KINETIC STUDIES

OF

CHORISMATE MUTASE - PREPHENATE DEHYDROGENASE

ISOLATED FROM

AEROBACTER AEROGENES

AND THE PREPARATION AND PURIFICATION

OF

SODIUM PREPHENATE

A THESIS SUBMITTED FOR
THE DEGREE OF
MASTER OF SCIENCE
OF THE
AUSTRALIAN NATIONAL UNIVERSITY

PAULINA KATARZYNA DUDZINSKI

DECEMBER 1980

Acknowledgement of work not performed by the author

The late Dr. R.K. Ghambeer performed some of the initial work in developing the method of the preparation and purification of sodium prephenate.

The NMR spectrum of prephenate was run and interpreted by Dr. M.D. Fenn of the Medical Chemistry Group, John Curtin School of Medical Research, in collaboration with Prof. L.M. Jackman.

The chemical analysis of sodium prephenate was performed by Analytical Services, the Medical Chemistry Group, John Curtin School of Medical Research.

P.K. Dudziński

P.K. Dudziński

ACKNOWLEDGEMENTS

I take pleasure in thanking Prof. F. Gibson for allowing me to work in the Department of Biochemistry, John Curtin School of Medical Research.

I wish to acknowledge with many thanks the supervision and advice of Dr. J.F. Morrison and Dr. T.E. Heyde during the course of the work.

I am pleased to acknowledge the contributions in various discussions and the smiling assistance of the other members of Laboratories 3077 and 3078, in particular Padmini SampathKumar, Keith Ellis, Ron Duggleby, Margaret Sneddon, Brian Crocker and Bernadette Mansour.

I wish to thank Margaret Sneddon, Brian Crocker and Bernadette Mansour for the preparation of some of the chorismate and enzyme used in the work described here.

I acknowledge the financial assistance of an Australian National University Scholarship.

ABSTRACT

This thesis is concerned with the enzyme chorismate mutase - prephenate dehydrogenase isolated from Aerobacter aerogenes. The enzyme catalyses the first two reactions in the tyrosine branch of the pathway of aromatic amino acid biosynthesis in the enterobacteria. These reactions are the rearrangement of chorismate to prephenate, and the subsequent aromatisation of the carbon ring to yield 4-hydroxyphenylpyruvate, accompanied by the conversion of NAD to NADH.

A method is described for the preparation of prephenate from chorismate utilising the enzyme's own catalytic function, the subsequent purification of prephenate as a barium salt and its conversion to the sodium salt to provide a more suitable substrate for enzyme kinetic investigations.

Steady state kinetic studies of the prephenate dehydrogenase reaction at pH 8.3 gave the following results: initial velocity patterns were intersecting; NADH inhibition was linear and competitive with respect to NAD and noncompetitive with respect to prephenate; 4-hydroxyphenylpyruvate inhibition was linear and noncompetitive with respect to both prephenate and NAD; sodium bicarbonate inhibition was competitive with respect to both NAD and prephenate, although certain peculiarities were observed, and probably resulted from considerable ionic strength changes. These results together with those of other inhibition experiments involving substrate analogues, and the quantitative analysis of the results are consistent with a mechanism that is essentially rapid equilibrium, the substrates binding randomly and synergistically (although 4-hydroxyphenylpyruvate is not the last product released), and involves the formation of the dead end complexes enzyme-prephenate-NADH, enzyme-prephenate-4-hydroxyphenylpyruvate and enzyme-NAD-4-hydroxyphenylpyruvate.

TABLE OF CONTENTS

	Acknowledgement of work not performed by the author		ii
	Acknowledgements		iii
	Abstract		iv
1	GENERAL INTRODUCTION		1
1.1	STEADY STATE ENZYME KINETICS		2
	1.1.1	Background	2
	1.1.2	Initial velocity studies in the absence of inhibitors	7
	1.1.3	Product inhibition	12
	1.1.4	Dead end inhibition	15
	1.1.5	Substrate inhibition	16
	1.1.6	Alternative substrate studies	18
	1.1.7	Isotope exchange studies	21
	1.1.8	Isotope partitioning	24
	1.1.9	Isotope effects	27
	1.1.10	pH effects	31
	1.1.11	Final remarks	49
1.2	THE BIOSYNTHESIS OF TYROSINE AND PHENYLALANINE : CHORISMATE MUTASE, PREPHENATE DEHYDROGENASE AND PREPHENATE DEHYDRATASE		50
	1.2.1	Organisms possessing a single monofunctional chorismate mutase	51
	1.2.2	Organisms possessing multiple monofunctional chorismate mutase isozymes	53
	1.2.3	Organisms possessing a single chorismate mutase as one activity of a bifunctional enzyme	55

1.2.4 Organisms possessing both the bifunctional enzymes chorismate mutase - prephenate dehydrogenase and chorismate mutase - prephenate dehydratase 61

1.3 AIMS OF THE WORK PRESENTED IN THIS THESIS 68

2. THE PREPARATION AND PURIFICATION OF SODIUM PREPHENATE 69

2.1 INTRODUCTION 70

2.2 MATERIALS AND METHODS 71

2.2.1 Chemicals 71

2.2.2 Preparation of enzyme 71

2.2.3 Determination of reactant concentrations 72

2.2.4 Test for barium 73

2.2.5 NMR spectra 73

2.2.6 Coupling of chorismate mutase - prephenate dehydrogenase to Sepharose 73

2.2.7 Estimation of chorismate mutase activity of Sepharose-bound enzyme 74

2.3 RESULTS

2.3.1 Preparation of prephenate using enzyme in free solution 75

2.3.2 Analysis of sodium prephenate 76

2.3.3 Use of Sepharose-linked enzyme 77

2.4 DISCUSSION 77

3 STEADY STATE KINETIC INVESTIGATIONS OF THE PREPHENATE DEHYDROGENASE REACTION 79

3.1 INTRODUCTION 80

3.2 MATERIALS AND METHODS 82

3.2.1 Chemicals 82

3.2.2 Isolation of enzyme 83

3.2.3 Enzyme assays 85

3.2.4 Estimation of substrate and other concentrations 87

3.2.5 Data analysis 88

3.2.6 Nomenclature and notation 89

3.3 RESULTS

3.3.1 Dependence of the steady state velocity on substrate concentrations 91

3.3.2 Steady state velocity investigations in the presence of products 92

3.3.3 Substrate analogue investigations 94

3.4 DISCUSSION

3.4.1 Qualitative assessment of the results 98

3.4.2 Quantitative aspects of the results 104

3.4.3 Conclusions 116

REFERENCES 119

CHAPTER 1

GENERAL INTRODUCTION

CHAPTER 1

GENERAL INTRODUCTION

This thesis reports steady state kinetic investigations of the bifunctional enzyme, chorismate mutase - prephenate dehydrogenase isolated from the enterobacterium Aerobacter aerogenes. The enzyme catalyses the first two reactions in the tyrosine branch of the pathway of aromatic amino acid biosynthesis in the enterobacteria (Fig. 1.1), the reactions being :

$$\text{chorismate} \xrightarrow[\text{mutase}]{\text{chorismate}} \text{prephenate} \qquad (1.1)$$

$$\text{prephenate} + \text{NAD} \xrightarrow[\text{dehydrogenase}]{\text{prephenate}} \text{4-hydroxyphenylpyruvate} + \text{NADH} + CO_2 \qquad (1.2)$$

The structural changes involved in these reactions are illustrated in Fig. 1.2.

Steady state enzyme kinetic technique, the approach used in this study, will be discussed in Section 1.1 of this Chapter, while Section 1.2 will deal with chorismate mutase - prephenate dehydrogenase and the functionally related enzyme, chorismate mutase - prephenate dehydratase, in various organisms. Finally, the aims of this investigation will be described in Section 1.3.

FIGURE 1.1 Pathways of biosynthesis of the aromatic amino acids.

(a) Reactions common to the biosynthesis of tyrosine, tryptophan and phenylalanine.

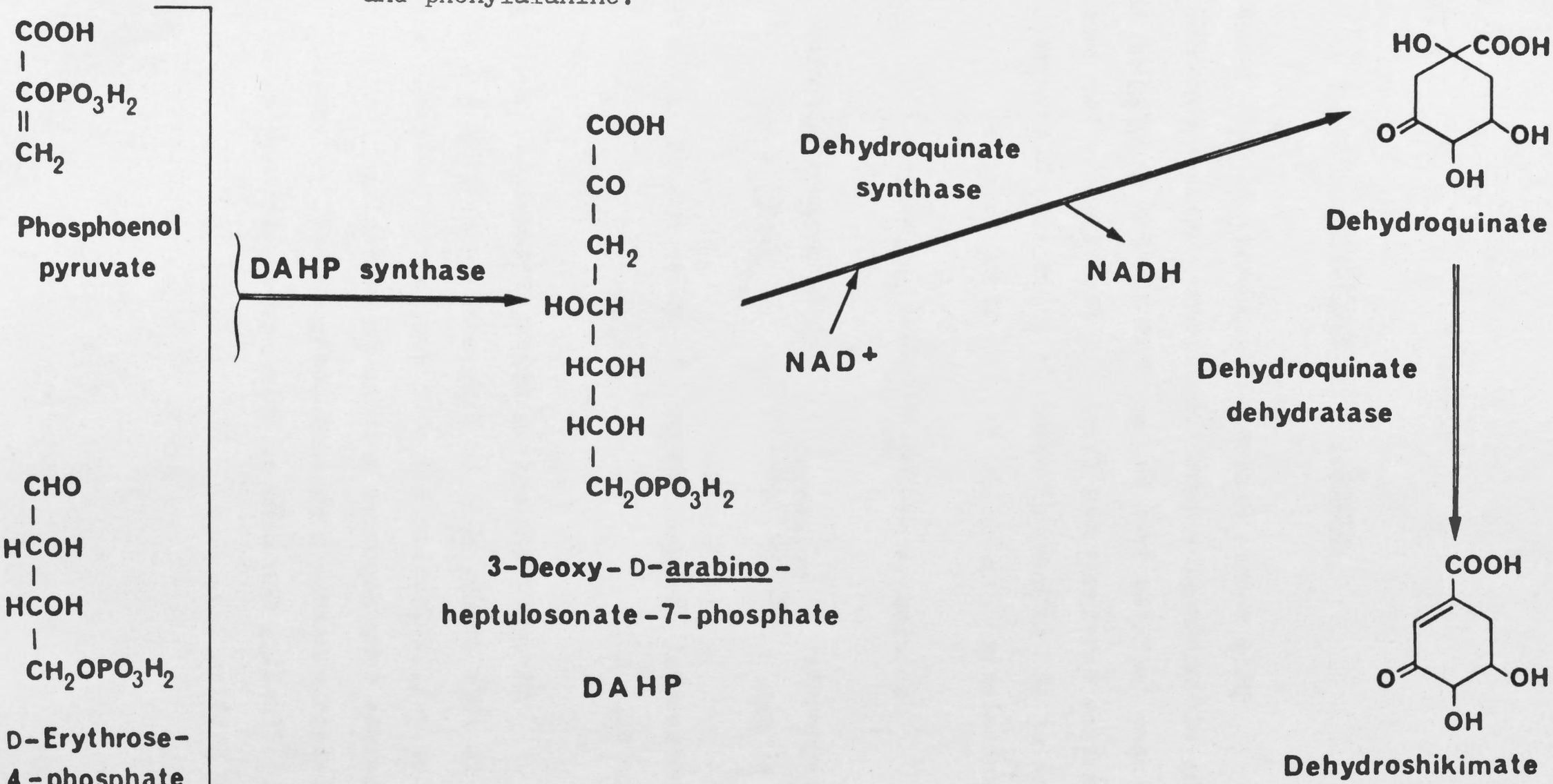

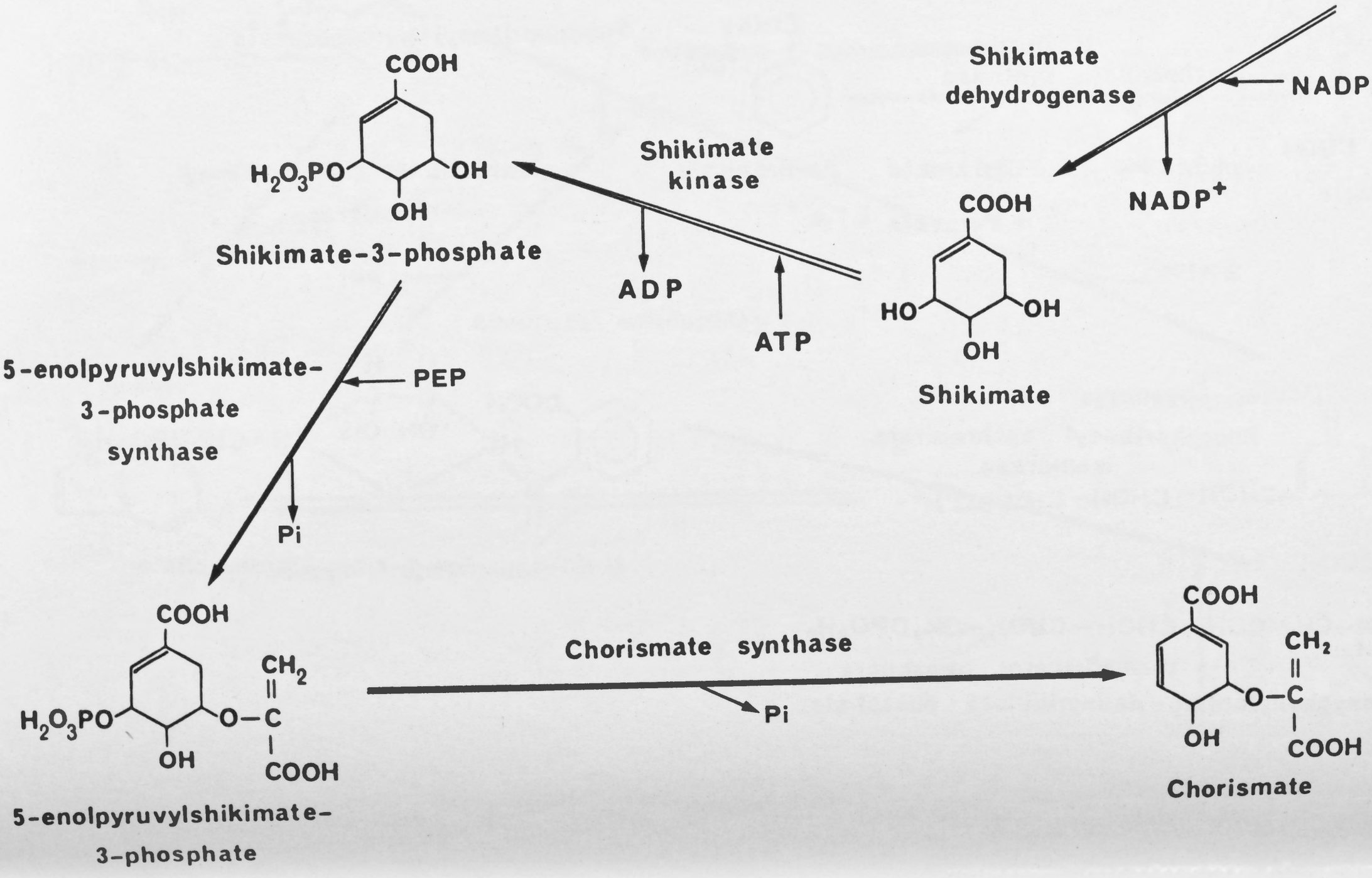
COOH
H_2O_3PO
OH
OH
Shikimate-3-phosphate
Shikimate kinase
ADP
ATP
Shikimate dehydrogenase
NADPH
$NADP^+$
COOH
HO
OH
OH
Shikimate
5-enolpyruvylshikimate-3-phosphate synthase
PEP
Pi
COOH
CH_2
H_2O_3PO
O—C
OH
COOH
5-enolpyruvylshikimate-3-phosphate
Chorismate synthase
Pi
COOH
CH_2
O—C
OH
COOH
Chorismate

FIGURE 1.1 (Continued) Pathways of biosynthesis of the aromatic amino acids.

(b) Reactions in the biosynthesis of tryptophan from chorismic acid.

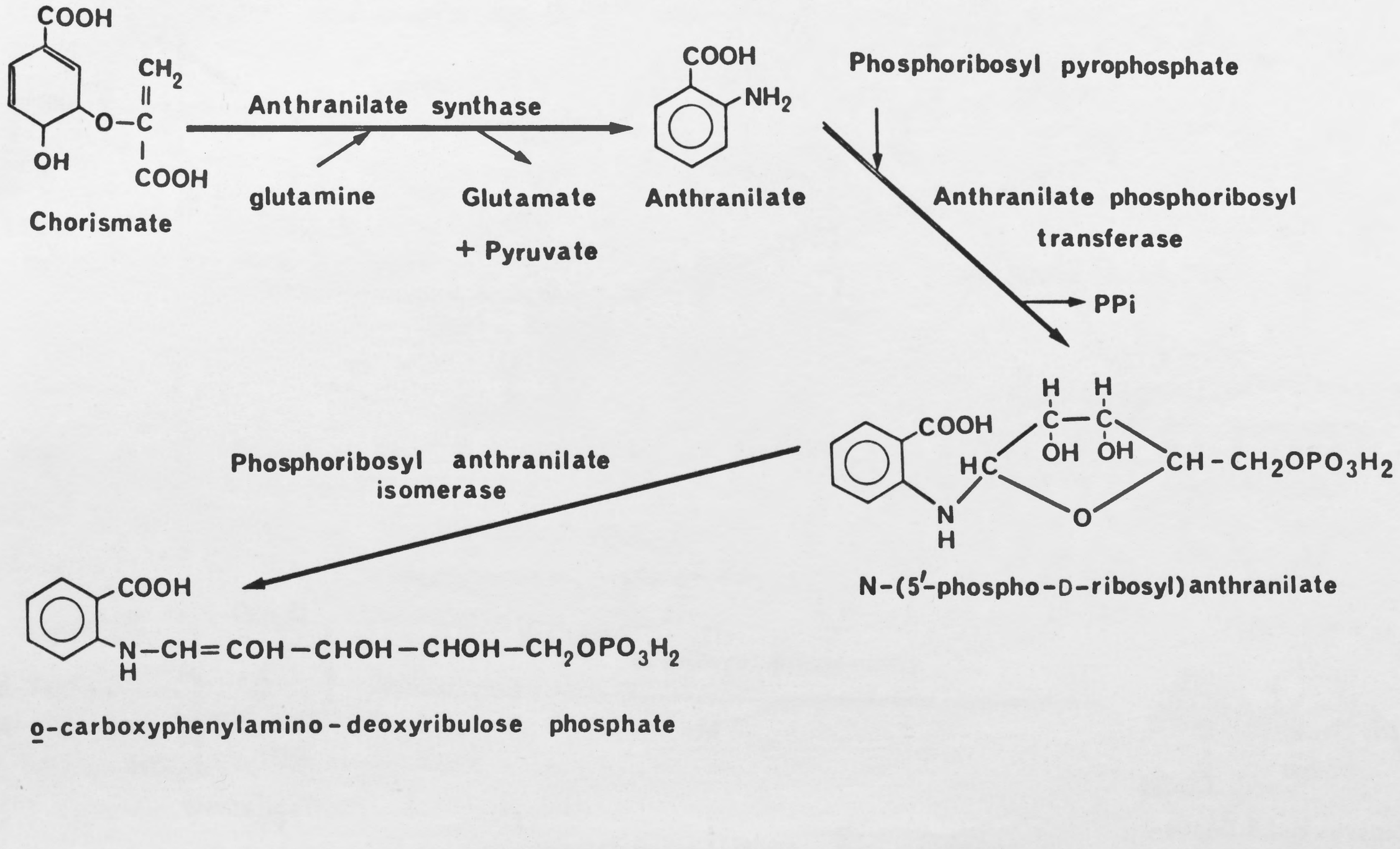

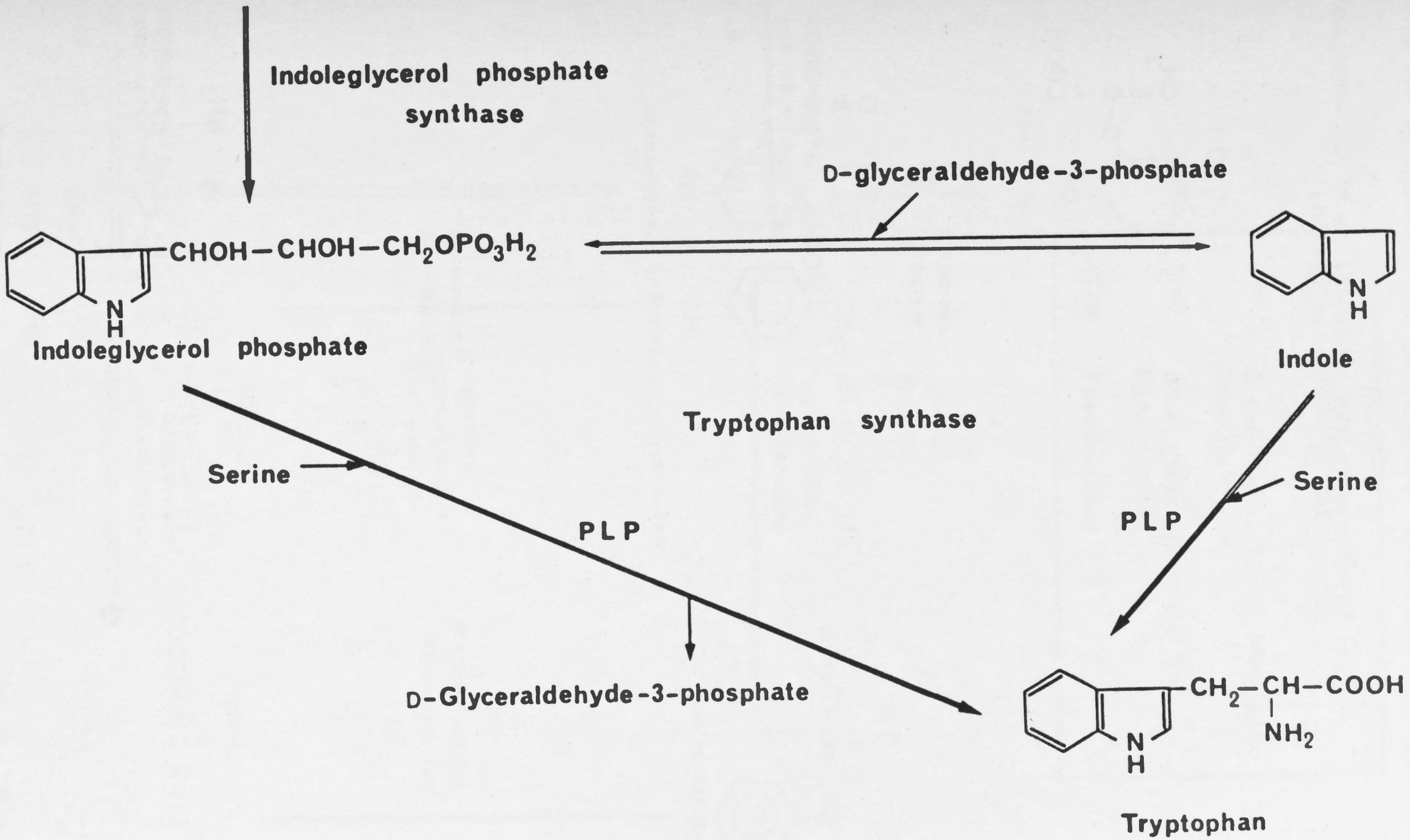
Indoleglycerol phosphate synthase
D-glyceraldehyde-3-phosphate
CHOH—CHOH—CH2OPO3H2
NH
Indoleglycerol phosphate
Indole
Tryptophan synthase
Serine
PLP
Serine
PLP
D-Glyceraldehyde-3-phosphate
CH2—CH—COOH
NH2
NH
Tryptophan

FIGURE 1.1 (Continued) Pathways of biosynthesis of the aromatic amino acids.

(c) Reactions in the biosynthesis of tyrosine and phenylalanine from chorismic acid.

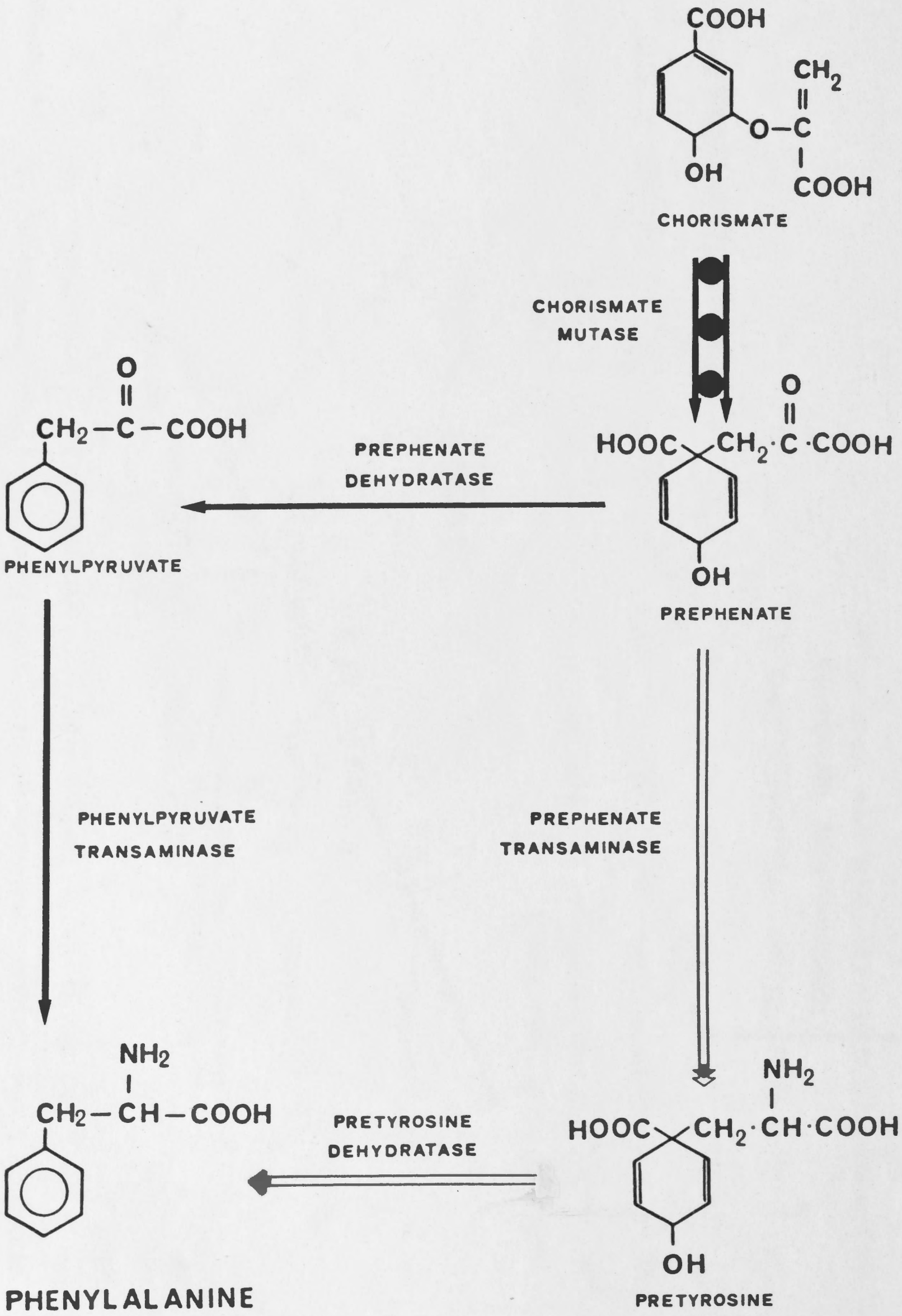

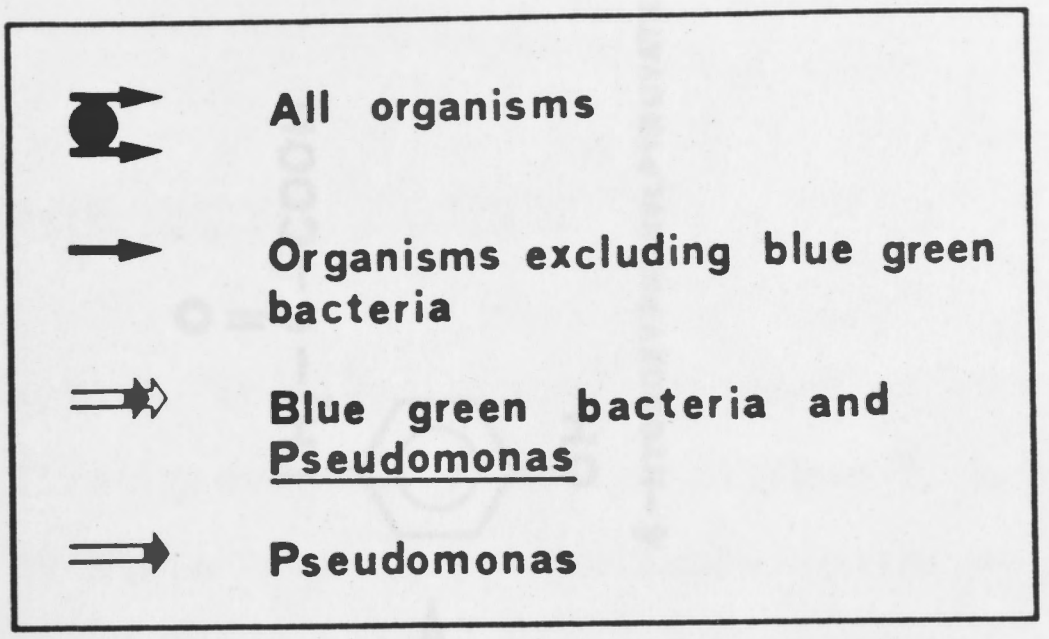
All organisms
Organisms excluding blue green bacteria
Blue green bacteria and Pseudomonas
Pseudomonas

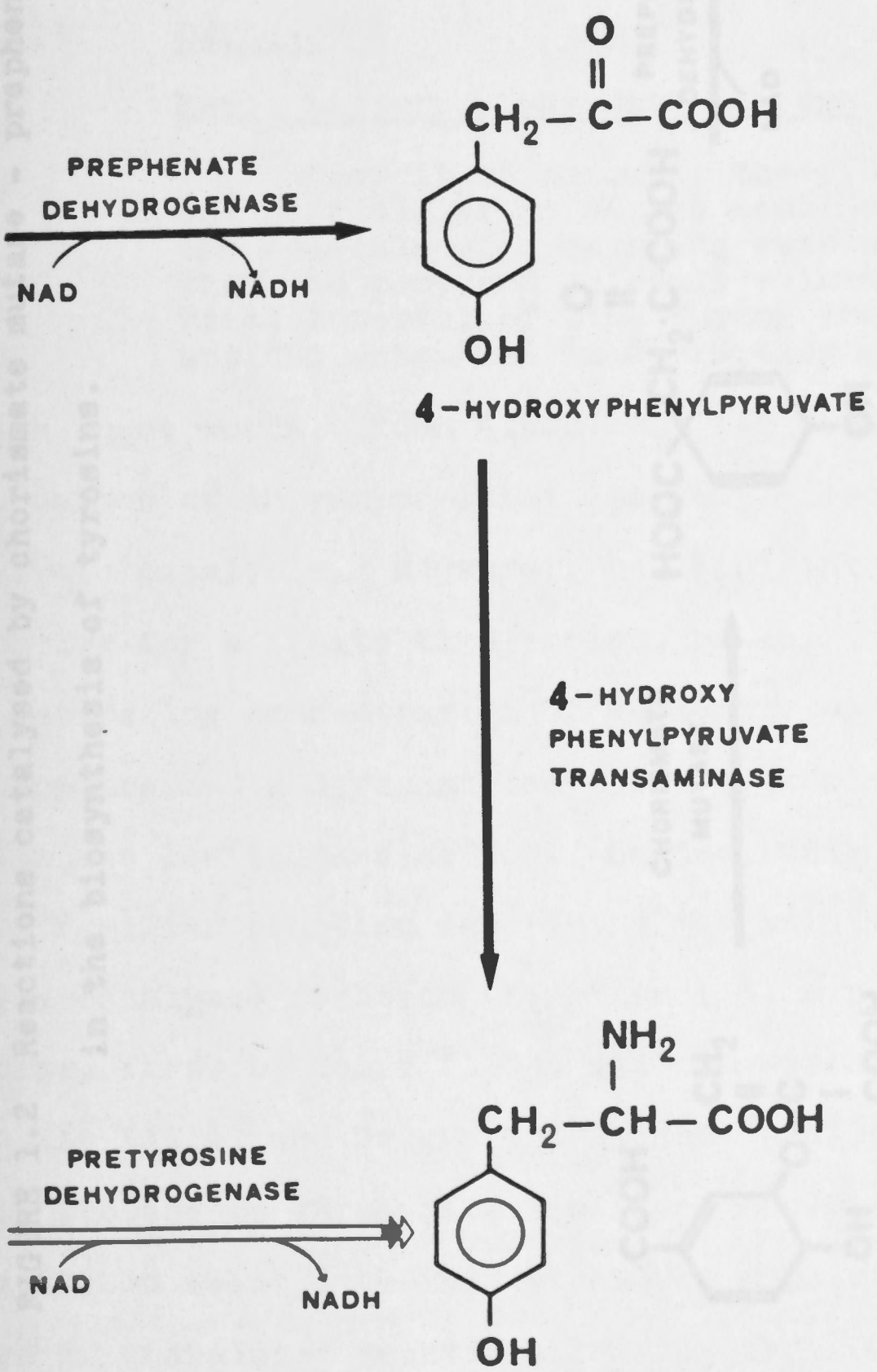
O
CH2 – C – COOH
PREPHENATE DEHYDROGENASE
NAD
NADH
OH
4 – HYDROXY PHENYLPYRUVATE
4 – HYDROXY PHENYLPYRUVATE TRANSAMINASE
NH2
CH2 – CH – COOH
PRETYROSINE DEHYDROGENASE
NAD
NADH
OH
TYROSINE

FIGURE 1.2 Reactions catalysed by chorismate mutase - prephenate dehydrogenase in the biosynthesis of tyrosine.

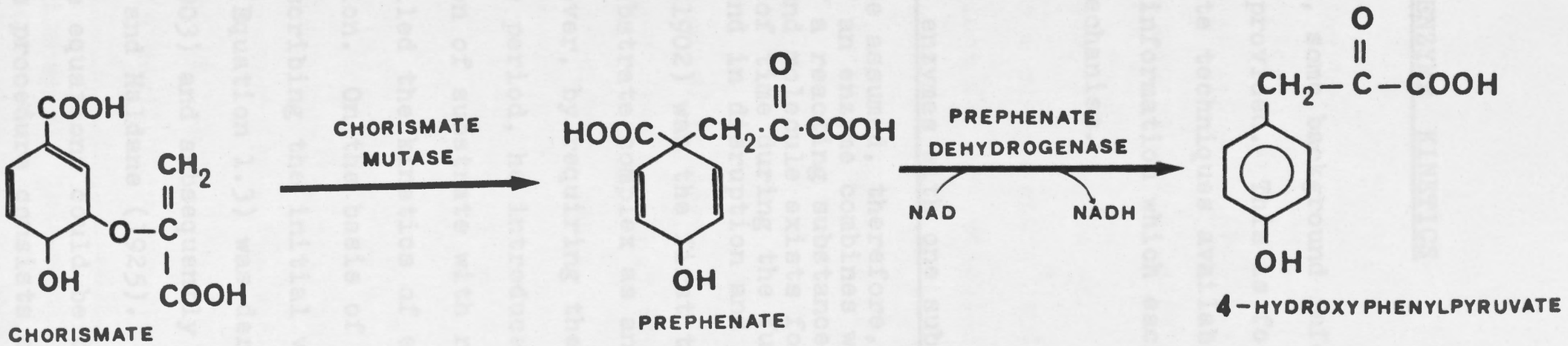

1.1 STEADY STATE ENZYME KINETICS

In this Section, some background information about enzyme kinetics is first provided. This is followed by a discussion of the steady state techniques available to the enzymologist, and the kind of information which each technique can yield about the enzymic mechanism.

1.1.1 BACKGROUND

Early history - enzymes with one substrate

> "Let it be assumed, therefore, that one molecule of an enzyme combines with one molecule of a reacting substance, and that the compound molecule exists for a brief interval of time during the further actions which end in disruption and change."

With these words, Brown (1902) was the first to postulate the formation of an enzyme-substrate complex as an intermediate in enzymic catalysis. Moreover, by requiring the existence of the complex for a finite time period, he introduced the concept of a saturating concentration of substrate with respect to enzyme concentration and reconciled the kinetics of enzymic catalysis with the law of mass action. On the basis of Brown's model, the now familiar equation describing the initial velocity of an enzyme-catalysed reaction (Equation 1.3) was derived in different forms, first by Henri (1903) and subsequently by Van Slyke and Cullen (1914) and Briggs and Haldane (1925). Henri also set out the process by which rate equations could be derived for enzyme-catalysed reactions; this procedure consists of writing a series of postulated reactions leading from substrate to product, setting up a rate equation for each step based on the law of

$$v = \frac{VA}{K_a + A}$$

where v = initial velocity

V = maximum velocity

A = initial substrate concentration

K_a = Michaelis constant for substrate (1.3)

mass action, making an assumption (where warranted) that the intermediates have reached a steady state* and then solving the set of simultaneous equations for the velocity in terms of measurable concentrations of reactants. This is the basis of all present methods of deriving rate equations for enzyme catalysed reactions.

Of the derivations of Equation 1.3 mentioned above, that of Briggs and Haldane (1925) required the least restrictive assumptions. The scheme considered was :

$$E + A \underset{k_2}{\overset{k_1}{\rightleftharpoons}} EA \xrightarrow{k_3} E + P \qquad (1.4)$$

One molecule of substrate (A) combines reversibly with one of enzyme (E) to form the binary complex (EA) which then breaks down to free enzyme and product (P). The rate constants for each step are as indicated in Scheme 1.4, above. When the total concentration of enzyme is negligibly small compared with the

---

* Actually, Henri assumed that the intermediates rapidly reach thermodynamic equilibrium. The concept of the "steady state" was introduced some years later by Bodenstein (1913) and was used by Briggs and Haldane (1925).

concentration of the reactants, the rate of change of the concentration of EA is (except during the first instant of the reaction) negligibly small compared with the rate of change of the substrate and product concentrations. (This is the steady state assumption.) An expression for the initial velocity of reaction may then be obtained which is identical in form with Equation 1.3, i.e.

$$v = \frac{k_3 . E_t . A}{\frac{k_2 + k_3}{k_1} + A} \qquad (1.5)$$

where E_t is the total concentration of enzyme = E + EA

The parameters V and K_a of Equation 1.3 are equal, respectively, to $k_3.E_t$ and $(k_2 + k_3)/k_1$ in the formulation of Equation 1.5. The familiar Equation 1.3 is now known as the Michaelis-Menten equation after those who first wrote it in that form (Michaelis and Menten, 1913), and the parameter K_a is referred to as the Michaelis constant, with no implications as to its meaning in terms of rate constants (which will vary with the mechanism under consideration). Those enzymes which conform in their kinetics to Equation 1.3 are said to display Michaelis-Menten behaviour. Many enzymes which catalyse reactions involving more than one substrate exhibit Michaelis-Menten kinetics if the concentration of only one substrate is varied with any other substrates being held at constant concentration.

Before the advent of statistical analysis in enzyme kinetics, the kinetic constants were determined graphically by

transforming the data and plotting according to an equation which linearises the Michaelis-Menten equation (which describes a rectangular hyperbola through the origin). Since these plots are now rarely used for purposes other than data display, only the double reciprocal plot will be dealt with. Inversion of Equation 1.3 yields Equation 1.6 which indicates that when 1/v

$$\frac{1}{v} = \frac{K_a}{V}.\frac{1}{A} + \frac{1}{V} \qquad (1.6)$$

is plotted against 1/A, a straight line of slope K_a/V is obtained. The values of the vertical and horizontal intercepts are $1/V$ and $-1/K_a$, respectively (see Fig. 1.3). This method has the advantages that it is the most familiar, it separates the variables and is therefore conceptually simpler than other plots which do not, and the effects of saturating with substrate are easily determined on the vertical axis ($1/A = 0$ corresponds to $A = \infty$).

Three basic types of inhibition by products and other substances were recognised by the early workers (e.g. Brown, 1902; Michaelis and Menten, 1913; Van Slyke and Cullen, 1914; Van Slyke and Zacharias, 1914; Michaelis and Pechstein, 1914; Michaelis and Rona, 1914). In modern nomenclature, inhibitors are "competitive", "uncompetitive" or "noncompetitive" depending on whether they increase the slopes of double reciprocal plots, the vertical intercepts, or both, respectively. (Some authors still reserve the term "noncompetitive" for the special case when double reciprocal plots intersect on the horizontal axis, and use the term "mixed" to describe the cases when the inter-

FIGURE 1.3 Relationship of double reciprocal plot to hyperbolic plot. (Corresponding points are indicated with the same symbol.)

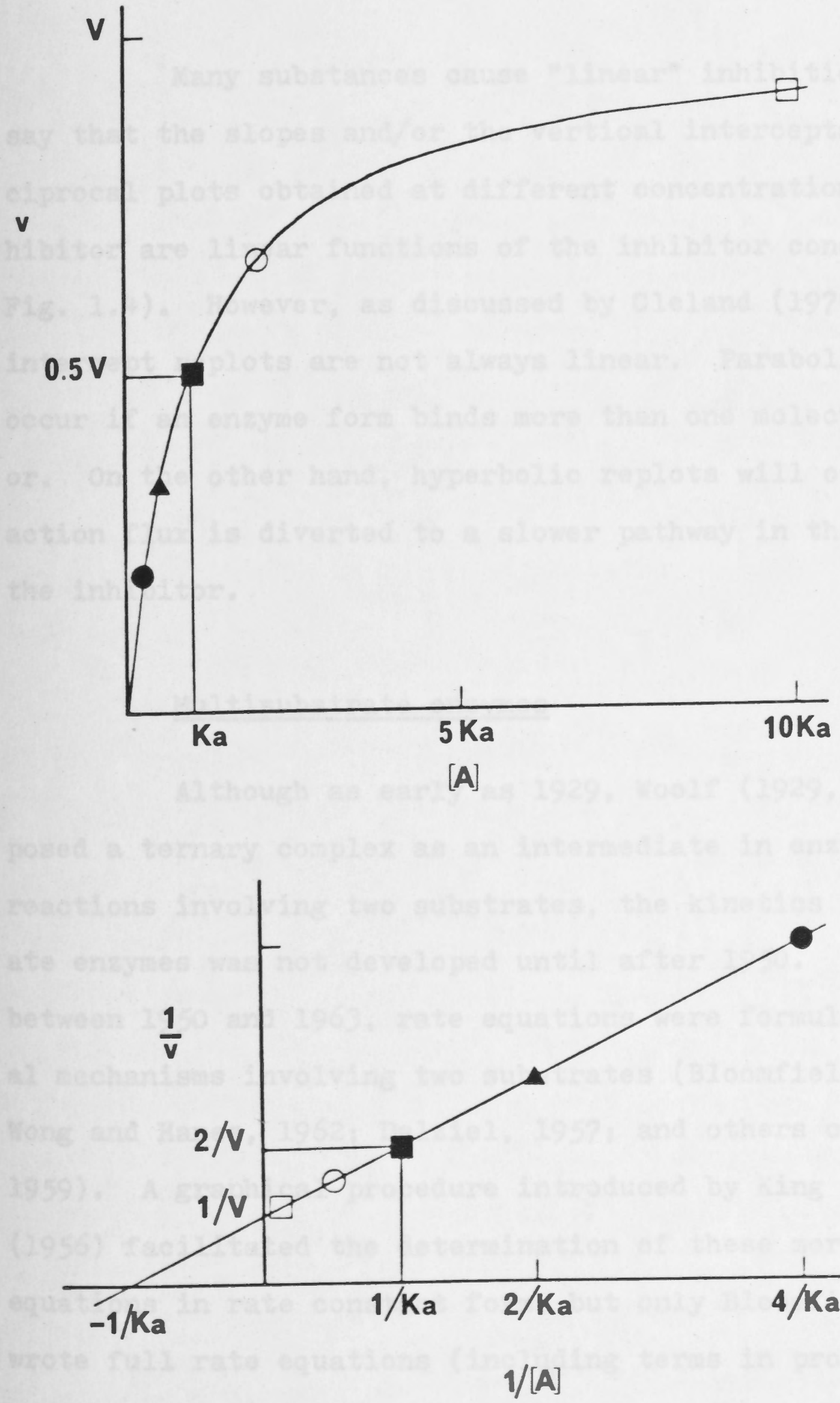

section point lies above or below the axis. As Dalziel (1957) pointed out, there seems no good theoretical reason for such a distinction.)

Many substances cause "linear" inhibition : that is to say that the slopes and/or the vertical intercepts of double reciprocal plots obtained at different concentrations of the inhibitor are linear functions of the inhibitor concentration (see Fig. 1.4). However, as discussed by Cleland (1970), slope or intercept replots are not always linear. Parabolic replots may occur if an enzyme form binds more than one molecule of inhibitor. On the other hand, hyperbolic replots will occur if the reaction flux is diverted to a slower pathway in the prescence of the inhibitor.

Multisubstrate enzymes

Although as early as 1929, Woolf (1929, 1931) had proposed a ternary complex as an intermediate in enzyme-catalysed reactions involving two substrates, the kinetics of multisubstrate enzymes was not developed until after 1950. In the years between 1950 and 1963, rate equations were formulated for several mechanisms involving two substrates (Bloomfield et al., 1962; Wong and Hanes, 1962; Dalziel, 1957; and others cited by Segal, 1959). A graphical procedure introduced by King and Altman (1956) facilitated the determination of these more complex rate equations in rate constant form, but only Bloomfield et al. (1962) wrote full rate equations (including terms in products as well as substrates), defining a kinetic constant for each term in the de-

FIGURE 1.4 Double reciprocal plots and slope and intercept replots for linear competitive, uncompetitive and noncompetitive inhibitions.

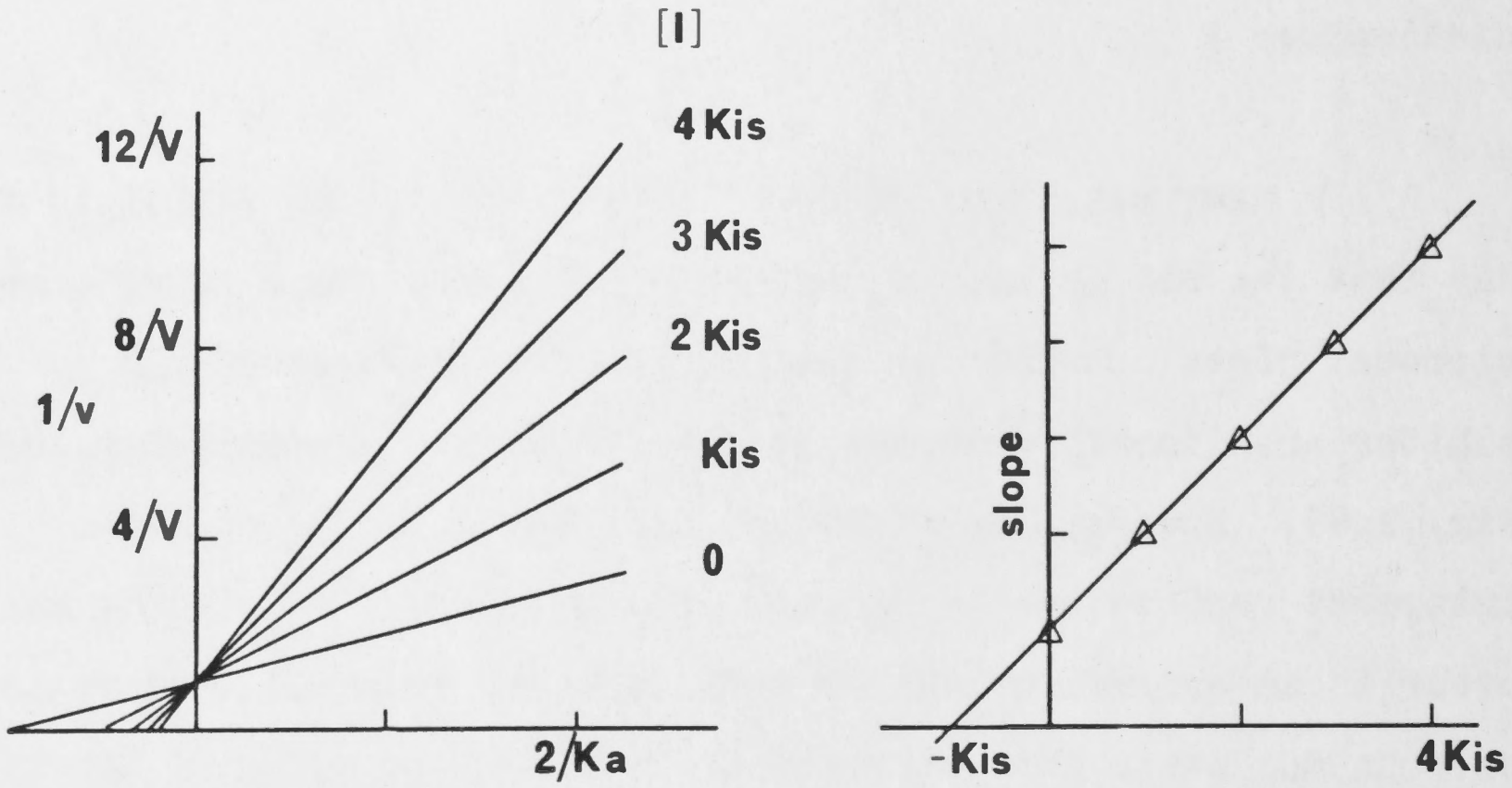

(a) Linear competitive inhibition.

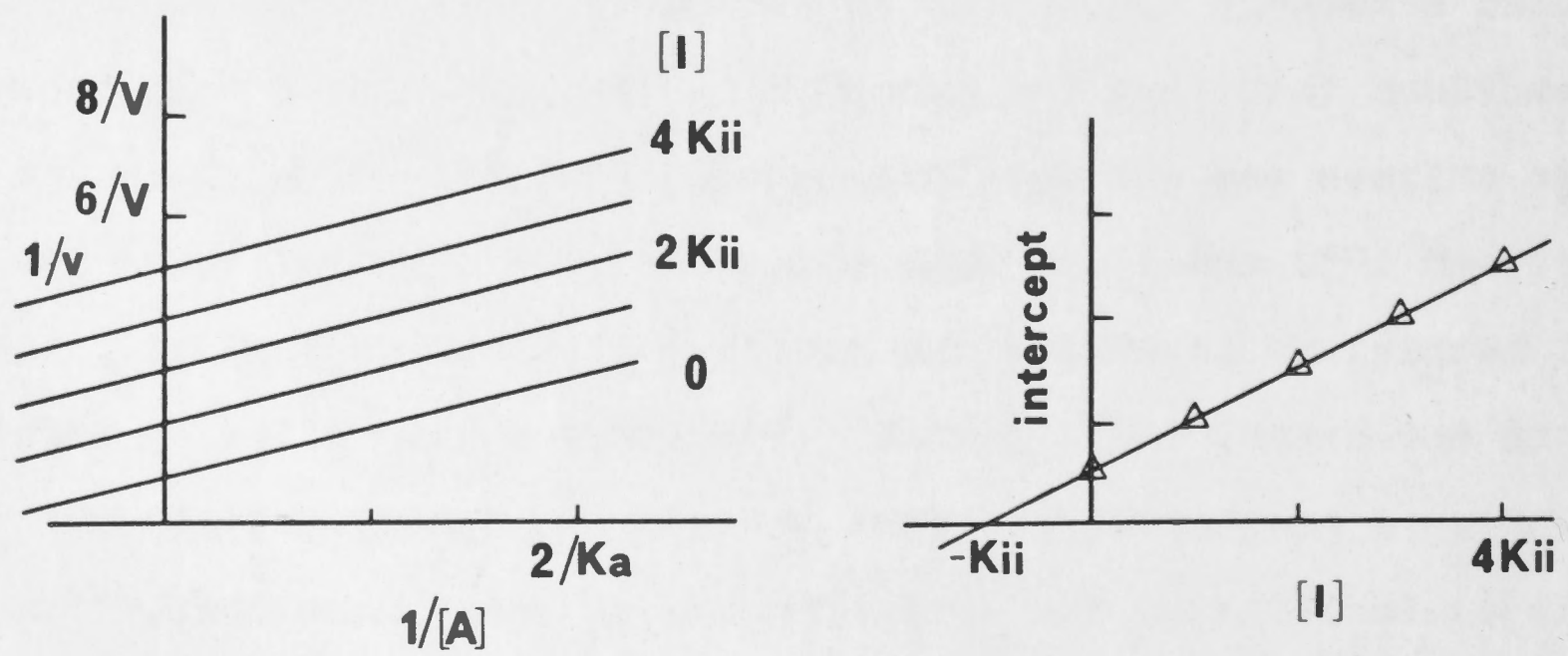

(b) Linear uncompetitive inhibition.

FIGURE 1.4 (Continued) Double reciprocal plots and slope and intercept replots for linear competitive, uncompetitive and noncompetitive inhibitions.

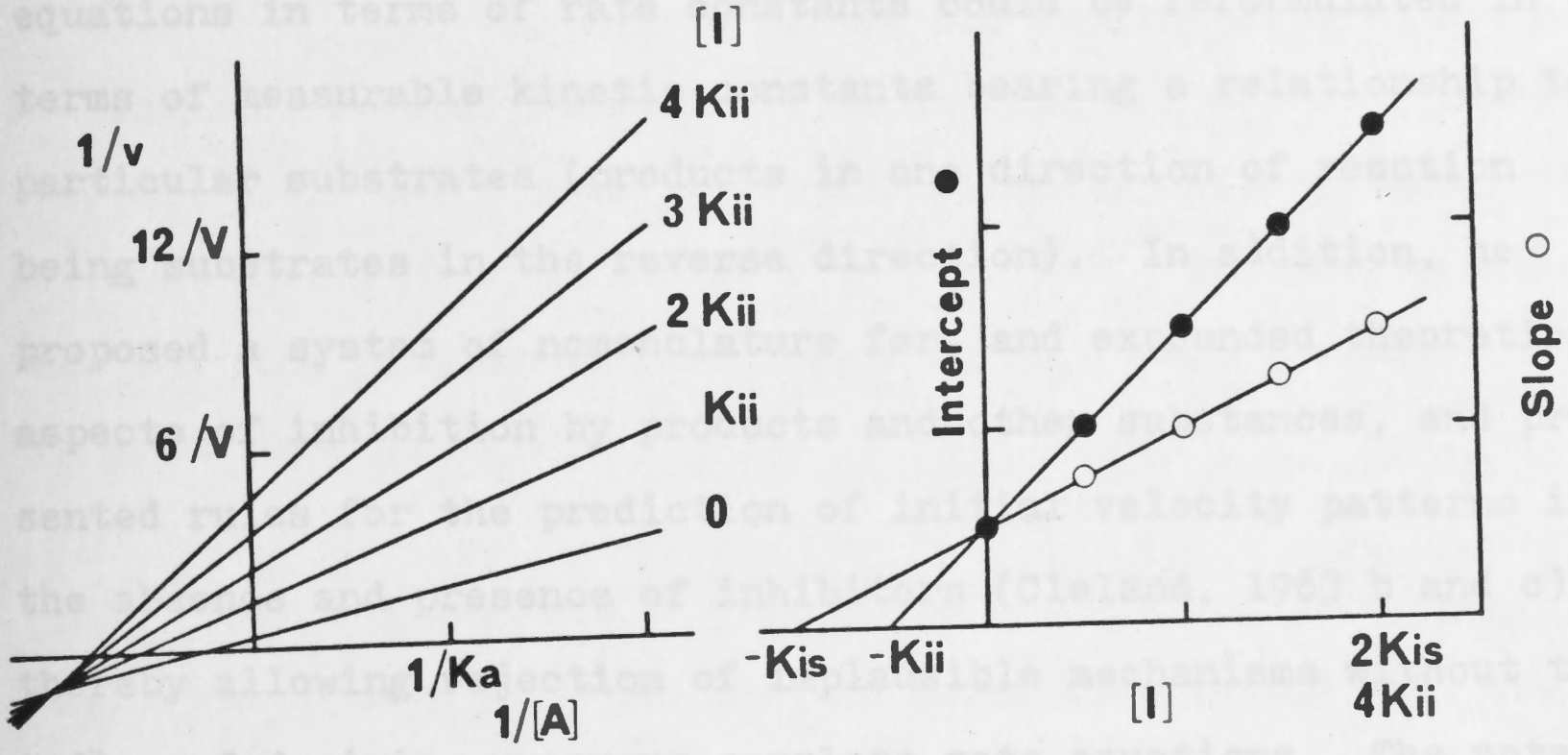

Kis > Kii ⇩ crossover point below horizontal axis

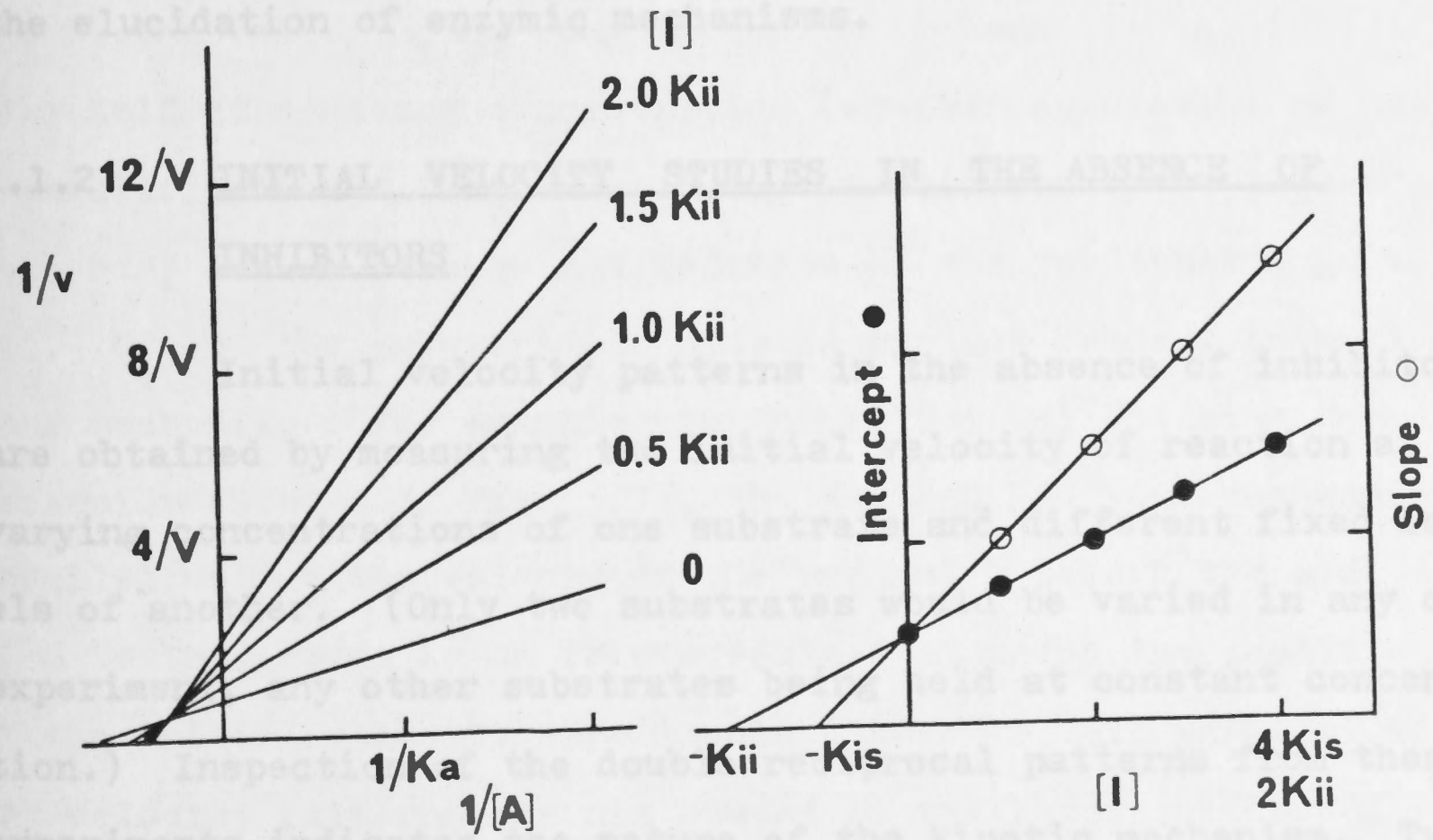

Kis < Kii ⇩ crossover point above horizontal axis

nominator. In 1963, Cleland (1963a) proposed a nomenclature and shorthand notation for the description of different mechanisms. Moreover, he also indicated how the complete initial velocity equations in terms of rate constants could be reformulated in terms of measurable kinetic constants bearing a relationship to particular substrates (products in one direction of reaction being substrates in the reverse direction). In addition, he proposed a system of nomenclature for, and expounded theoretical aspects of inhibition by products and other substances, and presented rules for the prediction of initial velocity patterns in the absence and presence of inhibitors (Cleland, 1963 b and c), thereby allowing rejection of implausible mechanisms without the tedium of deriving numerous complete rate equations. The notation and nomenclature of Cleland (1963 a and b) will be used in the following discussion of steady state kinetic techniques in the elucidation of enzymic mechanisms.

1.1.2 INITIAL VELOCITY STUDIES IN THE ABSENCE OF INHIBITORS

Initial velocity patterns in the absence of inhibitors are obtained by measuring the initial velocity of reaction at varying concentrations of one substrate and different fixed levels of another. (Only two substrates would be varied in any one experiment, any other substrates being held at constant concentration.) Inspection of the double reciprocal patterns from these experiments indicates the nature of the kinetic mechanism. Two types of mechanism have been defined by Cleland (1963a) :

Sequential - in which all substrates must be bound to to the enzyme before a product is released.

Ping pong - in which a product is released from the enzyme before all substrates have bound.

As examples, several bisubstrate mechanisms are depicted in Fig. 1.5, and their corresponding initial velocity patterns and initial rate equations are indicated in Fig. 1.6. Examples of sequential and ping pong mechanisms involving more than two substrates are given in Fig. 1.7.

An intersecting steady state velocity pattern (e.g. Fig. 1.6a) is obtained when the two substrates varied must coexist on the enzyme for reaction to proceed. Variation of A and B in an ordered bisubstrate reaction (Scheme 1, Fig. 1.5) would give an intersecting pattern, as would variation of A and B in the Bi Uni Uni Uni ping pong mechanism (Scheme 1, Fig. 1.7) if C were held at constant concentration (whether saturating or not). A parallel pattern (e.g. Fig. 1.6c) is obtained if an irreversible step occurs between the addition of the two substrates varied. Often, the irreversible step is product release in a ping pong mechanism : for example, in the Bi Uni Uni Uni ping pong mechanism (Scheme 1, Fig. 1.7), the A-C and B-C patterns would be parallel, since the release of the product P before the addition of C to the enzyme is an irreversible step under the conditions of the initial velocity experiments. However, all parallel initial velocity patterns are not caused by the interposition of product release (at zero concentration) between the addition of the two substrates varied. An example would be a Theorell-Chance

FIGURE 1.5 Examples of Bi Bi reaction mechanisms.

1. Ordered

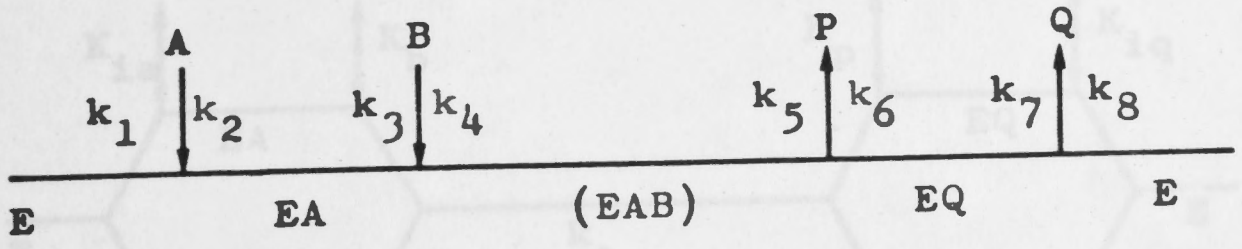

2. Theorell-Chance

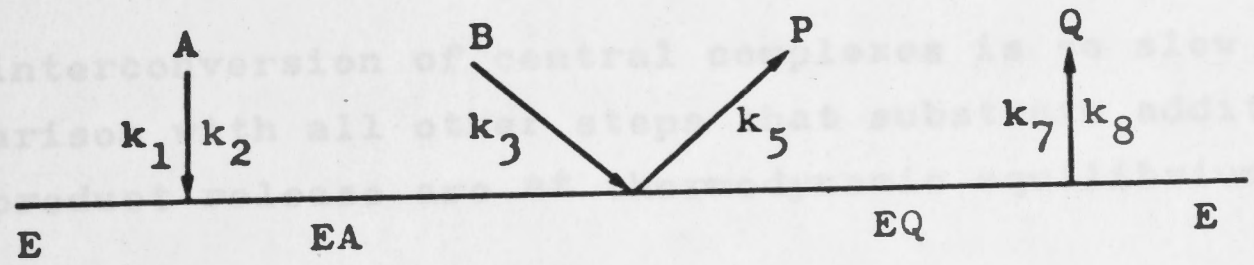

(There are no kinetically significant central complexes in a Theorell-Chance mechanism.)

3. Equilibrium ordered

(a)

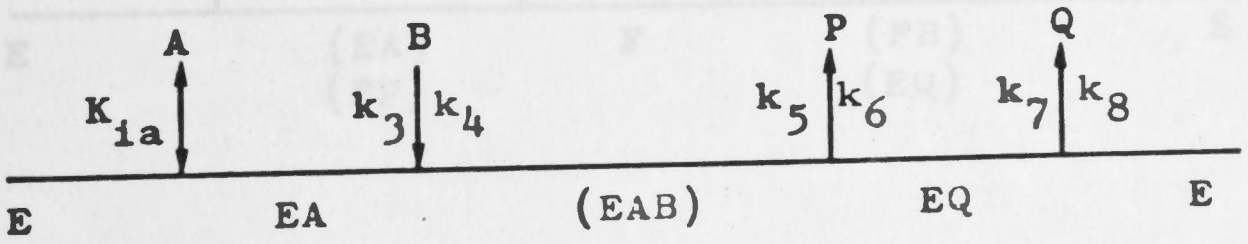

(b)

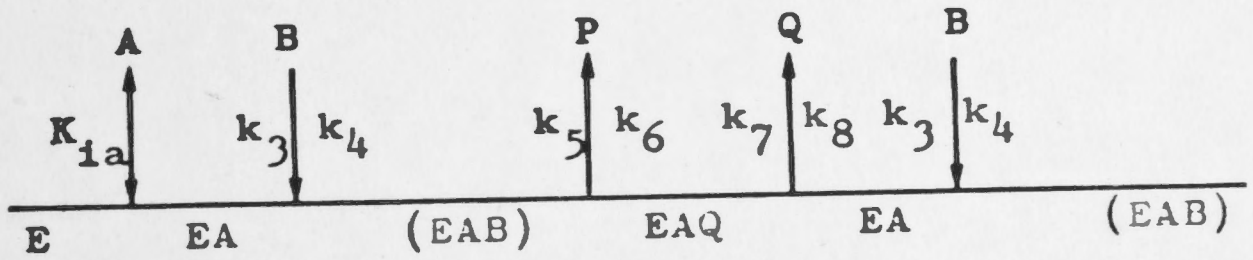

(A is a recycling activator.)

FIGURE 1.5 (Continued) Examples of Bi Bi reaction mechanisms.

4. Rapid equilibrium random

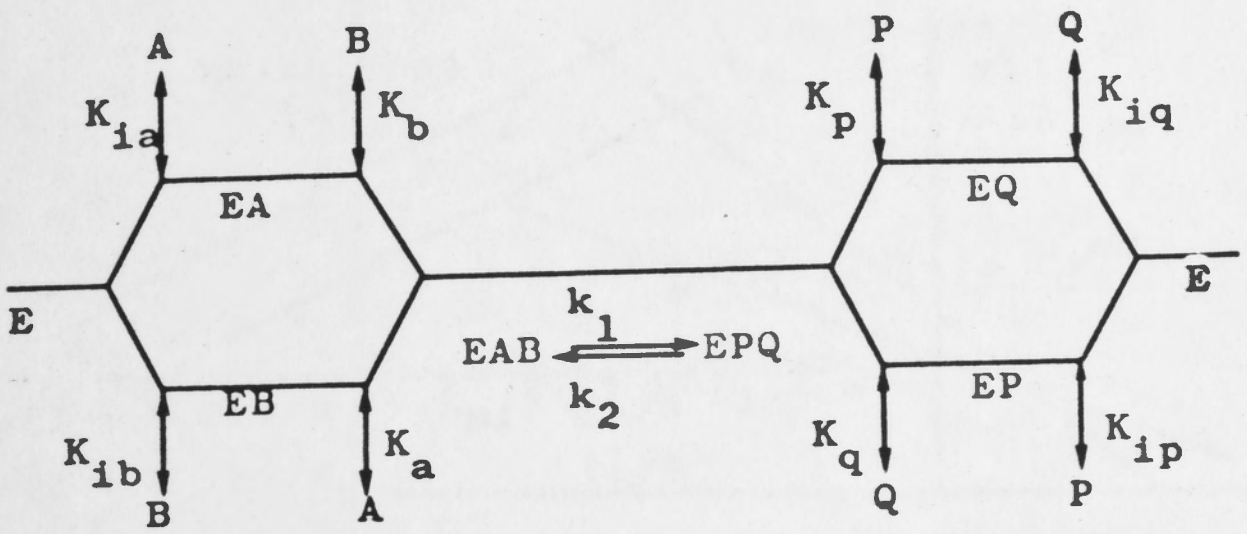

The interconversion of central complexes is so slow in comparison with all other steps that substrate addition and product release are at thermodynamic equilibrium.

5. Ping Pong

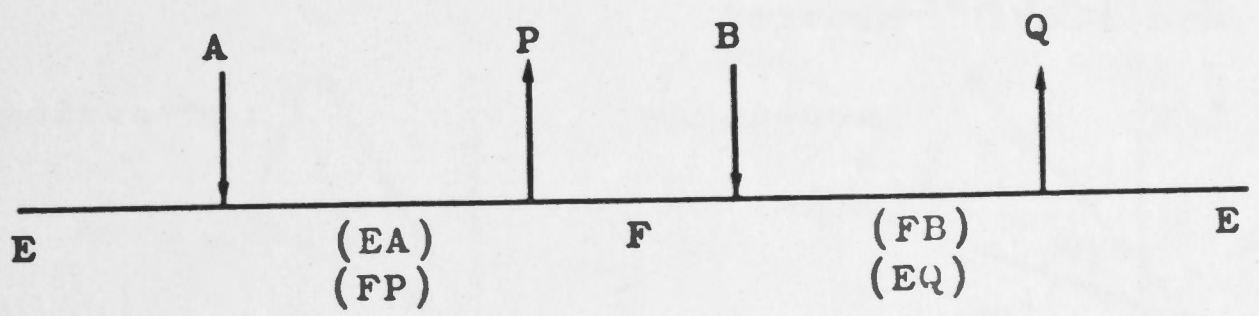

FIGURE 1.6 Common initial velocity patterns for bisubstrate mechanisms.

(a) Intersecting

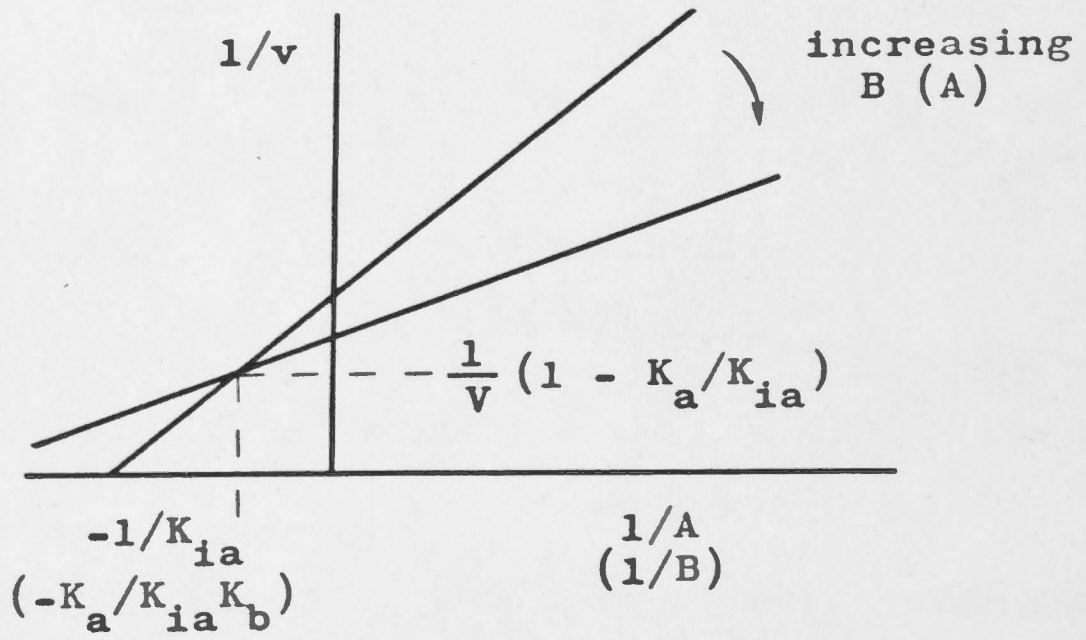

Sequential mechanism

$$v = \frac{VAB}{K_{ia}K_b + K_bA + K_aB + AB}$$

(e.g. Schemes 1,2,4, Fig. 1.5)

(b) Equilibrium ordered

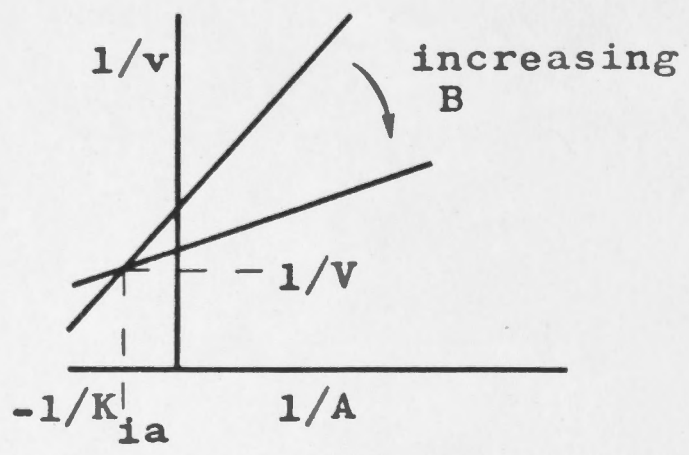

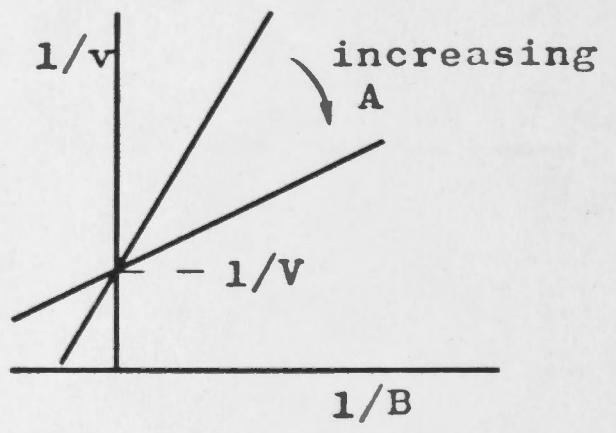

$$v = \frac{VAB}{K_{ia}K_b + K_bA + AB}$$

(e.g. Scheme 3, Fig. 1.5)

FIGURE 1.6 (Continued) Common initial velocity patterns for bisubstrate mechanisms.

(c) Parallel

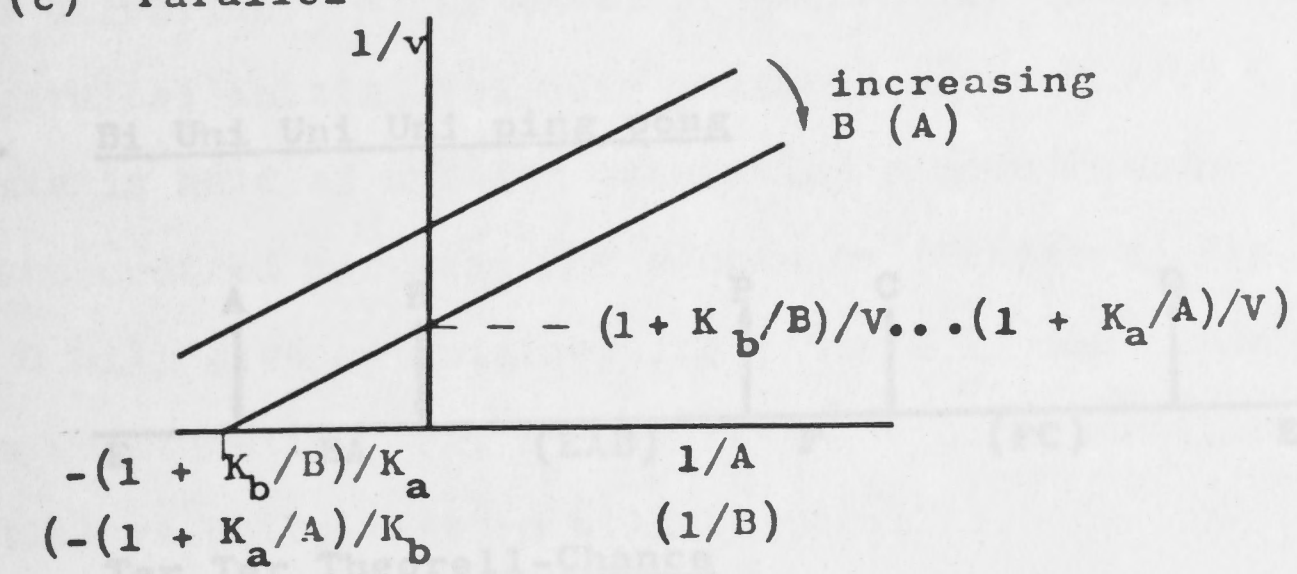

$$v = \frac{VAB}{K_b A + K_a B + AB}$$

(e.g. Scheme 5, Fig. 1.5 ;
Scheme 4, Fig. 1.5 if $K_{ia} \ll K_a$
Scheme 2, Fig. 1.5 if $k_2 \approx 0$
Scheme 1, Fig. 1.5 if $k_2 \ll k_5 k_7/(k_5 + k_7)$
i.e. $K_{ia} \ll K_a$

FIGURE 1.7 Examples of enzyme mechanisms involving three substrates.

1. Bi Uni Uni Uni ping pong

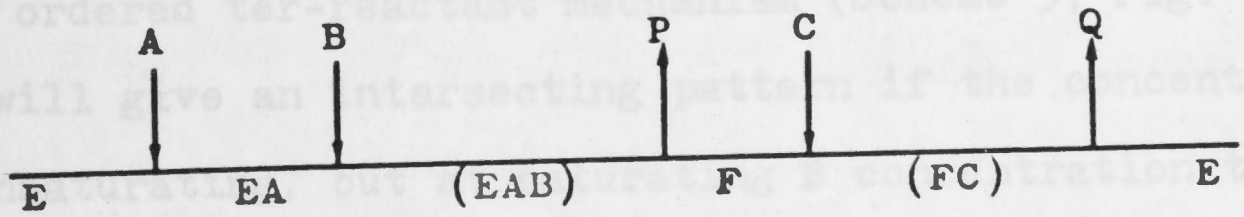

2. Ter Ter Theorell-Chance

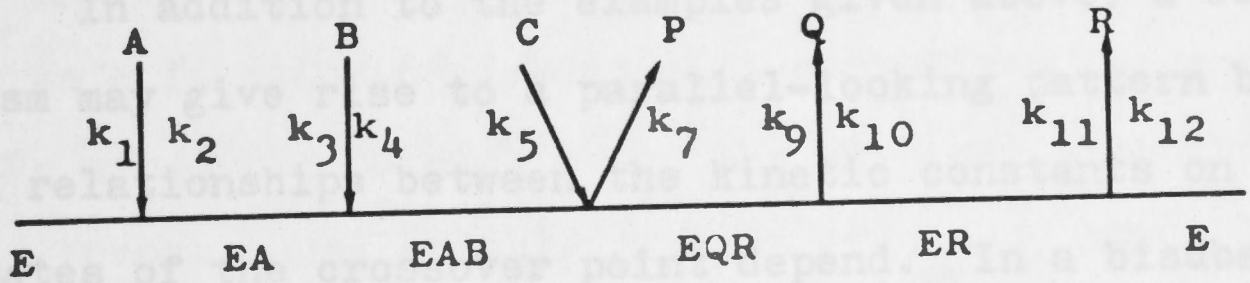

3. Ordered Ter Ter

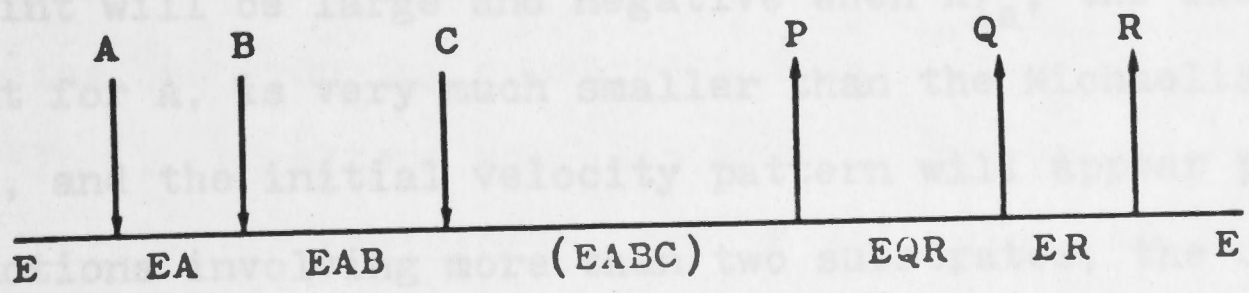

mechanism which is essentially irreversible because of the negligible rate of release of the first substrate to add in the forward direction. Other cases of sequential mechanisms giving rise to parallel initial velocity patterns may occur if a crucial substrate is held at a fixed saturating concentration. For example, in the ordered ter-reactant mechanism (Scheme 3, Fig. 1.7), A and C will give an intersecting pattern if the concentration of B is unsaturating, but at saturating B concentration the A-C initial velocity pattern will be parallel.

In addition to the examples given above, a sequential mechanism may give rise to a parallel-looking pattern because of certain relationships between the kinetic constants on which the coordinates of the crossover point depend. In a bisubstrate mechanism, the horizontal and vertical coordinates of the cross-over point will be large and negative when K_{ia}, the inhibition constant for A, is very much smaller than the Michaelis constant, K_a, and the initial velocity pattern will appear parallel. For reactions involving more than two substrates, the cross-over point coordinates may be defined by complex expressions involving kinetic constants and the concentrations of substrates held at fixed concentration, so it is not so easy to determine when the coordinates will be large and negative.

Generally speaking, initial velocity studies in the absence of inhibitors allow the determination of the mechanistic type (*i.e.* whether the reaction is sequential or ping pong) and evaluation of the kinetic parameters by statistical or graphical

analysis of the data (see Cleland, 1970). Usually, no information is obtained about the order (if any) in which the substrates bind to the enzyme, and such experiments can give no information about the order of product release. An exception to this general rule is the equilibrium ordered mechanism in which at least the first substrate addition is at thermodynamic equilibrium (Scheme 3, Fig. 1.5). Normally in a sequential mechanism, the intersection point of double reciprocal plots with each other is to the left of the vertical axis. In an equilibrium ordered mechanism, this will be so when the data are plotted as a function of 1/A at different fixed concentrations of B, but when plotted as a function of 1/B at different fixed concentrations of A, the crossover point lies on the vertical axis (Fig. 1.6b). The most common cause of this pattern (Cleland, 1970) is the participation of an activator which must bind to the enzyme prior to the first substrate, cannot dissociate after substrate binding and remains bound during subsequent catalytic cycles (Scheme 3b, Fig. 1.5). This pattern may also arise under certain circumstances in a rapid equilibrium random mechanism (Scheme 4, Fig. 1.5) if there is a marked synergism of substrate binding i.e. $K_{ia} >> K_a$ and $K_{ib} >> K_b$ (J.F. Morrison, personal communication). If the concentration of A is varied in the region of K_{ia} and that of B in the region of K_b, there is little tendency for B to combine with free enzyme since $K_{ib} >> K_b$. The reaction flux therefore goes through the equilibrium ordered pathway :

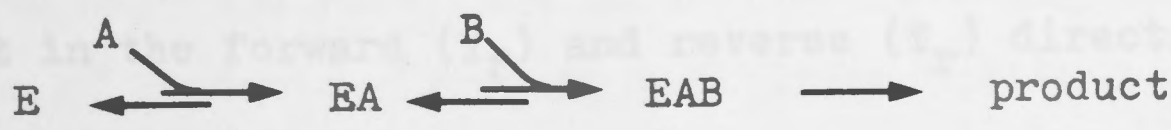

where A is the first substrate bound. Similarly, by manipulating the substrate concentrations, the reaction flux could be forced through the pathway :

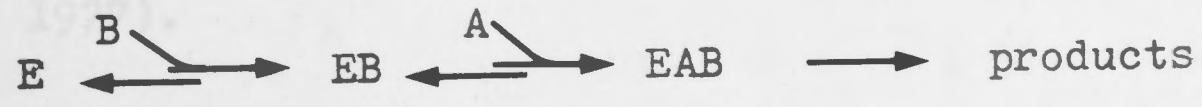

and the reaction becomes equilibrium ordered with B as the first substrate bound. Caution should therefore be exercised in assigning an equilibrium ordered mechanism on the basis of initial velocity experiments carried out over a single range of substrate concentrations.

Although initial velocity studies generally yield only qualitative information about a reaction (except for the values of the kinetic parameters), it is often worthwhile to consider theoretical aspects of a proposed mechanism, since corroborative information may be obtained or a proposed mechanism may be ruled out on the basis of initial velocity experiments. For example, if the intersection point of double reciprocal plots with each other lies on the horizontal axis in both forward and reverse directions, the reaction mechanism cannot be ordered (J.F. Morrison, personal communication). (For the ordered mechanism (Scheme 1, Fig. 1.5) the assumption that the vertical coordinate of the crossover point is zero in both directions leads to the impossible situation $k_4 = -k_5$.) For the Theorell-Chance mechanism (Scheme 2, Fig. 1.5) the vertical coordinates of the crossover point in the forward (Y_f) and reverse (Y_r) directions are :

$$Y_f = (1/k_5 - 1/k_2)/E_t \qquad (1.7)$$

$$Y_r = (1/k_2 - 1/k_5)/E_t \qquad (1.8)$$

Therefore the sum of the vertical coordinates in the forward and reverse directions must be zero for a Theorell-Chance mechanism (Cleland, 1977).

1.1.3 PRODUCT INHIBITION

The products of a reaction in one direction are substrates in the reverse direction, and therefore can be expected to form complexes with enzymes, thereby decreasing the effective concentration of enzyme and causing inhibition. A product inhibition pattern is determined by inspection of double reciprocal plots of initial velocity data obtained at varying concentrations of one substrate and different fixed levels of a product, keeping all other substrate concentrations fixed, usually at an unsaturating level. A pattern should be obtained for each product with respect to each substrate. As mentioned in Section 1.1.1, inhibition may be competitive, uncompetitive or noncompetitive depending on whether there is an increase in the slopes, vertical intercepts or both, respectively, of double reciprocal plots. While it is often true that slopes and intercepts are linear functions of product concentration, hyperbolic or more complex functions can be encountered if the product is involved in alternative reaction sequences (Cleland, 1963b). The usefulness of product inhibition experiments is in discriminating between mechanisms which have the same form of initial velocity equation in the absence of products. Product inhibition patterns can be predicted for any mechanism by the use of Cleland's (1963c) rules

for determining slope and intercept effects or from the complete rate equation (by eliminating terms in all products which are not added during a particular experiment). Use of the rules is simpler in the first instance, since this avoids the derivation of numerous complete rate equations which is a time-consuming task, especially for more complex mechanisms. When sufficient data have been accumulated to postulate a complete mechanism, the full rate equation will, however, be required in order to perform a critical quantitative assessment. The following examples indicate how product inhibition is used to discriminate between possible mechanisms.

Suppose that for an enzyme with two substrates (S_1 and S_2) and two products (P_1 and P_2), an intersecting initial velocity pattern has been obtained. One would then determine the product inhibition patterns for the hypothetical enzyme and compare them with those expected for the various sequential Bi Bi mechanisms (Table 1.1). If our supposed enzyme gave the patterns : P_1 competitive with respect to S_1 and noncompetitive with respect to S_2, and P_2 noncompetitive with respect to both substrates, this would be consistent with an ordered mechanism. The Theorell-Chance mechanism and a rapid equilibrium random mechanism with two dead end complexes (to be discussed later) do have the same product inhibition patterns, but can be distinguished by substrate analogue inhibition studies which will be discussed in the next section.

Suppose that parallel initial velocity patterns were

TABLE 1.1 Product inhibition patterns for sequential Bi Bi mechanisms.

Mechanism	Product	Varied substrate*	
		A	B
Ordered	P	NC**	NC
	Q	C	NC
Theorell-Chance	P	NC	C
	Q	C	NC
Rapid equilibrium random + dead end EAP complex	P	NC	C
	Q	C	C
Rapid equilibrium random + dead end EAP and EBQ complexes	P	NC	C
	Q	C	NC

* Patterns predicted on the assumption that the fixed substrate is not at a saturating level.

** Abbreviations used are :

C : competitive

UC : uncompetitive

NC : noncompetitive

obtained for this hypothetical enzyme. As mentioned in the previous section, a ping pong mechanism will definitely give the parallel pattern, but parallel patterns do not necessarily prove a ping pong mechanism. An irreversible Theorell-Chance mechanism would be distinguished from a ping pong mechanism by the fact that the former yields two uncompetitive product inhibition patterns, while the latter yields two noncompetitive patterns (Table 1.2). Once again, however, the irreversible Theorell-Chance mechanism would not be distinguished from a rapid equilibrium random mechanism with two dead end complexes and $K_{ia} \ll K_a$, since both mechanisms would have the same initial velocity and product inhibition patterns.

Products may form dead end complexes, especially in random mechanisms (Cleland, 1970), by binding on the substrate addition side of a reaction. For example, in a group transfer reaction, the substrate and the product missing the transferred group may be able to bind to the enzyme simultaneously, the product occupying the site for the second substrate. Since reaction may not take place until the product dissociates and the second substrate binds, the enzyme-substrate-product complex is dead end. The formation of dead end complexes does place some limitation on the usefulness of product inhibition studies, but these can be used in conjunction with other techniques for the elucidation of the kinetic mechanism.

TABLE 1.2 Product inhibition patterns for Bi-Bi mechanisms with parallel initial velocity patterns.

Mechanism	Product	Varied substrate*	
		A	B
Ping pong	P	NC**	C
	Q	C	NC
Irreversible Theorell-Chance	P	UC	C
	Q	C	UC
Rapid equilibrium random + dead end EAP and EBQ complexes. Kia ≪ Ka	P	UC	C
	Q	C	UC
Ordered. Kia ≪ Ka	P	NC***	NC
	Q	C	NC***

* Patterns predicted on the assumption that the fixed substrate is not at a saturating level.

** Abbreviations used are :

C : competitive

UC : uncompetitive

NC : noncompetitive

*** These patterns may be uncompetitive.

1.1.4 DEAD END INHIBITION

Dead end inhibitors are molecules which do not play a part in the normal reaction sequence but which can associate reversibly with the enzyme at substrate and product binding sites, thereby inhibiting reactions by tying up enzyme in nonproductive complexes. Dead end inhibition experiments are carried out in the same manner as described above (Section 1.1.3) for product inhibition. The experimentally determined patterns are then compared with predicted patterns for all plausible mechanisms. Once again, one may predict the patterns by the use of Cleland's (1963c) rules for dead end inhibition, or by deriving for each possible mechanism an initial rate equation which takes into account the inhibitor binding step.

Dead end inhibition experiments can provide corroborative evidence for a mechanism proposed on the basis of product inhibition, but are certainly useful in discriminating between those mechanisms which have the same initial velocity and product inhibition patterns. It will have been noted in the previous section, for example, that a reversible Bi Bi Theorell-Chance mechanism is indistinguishable on the basis of product inhibition from a rapid equilibrium random mechanism with **EAP** and **EBQ** dead end complexes. In the random mechanism, an analogue of either substrate will be competitive with its like substrate and non-competitive with respect to the unlike substrate. The Theorell-Chance mechanism is different in that only an analogue of the first substrate to bind to the enzyme could give this pattern. An analogue of the second substrate will be competitive with that

substrate but uncompetitive with respect to the first substrate in the binding sequence, thereby establishing a means of distinguishing between the two mechanisms.

1.1.5 SUBSTRATE INHIBITION

Some substrates when present at high concentrations associate with the enzyme at sites other than their normal binding sites, resulting in a piling up of nonproductive complexes and therefore inhibiting the reaction. Double reciprocal plots obtained while varying such an inhibitory substrate will show upward curvature near the vertical axis. Substrate inhibition is more likely to occur in the nonphysiological direction of reaction since there would have been little evolutionary pressure to eliminate characteristics unfavourable in the reverse direction.

Substrate inhibition experiments are carried out by varying a noninhibitory substrate at different fixed levels of the inhibitory substrate, spanning a range of concentrations below and in the inhibition region. The inhibition is called competitive, uncompetitive or noncompetitive depending on whether there is an increase in the slopes of double reciprocal plots, the intercepts, or both, respectively, and the type can be predicted for any postulated mechanism by the use of Cleland's (1963c) rules for predicting dead end inhibition patterns, as long as the varied substrate is the noninhibitory one (Cleland, 1970).

While experimentally obtained substrate inhibition

patterns may be consistent with a mechanism postulated on the basis of other data, one should be cautious in arriving at mechanistic conclusions from substrate inhibition data. Competitive and uncompetitive substrate inhibition have been said to be characteristic of ping pong and ordered mechanisms, respectively (Cleland, 1970), and this may be so for Bi Bi mechanisms. For example, in a ping pong Bi Bi mechanism, if the stable enzyme forms, E and F, are not entirely specific for their sustrates, at high substrate concentrations B may bind to E and/or A may bind to F. This would certainly result in competitive substrate inhibition. In an ordered mechanism, EA and EQ may be structurally similar (e.g. E-NAD and E-NADH), so that it is possible that at high levels, B binds to EQ resulting in uncompetitive substrate inhibition by B. If B could bind to free enzyme, however, blocking the addition of A, competitive inhibition would result. The following example shows how all three types of substrate inhibition can occur in the one mechanism. Consider an ordered Ter Bi mechanism :

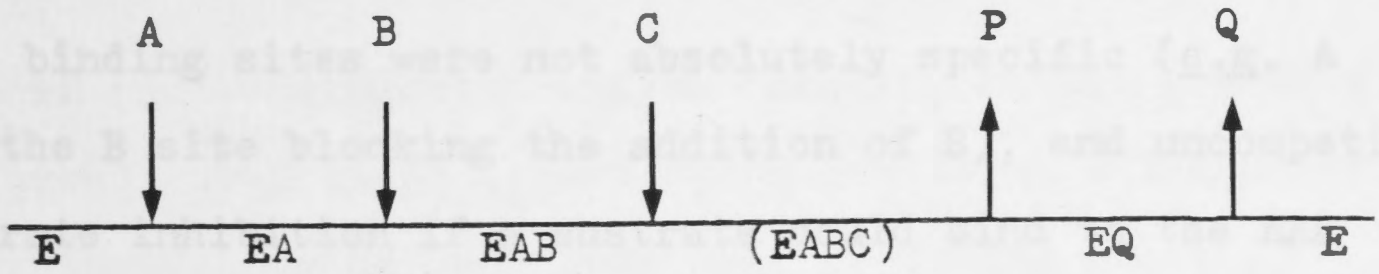

If B or C can bind to EQ forming EBQ or ECQ dead end complexes, uncompetitive inhibition with respect to A (and C or B, respectively) will result, since the second binding of the substrate occurs on the release side of reaction and, in the absence of added products, there is no reversible connection between the addition of the variable substrate and the inhibitory substrate.

If, in addition, either B or C can also bind to free enzyme forming EB or EC dead end complexes and blocking the addition of A, one would observe competitive inhibition with respect to A and noncompetitive inhibition with respect to the other substrate (i.e. C noncompetitive with respect to B or B noncompetitive with respect to C). In a truly rapid equilibrium random mechanism, one does not see substrate inhibition arising from substrate addition on the release side of reaction. This can easily be seen by considering a rapid equilibrium random Bi Bi mechanism, for which the initial velocity equation in the absence of added products is :

$$v = \frac{VAB}{K_{ia}K_b + K_bA + K_aB + AB} \qquad (1.9)$$

The addition of the formation of EBQ or EAP on the release side (or, for that matter, on the addition side) adds only a term in BQ or AP to the denominator, so that the formation of such a dead end complex would be seen only in the presence of added product. One would, however, see competitive substrate inhibition if the substrate binding sites were not absolutely specific (e.g. A binds at the B site blocking the addition of B), and uncompetitive substrate inhibition if a sustrate could bind to the EAB central complex.

1.1.6 ALTERNATIVE SUBSTRATE STUDIES

Many enzymes are not entirely specific for their substrates and will accept a substitute for the usual substrate. A molecule which will react in place of the usual substrate is call-

ed an alternative substrate, and can be used to obtain two kinds of information about an enzyme catalysed reaction.

In the first place, by testing substrate analogues for reactivity one may learn about the structure of the usual substrate during catalysis, since the alternative substrate must be able to assume the correct geometry and allow the required conformational changes in the protein for catalysis to proceed. (It should be pointed out that substrate analogues which are not reactive but act as competitive inhibitors with respect to the like substrate may yield information about groups on the substrate which are involved in binding to the enzyme.)

Another use of alternative substrates is in discrimination between ordered and random mechanisms, a technique pioneered by Fromm and his colleagues (Fromm, 1964; Zewe et al., 1964; Rudolph and Fromm, 1970. Some errors made by those authors were corrected by Darvey,1976.)

If one considers an enzyme reacting in the presence of both its usual substrates, S_1 and S_2, and also an alternative, S_1^*, of S_1, the following reactions will be taking place :

$$S_1 + S_2 \longrightarrow \text{products}$$

$$S_1^* + S_2 \longrightarrow \text{products}$$

One may measure the velocity of reaction by depletion of S_1 (v) or depletion of S_2 (v_t, which is the total velocity for S_1 and S_1^*). Alternatively, one may measure v and v_t in terms of the

formation of an appropriate product. The experiments are performed in the same manner as inhibition experiments : one measures the initial velocity (v or v_t) at various concentrations of one substrate and different fixed levels of the alternative substrate (including zero), while keeping the second substrate at a fixed concentration. The experimental data are then tested against the patterns predicted for the ordered and random mechanisms, which are listed in Table 1.3. Schemes for the various reaction mechanisms under consideration are presented in Fig. 1.8.

It will be seen from Table 1.3 that an ordered mechanism can be distinguished from a rapid equilibrium random mechanism on the basis of v or v_t measurements, but only if the alternative substrate is an analogue of the first bound substrate in the ordered mechanism. For the random mechanism, plots of 1/v against 1/A, 1/B and A^* are linear, and A^* acts as a competitive inhibitor with respect to A and a noncompetitive inhibitor with respect to B. In contrast, for the ordered mechanism, plots of 1/v against 1/B in the presence of A^* are two/one functions, i.e. nonrectangular hyperbolae (Darvey, 1976). It should be noted, however, that if $K_a^* = K_{ia}^*$, plots of 1/v against 1/B in the presence of A^* will be linear, and one is unable to discriminate between the ordered and the rapid equilibrium random mechanisms.

As indicated in Table 1.3b, measurements of v_t under various conditions will also allow discrimination between mechanisms. Plots of $1/v_t$ against 1/B at different concentrations of A^* will be linear for the random mechanism but two/one functions

TABLE 1.3 (a) Discrimination between random and ordered bisubstrate mechanisms by the use of alternative substrates. Measurements of v, the rate of disappearance of the usual substrate.

Mechanism	Usual and alternative substrates	Fixed substrate(s)	1/v plotted against	Form of plot	Remarks
Ordered	A, A^*	B A A & B	1/A 1/B A^*	linear two/one (1) linear	A^* is a linear competitive inhibitor with respect to A.
Rapid Equilibrium Random	A, A^* (2)	B A A & B	1/A 1/B A^*	linear " "	A^* is a linear competitive and a linear noncompetitive inhibitor with respect to A and B, respectively.
Ordered	B, B^*	B A A & B	1/A 1/B A^*	linear " "	B^* is a linear competitive and a linear noncompetitive inhibitor with respect to B and A, respectively.

Notes : (1) nonrectangular hyperbola (for non-zero concentrations of A^*). Becomes linear when $K_a^* = K_{ia}^*$ (see text).

(2) A and B are interchangeable in this mechanism.

TABLE 1.3 (b) Discrimination between random and ordered bisubstrate mechanisms by the use of alternative substrates. Measurement of v_t, the total velocity of reaction.

Mechanism	Usual and alternative substrates	Fixed substrate(s)	$1/v_t$ plotted against	Form of plot	Remarks
Ordered	A,A^*	B A	1/A 1/B	two/one (1) "	$1/v_t$ against 1/B becomes linear only if $K_a^* = K_{ia}^*$ AND $K_{ia}K_b = K_aK_b^*$.
Rapid Equilibrium Random	A,A^* (2)	B A A & B	1/A 1/B $1/A^*$	two/one (1) linear two/one (1)	A^* is a slope 2/1, intercept 2/1 noncompetitive inhibitor with respect to B.
Ordered	B,B^*	B A A & B	1/A 1/B $1/B^*$	linear two/one (1) "	B^* is a slope 2/1, intercept 2/1 noncompetitive inhibitor with respect to A.

Notes : (1) nonrectangular hyperbola for all non-zero concentrations of A^* (or B^*).

(2) A and B are interchangeable in this mechanism.

FIGURE 1.8 Schemes for the bisubstrate mechanisms considered in Table 1.3 - reactions taking place in the presence of an alternative substrate.

(a) Ordered - A^* is an alternative of A.

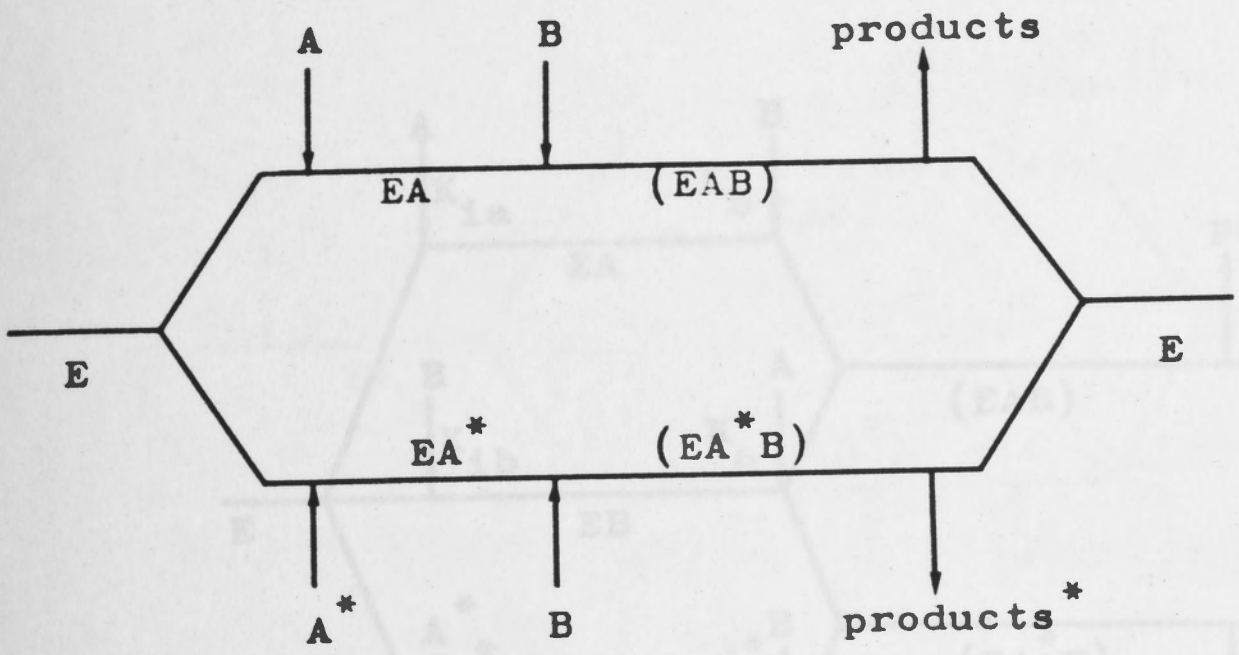

$$v = \frac{-dA}{dt} = \frac{VAB}{(X)}\left(1 + \frac{K_a^* B}{K_{ia}^* K_b^*}\right)$$

$$v_t = \frac{-dB}{dt} = \frac{VAB}{(X)}\left(1 + \frac{K_a^* B}{K_{ia}^* K_b^*}\right) + \frac{V^* A^* B K_{ia} K_b}{(X) K_{ia}^* K_b^*}\left(1 + \frac{K_a B}{K_{ia} K_b}\right)$$

$$(X) = \left(1 + \frac{K_a^* B}{K_{ia}^* K_b^*}\right)\left(K_{ia} K_b + K_b A + K_a B + AB\right)$$

$$+ \left(1 + \frac{K_a B}{K_{ia} K_b}\right)\left(1 + \frac{B}{K_b^*}\right)\left(\frac{K_{ia} K_b A^*}{K_{ia}^*}\right)$$

V, K_a, K_b and K_{ia} are kinetic constants defined according to Cleland (1963 a) for the reaction -

$$A + B \longrightarrow \text{products}$$

V^*, K_a^*, K_b^* and K_{ia}^* are kinetic constants defined for the reaction -

$$A^* + B \longrightarrow \text{products}$$

FIGURE 1.8(Continued) Schemes for the bisubstrate mechanisms considered in Table 1.3 - reactions taking place in the presence of an alternative substrate.

(b) Rapid Equilibrium Random - A^* is an alternative of A.

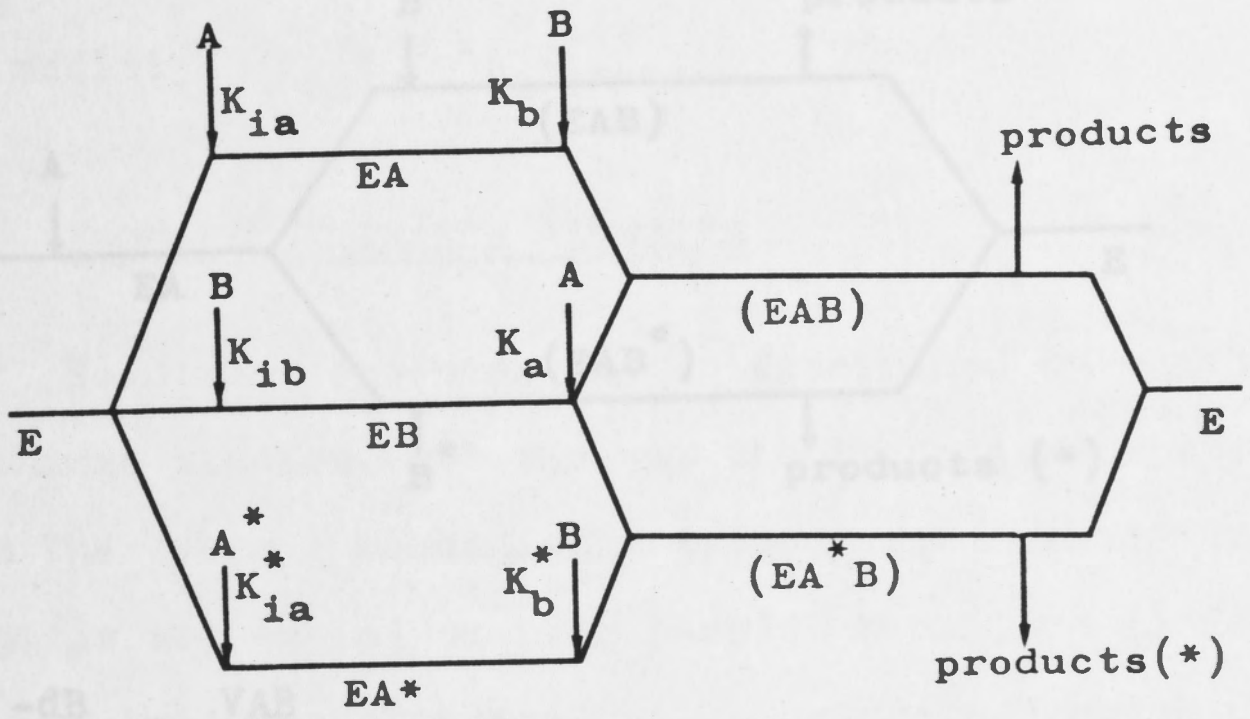

$$v = \frac{-dA}{dt} = \frac{VAB}{(X)}$$

$$v_t = \frac{-dB}{dt} = \frac{VAB}{(X)}\left(1 + \frac{K_a A^*}{K^*_a A}\right)$$

$$(X) = K_{ia}K_b + K_b A + K_a B + AB + \frac{K_a A^*}{K^*_a}(K^*_b + B)$$

V and V^* are the maximum velocities for the reactions $A + B \longrightarrow$ products, and $A^* + B \longrightarrow$ products, respectively.

Other kinetic constants are the dissociation constants indicated in the scheme above.

FIGURE 1.8(Continued) Schemes for the bisubstrate mechanisms considered in Table 1.3 - reactions taking place in the presence of an alternative substrate.

(c) Ordered - B^* is an alternative of B.

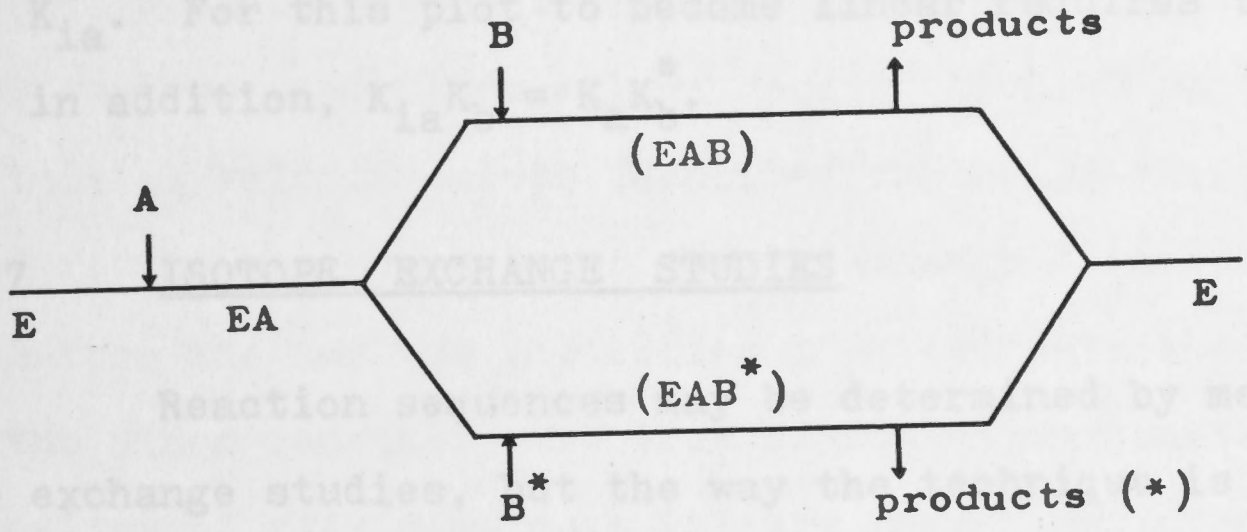

$$v = \frac{-dB}{dt} = \frac{VAB}{(X)}$$

$$v_t = \frac{-dA}{dt} = \frac{VAB}{(X)}\left(1 + \frac{V^* B^* K_b}{V B K_b^*}\right)$$

$$(X) = K_{ia}K_b + K_bA + K_aB + AB + \frac{K_a^* K_b B^*}{K_a K_b^*}(K_a + A)$$

V, K_a, K_b and K_{ia} are kinetic constants defined according to Cleland (1963 a) for the reaction A + B $\longrightarrow$ products, while V^*, K_a^* and K_b^* are the kinetic constants defined for the reaction A + B^* $\longrightarrow$ products.

for the ordered mechanism. It should be noted that the v_t plot is less likely than v plots to fail to discriminate between the mechanisms, since $1/v_t$ against 1/B will be nonlinear even if $K_a^* = K_{ia}^*$. For this plot to become linear requires that $K_a^* = K_{ia}^*$ and, in addition, $K_{ia}K_b = K_aK_b^*$.

1.1.7 ISOTOPE EXCHANGE STUDIES

Reaction sequences may be determined by means of isotope exchange studies, but the way the technique is applied depends on the overall mechanistic type (i.e. whether the reaction mechanism is sequential or ping pong). Equations to describe the velocity of isotopic exchange can be determined using Cleland's (1967) adaptation of the method of King and Altman (1956).

Ping Pong Mechanisms

In ping pong mechanisms the overall reaction sequence is composed of partial reactions, and isotopic exchange between the components of each partial reaction should be demonstrable in the absence of any other substrates or products. For example, in the Bi Bi ping pong mechanism (Scheme 1.10) an A-P exchange will

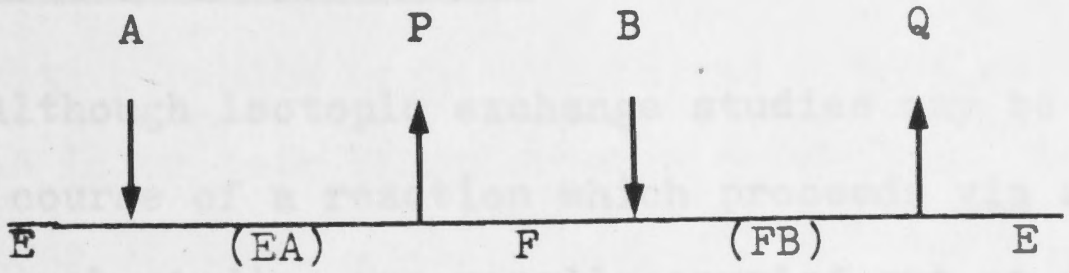

(1.10)

occur in the absence of added B or Q, and similarly the B-Q exchange should be detected in the absence of added A or P. Because only partial reactions are considered, the system under

investigation will always be at thermodynamic equilibrium once the steady state has been reached, and reactants can be varied individually at fixed levels of others. Determination of the velocity of exchange of isotope from one reactant to another under various conditions allows construction of plots similar to the initial velocity plots described in the previous sections. However, the maximum velocities of exchange differ in interpretation from the maximum velocities of steady state experiments, and the other constants are true dissociation constants and not composites of rate constants (as are many kinetic constants).

The usefulness of isotopic exchange studies for the detection of ordered or random addition in partial reactions involving more than one substrate (e.g. the E ⟶ F portion of Scheme 1.11) was demonstrated by Cedar and Schwartz (1969).

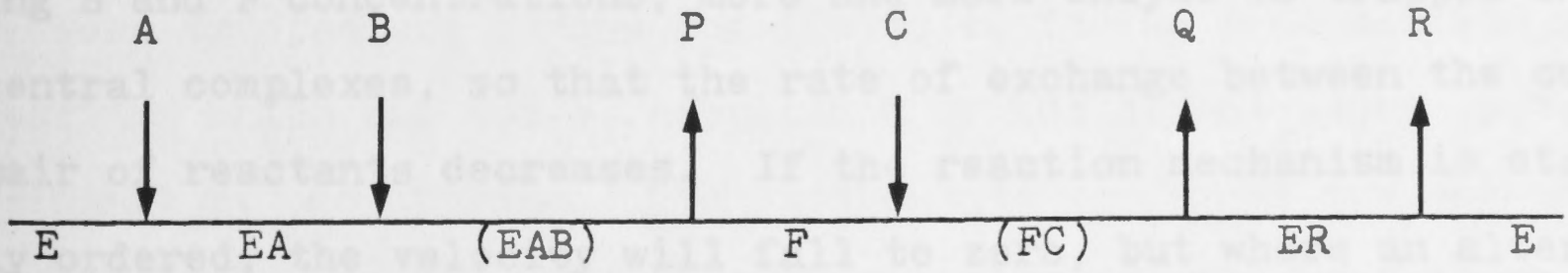

(1.11)

Sequential Mechanisms

Although isotopic exchange studies may be undertaken during the course of a reaction which proceeds via a sequential mechanism, such studies are usually carried out at chemical equilibrium. This means that a substrate and a product must be increased in a constant ratio, otherwise equilibrium is perturbed. As an example of the use of the technique, the ordered and random

Bi Bi mechanisms will be considered.

For an ordered Bi Bi mechanism, exchange patterns for the A-Q and B-P pairs of reactants are more diagnostic of the mechanism, although the exchanges between the reactant pairs A-Q, B-P and either of A-P or B-Q (but not both) can conceivably be measured (Cleland, 1970). If one has no idea of the order, then all possible exchanges must be measured.

The velocity of exchange between the inner pair of reactants (B and P) in an ordered mechanism is a hyperbolic function of the concentration of A (and Q, since A and Q are increased in constant ratio). However, the velocity of the A-Q exchange rises and is subsequently inhibited as the concentrations of B and P are increased. This inhibition occurs because at increasing B and P concentrations, more and more enzyme is trapped in central complexes, so that the rate of exchange between the outer pair of reactants decreases. If the reaction mechanism is strictly ordered, the velocity will fall to zero, but where an alternative pathway is available for exchange, the velocity will taper to a non-zero level.

With a random mechanism, A and Q or B and P will always behave as an inner pair of an ordered mechanism. Increasing the concentrations of A and Q will force the B-P exchange through the upper pathway (Scheme 4, Fig. 1.5), while raising the concentrations of B and P forces the A-Q exchange to occur through the lower pathway. Therefore, in both cases the hyperbolic pattern will be observed.

The isotopic exchange technique is particularly useful in determining whether a random mechanism is truly rapid equilibrium. Since the same step (the interconversion of central complexes) limits all exchanges in a rapid equilibrium mechanism, all exchanges must proceed at the same velocity. Failure to comply with this condition indicates that the release of a product must be partially rate limiting.

1.1.8 ISOTOPE PARTITIONING

The technique of isotope partitioning, which was introduced by Rose (Rose *et al.*, 1974), involves the use of radioactively labelled substrate to determine which steps of the reaction sequence may be rate limiting. For bisubstrate reactions it is applicable to the first-bound substrate in an ordered and both substrates in a random mechanism, and can be used to discriminate between ordered and random possibilities for an irreversible reaction which can not be approached by the technique of isotope exchange at equilibrium. The experiments performed are essentially single turnover experiments since all product formed comes from a pre-equilibrated mixture of enzyme and a labelled substrate. One measures the amount of product formed from a known amount of enzyme-labelled substrate complex at different concentrations of the second substrate. (The detailed experimental procedure is described by Rose *et al.*, 1976.) Essentially one is measuring the fraction of complex which reacts to form product rather than dissociating to free enzyme and substrate. If one considers the scheme :

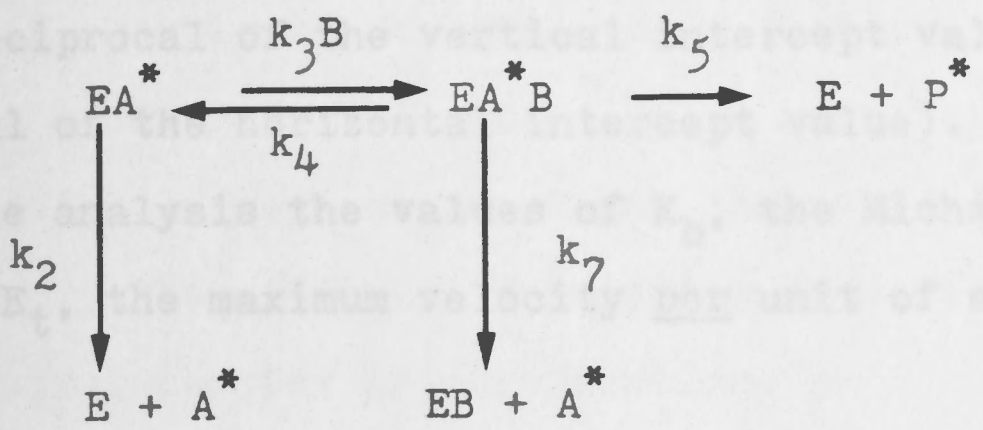

(1.12)

where E, B, A^* and P^* are free enzyme, varied substrate, and labelled substrate and product, respectively. For the following discussion it is assumed that A^* is present at a saturating level in the pre-equilibration mixture, so that the total enzyme concentration, E_t, is equal to the concentration of EA^*. (It may not be possible to set this up experimentally if the dissociation constant for A is high, and one must make allowance for non-saturation in the interpretation of data if this is the case.) The experimental data should conform to the equation :

$$\frac{P^*}{E_t} = \frac{(P^*_{max}/E_t).B}{K^*_b + B}$$

where P^*/E_t = proportion of EA^* which goes to product

P^*_{max}/E_t = maximum proportion of EA^* which can go to product formation (at saturating B concentration)

K^*_b = concentration of B at which half of EA^* goes to product and half dissociates releasing A^*

B = concentration of the varied substrate

(1.13)

The parameters P^*_{max}/E_t and K^*_b are determined from the double reciprocal plot of the experimental data (P^*_{max}/E_t being the

reciprocal of the vertical intercept value, and $-K_b^*$ the reciprocal of the horizontal intercept value). One also requires for the analysis the values of K_b, the Michaelis constant for B, and V/E_t, the maximum velocity per unit of enzyme.

It can be shown that :

$$\frac{k_7}{V/E_t} = \frac{E_t}{P^*_{max}} - 1 \qquad (1.14)$$

$$\frac{K_b^*}{K_b} = \frac{k_2(1 + k_7/(k_4 + k_5))}{(V/E_t)(1 + k_7/k_5)} \qquad (1.15)$$

One can therefore calculate the value of k_7 directly from Equation 1.14. If the reaction mechanism is strictly ordered, then k_7 must equal zero, since the binding of B locks A into the ternary complex, and P^*_{max} will be equal to E_t. When this is the case, $k_2/(V/E_t) = K_b^*/K_b$ and k_2 can be calculated. If $k_7 \neq 0$, then it can be shown that $k_2/(V/E_t)$ will be larger than K_b^*/K_b but smaller than $(K_b^*/K_b)(E_t/P^*_{max})$ and at least the upper and lower limits can be determined for the value of k_2 relative to V/E_t, even if the value can not be calculated. When the technique is applied to the reverse reaction (if this is possible), one can determine the rates of all reactant release steps relative to a fixed standard (V_1/E_t or V_2/E_t where V_1 and V_2 are the maximum velocities in the forward and reverse directions, respectively).

It should be noted that if a random mechanism were truly rapid equilibrium, no formation of P^* would be detected

(J.F. Morrison, personal communication), since by definition of the mechanism, all steps are so much faster than the interconversion of central complexes that this is the sole rate limiting step. Therefore all substrates must dissociate faster than the central complex interconversion.

1.1.9 ISOTOPE EFFECTS

Enzymic catalysis involves the breakage and formation of certain bonds and changes in the hybridisation of others. Since isotopic substitution can influence the energetics of the reaction, the study of isotope effects can yield information about the transition states and rate limiting steps in the reaction sequence. Isotope effects can be of two types : primary or secondary.

A primary isotope effect occurs when the isotopically substituted atom is involved in a bond which is broken during the reaction. These effects will be considered below in more detail. Secondary isotope effects are smaller than primary effects, and are associated with isotopic substitution of an atom not actually involved in a bond which is made or broken during reaction. Such effects will be seen if, in the transition state of the rate limiting step, a bond to the substituted atom differs in energy from the ground state (Rose, 1970), and therefore secondary isotope effects can provide clues about the nature of the transition state. Richards (1970) has briefly discussed secondary isotope effects on the reactions catalysed by fumarase and lysozyme.

Secondary effects will not be considered further in this discussion.

It is well known that substitution of deuterium or tritium for a hydrogen atom in a bond which is broken during a reaction will result in reduction of the rate of bond breakage. However, the full effect is not normally seen in steady state enzyme kinetic studies because the bond-breaking step is not isolated in the kinetic parameters from other steps such as substrate binding, product release and conformational changes in the reactants and enzyme. In spite of this complication, it is possible under certain circumstances to determine the true isotope effect on the bond-breaking step with a method developed by Northrop (1975). Using the relationship established for chemical reactions between the deuterium and tritium effects on a bond-breaking step :

$$k_H/k_T = (k_H/k_D)^{1.44} = a^{1.44}$$

where k_H/k_T and k_H/k_D are the tritium and deuterium effects, respectively, on the bond-breaking step. (1.16)

Northrop has shown that the true deuterium effect, a, is related to the deuterium and tritium effects expressed in V/K by the expression :

$$\frac{(V/K)_H/(V/K)_D - 1}{(V/K)_H/(V/K)_T - 1} = \frac{a - 1}{a^{1.44} - 1}$$

where $(V/K)_H/(V/K)_D$ and $(V/K)_H/(V/K)_T$ are the measured deuterium and tritium effects on V/K. (1.17)

Since there is only one unknown in the relationship, the deuterium effect on the bond breaking step can be determined. (It should be noted that the methods for determining deuterium and tritium effects differ because tritium can be used only as a trace label (see Schimerlik *et al.*, 1975)). Having calculated the true isotope effect, one may then consider how the extent to which it is expressed in the kinetic parameters can be used to deduce the rate limiting steps.

Consider the ordered Bi Ter reaction (Scheme 1.18), where the bond breaking step is represented by EAB $\rightleftharpoons$ EPQR with forward and reverse rate constants k_5 and k_6, respectively.

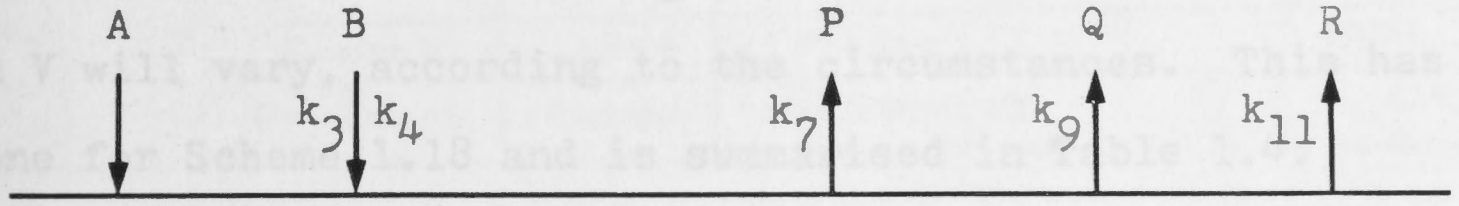

$$E \quad EA \quad EAB \underset{k_6}{\overset{k_5}{\rightleftharpoons}} EPQR \quad EQR \quad ER \quad E \qquad (1.18)$$

The expressions for the V/K and V isotope effects can be shown to be :

$$\frac{(V/K)_H}{(V/K)_D} = \frac{a + k_5/k_4 + k_6/k_7}{1 + k_5/k_4 + k_6/k_7} \qquad (1.19)$$

$$\frac{(V)_H}{(V)_D} = \frac{a + k_6/k_7 + k_5/k_7 + k_5/k_9 + k_5/k_{11}}{1 + k_6/k_7 + k_5/k_7 + k_5/k_9 + k_5/k_{11}} \qquad (1.20)$$

where a is the absolute isotope effect on the bond breaking step, and $(V/K)_H/(V/K)_D$ and $(V)_H/(V)_D$ are the isotope effects on the

V/K ratio and the maximum velocity, respectively. Whenever the commitment of both central complexes to catalysis is low (B and P dissociate rapidly), the isotope effect on the V/K ratio will be relatively large. If either B or P (or both) dissociate relatively slowly, the isotope effect on V/K will be small. The expression for the isotope effect on the maximum velocity does not take into account the commitment of EAB to catalysis, but depends on the commitment of EPQR and also the rate of catalysis in the forward direction relative to the rates of release of the products, and therefore the effects on V/K and V may well differ. The simplest way to approach the interpretation of the possible isotope effects is to consider the circumstances in which the V/K effect will be small or large, and then to consider how the effect on V will vary, according to the circumstances. This has been done for Scheme 1.18 and is summarised in Table 1.4.

Although some enzymes may show good isotope effects on V/K and V, others may not, and for these latter enzymes, the determination of the absolute isotope effect on the bond breaking step can be difficult. The method of equilibrium perturbation by isotopic substitution can be of use in these cases. The method relies on the fact that if a reaction mixture is made up at equilibrium concentrations using the normal product, but a substrate deuterated at a position which undergoes cleavage, then the addition of enzyme will perturb equilibrium in the direction of the deuterated substrate. This occurs because the rate of cleavage of the hydrogen-containing bond is faster than the rate for a corresponding deuterated bond. Equilibrium is re-established when isotopic equilibrium between the substrate and product has

TABLE 1.4 Interpretation of V/K and V isotope effect for the ordered Bi Ter mechanism (Scheme 1.18)

V/K effect	C_f *	C_r **	Rate limiting step	V effect
LARGE	small	small	catalysis	LARGE
			product release	SMALL
SMALL	large	small	catalysis	LARGE
			product release	SMALL
	small	large	immaterial	SMALL
	large	large	immaterial	SMALL

* C_f : commitment of EAB to catalysis

$$= \frac{k_5 \text{ (rate of EAB} \longrightarrow \text{EPQR)}}{k_4 \text{ (rate of EAB} \longrightarrow \text{EA + B)}}$$

** C_r : commitment of EPQR to catalysis

$$= \frac{k_6 \text{ (rate of EPQR} \longrightarrow \text{EAB)}}{k_7 \text{ (rate of EPQR} \longrightarrow \text{EQR + P)}}$$

been attained. Schimerlik *et al*. (1975) have discussed the theory behind the method, including the effect of a change in equilibrium constant on isotopic substitution.

The preceding discussion has centred on the effects of isotopic substitution on the parameters V/K and V in sequential mechanisms. Bardsley and Waight (1976) have considered how isotopic substitution will affect the initial velocity under various conditions of substrate and product concentrations for some simple mechanisms, but the interpretation of the effects seems far more complex than that of the effects on defined kinetic parameters. Finally, it should be pointed out that the approaches discussed (including that of Bardsley and Waight (1976)) depend on the assumption that only the bond-breaking step is affected by isotopic substitution, an assumption that may well be unjustified.

1.1.10 pH EFFECTS

The early recognition of the influence of hydrogen ion concentration on enzymic activity led to the introduction by Sorensen (1909) of the concept of pH. The later suggestion by Haldane (1930) that it is the charge distribution of certain functional groups on the enzyme which is responsible for variations in the rates of enzymic reactions with varying pH led to the idea that these functional groups might be identified from the response of the kinetic parameters to pH changes. While the study of pH effects on enzymic activity is not a new technique, the interpretation of data obtained has often been limited in the past by the oversimplification of the models considered. Doubts about

the usefulness of such studies have been expressed (e.g. Knowles, 1976), but it need not be true that no useful information about an enzyme can be obtained, and this may be so even if the identity of a group whose pK is established remains unknown. Cleland (1977) has expounded the theory and analytical geometry of pH profiles. It is the aim of the following discussion to indicate the kind of information which is accessible from an analysis of the effects of variation of pH on enzymic activity by considering the basic theory briefly and then certain specific models.

Ionisation of a dibasic acid

Consider a molecule, E, which possesses two groups, X and Y, which undergo ionisation as follows* :

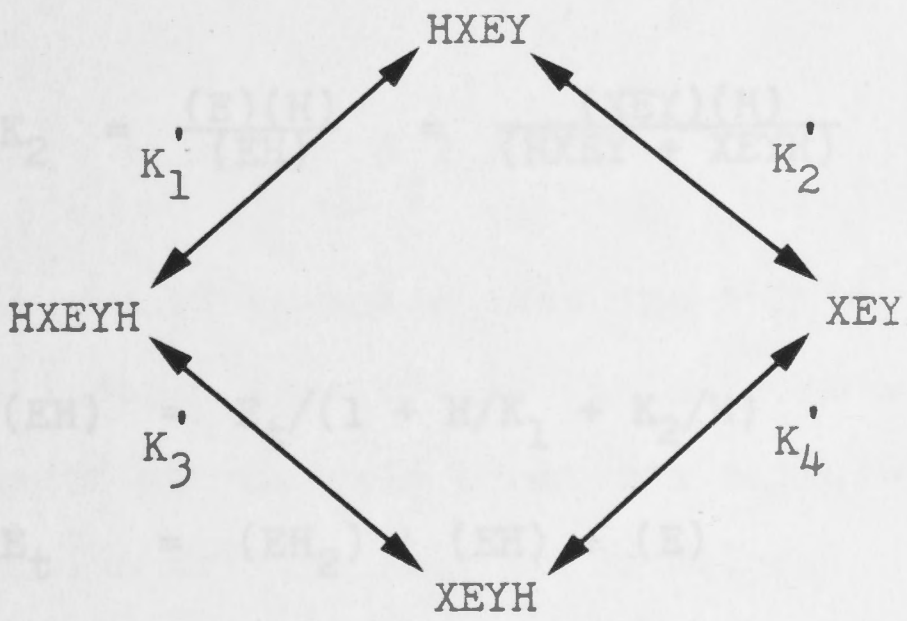

(1.21)

It is easily deduced that the ratio of the two singly protonated species is :

$$\frac{(HXEY)}{(XEYH)} = K_2'/K_4' = K_3'/K_1' \qquad (1.22)$$

where the Ks are the dissociation constants of Scheme 1.21.

---

* Charges and free hydrogen ions are omitted throughout.

It is clear from Equation 1.22 that the ratio of the two singly protonated species is independent of the concentration of hydrogen ions. If the molecule under consideration is an enzyme, it follows that if pH variation affects any kinetic parameter it is not possible to determine whether the variation results from a change in the concentration of HXEY or that of XEYH. Therefore, the two singly protonated species must be considered together, and Scheme 1.21 can be rewritten as :

$$EH_2 \overset{K_1}{\longleftrightarrow} EH \overset{K_2}{\longleftrightarrow} E \qquad (1.23)$$

with :

$$K_1 = \frac{(EH)(H)}{(EH_2)} = \frac{(HXEY + XEYH)(H)}{(HXEYH)} \qquad (1.24)$$

$$K_2 = \frac{(E)(H)}{(EH)} = \frac{(XEY)(H)}{(HXEY + XEYH)} \qquad (1.25)$$

and :

$$(EH) = E_t/(1 + H/K_1 + K_2/H) \qquad (1.26)$$

$$E_t = (EH_2) + (EH) + (E) \qquad (1.27)$$

The relationships of the macroscopic (molecular) dissociation constants, K_1 and K_2, to the microscopic (group) dissociation constants of Scheme 1.21 are given by the expressions :

$$K_1 = K_1' + K_3' \qquad (1.28)$$

$$1/K_2 = 1/K_2' + 1/K_4' \qquad (1.29)$$

It is these macroscopic dissociation constants which may be experimentally accessible when changes in the kinetic parameters of an enzyme-catalysed reaction accompany pH variation and, even supposing that pK_1 and pK_2 are correctly estimated, the values of the microscopic constants remain unknown.

In the event that all the microscopic constants are equal ($K_1' = K_2' = K_3' = K_4'$) it is easily shown that $K_1 = 4K_2$ and $pK_2 - pK_1 = 0.6$ (log 4). If the dissociation constant for group X is unaffected by the state of ionisation of group Y and *vice versa* (*i.e.* $K_1' = K_4'$ and $K_3' = K_2'$) then the microscopic constants are related to the macroscopic constants by the expressions :

$$K_1' = K_4' = \frac{K_1 + \sqrt{(K_1)^2 - 4K_1K_2}}{2} \qquad (1.30)$$

$$K_2' = K_3' = K_1K_2/K_1' \qquad (1.31)$$

However, it should be noted that there is no *a priori* reason to assume the independence of the ionisations at X and Y, and therefore values of microscopic constants calculated on the basis of this assumption are unlikely to be helpful. Consequently it seems more reasonable to deal with the macroscopic (molecular) constants : fewer of them are needed to describe a system, and measurements of microscopic (group) constants, even for less complex molecules than enzymes, are inherently unreliable (Dixon, 1976).

Since enzymes and often their substrates, inhibitors

and activators, contain ionisable groups, in the consideration of variation of kinetic parameters with varying pH, the kind of function described by Equation 1.26 is often encountered, viz. :

$$y = a/(1 + H/K_1 + K_2/H) \qquad (1.32)$$

with :

$$\log y = \log a - \log (1 + H/K_1 + K_2/H) \qquad (1.33)$$

Now :

$$\lim_{H\to\infty} (\log y) = \log a - \log H + \log K_1$$
$$= \log a + pH - pK_1 \qquad (1.34)$$

$$\lim_{H\to 0} (\log y) = \log a - \log K_2 + \log H$$
$$= \log a + pK_2 - pH \qquad (1.35)$$

Therefore, a plot of log y against pH (Fig. 1.9) will have straight line asymptotes of slope +1 at low pH, and of slope -1 at high pH, and the point of intersection of these asymptotes will be at pH = $(pK_1 + pK_2)/2$. If the pKs are well separated, there will be an intermediate region where both H/K_1 and K_2/H are very much less than one, and the contribution of these terms to the value of log y will be negligible, resulting in a segment of the curve having slope zero between the values of pK_1 and pK_2. The intersection of this zero slope segment with the acid asymptote will be at pH = pK_1 while the intersection with the high pH asymptote will occur at pH = pK_2 (Fig. 1.9) and the pKs can be determined graphically. As the pKs come closer than about three pH units, the intermediate segment of slope zero shortens until

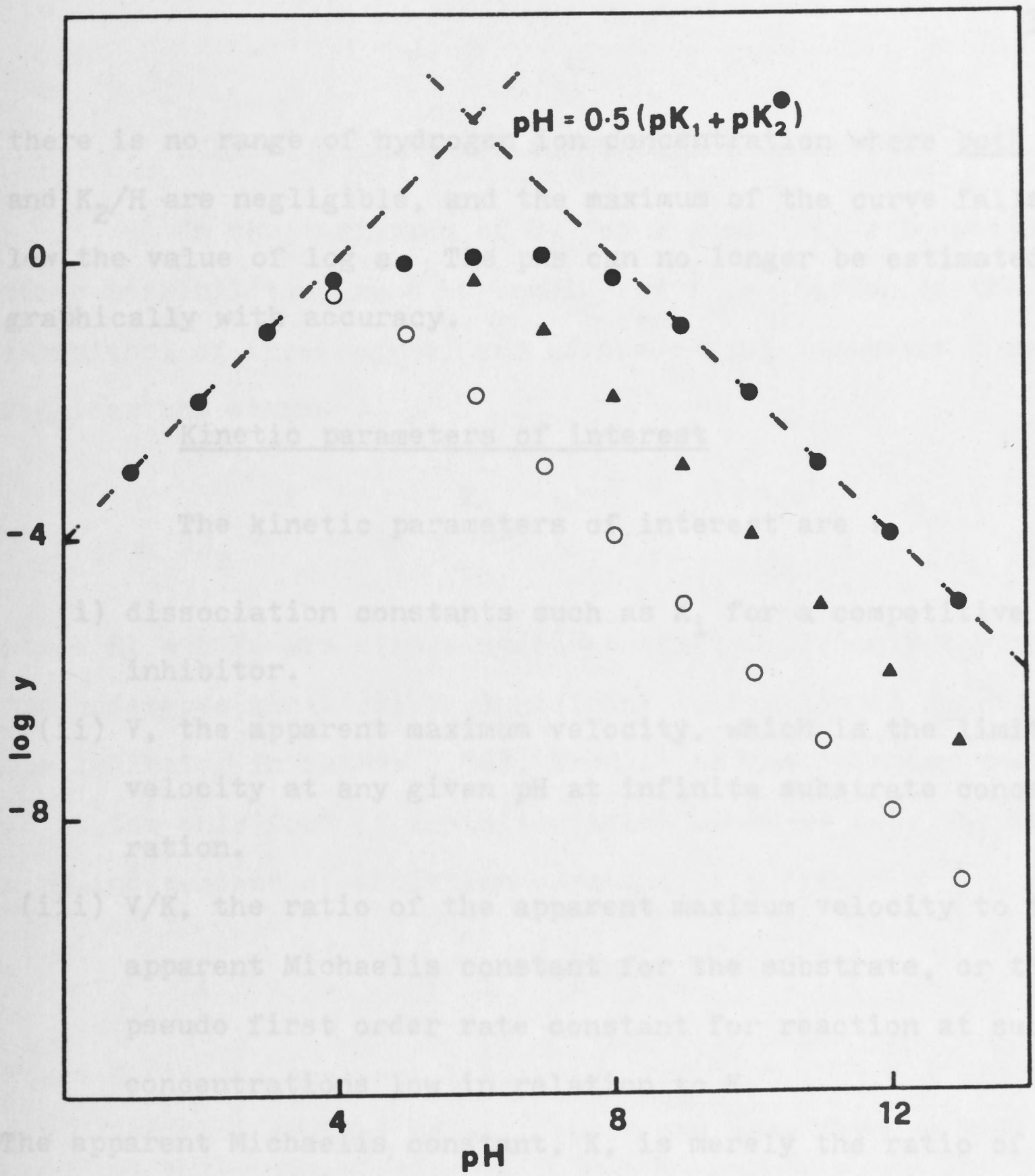

FIGURE 1.9 Plots of log y against pH.

$\log y = \log a - \log (1 + H/K_1 + K_2/H)$

$a = 1$; $pK_1 = 4$; $pK_2 = 4(\circ), 6(\blacktriangle), 8(\bullet)$.

Low (←· –) and high (– ·→) pH asymptotes.

there is no range of hydrogen ion concentration where <u>both</u> H/K_1 and K_2/H are negligible, and the maximum of the curve falls below the value of log a. The pKs can no longer be estimated graphically with accuracy.

Kinetic parameters of interest

The kinetic parameters of interest are :

(i) dissociation constants such as K_i for a competitive inhibitor.

(ii) V, the apparent maximum velocity, which is the limiting velocity at any given pH at infinite substrate concentration.

(iii) V/K, the ratio of the apparent maximum velocity to the apparent Michaelis constant for the substrate, or the pseudo first order rate constant for reaction at substrate concentrations low in relation to K.

The apparent Michaelis constant, K, is merely the ratio of the two fundamental parameters, V and V/K. Moreover, except in the case that the Michaelis constant is independent of pH (as discussed by Cornish-Bowden (1976), it is simpler to consider V/K, since K depends on the state of ionisation of both the free enzyme and the enzyme-substrate complex, and even for relatively simple models, the variation of K with pH is less amenable to interpretation than that of V/K.

Variation of K_i for a competitive inhibitor

In the variation of K_i for a competitive inhibitor, three possibilities must be considered : ionisation of the inhibitor, of free enzyme, and of the enzyme-inhibitor complex. Consider the scheme :

$$XH_2 \overset{K_1}{\longleftrightarrow} XH \overset{K_2}{\longleftrightarrow} X \qquad (1.36)$$

where K_1 and K_2 are dissociation constants. If only the inhibitor undergoes kinetically significant ionisation (X represents the inhibitor in Scheme 1.36), then it is easily shown that if XH is the only form of inhibitor which binds to free enzyme (with a pH-independent dissociation constant of K_i') then :

$$K_i = K_i'(1 + H/K_1 + K_2/H) \qquad (1.37)$$

where K_i is the apparent inhibition constant. A plot of pK_i (= -log K_i) against pH will be of the same form as Fig. 1.9. The plateau region, if it exists, will be at $pK_i = pK_i'$. If it is only free enzyme which undergoes kinetically significant ionisation (X represents the enzyme in Scheme 1.36), and only XH binds inhibitor with a dissociation constant of K_i', then Equation 1.37 again describes K_i, and a plot of pK_i against pH will be of the same form as that described above, but will yield the pKs of free enzyme.

If both free enzyme and the enzyme-inhibitor complex undergo ionisation, with :

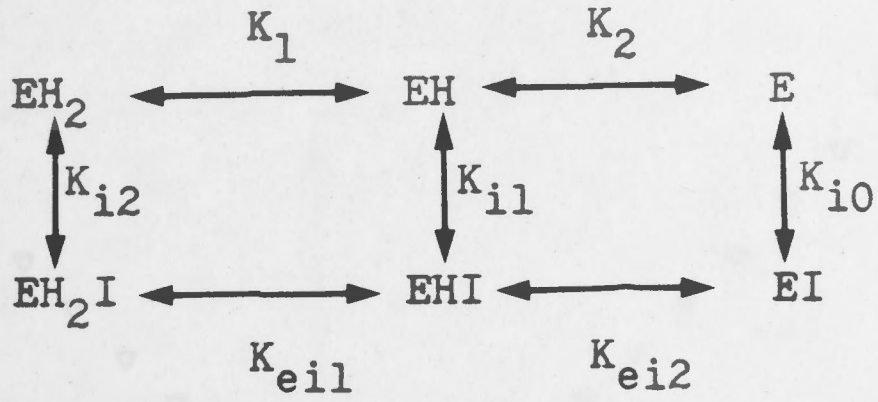

where all the Ks are dissociation constants (1.38)

then :

$$K_i = \frac{K_{i1}(1 + H/K_1 + K_2/H)}{(1 + H/K_{ei1} + K_{ei2}/H)} \qquad (1.39)$$

A plot of pK_i against pH is the difference between two curves of the same form as Fig. 1.9, with the horizontal position of the curve determined by the value of pK_{i1}. The curve has high and low pH asymptotes of slope zero, and undergoes changes of slope of -1 as the pKs of free enzyme are passed, and of +1 as the pKs of the enzyme-inhibitor complex are passed. Fig. 1.10 gives an example of this type of curve.

Variation of V and V/K with pH : Specific Models

(A) All protonations are undisturbed equilibria

Brocklehurst and Dixon (1976) have considered in considerable detail the general model of Scheme 1.40 where only the protonations are regarded as unperturbed equilibria.

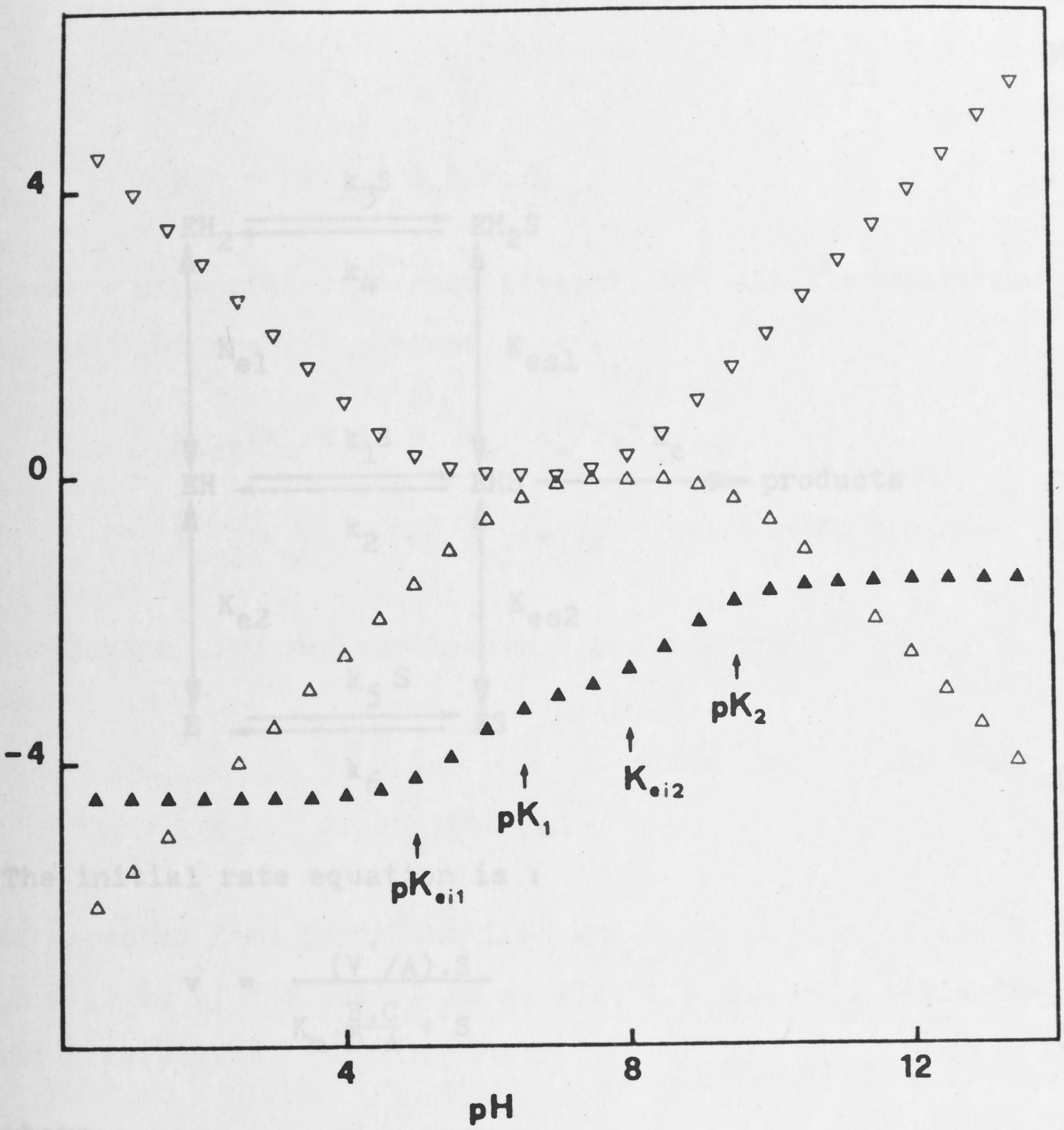

FIGURE 1.10 Plots of pK_i(▲), log $(1 + H/K_{ei1} + K_{ei2}/H)$(▽) and -log $(1 + H/K + K/H)$(△) for Scheme 1.38.

$$pK_i = pK_{i1} + \log (1 + H/K_{ei1} + K_{ei2}/H) - \log (1 + H/K_1 + K_2/H)$$

$pK_{i1} = 3$; $pK_{ei1} = 5$; $pK_1 = 6.5$; $pK_{ei2} = 8$; $pK_2 = 9.5$.

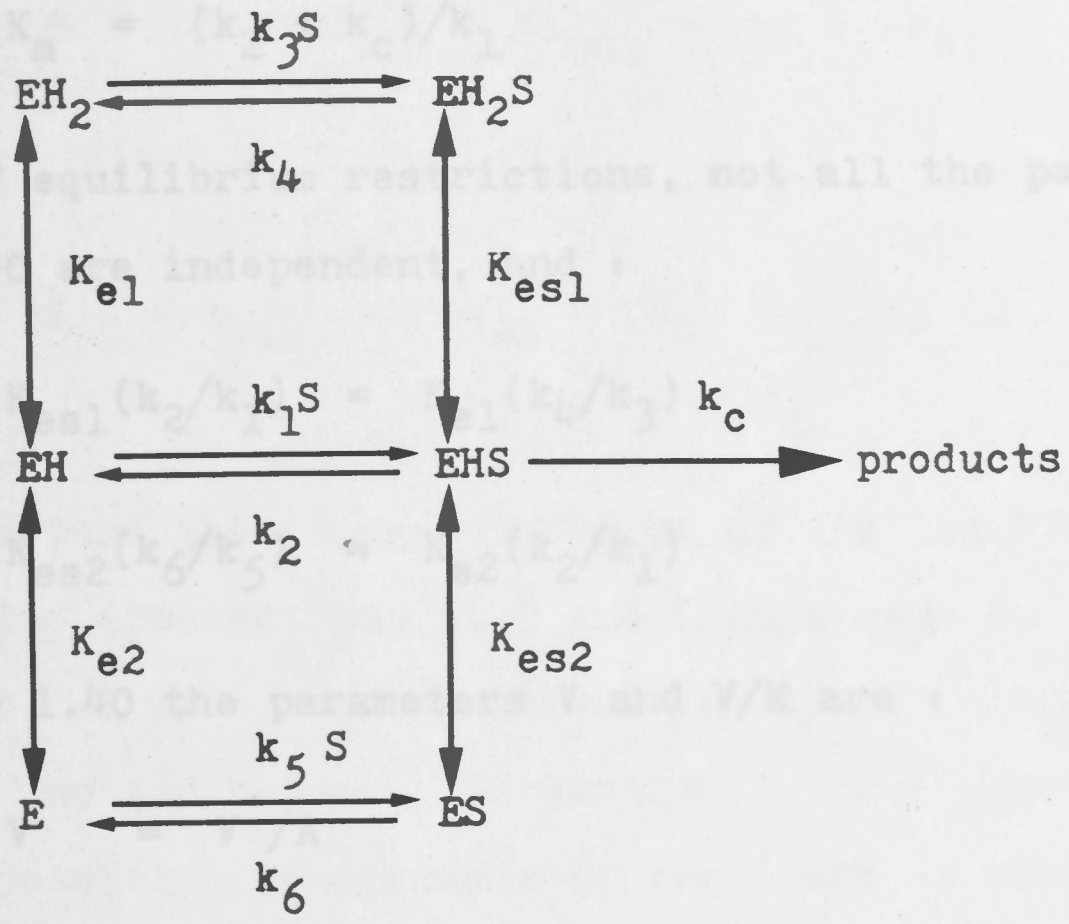

(1.40)

The initial rate equation is :

$$v = \frac{(V'/A).S}{K_m.\frac{B.C}{D.A} + S} \qquad (1.41)$$

where :

$$V' = k_c.E_t \qquad (1.42)$$

$$A = 1 + H/K_{esl} + K_{es2}/H \qquad (1.43)$$

$$B = 1 + H/K_{el} + K_{e2}/H \qquad (1.44)$$

$$C = 1 + \frac{k_4}{k_2+k_c}.\frac{H}{K_{esl}} + \frac{k_6}{k_2+k_c}.\frac{K_{es2}}{H} \qquad (1.45)$$

$$D = 1 + \frac{k_3}{k_1}.\frac{H}{K_{el}} + \frac{k_5}{k_1}.\frac{K_{e2}}{H} \qquad (1.46)$$

$$K_m = (k_2 + k_c)/k_1 \qquad (1.47)$$

Because of equilibrium restrictions, not all the parameters of Scheme 1.40 are independent, and :

$$K_{es1}(k_2/k_1) = K_{e1}(k_4/k_3) \qquad (1.48)$$

$$K_{es2}(k_6/k_5) = K_{e2}(k_2/k_1) \qquad (1.49)$$

For Scheme 1.40 the parameters V and V/K are :

$$V = V'/A \qquad (1.50)$$

$$V/K = (V'/K_m)(D/B.C) \qquad (1.51)$$

As expected from Equations 1.50 and 1.43, a plot of log V against pH will be of the same form as Fig. 1.9 and will yield the pKs of the free enzyme.

The plot of log V/K against pH will be the result of addition and subtraction of curves whose general shape was illustrated in Fig. 1.9, with the horizontal position depending on the value of the pH-independent parameter, log (V'/K_m). At low pH, the log V/K plot will have a straight line asymptote of slope +1. As the pH rises, the curve changes slope four times by a factor of -1 as the pKs in B and C are passed, and twice by +1 as those in D are passed, with the high pH asymptote having a slope of -1. A constraint on the shape of the plot arises because the pKs in C and D are not independent of each other : it can easily be shown that the high and low pH asymptotes of both log C and log D intersect at :

$$pH = 0.5(pK_{es1} + pK_{es2} + \log k_4/k_6) \qquad (1.52)$$

and that :

$$pK_{1D} - pK_{1C} = pK_{2C} - pK_{2D} = \log (1 + k_c/k_2) \qquad (1.53)$$

This means that the changes in slope of the log V/K plot that arise at the apparent pKs in C and D must come in the order : -1, +1, +1, -1 with equal intervals of log $(1 + k_c/k_2)$ between the first two and between the last two. As a consequence, there are four possible arrangements of the order of slope changes in the plot of log V/K against pH : (1) -1, -1, +1, +1, -1, -1; (2) -1, +1, -1, -1, +1, -1;(3) -1, -1, -1, +1, +1, -1 (and its reverse);(4) -1, -1, +1, -1, +1, -1 (and its reverse).

Arrangement (1) leads to a double optimum as illustrated in Fig. 1.11, and occurs only when both pKs in D fall between the pKs in B. When $pK_{1B} < pK_{2B}$ this will happen only in the unlikely event that k_3 and k_5 are both greater than k_1, i.e. when S binds to EH more slowly than to EH_2 and E. The ratio K_{e1}/K_{e2} must be greater than both the ratios k_3/k_1 and k_5/k_1. (Other arrangements can also give $k_3 > k_1$ and $k_5 > k_1$ but the relationship of K_{e1}/K_{e2} to the rate constants is different as summarised in Table 1.5.) Arrangement (2) leads to a two stage fall from the optimum on both sides, as illustrated in Fig. 1.12, and arises when both the pKs in B fall between the pKs in D. When pK_{1D} is smaller than pK_{2D} this will occur only when k_3 and k_5 are both smaller than k_1, i.e. when S binds to EH faster than to EH_2 and

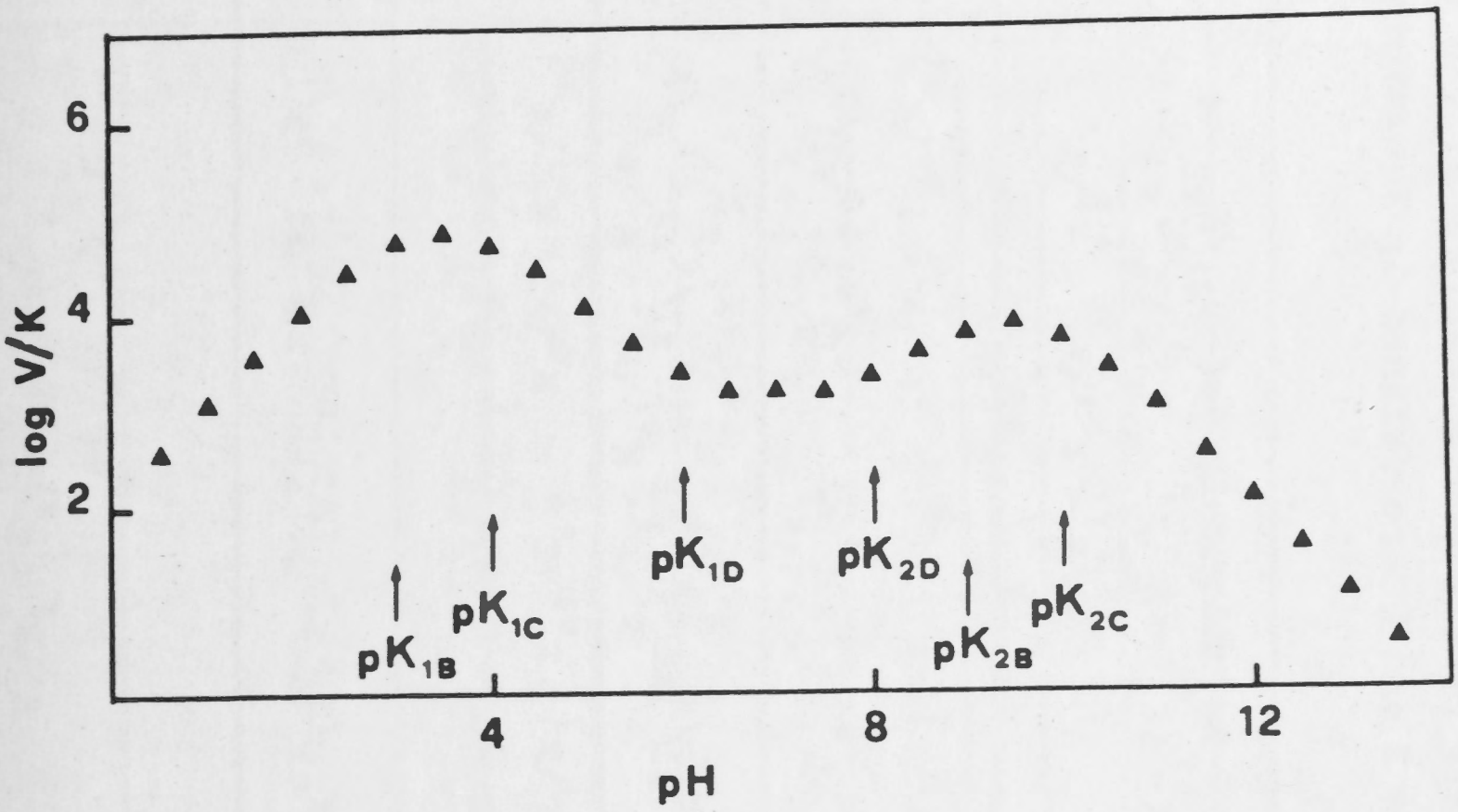

FIGURE 1.11 Plot of log V/K against pH for Scheme 1.40.

$\log V/K = \log (V'/K_m) + \log D - \log B - \log C$

with V', K_m, B, C and D defined in Equations 1.42 - 1.47. The slope changes occur in the order : -1, -1, +1, +1, -1, -1 (Arrangement 1; see text). $V'/K_m = 1$.

TABLE 1.5 Relationships between acid dissociation constants and rate constants for direct i formation of enzyme-substrate complexes for all possible combinations of pKs in i the terms B and D for Scheme 1.40. The terms B and D are defined in Equations i 1.44 and 1.46.

Arrangement of slope changes in log V/K plots	pKs in ascending order	Relationships of k_1, k_3, k_5	Relationships of K_{e1}/K_{e2} to k_3/k_1 and k_5/k_1
(1) -1,-1,+1,+1,-1,-1	$B_1\ D_1\ D_2\ B_2$ $B_1\ D_2\ D_1\ B_2$	$k_1 < k_3$ $k_1 < k_5$	$k_3/k_1 < K_{e1}/K_{e2}$ $k_5/k_1 < K_{e1}/K_{e2}$
	$B_2\ D_1\ D_2\ B_1$ $B_2\ D_2\ D_1\ B_1$	$k_3 < k_1$ $k_5 < k_1$	$K_{e1}/K_{e2} < k_3/k_1$ $K_{e1}/K_{e2} < k_5/k_1$
(2) -1,+1,-1,-1,+1,-1	$D_1\ B_1\ B_2\ D_2$ $D_1\ B_2\ B_1\ D_2$	$k_3 < k_1$ $k_5 < k_1$	$k_3/k_1 < K_{e1}/K_{e2}$ $k_5/k_1 < K_{e1}/K_{e2}$
	$D_2\ B_1\ B_2\ D_1$ $D_2\ B_2\ B_1\ D_1$	$k_1 < k_3$ $k_1 < k_5$	$K_{e1}/K_{e2} < k_3/k_1$ $K_{e1}/K_{e2} < k_5/k_1$
(3) -1,-1,-1,+1,+1,-1	$B_1\ B_2\ D_1\ D_2$ $B_1\ B_2\ D_2\ D_1$	$k_5 < k_1 < k_3$	$k_5/k_1 < K_{e1}/K_{e2} < k_3/k_1$

	$B_2\ B_1\ D_1\ D_2$ $B_2\ B_1\ D_2\ D_1$	$k_5 < k_1 < k_3$	$k_5/k_1 < K_{e1}/K_{e2} < k_3/k_1$
Reverse (3) -1,+1,+1,-1,-1,-1	$D_1\ D_2\ B_1\ B_2$ $D_1\ D_2\ B_2\ B_1$ $D_2\ D_1\ B_1\ B_2$ $D_2\ D_1\ B_2\ B_1$	$k_3 < k_1 < k_5$	$k_3/k_1 < K_{e1}/K_{e2} < k_5/k_1$
(4) -1,-1,+1,-1,+1,-1	$B_1\ D_1\ B_2\ D_2$	$k_5 < k_1 < k_3$	$k_3/k_1 < K_{e1}/K_{e2}$ $k_5/k_1 < K_{e1}/K_{e2}$
	$B_1\ D_2\ B_2\ D_1$	$k_1 < k_5 < k_3$	$k_5/k_1 < K_{e1}/K_{e2} < k_3/k_1$
	$B_2\ D_1\ B_1\ D_2$	$k_5 < k_3 < k_1$	$k_5/k_1 < K_{e1}/K_{e2} < k_3/k_1$
	$B_2\ D_2\ B_1\ D_1$	$k_5 < k_1 < k_3$	$K_{e1}/K_{e2} < k_3/k_1$ $K_{e1}/K_{e2} < k_5/k_1$
Reverse (4) -1,+1,-1,+1,-1,-1	$D_1\ B_1\ D_2\ B_2$	$k_3 < k_1 < k_5$	$k_3/k_1 < K_{e1}/K_{e2}$ $k_5/k_1 < K_{e1}/K_{e2}$
	$D_1\ B_2\ D_2\ B_1$	$k_3 < k_5 < k_1$	$k_3/k_1 < K_{e1}/K_{e2} < k_5/k_1$
	$D_2\ B_1\ D_1\ B_2$	$k_1 < k_3 < k_5$	$k_3/k_1 < K_{e1}/K_{e2} < k_5/k_1$
	$D_2\ B_2\ D_1\ B_1$	$k_3 < k_1 < k_5$	$K_{e1}/K_{e2} < k_3/k_1$ $K_{e1}/K_{e2} < k_5/k_1$

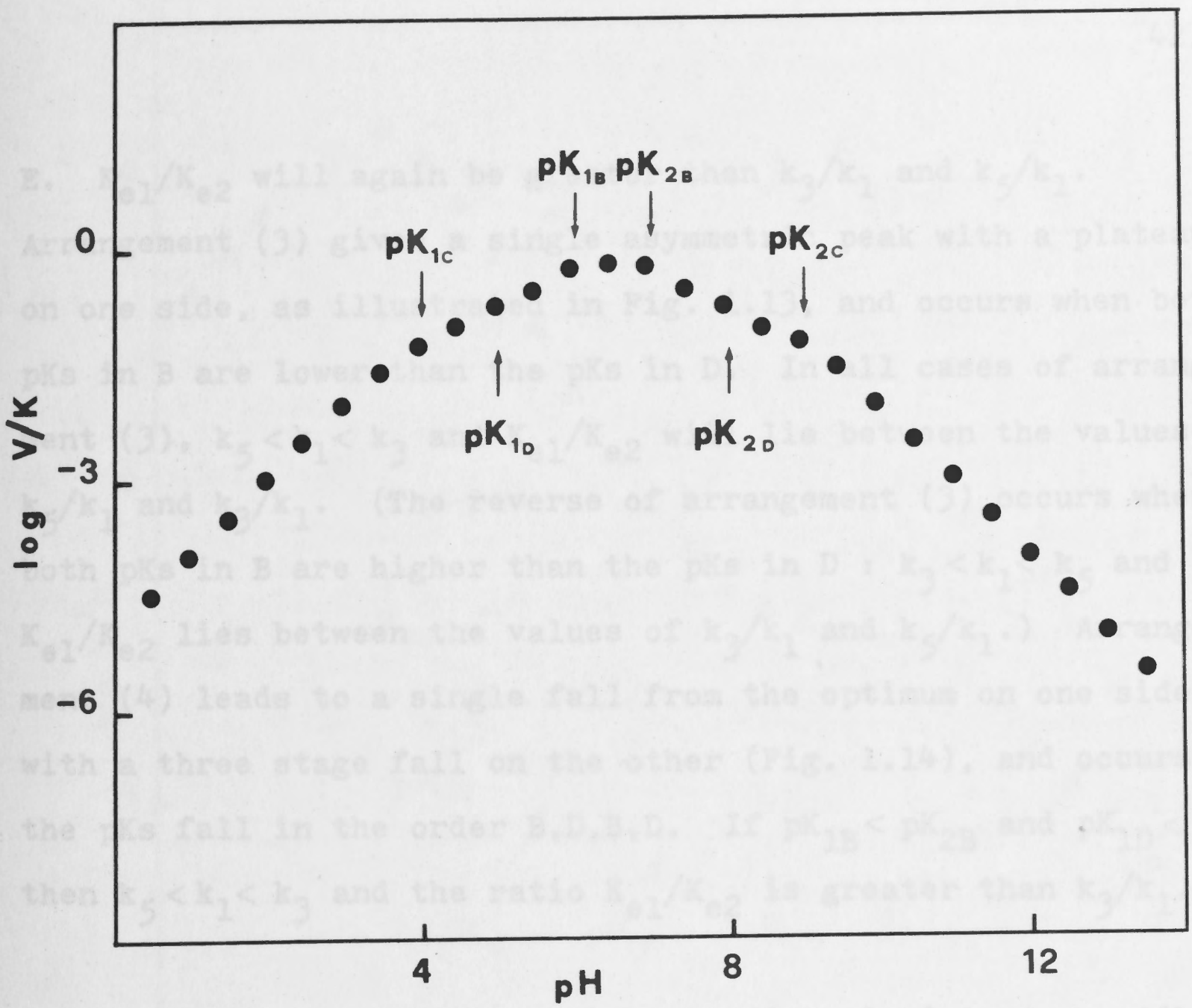

FIGURE 1.12 Plot of log V/K against pH for Scheme 1.40.

$$\log V/K = \log (V'/K_m) + \log D - \log B - \log C$$

with V', K_m, B, C and D defined in Equations 1.42 - 1.47. The slope changes occur in the order : -1, +1, -1, -1, +1, -1 (Arrangement 2; see text). $V'/K_m = 1$.

E. K_{e1}/K_{e2} will again be greater than k_3/k_1 and k_5/k_1. Arrangement (3) gives a single asymmetric peak with a plateau on one side, as illustrated in Fig. 1.13, and occurs when both pKs in B are lower than the pKs in D. In all cases of arrangement (3), $k_5 < k_1 < k_3$ and K_{e1}/K_{e2} will lie between the values of k_5/k_1 and k_3/k_1. (The reverse of arrangement (3) occurs when both pKs in B are higher than the pKs in D : $k_3 < k_1 < k_5$ and K_{e1}/K_{e2} lies between the values of k_3/k_1 and k_5/k_1.) Arrangement (4) leads to a single fall from the optimum on one side, with a three stage fall on the other (Fig. 1.14), and occurs when the pKs fall in the order B,D,B,D. If $pK_{1B} < pK_{2B}$ and $pK_{1D} < pK_{2D}$ then $k_5 < k_1 < k_3$ and the ratio K_{e1}/K_{e2} is greater than k_3/k_1.

If EH and EHS are the only directly interconvertible forms of free enzyme and enzyme-substrate complex, then $k_3 = k_4 = k_5 = k_6 = 0$, and both C and D reduce to unity, leaving :

$$V/K = (V'/K_m)/B$$

$$= \frac{V'/K_m}{1 + H/K_{e1} + K_{e2}/H} \qquad (1.54)$$

A plot of log V/K against pH yields the pKs of free enzyme, and these pKs should agree with those determined from a plot of pK_i for a competitive inhibitor against pH.

If all reversible steps are at equilibrium, the expression for V/K is identical in form with Equation 1.54 above, with the only difference being in the interpretation of K_m, which is now a true dissociation constant.

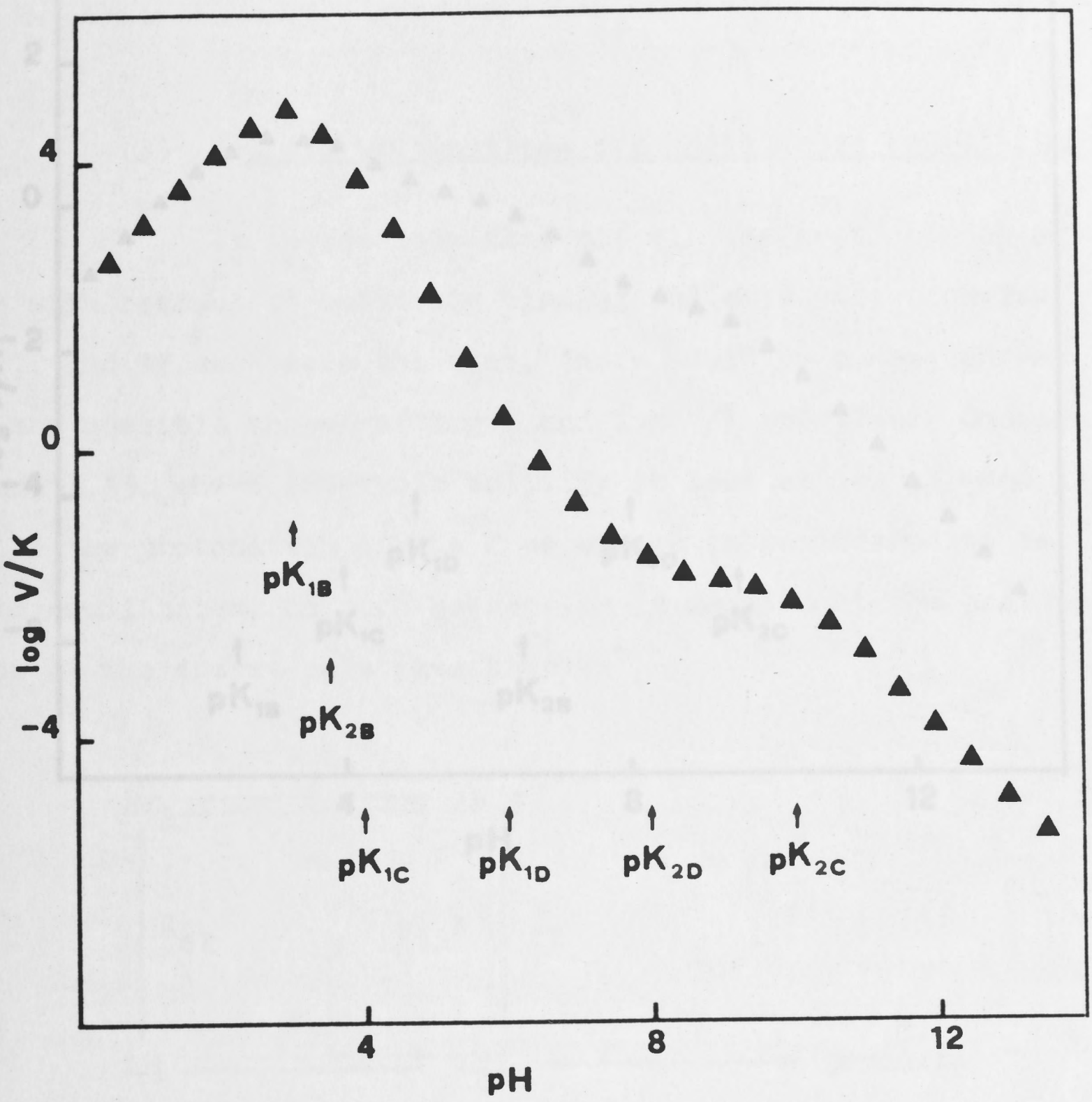

FIGURE 1.13 Plot of log V/K against pH for Scheme 1.40.

$$\log V/K = \log (V'/K_m) + \log D - \log B - \log C$$

with V', K_m, B, C and D defined in Equations 1.42 - 1.47. The slope changes occur in the order : -1, -1, -1, +1, +1, -1 (Arrangement 3; see text). $V'/K_m = 1$.

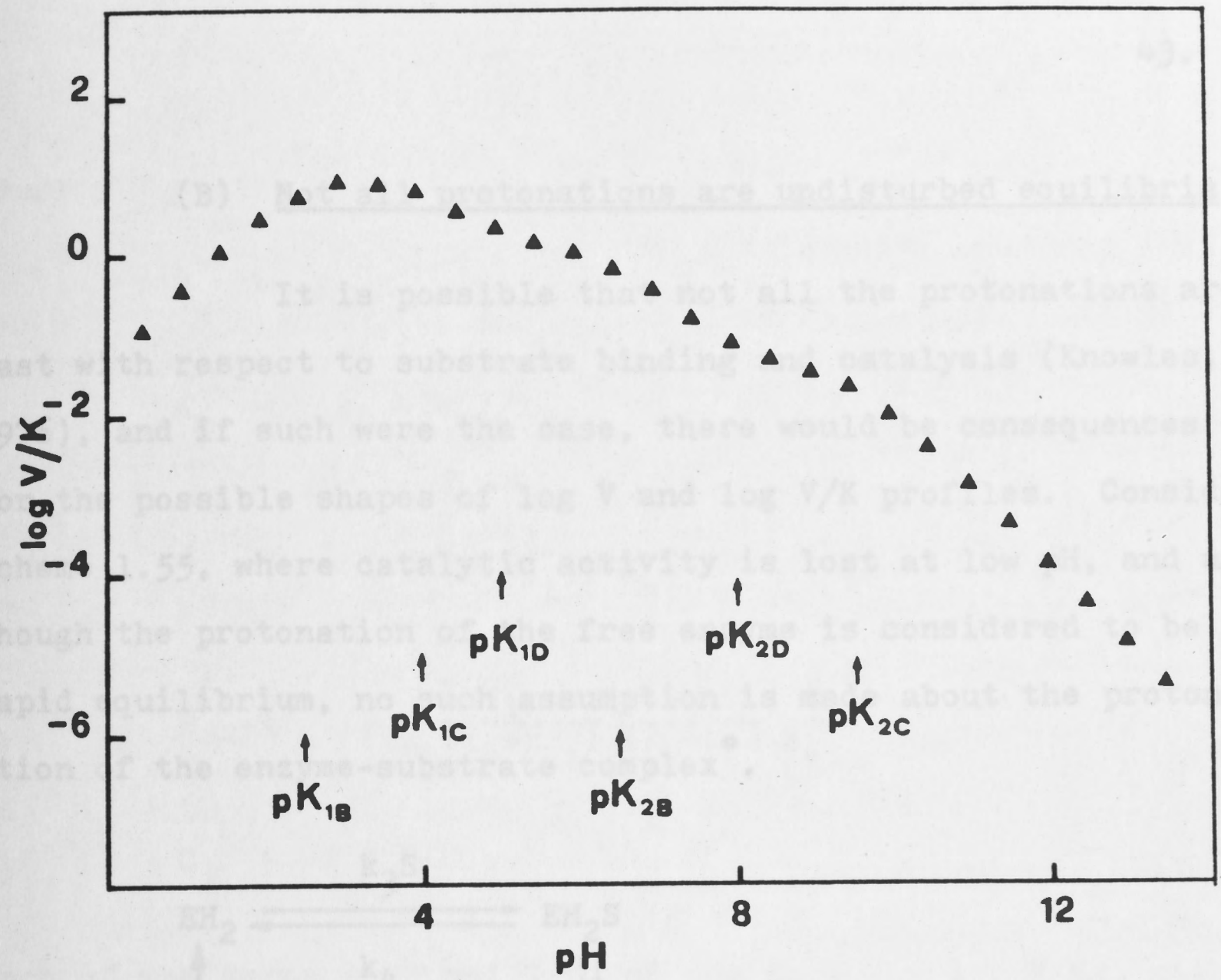

FIGURE 1.14 Plot of log V/K against pH for Scheme 1.40.

$$\log V/K = \log (V'/K_m) + \log D - \log B - \log C$$

with V', K_m, B, C and D defined in the Equations 1.42 - 1.47. The slope changes occur in the order : -1, -1, +1, -1, +1, -1 (Arrangement 4; see text). $V'/K_m = 1$.

(B) Not all protonations are undisturbed equilibria

It is possible that not all the protonations are fast with respect to substrate binding and catalysis (Knowles, 1976), and if such were the case, there would be consequences for the possible shapes of log V and log V/K profiles. Consider Scheme 1.55, where catalytic activity is lost at low pH, and although the protonation of the free enzyme is considered to be rapid equilibrium, no such assumption is made about the protonation of the enzyme-substrate complex*.

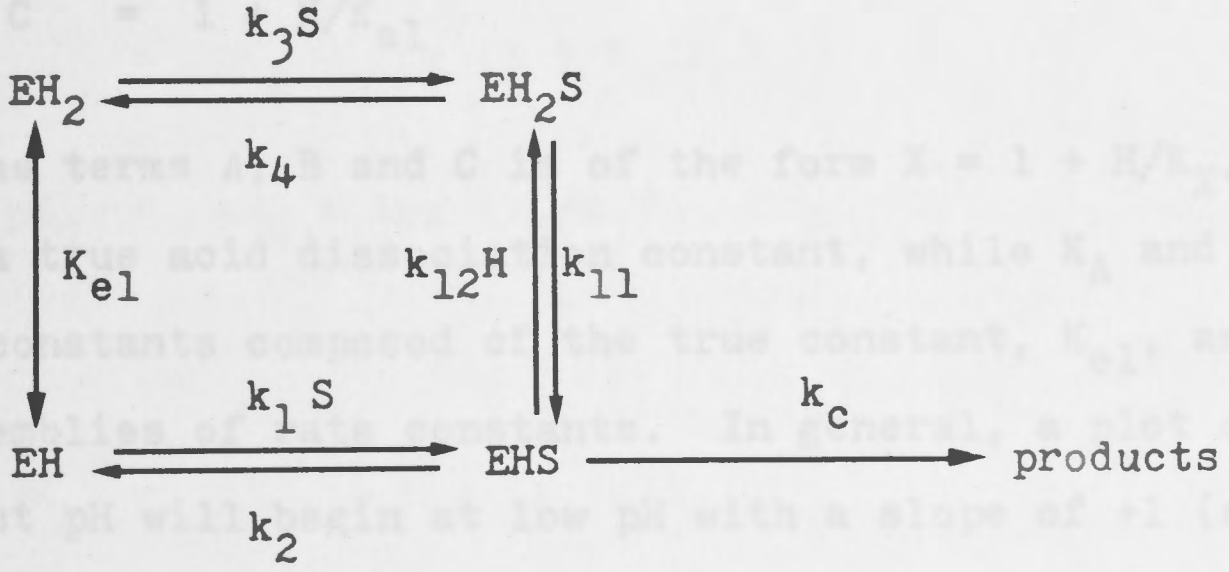

(1.55)

For Scheme 1.55, the expression for V/K is :

$$V/K = (V'/K_m) \cdot \frac{A}{B.C} \qquad (1.56)$$

---

* (1) There is no reason to assume both protonations to be slow since this would lead to non-linear double reciprocal plots with S as the varied substrate.

(2) Although the rate equation has been derived for a scheme in which activity is lost at both high and low pH, the complexity of the equation renders it more convenient to consider the two cases separately. In the interests of brevity, loss of activity at high pH will not be dealt with here. The analysis is similar, but varies in details (Cleland, 1977).

where :

$$V' = k_c.E_t \tag{1.57}$$

$$K_m = (k_2 + k_c)/k_1 \tag{1.58}$$

$$A = 1 + \frac{k_3 k_{11}}{k_1(k_4+k_{11})} \cdot \frac{H}{K_{e1}} \tag{1.59}$$

$$B = 1 + \frac{k_3 k_{11}}{k_1(k_4+k_{11})} \cdot \frac{k_2}{(k_2+k_c)} \cdot \frac{H}{K_{e1}} \tag{1.60}$$

$$C = 1 + H/K_{e1} \tag{1.61}$$

Each of the terms A, B and C is of the form $X = 1 + H/K_X$, with K_C being a true acid dissociation constant, while K_A and K_B are apparent constants composed of the true constant, K_{e1}, and different assemblies of rate constants. In general, a plot of log V/K against pH will begin at low pH with a slope of +1 (since the low pH asymptotes of log A, -log B and -log c have slopes of +1, -1 and -1, respectively). As the pH rises the curve changes slope twice by -1 as the pKs in B and C are passed, and once by +1 as the pK in A is passed, so that the final slope of the curve is zero. The high and low pH asymptotes of the curve are :

$$\lim_{H \to 0} (\log (V/K)) = \log (V'/K_m) \tag{1.62}$$

$$\lim_{H \to \infty} (\log (V/K)) = \log (V'/K_m) + pH - pK_{e1} + \log (1 + k_c/k_2) \tag{1.63}$$

with the intersection of the asymptotes at :

$$pH = pK_{e1} - \log (1 + k_c/k_2) \tag{1.64}$$

It is clear that the true value of pK_{el} will not be obtained unless k_c is very much smaller than k_2, in which case the terms A and B in Equation 1.56 cancel, and the plot of log V/K has only a single slope change at the pK value in C, i.e. at pK_{el}. In general, however, there will be three slope changes in the curve. Now the pKs in A, B and C are related in the following way :

$$pK_A = pK_D - \log (1 + k_4/k_{11}) \qquad (1.65)$$

$$pK_B = pK_D - \log (1 + k_4/k_{11}) - \log (1 + k_c/k_2)$$

$$= pK_A - \log (1 + k_c/k_2) \qquad (1.66)$$

$$pK_C = pK_D - \log (k_3/k_1) \qquad (1.67)$$

where:

$$pK_D = pK_{el} - \log (k_1/k_3) \qquad (1.68)$$

It is clear from Equations 1.65 and 1.66 that pK_B lies below pK_A, and therefore the slope changes due to pK_A and pK_B in the log V/K profile must come in the order -1, +1. Therefore, there are only two possible arrangements of all the slope changes : (1) -1, -1, +1; and (2) -1, +1, -1.

Arrangement (1) leads to a single fall from the optimum on the acid side, with a drop to the limiting value of log V'/K_m on the alkaline side, as illustrated in Fig. 1.15. (The profile might be considered to have a hump.) This arrangement occurs only when the pK in C falls below the pK in A. Inspec-

FIGURE 1.15 Plots of log V/K (■), log A (□), -log B (○) and -log C (△) for Scheme 1.55.

$$\log V/K = \log (V'/K_m) + \log A - \log B - \log C$$

with V', K_m, A, B and C defined in Equations 1.57 - 1.61. $pK_{el} = 6$; $k_4/k_{11} = 9$; $k_c/k_2 = 9$; $k_3/k_1 = 1000$; $V'/K_m = 1$; $pK_A = 8$; $pK_B = 7$; $pK_C = 6$.

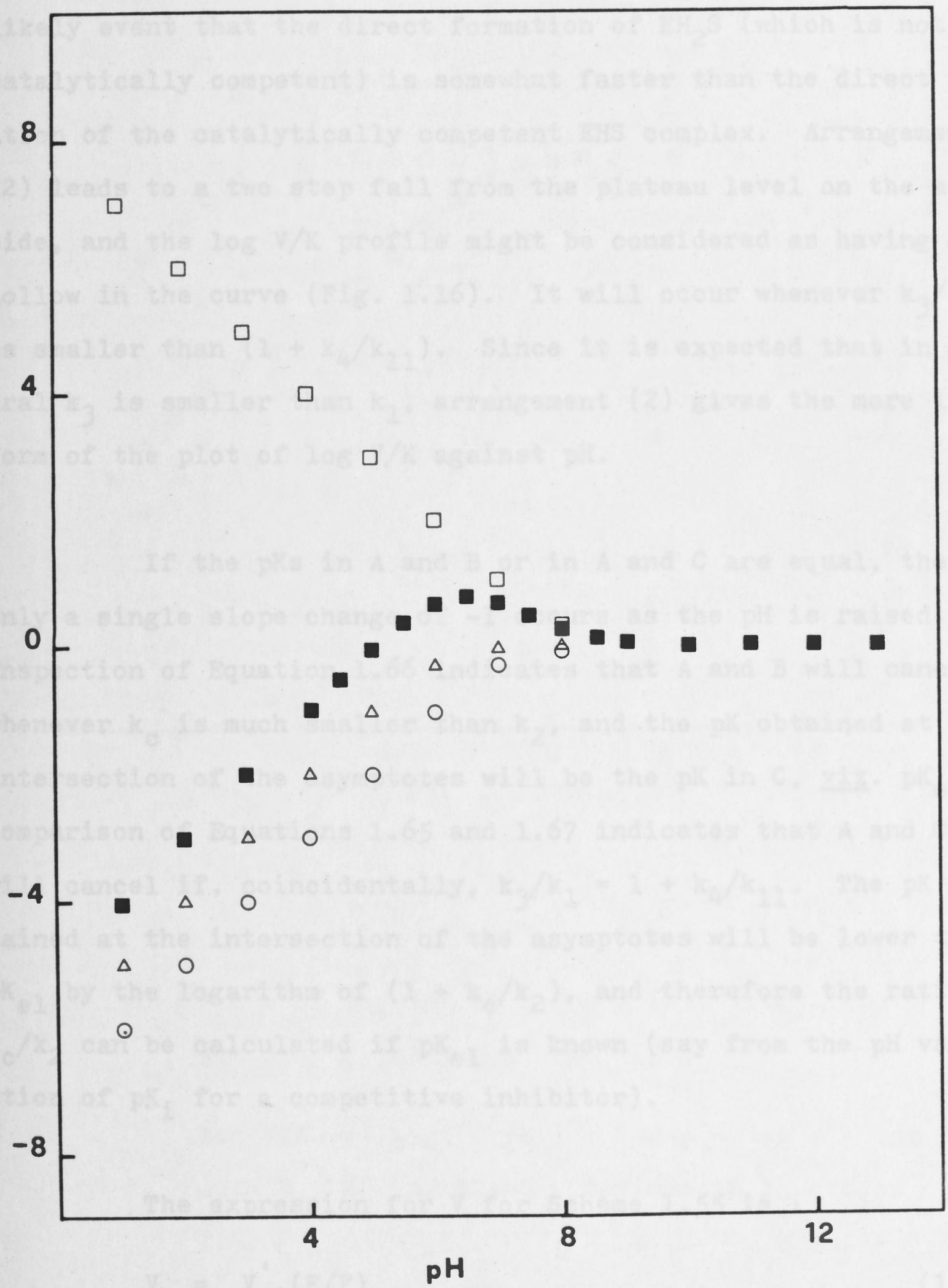
8
4
0
-4
-8
4
8
12
pH

tion of Equations 1.65 and 1.67 indicates that this will occur only when k_3/k_1 is greater than $(1 + k_4/k_{11})$, *i.e.* in the unlikely event that the direct formation of EH_2S (which is not catalytically competent) is somewhat faster than the direct formation of the catalytically competent EHS complex. Arrangement (2) leads to a two step fall from the plateau level on the acid side, and the log V/K profile might be considered as having a hollow in the curve (Fig. 1.16). It will occur whenever k_3/k_1 is smaller than $(1 + k_4/k_{11})$. Since it is expected that in general k_3 is smaller than k_1, arrangement (2) gives the more likely form of the plot of log V/K against pH.

If the pKs in A and B or in A and C are equal, then only a single slope change of -1 occurs as the pH is raised. Inspection of Equation 1.66 indicates that A and B will cancel whenever k_c is much smaller than k_2, and the pK obtained at the intersection of the asymptotes will be the pK in C, *viz.* pK_{el}. Comparison of Equations 1.65 and 1.67 indicates that A and C will cancel if, coincidentally, $k_3/k_1 = 1 + k_4/k_{11}$. The pK obtained at the intersection of the asymptotes will be lower than pK_{el} by the logarithm of $(1 + k_c/k_2)$, and therefore the ratio k_c/k_2 can be calculated if pK_{el} is known (say from the pH variation of pK_i for a competitive inhibitor).

The expression for V for Scheme 1.55 is :

$$V = V'.(E/F) \qquad (1.69)$$

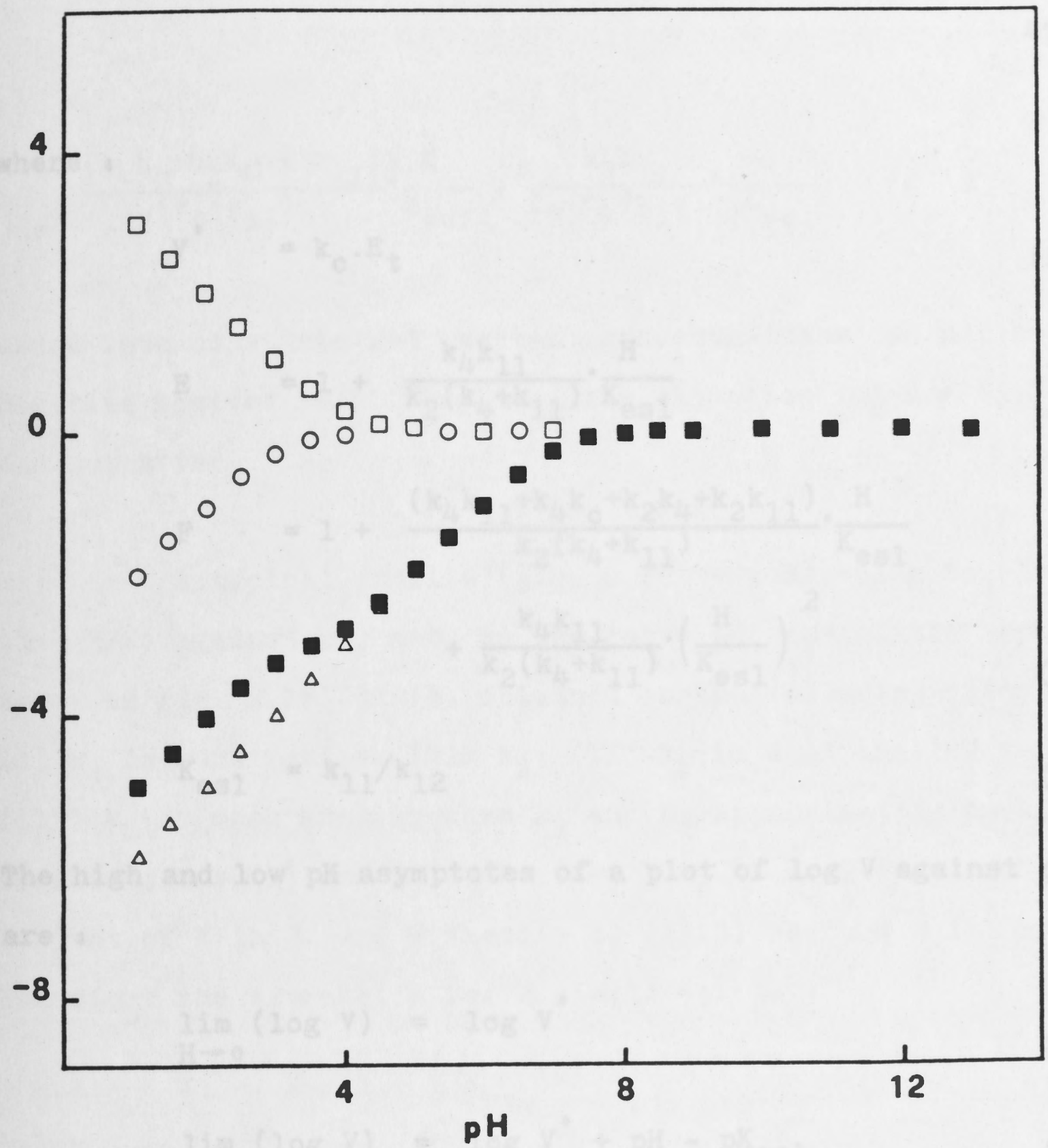

FIGURE 1.16 Plots of log V/K (■), log A (□), -log B (○) and -log C (△) for Scheme 1.55.

$$\log V/K = \log (V'/K_m) + \log A - \log B - \log C$$

with V', K_m, A, B and C defined in Equations 1.57 - 1.61. $pK_{el} = 7$; $k_4/k_{11} = 9$; $k_c/k_2 = 9$; $k_3/k_1 = 0.01$; $V'/K_m = 1$; $pK_A = 4$; $pK_B = 3$; $pK_C = 7$.

where :

$$V' = k_c . E_t \tag{1.70}$$

$$E = 1 + \frac{k_4 k_{11}}{k_2(k_4+k_{11})} \cdot \frac{H}{K_{es1}} \tag{1.71}$$

$$F = 1 + \frac{(k_4 k_{11}+k_4 k_c+k_2 k_4+k_2 k_{11})}{k_2(k_4+k_{11})} \cdot \frac{H}{K_{es1}} + \frac{k_4 k_{11}}{k_2(k_4+k_{11})} \cdot \left(\frac{H}{K_{es1}}\right)^2 \tag{1.72}$$

$$K_{es1} = k_{11}/k_{12} \tag{1.73}$$

The high and low pH asymptotes of a plot of log V against pH are :

$$\lim_{H \to o} (\log V) = \log V' \tag{1.74}$$

$$\lim_{H \to \infty} (\log V) = \log V' + pH - pK_{es1} \tag{1.75}$$

which intersect at $pH = pK_{es1}$. Although the intersection of the asymptotes yields the pK of the enzyme-substrate complex, the shape of the log V curve need not be simple. Moreover, while E is a term of the type found in the expression for V/K, the term F is quadratic and in the general case the log V profile has different characteristics from the log V/K profile. In particular, the "hump" (as in Fig. 1.15) is not possible since this would require log E to be greater than log F for some pH range. This can only occur if it is possible that :

$$\frac{(k_4k_c+k_2k_4+k_2k_{11})}{k_2(k_4+k_{11})}\cdot\frac{H}{K_{es1}} + \frac{k_4k_{11}}{k_2(k_4+k_{11})}\cdot\left(\frac{H}{K_{es1}}\right)^2 < 0 \qquad (1.76)$$

Since rate constants and reactant concentrations can not be negative however small they are, the situation log E > log F can not arise.

A typical profile (i.e. a curve conforming to -log (1 + H/K) against pH, such as the curve for any of the separate terms in Fig. 1.16) can be obtained in the following situations : (i) k_c is much smaller than k_2; (ii) k_c is much smaller than k_{11}; (iii) k_4 is much smaller than k_2 and k_c approximately equals k_{11}. In situations (i) and (ii) the term k_4k_c is lost from the coefficient of H in F, and F factors to (E)(G) where $G = 1 + H/K_{es1}$. Therefore the expression for V simplifies to :

$$V = V'/(1 + H/K_{es1}) \qquad (1.77)$$

In situation (iii) when k_4 is much smaller than k_2, the term k_4k_{11} is lost from the coefficient of H in F, and F will factor into (E)(G) if k_c and k_{11} are approximately equal. (There are some other situations in which a normally-shaped profile will be obtained, but they require even more remotely coincidental circumstances than situation (iii) above.)

If none of the above situations holds, the log V profile can show more or less of a hollow. If k_{11}/k_2 is large (EH_2S dissociates to EHS much more rapidly than S dissociates from the EHS complex) then the log V profile will be normal or

nearly normal (the intersection of the asymptotes can be more than 0.3 unit above the curve). When k_{11}/k_2 is small, however, there is a hollow in the log V profile, which becomes more pronounced as k_4/k_{11} becomes larger. (Compare Figs. 1.17 (a) and (b).) The log V profile will tend toward a "typical" curve, then, if a relatively large supply of EHS complex can be maintained. (As may be observed in Fig. 1.17, a slope of +1 in the log V profile can be approximated without the final low pH asymptote being reached. In such a case, the intersection of the high pH asymptote with the apparent low pH asymptote yields pK_X where K_X is the reciprocal of the coefficient of H in the term F.)

1.1.11 FINAL REMARKS

The techniques described above for the investigation of an enzymic reaction are by no means the only ones, but they are the most reliable as far as the interpretation of results is concerned (with the possible exception of pH effects). Among other techniques available to the enzymologist are the study of the variation of kinetic parameters under conditions of solvent, temperature and ionic strength perturbation, and the effects of chemical and mutational modification of primary structure. It is not, however, the purpose of this section to catalogue exhaustively and to describe in detail all possible techniques but to indicate the major approaches to the determination of the kinetic mechanism of an enzyme-catalysed reaction, and, therefore, the approaches just mentioned will not be elaborated further.

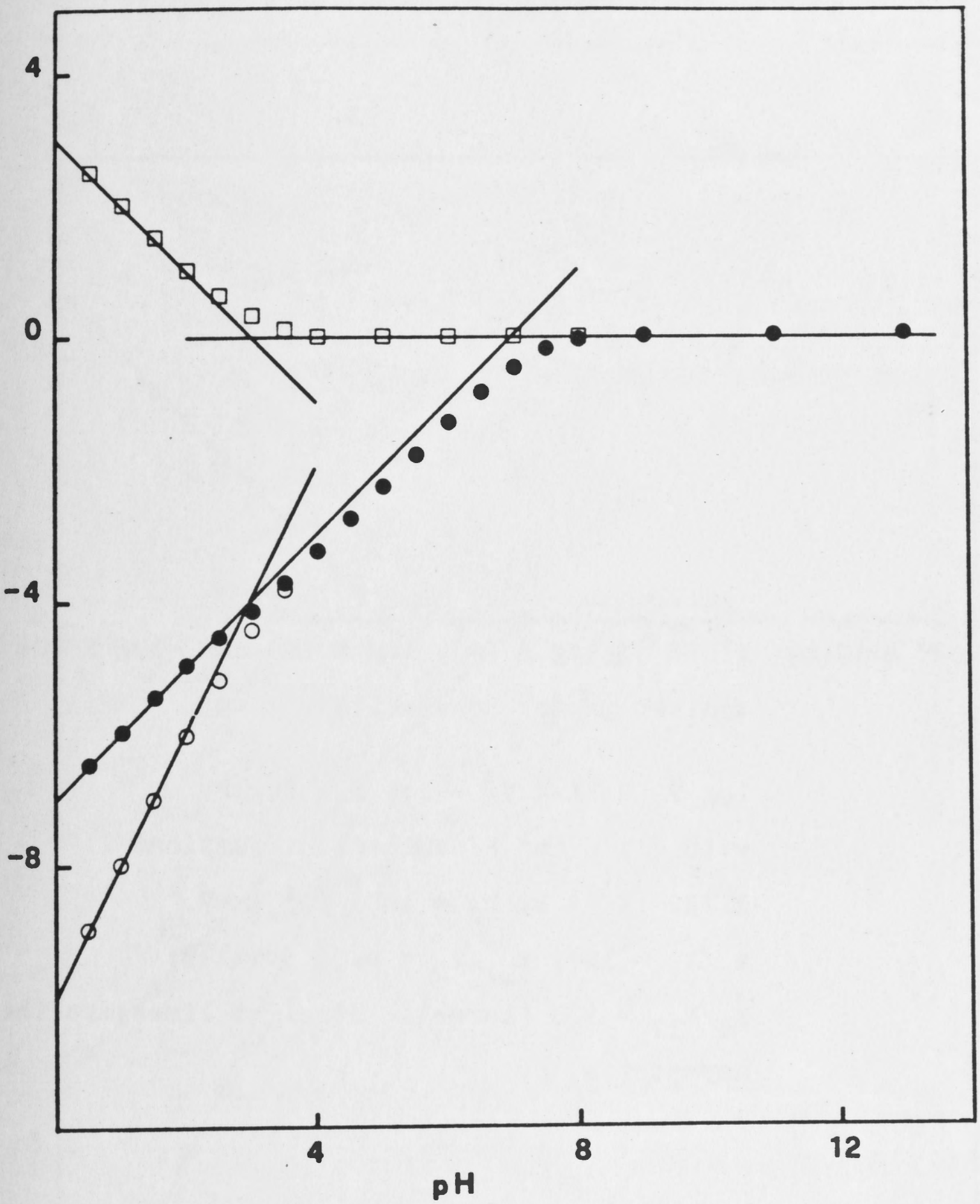

FIGURE 1.17(a) Plots of log V (●), log E (□) and -log F (○) against pH for Scheme 1.55.

log V = log V' + log E - log F

with V', E and F defined in Equations 1.70 - 1.73. V' = 1; k_2 = 100; pK_{es1} = 7; k_c/k_2 = 100; k_{11}/k_2 = 0.01 (small); k_4/k_{11} = 0.01 (small). Straight lines are the asymptotes.

FIGURE 1.17(b) Plots of log V (●), log E (□) and -log F (○) against pH for Scheme 1.55.

$\log V = \log V' + \log E - \log F$

with V', E and F defined in Equations 1.70 - 1.73. $V' = 1$; $k_2 = 100$; $pK_{es1} = 7$; $k_c/k_2 = 100$; $k_{11}/k_2 = 0.01$ (small); $k_4/k_{11} = 100$ (large). Straight lines are the asymptotes.

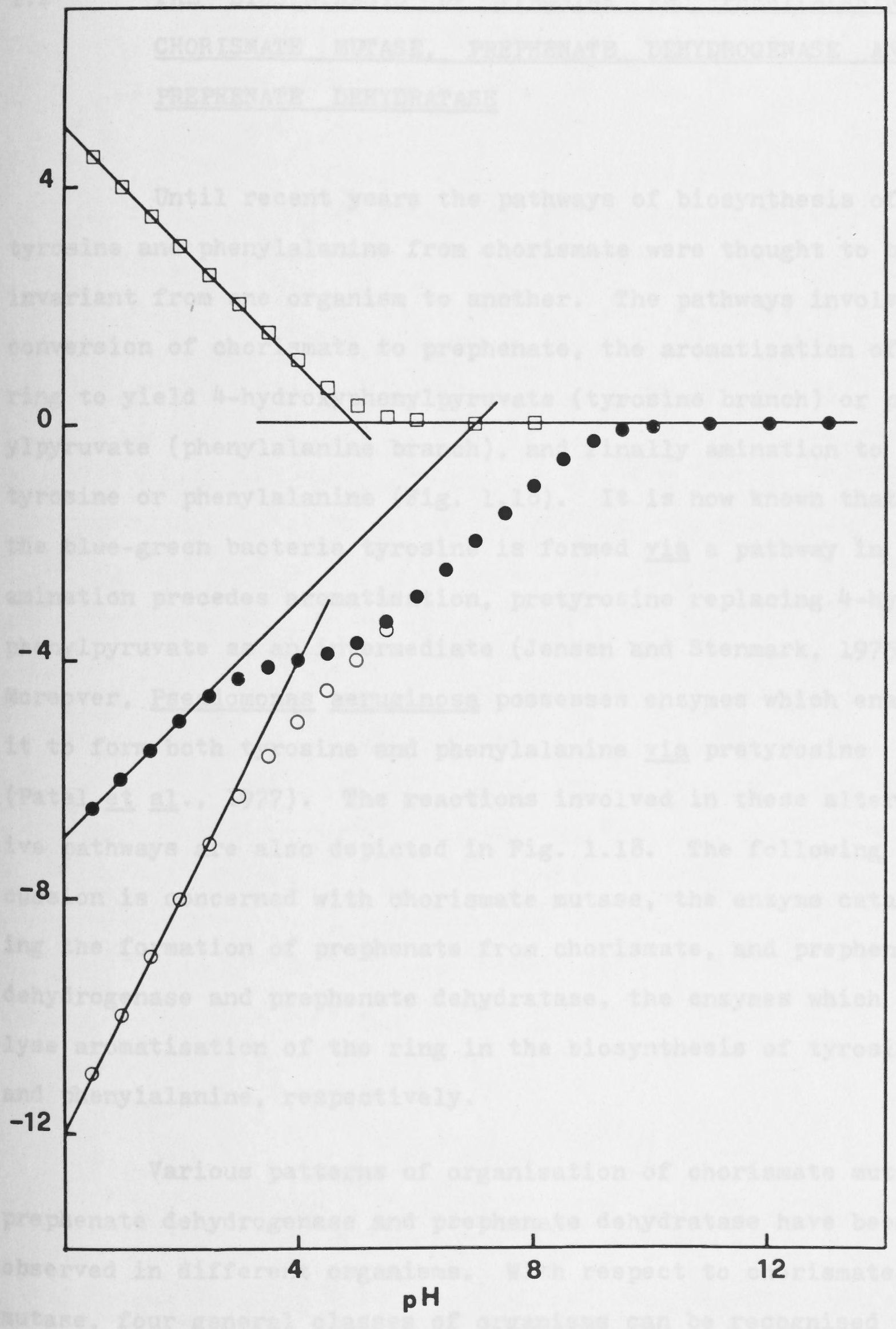
4
0
-4
-8
-12
4
8
12
pH

1.2 THE BIOSYNTHESIS OF TYROSINE AND PHENYLALANINE : CHORISMATE MUTASE, PREPHENATE DEHYDROGENASE AND PREPHENATE DEHYDRATASE

Until recent years the pathways of biosynthesis of tyrosine and phenylalanine from chorismate were thought to be invariant from one organism to another. The pathways involve the conversion of chorismate to prephenate, the aromatisation of the ring to yield 4-hydroxyphenylpyruvate (tyrosine branch) or phenylpyruvate (phenylalanine branch), and finally amination to form tyrosine or phenylalanine (Fig. 1.18). It is now known that in the blue-green bacteria tyrosine is formed *via* a pathway in which amination precedes aromatisation, pretyrosine replacing 4-hydroxyphenylpyruvate as an intermediate (Jensen and Stenmark, 1975). Moreover, *Pseudomonas aeruginosa* possesses enzymes which enable it to form both tyrosine and phenylalanine *via* pretyrosine (Patel *et al.*, 1977). The reactions involved in these alternative pathways are also depicted in Fig. 1.18. The following discussion is concerned with chorismate mutase, the enzyme catalysing the formation of prephenate from chorismate, and prephenate dehydrogenase and prephenate dehydratase, the enzymes which catalyse aromatisation of the ring in the biosynthesis of tyrosine and phenylalanine, respectively.

Various patterns of organisation of chorismate mutase, prephenate dehydrogenase and prephenate dehydratase have been observed in different organisms. With respect to chorismate mutase, four general classes of organisms can be recognised :

FIGURE 1.18 Pathways of biosynthesis of tyrosine and phenylalanine from chorismate.

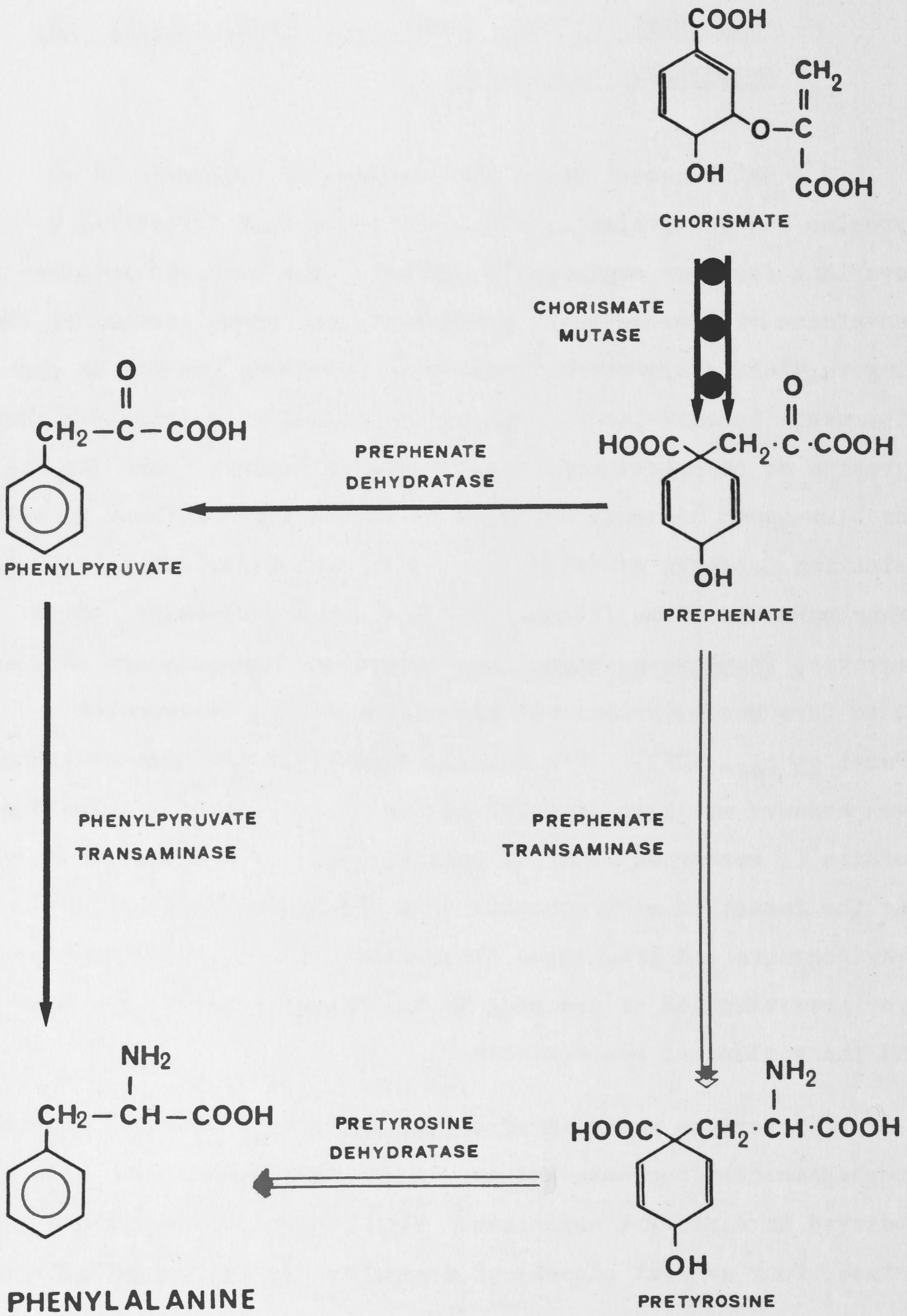

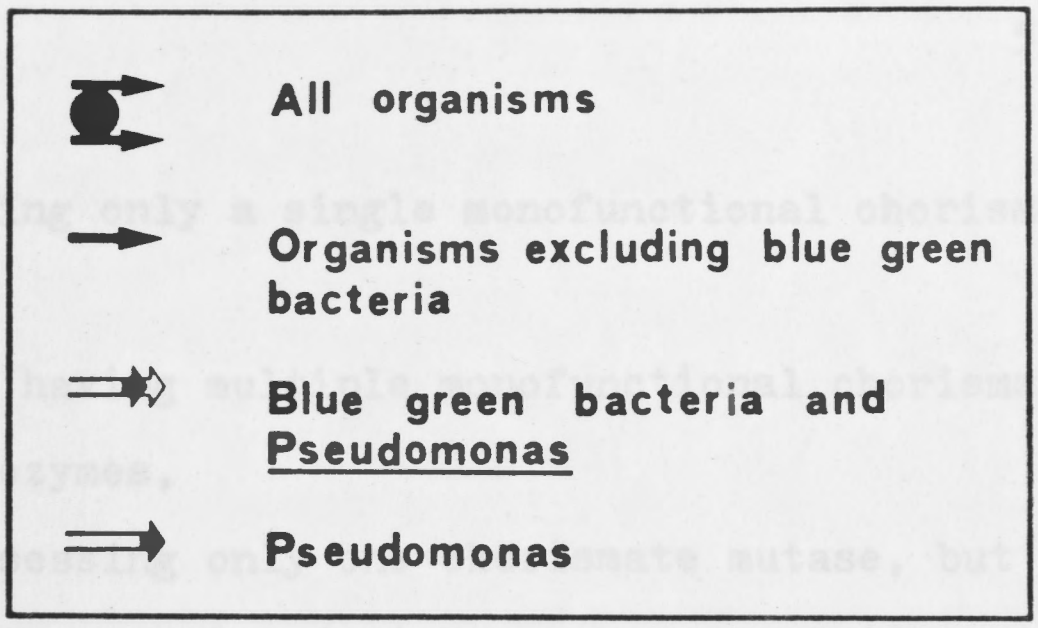
All organisms
Organisms excluding blue green bacteria
Blue green bacteria and Pseudomonas
Pseudomonas

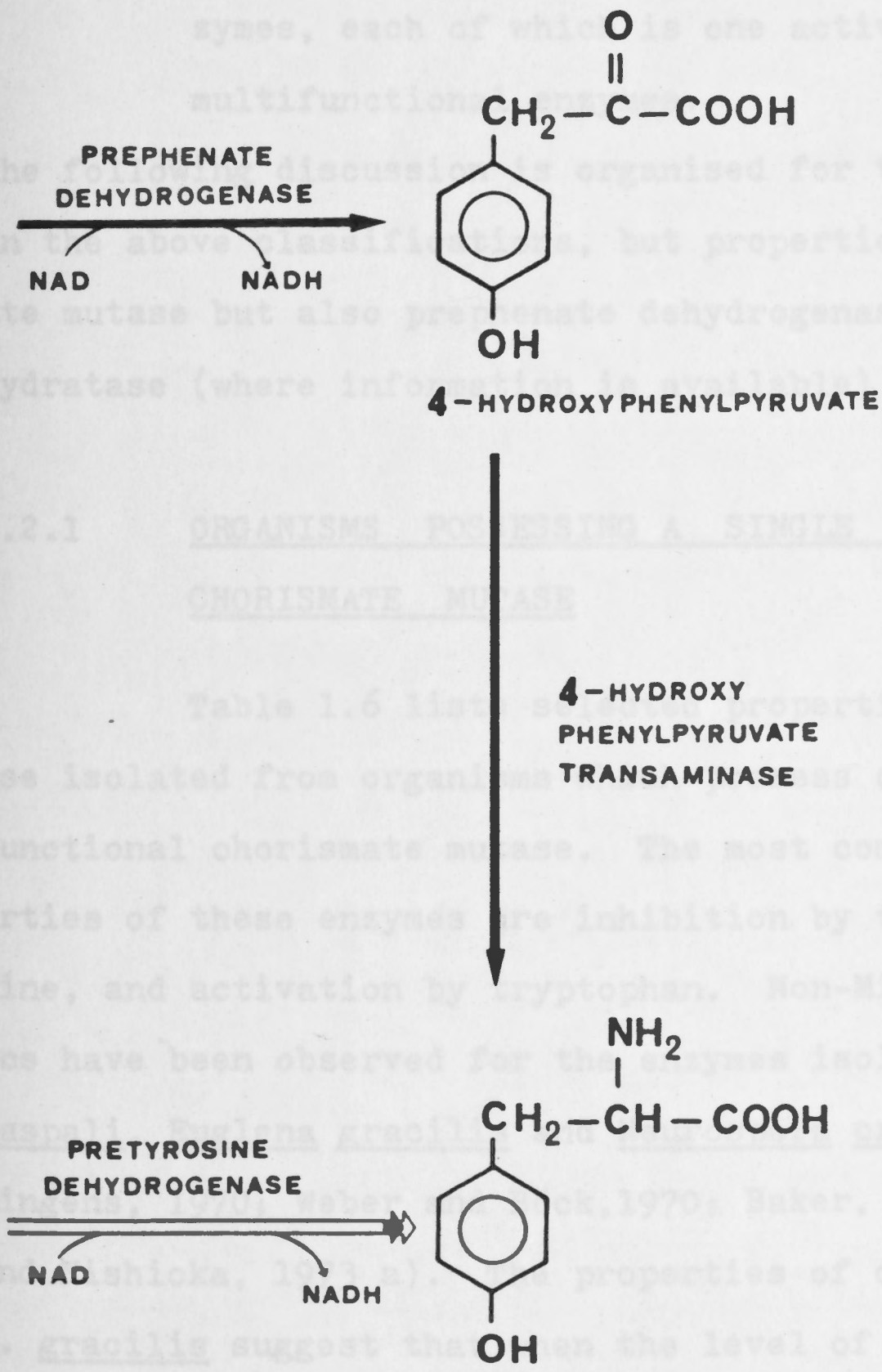
O
||
CH2—C—COOH
PREPHENATE DEHYDROGENASE
NAD
NADH
OH
4-HYDROXY PHENYLPYRUVATE
4-HYDROXY PHENYLPYRUVATE TRANSAMINASE
NH2
|
CH2—CH—COOH
PRETYROSINE DEHYDROGENASE
NAD
NADH
OH
TYROSINE

(a) those having only a single monofunctional chorismate mutase,

(b) organisms having multiple monofunctional chorismate mutase isozymes,

(c) those possessing only one chorismate mutase, but this activity is associated with another catalytic activity in a bifunctional enzyme, and

(d) those organisms having multiple chorismate mutase enzymes, each of which is one activity of different multifunctional enzymes.

The following discussion is organised for the sake of simplicity on the above classifications, but properties of not only chorismate mutase but also prephenate dehydrogenase and prephenate dehydratase (where information is available) will be dealt with.

1.2.1 ORGANISMS POSSESSING A SINGLE MONOFUNCTIONAL CHORISMATE MUTASE

Table 1.6 lists selected properties of chorismate mutase isolated from organisms which possess only a single monofunctional chorismate mutase. The most commonly observed properties of these enzymes are inhibition by tyrosine and phenylalanine, and activation by tryptophan. Non-Michaelis-Menten kinetics have been observed for the enzymes isolated from Claviceps paspali, Euglena gracilis and Neurospora crassa (Sprössler and Lingens, 1970; Weber and Böck,1970; Baker, 1966 and 1968; Woodin and Nishioka, 1973 a). The properties of certain enzymes from E. gracilis suggest that when the level of tryptophan is high, synthesis of tryptophan is slowed by inhibition of anthranilate

TABLE 1.6 Selected properties of chorismate mutase from various organisms possessing only a single monofunctional chorismate mutase enzyme.

ORGANISM	PURITY OF PREPARATION	M.W.*	M.W. OF SUBUNITS	KINETICS	K_m or $S_{0.5}$ (mM)	EFFECTS OF TYR	PHE	TRP	REFERENCES
Chlamydomonas reinhardii	partial	61 000	?	linear	0.46	Inh.	Inh.	Ant.	Zurawski and Brown, 1975.
Claviceps paspali	partial	60 000	?	nonlinear	0.46	Inh.	Inh.	Act.	Sprössler and Lingens, 1970.
Euglena gracilis	85%	160 000	?	nonlinear	1.0	Inh.	Inh.	Act.	Weber and Böck, 1970.
Neurospora crassa	crude	?	?	nonlinear	0.1	Inh.	Inh.	Act.	Baker, 1966 and 1968.
Saccharomyces cerevisiae	homogeneous	35 000	?	?	?	Inh.	N.E.	Act.	Lingens et al., 1966. Sprössler et al., 1970.
Streptomyces aureofaciens	homogeneous	51 000 -63 000	14 500	linear	0.52	N.E.	N.E.	N.E.	Görisch and Lingens, 1974.
Streptomyces Sp. 3022a	partial	75 000	?	linear	0.6	N.E.	N.E.	N.E.	Lowe and Westlake, 1972.
Streptomyces venezuelae	partial	55 000	?	linear	0.38	N.E.	N.E.	N.E.	Görisch and Lingens, 1972.

* Abbreviations used are :

M.W.	:	molecular weight
K_m	:	Michaelis constant
$S_{0.5}$	:	substrate concentration giving half-maximum velocity
TYR	:	tyrosine
PHE	:	phenylalanine
TRP	:	tryptophan
Inh.	:	inhibition
Act.	:	activation
Ant.	:	antagonism of phenylalanine and tyrosine inhibition
N.E.	:	no effect.

synthase*, and chorismate mutase is activated by tryptophan, diverting chorismate to tyrosine and phenylalanine biosynthesis (Weber and Böck, 1969). When phenylalanine and tyrosine levels increase, chorismate mutase is inhibited, slowing down the synthesis of these two amino acids, and DAHP synthase (the first enzyme of the shikimate pathway) is also feedback inhibited by tyrosine (Weber and Böck, 1968), thereby cutting down the flow of carbon into the biosynthesis of the aromatic amino acids. Little information is available about the enzymes prephenate dehydrogenase and prephenate dehydratase in these organisms, but the feedback inhibition properties are as expected. Prephenate dehydrogenase from N. crassa is inhibited by tyrosine, activated by phenylalanine and unaffected by tryptophan (Catcheside, 1969), while prephenate dehydratase from C. paspali is inhibited by phenylalanine and unaffected by the other aromatic amino acids (Lingens et al., 1967).

Unlike the enzymes described above, chorismate mutase isolated from several species of Streptomyces is not affected by the aromatic amino acids (Görisch and Lingens, 1972 and 1974; Lowe and Westlake, 1972). In these organisms, the early steps in the biosynthesis of the antibiotic chloramphenicol (whose structure is shown in Fig. 1.19) are common with the biosynthetic pathway for the aromatic amino acids (Vining and Westlake, 1964). Görisch and Lingens (1972) and Lowe and Westlake (1972) suggest that prephenate is the branch-point for the biosynthesis of the phenylpropanoid moiety of chloramphenicol, and the characteris-

---

* The reactions involved in the biosynthesis of the aromatic amino acids have been illustrated in Fig. 1.1

FIGURE 1.19 Structure of chloramphenicol.

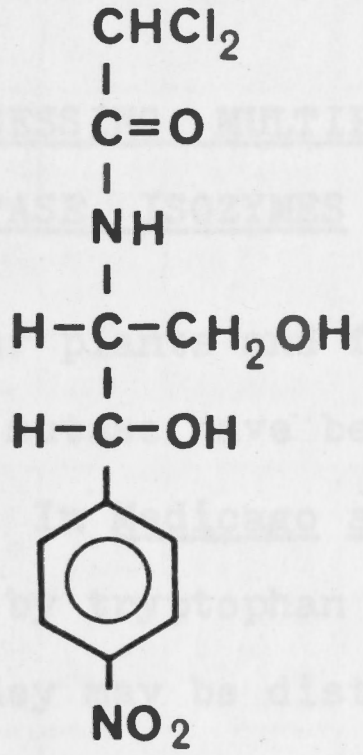

tics of some of the enzymes involved are consistent with this hypothesis (Lowe and Westlake, 1972). While chorismate mutase activity is unaffected by the aromatic amino acids, prephenate dehydratase is feedback inhibited by phenyalanine, and anthranilate synthase by tryptophan, thus providing some control for two of the branches. (Prephenate dehydrogenase has not yet been isolated as a stable preparation.) This pattern of control would ensure a supply of prephenate for the biosynthesis of chloramphenicol when prephenate is no longer required for aromatic amino acid biosynthesis.

1.2.2 ORGANISMS POSSESSING MULTIPLE MONOFUNCTIONAL CHORISMATE MUTASE ISOZYMES

Among the higher plants and fungi, three definite types of isozyme of chorismate mutase have been described (Woodin and Nishioka, 1973 a and b). In Medicago sativa, CM1 and CM3 isozymes are both activated by tryptophan and inhibited by tyrosine and phenylalanine, but they may be distinguished on the basis of electrophoretic mobility, activation energy and the effects of lignin precursors (see Table 1.7 which lists selected properties of the isozymes from some species of plants and fungi). On the other hand, although CM2 is similar to CM1 in its response to lignin and coumarin precursors, it remains unaffected by the aromatic amino acids (Woodin and Nishioka, 1973 b).

The situation in higher plants parallels that in the chloramphenicol-producing Streptomyces species in that the aromatic amino acids are not the final product of the shikimate path-

TABLE 1.7 Selected properties of chorismate mutase isolated from organisms possessing multiple monofunctional enzymes.

ORGANISM	ISOZYMES DETECTED	MOLECULAR WEIGHT	EFFECTS OF						REFERENCES
			TRP*	TYR	PHE	CAFFEATE	3,4-DIMETHOXY CINNAMATE	FERULATE	
Medicago sativa	CM1	46 000	Act.	Inh.	Inh.	Inh.	N.E.	N.E.	Woodin and Nishioka, 1973 b.
	CM2	58 000	N.E.	N.E.	N.E.	Inh.	N.E.	N.E.	
	CM3	69 000	Act.	Inh.	Inh.	N.E.	Act.	Inh.	
Penicillium chrysogenum	CM1	?	Act.	Inh.	Inh.	Inh.	N.E.	?	Woodin and Nishioka, 1973 a.
	CM3	?	Act.	Inh.	Inh.	N.E.	Act.	?	
Penicillium duponti	CM1	?	Act.	Inh.	Inh.	Inh.	N.E.	N.E.	Woodin and Nishioka, 1973 a.
	CM2	?	N.E.	N.E.	N.E.	Inh.	N.E.	N.E.	
	CM3	?	Act.	Inh.	Inh.	Act.	Act.	Inh.	
Phaseolus aureus	CM1	50 000	Act. & Ant	Inh.	Inh.	Inh.	N.E.	?	Gilchrist and Kosuge, 1974 and 1975.
	CM2	36 000	N.E.	N.E.	N.E.	Inh.	N.E.	?	

* Abbreviations used are :-

TRP : tryptophan
TYR : tyrosine
PHE : phenylalanine

Act. : activation
Inh. : inhibition
N.E. : no effect
Ant. : antagonism of tyrosine and phenylalnine inhibition.

way : these amino acids are precursors in their turn of the alkaloids, coumarins and lignin (see Fig. 1.20). The existence of the isozymes ensures production of at least low levels of prephenate regardless of the plant's requirements for aromatic amino acids, thus ensuring the production of precursors of the structural product lignin, and the coumarins and alkaloids.

Although similar isozymes have been described in the fungi Penicillium chrysogenum and P. duponti (Woodin and Nishioka, 1973 a), not enough is known of aromatic metabolism in the fungi to draw conclusions about their role. It is possible that their function is associated with the biosynthesis of alkaloids.

Once again, little information is available about prephenate dehydrogenase and prephenate dehydratase in these organisms. Gamborg and Keeley (1966) reported that prephenate dehydrogenase from Phaseolus vulgaris L. is unaffected by aromatic acids or benzoic acid derivatives. This observation is consistent with the conclusion of Woodin and Nishioka (1973 b) that it is the rearrangement of chorismate to prephenate which is highly regulated in plants, rather than subsequent steps. It is interesting to note that prephenate dehydrogenase from P. vulgaris L. requires NADP rather than NAD; NADP may replace NAD in the case of prephenate dehydrogenase from Aerobacter aerogenes but was reported to be less effective (Cotton and Gibson, 1967).

FIGURE 1.20 Some possible metabolites of chorismate in the higher plants. (Adapted from Fig. 2, Woodin and Nishioka, 1973 b.)

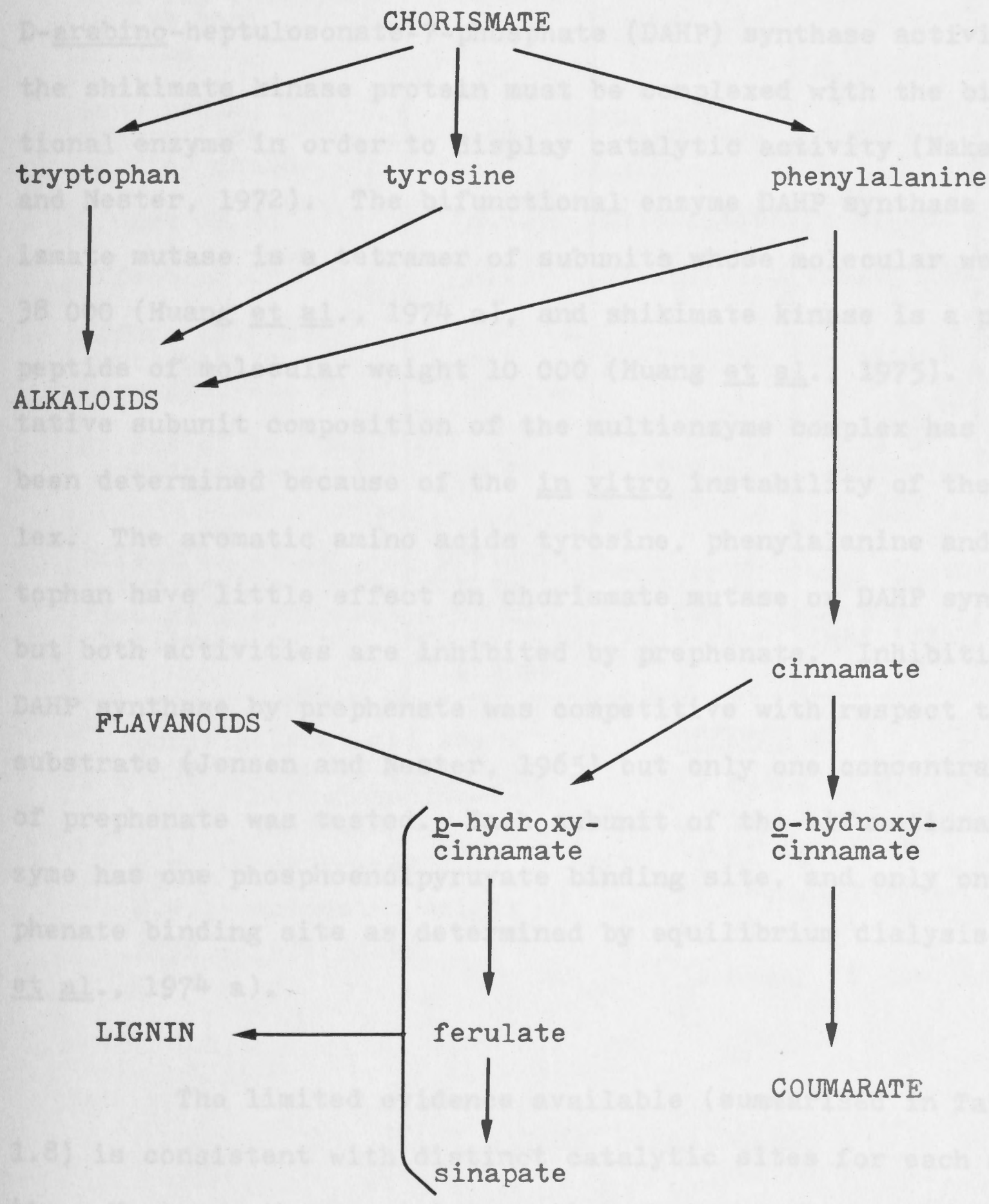

1.2.3 ORGANISMS POSSESSING A SINGLE CHORISMATE MUTASE AS ONE ACTIVITY OF A BIFUNCTIONAL ENZYME

In Bacillus subtilis 168, only one form of chorismate mutase has been identified. This protein also possesses 3-deoxy-D-arabino-heptulosonate-7-phosphate (DAHP) synthase activity, and the shikimate kinase protein must be complexed with the bifunctional enzyme in order to display catalytic activity (Nakatsukasa and Nester, 1972). The bifunctional enzyme DAHP synthase - chorismate mutase is a tetramer of subunits whose molecular weight is 38 000 (Huang et al., 1974 a), and shikimate kinase is a polypeptide of molecular weight 10 000 (Huang et al., 1975). Quantitative subunit composition of the multienzyme complex has not been determined because of the in vitro instability of the complex. The aromatic amino acids tyrosine, phenylalanine and tryptophan have little effect on chorismate mutase or DAHP synthase, but both activities are inhibited by prephenate. Inhibition of DAHP synthase by prephenate was competitive with respect to each substrate (Jensen and Nester, 1965) but only one concentration of prephenate was tested. Each subunit of the bifunctional enzyme has one phosphoenolpyruvate binding site, and only one prephenate binding site as determined by equilibrium dialysis (Huang et al., 1974 a).

The limited evidence available (summarised in Table 1.8) is consistent with distinct catalytic sites for each activity. However, there are interactions between the catalytic site for chorismate mutase and each of the other activities. The

TABLE 1.8 DAHP synthase - chorismate mutase : shikimate kinase:- evidence consistent with distinct catalytic sites for each activity.

	CATALYTIC ACTIVITY			
	SHIKIMATE KINASE	DAHP* SYNTHASE	CHORISMATE MUTASE	REFS.
Activity catalysed by 10 000 M.W. species	+	-	-	1
Activity catalysed by $(38\ 000)_4$ species	-	+	+	1
Gene coding for appropriate poly-peptide chain	*aro* I	*aro* (AG)	*aro* (AG)	2,3
Effect of Cd^{2+}	n.t.	stimulation	no effect	4
Effect of Cu^{2+}	n.t.	stimulation	inhibition	4
Effect of p-mercuribenzoate, bromopyruvate	n.t.	inhibition	no effect	4
Effect of limited trypsin treatment	n.t.	little effect	almost complete loss	5
Effect of anti-serum against purified DAHP synthase-chorismate mutase	prevents activation by bi-functional enzyme	maximum 20% inhibition	maximum 80% inhibition	5

* Abbreviations used are :
DAHP : 3-deoxy-D-*arabino*-heptulosonate-7-phosphate
n.t. : not tested
M.W. : molecular weight
REFS : references

REFERENCES :

1. Huang *et al.*, 1975.
2. Lepesant-Kejzlarovà *et al.*, 1975.
3. Hoch and Nester, 1973.
4. Huang *et al.*, 1974 b.
5. Huang *et al.*, 1974 a.

expression of shikimate kinase activity is dependent on association of the enzyme with a catalytically competent chorismate mutase, as indicated by genetic studies (Nakatsukasa and Nester, 1972) and comparison of the effects of native DAHP synthase - chorismate mutase and its tryptic fragments on shikimate kinase activity (Huang et al., 1974 a). DAHP synthase activity is also influenced by events at the chorismate mutase catalytic site. As chorismate mutase activity is progressively lost on tryptic digestion of the bifunctional enzyme, there is a parallel decrease in the sensitivity of DAHP synthase to inhibition by prephenate (Huang et al., 1974 a). Since there is only one prephenate binding site per subunit, this is presumably lost with chorismate mutase activity, suggesting that the prephenate inhibition of DAHP synthase is mediated by binding of prephenate at the chorismate mutase site.

Champney and Jensen (1970) have reported several properties of a crude preparation of prephenate dehydrogenase from B. subtilis NP 40, a spontaneous full revertant of strain 168. (Strain 168 carries a mutation in the gene specifying indoleglycerol phosphate synthase and is, therefore, blocked in tryptophan biosynthesis (Crawford, 1975).) Intersecting initial velocity patterns were obtained for prephenate dehydrogenase, and tyrosine and phenylalanine were competitive inhibitors with respect to prephenate, while tryptophan and the product of the reaction, 4-hydroxyphenylpyruvate, were noncompetitive with respect to prephenate. All inhibitors were tested at a single concentration.

However, neither the inhibition by these compounds with respect to NAD nor the inhibition by NADH was investigated. Moreover, it is possible that the results reported by Champney and Jensen were complicated by the presence of prephenate dehydratase in their crude preparation, but the authors make no mention of this, nor of the possibility of interference by nonspecific dehydrogenases.

Prephenate dehydratase isolated from B. subtilis 168 is susceptible to competitive inhibition by phenylalanine and tryptophan which are about equally effective. Double reciprocal plots were linear at the single concentration of each compound for which data are presented (Rebello and Jensen, 1970). The role of tyrosine is not clear. While Nester and Jensen (1966) reported inhibition by tyrosine at concentrations exceeding 0.1 mM, a subsequent report indicated that although tyrosine alone has little effect, at relatively high concentrations it relieves the inhibition by tryptophan (Rebello and Jensen, 1970). Finally, Pierson and Jensen (1974) reported that the antagonistic effect of tyrosine towards phenylalanine inhibition could not be repeated, but did not clarify the situation with respect to the effect of tyrosine alone. The inhibitors phenylalanine and tryptophan promote dissociation of the enzyme from a 210 000 molecular weight species to one with molecular weight 55 000 (Pierson and Jensen, 1974). The enzyme may also be regulated by means of activation by leucine and methionine (Jensen, 1969; Rebello and Jensen, 1970). These non-aromatic amino acids promote association of the enzyme even in the presence of tryptophan, but not in the presence of phenylalanine (Pierson and Jensen, 1974).

From the properties of the enzyme DAHP synthase - chorismate mutase and prephenate dehydratase isolated from B. subtilis 168, and prephenate dehydrogenase from a close relative, it would appear that chorismate mutase is not inhibited until the prephenate concentration has risen, as a result of the feedback inhibition of the dehydrogenase and dehydratase activities. Moreover, DAHP synthase activity is inhibited by prephenate concomitantly with chorismate mutase, thereby slowing the flow of phosphoenolpyruvate and erythrose-4-phosphate into aromatic amino acid biosynthesis.

The only other organism known to possess a single chorismate mutase which exists as one activity of a bifunctional enzyme is the bacterium Alcaligenes eutrophus whose chorismate mutase protein also displays prephenate dehydratase activity (Friedrich et al., 1976 a and b). Native chorismate mutase - prephenate dehydratase from this organism has a molecular weight of 180 000 with subunits of 47 000 molecular weight, suggesting a tetrameric structure. Substrate saturation curves for both chorismate and prephenate are hyperbolic in the absence of modifiers, and Michaelis constants for chorismate and prephenate are 0.2 and 0.67 mM, respectively, at pH 7.8. Phenylalanine inhibits the mutase activity above pH 7.2. At pH 7.8, phenylalanine induces concave-up double reciprocal plots and is competitive with respect to chorismate on the basis that double reciprocal plots at different phenylalanine concentrations appear to have a common point of intersection on the vertical axis. Prephenate is also a competitive inhibitor of chorismate mutase (on the same

basis as phenylalanine) but induces double reciprocal plots which are concave-down. On the other hand, prephenate dehydratase exhibits Michaelis-Menten kinetics even in the presence of the linear competitive inhibitors phenylalanine and tryptophan, or the activator tyrosine, which decreases the apparent Michaelis constant for prephenate and increases the apparent maximum velocity. Friedrich et al. (1976 b) have suggested that the active sites for chorismate mutase and prephenate dehydratase are not identical because (a) mutants with normal chorismate mutase activity but which lack prephenate dehydratase activity have been isolated and (b) in the overall reaction (chorismate → prephenate → phenylpyruvate) prephenate accumulates in the medium to a relatively high concentration before prephenate dehydratase activity can be detected. Other suggestive evidence is the differential effect of bivalent cations which inhibit the dehydratase activity to a greater extent than the mutase activity.

Friedrich et al. (1976 a and b) have also investigated prephenate dehydrogenase isolated from A. eutrophus. It is a monofunctional enzyme of molecular weight about 55 000, whose kinetics are Michaelis-Menten with respect to both substrates in the absence of modifiers. However, a full kinetic study has not been reported, and the Michaelis constant for prephenate (0.045 mM) was determined at a high fixed concentration of NAD. The product 4-hydroxyphenylpyruvate was reported to be a competitive inhibitor with respect to prephenate (data not shown) and tyrosine, the end product, is a linear noncompetitive inhibitor with respect to NAD. Tyrosine induces concave-up double reciprocal plots when

prephenate is the varied substrate, but plots of 1/v against tyrosine concentration at different fixed prephenate concentrations (Dixon plots) are linear with a common point of intersection whose vertical coordinate is positive (horizontal coordinate negative), indicative of competitive inhibition. The authors also indicated that the compounds dihydroxyphenylalanine and hydroxycinnamate (coumarate) inhibited competitively, but did not specify which substrate was varied.

Although tyrosine can be formed by hydroxylation of phenylalanine in tyrosine auxotrophic mutants of A. eutrophus, the normal role of phenylalanine hydroxylase is believed to be in the catabolism of phenylalanine (Friedrich and Schlegel, 1972). Therefore, prephenate dehydrogenase must compete effectively with prephenate dehydratase for the prephenate formed by chorismate mutase. This is supported by the difference in turnover numbers between chorismate mutase and prephenate dehydratase (2210 and 350 mol/min/mol enzyme, respectively). Friedrich et al. (1976 b) assume that because chorismate mutase and prephenate dehydratase activities reside on the same protein, there is normally a preferential flow of chorismate into phenylalanine biosynthesis, but the available evidence suggests the contrary. Were chorismate to be channelled preferentially into phenylalanine biosynthesis, not only prephenate dehydratase but also chorismate mutase would be inhibited when the phenylalanine level rises, and therefore both tyrosine and phenylalanine biosynthesis would be slowed. However, preferential flow of chorismate into tyrosine biosynthesis would have the result that an excessive level of tyrosine would

inhibit prephenate dehydrogenase, but activate prephenate dehydratase, thus diverting the flow of prephenate to phenylalanine biosynthesis. Only when the requirements for both these amino acids were filled would chorismate mutase be inhibited by a high level of phenylalanine.

1.2.4 ORGANISMS POSSESSING BOTH THE BIFUNCTIONAL ENZYMES CHORISMATE MUTASE - PREPHENATE DEHYDROGENASE AND CHORISMATE MUTASE - PREPHENATE DEHYDRATASE

The enterobacteria *Aerobacter aerogenes*, *Escherichia coli* and *Salmonella typhimurium* have been shown to possess two chorismate mutase enzymes, each of which is one activity of a bifunctional enzyme. These enzymes, chorismate mutase - prephenate dehydrogenase and chorismate mutase - prephenate dehydratase, catalyse the first two steps in the reaction pathway from chorismate to tyrosine and phenylalanine, respectively, the reactions being :

$$\text{chorismate} \xrightarrow[\text{mutase}]{\text{chorismate}} \text{prephenate}$$

$$\text{prephenate} + \text{NAD} \xrightarrow[\text{dehydrogenase}]{\text{prephenate}} \text{4-hydroxyphenylpyruvate} + \text{NADH} + CO_2 \qquad (1.78)$$

$$\text{chorismate} \xrightarrow[\text{mutase}]{\text{chorismate}} \text{prephenate}$$

$$\text{prephenate} \xrightarrow[\text{dehydratase}]{\text{prephenate}} \text{phenylpyruvate} + CO_2 \qquad (1.79)$$

Table 1.9 compares some physical properties of the enzymes chor-

TABLE 1.9(a) Comparison of some physical properties of chorismate mutase - prephenate dehydrogenase isolated from A. aerogenes and E. coli and chorismate mutase - prephenate dehydratase isolated from E. coli and S. typhimurium.

Enzyme	Chorismate mutase-prephenate dehydrogenase		Chorismate mutase-prephenate dehydratase	
Source	A. aerogenes	E. coli	E. coli	S. typhimurium
Purity of preparation	95%	95-100%	95-100%	partial
Molecular weight	76 000	82 000	85 000	~109 000
Subunit molecular weight	39 000	41 000	40 000	N.D.*
Number of tryptic peptides :				
obtained	35-40	35-40	37-43	N.D.
predicted for				
—identical subunits	38	38	38	N.D.
—nonidentical subunits	76	75	75	N.D.
Polymerisation induced by feedback inhibitor	N.D.	yes	yes	yes
References	1-2	3-5	6-8	9-10

* N.D. : not determined

TABLE 1.9(b) Comparison of the amino acid compositions of chorismate mutase - prephenate dehydratase from E. coli and chorismate mutase - prephenate dehydrogenase from E. coli and A. aerogenes.*

Enzyme	Chorismate mutase - prephenate dehydratase	Chorismate mutase - prephenate dehydrogenase	
Source	E. coli	E. coli	A. aerogenes
Lys	34	34	36
His	26	17	17
Arg	39	43	44
Cya	7	8	8
Asp	61	72	73
Thr	38	36	38
Ser	37	33	38
Glu	97	85	86
Pro	29	32	36
Gly	39	58	61
Ala	71	79	85
Val	47	50	53
Met	13	18	18
Ile	43	38	37
Leu	91	70	72
Tyr	19	19	21
Phe	22	24	28
Trp	4	7	8

* The numbers in the table are the nearest integral values calculated for a "standard" molecular weight of 80 000. Originally published figures were based on molecular weights of 40 6000 for E. coli chorismate mutase - prephenate dehydratase (Ref. 5), and 82 000 and 76 000 for chorismate mutase - prephenate dehydrogenase isolated from E. coli and A. aerogenes, respectively (Ref. 3 and 1).

TABLE 1.9 REFERENCES

1. Koch *et al.*, 1970 a.
2. Koch *et al.*, 1970 b.
3. Koch *et al.*, 1971 a.
4. Koch *et al.*, 1971 b.
5. Llewellyn and Smith, 1977.
6. Davidson *et al.*, 1972.
7. Gething and Davidson, 1976.
8. Baldwin, 1974.
9. Schmit and Zalkin, 1969.
10. Schmit and Zalkin, 1971.

ismate mutase - prephenate dehydrogenase isolated from A. aerogenes and E. coli and chorismate mutase - prephenate dehydratase from E. coli and S. typhimurium. Little information about chorismate mutase - prephenate dehydrogenase from S. typhimurium or the chorismate mutase-prephenate dehydratase from A. aerogenes has been reported.

Chorismate mutase - prephenate dehydrogenase isolated from A. aerogenes and E. coli and chorismate mutase - prephenate dehydratase from E. coli are similar in their molecular weights, subunit size, amino acid composition and the number of peptides obtained by tryptic digestion. About 50% homology has been reported for the chorismate mutase - prephenate dehydrogenase enzymes of E. coli and A. aerogenes on the superficial basis of position and intensity of spots on peptide maps of the enzymes (Koch et al., 1971 b). Sequence data are available only for chorismate mutase - prephenate dehydratase from E. coli (Gething and Davidson, 1976; Baldwin, 1974) and therefore it is not possible to say how closely the enzymes are related in their primary structure.

The molecular weight of chorismate mutase - prephenate dehydratase isolated from S. typhimurium appears to be much greater than those of the other enzymes considered in Table 1.9 but the apparent molecular weight depends on the method of estimation, 109 000 obtained by sucrose gradient centrifugation and 88 000 by gel filtration. However, using both methods, Schmit and Zalkin (1971) have shown that the enzyme undergoes dimerisation in the presence of the feedback inhibitor phenyl-

TABLE 1.10 Comparison of some kinetic properties of chorismate mutase - prephenate dehydrogenase and chorismate mutase - prephenate dehydratase from selected organisms.

Enzyme	Chorismate mutase-prephenate dehydrogenase	
Organism	*A. aerogenes*[e]	*E. coli*
Purity of enzyme preparation	95%	95-100%
Kinetics with respect to :		
chorismate	Linear	Nonlinear[a,b]
prephenate	Linear	Nonlinear[a,b]
NAD	Linear	Linear
K_m[c] or $[S]_{0.5}$ (mM)		
chorismate	1.3	0.39
prephenate	0.35 (app)	0.37 (app)
NAD	0.6 (app)	0.33 (app)
Feedback inhibitor	Tyrosine	Tyrosine
Effects of feedback inhibitor with respect to :		
chorismate	No effect up to 3 mM	No effect up to 4 mM
prephenate	Competitive[a] inhibition	Competitive[a] inhibition
NAD	Noncompetitive inhibition	Noncompetitive inhibition
Prephenate inhibition of chorismate mutase	Competitive K_i = 0.31 mM	Not determined
References	1 - 3	3 - 4

Enzyme	Chorismate mutase - prephenate dehydratase	
Organism	*E. coli*	*S. typhimurium*
Purity of enzyme preparation	95-100%	partial
Kinetics with respect to : chorismate prephenate NAD	Linear Linear Not applicable	Linear Nonlinear Not applicable
K_m [c] or $[S]_{0.5}$ (mM) chorismate prephenate NAD	0.045 (0.024) 1.0 (0.47) Not applicable	0.08 0.35 Not applicable
Feedback inhibitor	Phenylalanine	Phenylalanine
Effects of feedback inhibitor with respect to : chorismate prephenate	Competitive[d] inhibitor ? Competitive[a,d] inhibitor ?	Competitive[a] inhibitor Competitive[a] inhibitor
Prephenate inhibition of chorismate mutase	Competitive K_i=0.06 mM (0.031 mM)	Linear competitive K_i = 0.1 mM
References	5 - 7 (9)	8

TABLE 1.10 (Continued).

Notes :

(a) Double reciprocal plots concave-up.

(b) Chorismate mutase - prephenate dehydrogenase purified from E. coli JP2132 exhibits Michaelis-Menten kinetics (P. Sampathkumar, personal communication).

(c) Abbreviations used are :

K_m - Michaelis constant.

$S_{0.5}$ - substrate concentration giving half maximum velocity.

app - apparent.

K_i - inhibition constant.

(d) Relevant data of Reference 6 plotted as substrate saturation curves and Dixon plots (chorismate mutase) or Hill plots (prephenate dehydratase). Replotting data in double reciprocal form yields (nonlinear) competitive inhibition of chorismate mutase and, for prephenate dehydratase, concave-up double reciprocal plots which may have a common point of intersection on the vertical axis.

(e) Data of Heyde and Morrison (1978) will be discussed in Chapter 3.

REFERENCES :

1. Koch et al., 1970 a.
2. Cotton and Gibson, 1965.
3. Koch et al., 1972.
4. Koch et al., 1971 a.
5. Davidson et al., 1972.
6. Dopheide et al., 1972.
7. Davidson, B.E., and Dopheide, T.A.A., unpublished results cited by Gething, 1973.
8. Schmit and Zalkin, 1969.
(9) Duggleby et al., 1978.

alanine. A similar phenomenon has been observed with chorismate mutase - prephenate dehydratase from E. coli, the smallest polymer observed having a molecular weight of 162 000 (Baldwin, 1974). Cotton and Gibson (1968) reported that tyrosine did not prevent acid-promoted dissociation of chorismate mutase - prephenate dehydrogenase from A. aerogenes but did not indicate what effect tyrosine alone might have. Chorismate mutase - prephenate dehydrogenase isolated from E. coli K12 is, in solution, an equilibrium mixture of dimers and tetramers. In the absence of tyrosine, the equilibrium favours the dimer, while in its presence the tetramer is the predominant form (Llewellyn and Smith, 1977).

Table 1.10 summarises certain kinetic properties of chorismate mutase - prephenate dehydrogenase isolated from A. aerogenes and E. coli and chorismate mutase - prephenate dehydratase from E. coli and S. typhimurium. Except in the case of prephenate dehydratase from S. typhimurium, these enzymes normally exhibit Michaelis-Menten behaviour. Although Koch et al. (1971 a) reported nonlinear kinetics with respect to chorismate and prephenate for E. coli chorismate mutase - prephenate dehydrogenase, more recent investigation has established that the enzyme displays Michaelis-Menten kinetics (P. Sampathkumar, personal communication). Although prephenate dehydrogenase catalyses a bisubstrate reaction, a full steady state investigation had not been reported for the enzymes from A. aerogenes or E. coli when the work reported in this thesis was begun. Preliminary results obtained with the enzyme from A. aerogenes

were consistent with a rapid equilibrium random mechanism involving the formation of two dead end complexes, enzyme-NAD-4-hydroxyphenylpyruvate and enzyme-prephenate-NADH. (These investigations were performed by the late Dr. R.K. Ghambeer.) While there was no evidence in the literature that the mutase activity of chorismate mutase - prephenate dehydrogenase is inhibited by the end product, tyrosine, the mutase activity of chorismate mutase - prephenate dehydratase is inhibited competitively by phenylalanine. Both prephenate dehydrogenase and prephenate dehydratase are inhibited by the end product (tyrosine or phenylalanine, respectively) with prephenate dehydratase being more susceptible to phenylalanine inhibition than the mutaseactivity (Dopheide et al., 1972; Schmit and Zalkin, 1969).

Several workers have addressed themselves to the question of whether these bifunctional enzymes catalyse both reactions at the same or overlapping active centre(s), or whether the active sites are located in separate domains of the protein. Crystallographic data are not available for either of the enzymes under discussion, so that conclusions about the relationship of the active sites have been based on the following lines of evidence : (a) effects of mutations, (b) differential effects of inhibitors and chemical modification of the protein structure, and (c) studies of the overall reaction.

In the case of chorismate mutase - prephenate dehydratase, the evidence is consistent with there being separate active sites. Schmit et al. (1970) and Pittard and Wallace (1966) have described S. typhimurium and E. coli strains which

lack only the mutase activity of chorismate mutase - prephenate dehydratase, while Baldwin (1974) has, from two mutant strains of E. coli, purified to homogeneity a protein which behaves like wild type chorismate mutase - prephenate dehydratase during purification, but which lacks prephenate dehydratase activity. Gething (1973) has found that modification of chorismate mutase - prephenate dehydratase from E. coli by sulphydryl reagents or tetranitromethane results in a loss of dehydratase activity but mutase activity is retained. Enzyme modified with 5,5'-dithio-bis-(2-nitrobenzoic acid) (DTNB) still binds prephenate although it is no longer catalytically competent in the dehydratase reaction. Similarly, sulphydryl reagents cause preferential loss of the dehydratase activity of the enzyme from S. typhimurium (Schmit et al., 1970). Limited investigations of the overall reaction catalysed by chorismate mutase - prephenate dehydratase from E. coli and S. typhimurium (B.E. Davidson and T.A.A. Dopheide, unpublished results cited by Gething, 1973; Schmit and Zalkin, 1969) have shown that prephenate generated from chorismate dissociates significantly from the enzyme, and there is a significant lag in the production of phenylpyruvate. This parallels the situation with chorismate mutase - prephenate dehydratase isolated from Alcaligenes eutrophus (discussed in Section 1.2.3). At least in the case of the enzyme from E. coli, the concentration of prephenate attained in the overall reaction is high enough to account for the rate of the dehydratase reaction. Duggleby et al. (1978) deduced that if both the mutase and dehydratase reactions are catalysed at a single active site, the K_m value for prephenate as a substrate for the

dehydratase reaction must equal its K_i value as an inhibitor of the mutase reaction. In fact, this relationship does not hold for the enzymes isolated from S. typhimurium and E. coli (see Table 1.10), and, at least in the case of the enzyme from E. coli, there is no evidence for direct channeling of prephenate from the mutase to the dehydratase site, or for any strong interaction between the sites.

In contrast with the above results, experiments with chorismate mutase - prephenate dehydrogenase isolated from E. coli and A. aerogenes have yielded results consistent with a model involving a common site for the two catalytic activities. Koch et al. (1972) reported that in the overall reaction, no significant concentration of free prephenate is established before prephenate dehydrogenase activity is detected, and the maximum prephenate concentration attained is by no means high enough to account for the rate of dehydrogenase activity measured. Although the enzyme from E. coli displayed a slight lag in reaching the maximum rate of NADH production, this was not the case with the enzyme isolated from A. aerogenes. More recently, Heyde (1978) has reported that the enzyme from A. aerogenes converts chorismate and NAD to 4-hydroxyphenylpyruvate and NADH faster than expected on the basis of separate non-interacting sites. Comparison of simulations of the time course of the overall reaction with experimental data was consistent with a model based on a single active site if a minor proportion of chorismate that reacts can be converted to 4-hydroxyphenylpyruvate without the intermediate release of prephenate; consistent

with this requirement, some channeling of radioactivity from chorismate to 4-hydroxyphenylpyruvate was detected (Heyde, 1978). Koch et al. (1972) and Heyde (1978) found that the mutase and dehydrogenase activities of chorismate mutase - prephenate dehydrogenase from A. aerogenes were not affected differentially by sulphydryl reagents, tetranitromethane, N-bromosuccinimide, carboxypeptidase A and other treatments, and equal protection was afforded by chorismate and prephenate but neither NAD nor tyrosine protected against inactivation. Similarly, trypsin nonselectively inactivates the mutase and dehydrogenase activities with some protection afforded by prephenate but not by NAD (P.K. Dudziński, unpublished results). Koch also demonstrated that the modification of a single sulphydryl group which is protected by prephenate leads to equal loss of both the mutase and dehydrogenase activities. Finally, mutant strains of E. coli and A. aerogenes with lesions in the gene specifying chorismate mutase - prephenate dehydrogenase have lacked both enzymic activities of this protein (Cotton and Gibson, 1965).

1.3 AIMS OF THE WORK PRESENTED IN THIS THESIS

The general aim of the work presented in this thesis was to further the knowledge of the way enzymes function. Without enzymes, the chemical reactions which occur in living organisms would take place far too slowly to sustain life as we know it. Moreover, a proper balance is usually maintained between the synthesis and degradation of a wide variety of compounds. It is a challenging problem, therefore, to try to understand how enzymes function as catalysts, and how the coordination of their activities is acheived so that imbalances do not occur. The investigation of the kinetic properties of a particular enzyme, chorismate mutase - prephenate dehydrogenase, was a way of approaching this aim.

Specifically, the aims were :

to develop a procedure for the preparation and purification of the substrate, prephenate, in reasonable quantities and in a form suitable for enzyme kinetic studies, and

to investigate the steady state kinetic properties of the dehydrogenase reaction catalysed by chorismate mutase - prephenate dehydrogenase in order to determine the sequence of events on the enzyme surface i.e. to determine the kinetic mechanism.

CHAPTER 2

THE PREPARATION AND PURIFICATION OF SODIUM PREPHENATE

CHAPTER 2

THE PREPARATION AND PURIFICATION OF SODIUM PREPHENATE

2.1 INTRODUCTION

In order to carry out the kinetic studies reported in this thesis it was essential to have reasonable amounts of the substrates chorismate and prephenate which are not commercially available in pure form. The procedure of Gibson (1968) for the isolation and purification of chorismic acid gave good yields of pure material. A variety of methods has been used to prepare prephenate in connection with studies of prephenate dehydrogenase and prephenate dehydratase. Barium prephenate has been isolated from culture filtrates of a phenylalanine-requiring mutant of Escherichia coli (Weiss et al., 1954), a tyrosine auxotroph of Salmonella typhimurium (Dayan and Sprinson, 1970) and a triple mutant of Neurospora crassa (Metzenberg and Mitchell, 1956). The yields from these procedures were 20-50% and the product was 93-99% pure. Only impure samples of barium prephenate have been obtained either by chemical synthesis (Plieninger, 1962) or by heating chorismate at alkaline pH (Gibson, 1964). Prephenate has also been prepared enzymically from chorismate using chorismate mutase - prephenate dehydrogenase (Koch et al., 1970 a). The product of that procedure, however, was not isolated, and it seems likely that prephenate solutions used for subsequent experimentation would have been contaminated by compounds which may

arise non-enzymically from chorismate (Young et al., 1969).

Because chorismic acid and chorismate mutase - prephenate dehydrogenase were already being prepared in our laboratory it seemed preferable to isolate prephenate following its enzymic formation from chorismate, rather than to obtain the compound from culture filtrates.

2.2 MATERIALS AND METHODS

2.2.1 CHEMICALS

Chorismic acid was prepared by the method of Gibson (1968), recrystallised from ethyl acetate/petroleum ether and stored over dessicant at -15°C until use. Rhodizonic acid was a product of B.D.H. CNBr-Sepharose was purchased from Pharmacia. All other chemicals were of analytical grade or of the best grade available.

2.2.2 PREPARATION OF ENZYME

Chorismate mutase - prephenate dehydrogenase was purified from extracts of a multiple aromatic auxotroph, Aerobacter aerogenes Poly 3 by a modification of the procedure described by Koch et al. (1970 a). Although impure enzyme was used originally, the procedure has been repeated with nearly pure enzyme. For the particular preparation reported here, enzyme used was free of prephenate dehydratase activity (assayed by a modification of the

procedure of Cotton and Gibson (1965)) and had a specific activity of 3.1 units/mg of protein. One unit of activity is defined as the amount of enzyme which produces one μmole of prephenate per minute in the presence of 1.5 mM chorismate at pH 7.5 and 30°C. Enzyme used for coupling to Sepharose had a specific activity of 4.0 units/mg of protein. In comparison, pure enzyme has a specific activity of about 30 units/mg.

2.2.3 DETERMINATION OF REACTANT CONCENTRATIONS

(a) Chorismate

Routine determinations of chorismate concentrations were carried out by conversion of chorismate to 4-hydroxyphenylpyruvate by chorismate mutase - prephenate dehydrogenase. The reaction was performed at 30°C in 0.1 M Tris-HCl, pH 7.5, in the presence of excess NAD. The concentration of chorismate was determined from the amount of NAD reduced, which was calculated from the change in absorbance at 340 nm using a molar extinction coefficient of 6 500 for equimolar mixtures of NADH and 4-hydroxyphenylpyruvate (R.K. Ghambeer, unpublished results). Rapid estimations of chorismate concentrations were based on its absorbance at 273 nm using a molar extinction coefficient of 2 630 (Edwards and Jackman, 1965).

(b) Prephenate

Prephenate concentrations were estimated by either of the following two methods :

(i) acid hydrolysis to phenylpyruvate, whose molar extinction coefficient was taken to be 17 600 at 320 nm (Gibson

and Gibson, 1964).

(ii) conversion of prephenate to 4-hydroxyphenylpyruvate by chorismate mutase - prephenate dehydrogenase. The reaction was performed at 30°C in 0.1 M Tris-HCl, pH 7.5, in the presence of excess NAD, and the concentration of prephenate was determined from the amount of NAD reduced, which was calculated as described above.

(c) Protein

The concentration of partially purified preparations of chorismate mutase - prephenate dehydrogenase was estimated spectrophotometrically at 280 nm using an extinction coefficient of 1.0 absorbance unit per cm per mg.

2.2.4 TEST FOR BARIUM

Rhodizonic acid was used to test for the presence of barium. In the absence of barium, filter paper soaked in rhodizonic acid solution is yellow; in the presence of barium a pink colour is observed.

2.2.5 NMR SPECTRA

NMR spectra were obtained on a Varian T60A instrument using tetramethyl silane as an external standard.

2.2.6 COUPLING OF CHORISMATE MUTASE - PREPHENATE DEHYDROGENASE TO SEPHAROSE

1.1 g CNBr-Sepharose 4B was swollen in and extensively

washed with 1 mM HCl. The gel was then washed in 10 ml 0.1 M $NaHCO_3$ containing 0.5 M NaCl, pH 8.0, and suspended in 10 ml of the same buffer. To the gel suspension was added 0.5 ml of a solution containing 6.4 units of chorismate mutase (1.6 mg of protein) per ml. The mixture was incubated in a shaking water bath at room temperature for one hour, and after this time the gel was collected by filtration and washed extensively with the following buffers : 0.1 M acetate, 0.5 M NaCl (pH 5.0); 0.1 M $NaHCO_3$, 0.5 M NaCl (pH 8.0); 0.1 M Tris-HCl, pH 7.5, containing 1 mM EDTA and 1 mM dithiothreitol (DTT). The final product was stored in the last-mentioned buffer at $4^{\circ}C$.

2.2.7 ESTIMATION OF CHORISMATE MUTASE ACTIVITY OF SEPHAROSE - BOUND ENZYME

1 ml of packed gel was equilibrated with, then resuspended in 0.1 M Tris-HCl, pH 7.5, containing 1 mM EDTA, 1 mM DTT and 1.5 mM sodium chorismate. The suspension was incubated in a shaking water bath at $30^{\circ}C$ for an appropriate time, when the gel was separated from the test solution. An aliquot of the test solution incubated under the same conditions but not in contact with gel served as the control. The concentrations of prephenate in the test, the control and the original solutions were estimated by acid hydrolysis to phenylpyruvate (2.2.3 (c) above).

2.3 RESULTS

2.3.1 PREPARATION OF PREPHENATE USING ENZYME IN FREE SOLUTION

The reaction mixture, which contained 0.1 M Tris-HCl buffer (pH 7.5), 88 mM chorismate and 26 units (8.5 mg) of purified chorismate mutase - prephenate dehydrogenase in a total volume of 21 ml, was incubated at 37°C until the rate of disappearance of chorismate was negligible (50 min). Disappearance of chorismate was followed at 273 nm after a 1 to 300 dilution of samples with 50 mM NaOH. In a typical preparation the absorbance of diluted samples was allowed to decrease from 0.77 to 0.06. The mixture was cooled to 4°C and all further processing was carried out at the same temperature. The concentration of prephenate was estimated by acid hydrolysis and the solution was diluted to 20 mM prephenate with glass-distilled water. (If this step was omitted the final product was contaminated by Tris as judged by the presence of nitrogen.) To each 100 ml of diluted prephenate solution was added, with stirring, 33 ml of 1.4% (w/v) barium bromide in 80% (v/v) ethanol. The mixture was allowed to stand for 1 hr and then centrifuged at 27 000 x g for 10 min to remove a small precipitate. The clear supernatant solution was stirred during the addition, to each 100 ml, of 50 ml of chilled 80% (v/v) ethanol containing 1.4% (w/v) barium bromide and then 450 ml of absolute ethanol. The final concentration of ethanol was 85%. The white gelatious precipitate was allowed to stand overnight before collection by centrifuging at 23 000 x g for 10 min. The precipitate was washed twice with absolute ethanol, and twice

with ether, then dried overnight *in vacuo* over P_2O_5 and paraffin wax.

The barium prephenate was dissolved in 65 ml of glass-distilled water to give a prephenate concentration of about 20 mM and the insoluble material was removed by centrifuging at 27 000 x g for 15 min. The barium salt of prephenate was converted to a sodium salt by passage of the supernatant through a column (1 x 20 cm) of Zeokarb 225 (Na^+ form). The solution of sodium prephenate, which was free of barium, was lyophilised.

In different preparations the overall recovery of prephenate from chorismate was about 65% and the colour of the final product varied from dark to pale pink. The solid was stored over dessicant at -15°C. Solutions of the compound at a concentration of 2 mM were stable for at least two months when stored at -15°C.

2.3.2 ANALYSIS OF SODIUM PREPHENATE

Chemical estimation showed that the product contained less than 0.5% phenylpyruvate. Elementary analysis was compatible with the formula $C_{10}H_8O_{16}.1.5H_2O$ (*Found* : C, 40.7%; H, 3.4%; *Calculated* : C, 40.4%; H, 3.7%; MW 297). The product was calculated to be 96% pure on the basis of assay by the dehydrogenase method, and using a molecular weight of 297. The NMR spectrum revealed the presence of three major peaks attributable to the four olefinic protons, the protons *para* to the carboxyl group, and the two methylene protons at δ values of 6.05, 4.55 and 3.2,

respectively. The integrated peak ratios were 4:1:2 as would be expected from the structure of prephenate. No peaks corresponding to those published by Edwards and Jackman (1965) for chorismic acid were observed.

2.3.3 USE OF SEPHAROSE - LINKED ENZYME

To determine the feasibility of using enzyme linked to Sepharose for the conversion of chorismate to prephenate, a small amount of chorismate mutase - prephenate dehydrogenase was coupled to Sepharose 4B as described in Section 2.2.6. The product was found to be capable of converting chorismate to prephenate; it possessed a mutase activity of 0.07 units per ml of packed gel at 30°C and contained 7% of the enzymic activity present in the coupling mixture. Because the total catalytic activity of the product was low and as larger amounts of enzyme were not available for coupling at that time, prephenate was not routinely prepared using bound enzyme. Nevertheless, this approach has considerable potential, especially as bound enzyme is stable over six months at 4°C.

2.4 DISCUSSION

The procedure developed for the preparation and isolation of sodium prephenate gives a good yield of pure product and has been found to be reproducible. Further, it allows the use of any preparation of chorismate mutase which is free of contaminating activities, such as prephenate dehydratase which will convert

the desired product to phenylpyruvate.

While prephenate has been prepared for the work reported here using enzyme only in free solution, the preliminary results obtained with enzyme bound to Sepharose are encouraging. There was no need to develop the method further in our laboratory, but if there were a problem of high usage of prephenate, or conservation of enzyme, the development of the procedure using Sepharose-linked enzyme would be warranted.

CHAPTER 3

STEADY STATE KINETIC INVESTIGATIONS OF THE PREPHENATE DEHYDROGENASE REACTION

CHAPTER 3

STEADY STATE KINETIC INVESTIGATIONS OF THE PREPHENATE DEHYDROGENASE REACTION

3.1 INTRODUCTION

At the time that this work was commenced, no extensive kinetic study of the dehydrogenase reaction catalysed by chorismate mutase - prephenate dehydrogenase had been reported. What little information was available is summarised below.

(a) Reaction essentially irreversible (1).*

(b) Michaelis-Menten behaviour with respect to both prephenate and NAD (1 and 2).

(c) Apparent Michaelis constants :

Prephenate : 0.11 mM at 1.67 mM NAD, in 50 mM Tris buffer, pH 8.8, and at 37°C (1). 0.35 mM at 2.0 mM NAD, in 50 mM Tris-HCl buffer, pH 8.1, and at 37°C (2).

NAD : 0.15 mM at 0.67 mM prephenate, in 50 mM Tris buffer, pH 8.8, and at 37°C (1). 0.6 mM at 8 mM prephenate, in 50 mM Tris-HCl buffer, pH 8.1, and at 37°C (2).

---

* (1) Cotton and Gibson (1967).
(2) Koch et al. (1970 a).

(d) Inhibitors.

Tyrosine :

Competitive with respect to prephenate; induces concave-up double reciprocal plots (1 and 2). When NAD is varied, double reciprocal plots are linear and intersect in the first quadrant (1). Noncompetitive at the single concentration of tyrosine tested (2).

4-hydroxyphenylpyruvate :

Linear double reciprocal plots; type of inhibition with respect to prephenate not reported (data not shown). As for tyrosine with respect to NAD (1).

4-hydroxybenzoate :

Nonlinear double reciprocal plots with prephenate as varied substrate; type of inhibition not reported (data not shown). Inhibition with respect to NAD not reported (1).

4-hydroxyphenyllactate, 4-hydroxycinnamate, D-tyrosine :

Only percentage inhibition data reported at arbitrary substrate concentrations (2).

Preliminary results obtained in this laboratory by the late Dr. R.K. Ghambeer using partially purified enzyme were consistent with a rapid equilibrium random mechanism involving the formation of the two dead end complexes, enzyme-NAD-4-hydroxyphenylpyruvate and enzyme-prephenate-NADH. However, the experiments had been performed at pH 7.5, and at this pH the patterns of product inhibition by bicarbonate could not be determined because the release of carbon dioxide interferes with velocity

measurements. Therefore, a pH of 8.3 was chosen to facilitate a full product inhibition study.

3.2 MATERIALS AND METHODS

3.2.1 CHEMICALS

Chorismic acid was prepared as described in Section 2.2.1. Sodium prephenate was prepared and purified by the method described in Chapter 2. Chorismic acid, sodium prephenate and NAD (Calbiochem) were stored over dessicant at -15°C. Tris used in kinetic experiments was purchased from Merck and was of analytical reagent grade, while that used in enzyme purification was Sigma 7-9. Mimosine was a gift of Dr. R. Harris of the Division of Plant Industry, CSIRO. All other chemicals were of analytical reagent grade, or of the best grade available.

Solutions of NADH (P.L. Biochemicals) were made up at pH 7.5 on the day of use. 4-Hydroxyphenylpyruvate (Sigma, A grade) solutions were prepared on the day before use by dissolving the solid in 0.2 M Tris-HCl buffer, pH 7.5, readjusting to pH 7.5 with 0.01 M NaOH and making up to an appropriate volume with glass-distilled water. The solution was stored overnight at -15°C, thawed in the morning of the experiment, kept on ice while in use, and any remaining solution discarded at the end of the experiment. When this procedure was adopted, UV spectra of solutions before and after experimentation were the same, but storing such a solution at -15°C for yet another night resulted

in spectral changes, and also quantitative (but not qualitative) differences between inhibition experiments carried out on the successive days. 4-Hydroxyphenylpyruvate is unstable to alkaline pH and decomposes to hydroxybenzaldehyde and other unknown products (Painter and Zilva, 1947; Knox and Pitt, 1957; Doy, 1960).

Buffers and salt solutions were stored at -4°C and kept on ice while in use.

3.2.2 ISOLATION OF ENZYME

Chorismate mutase - prephenate dehydrogenase was prepared by the method of Heyde and Morrison (1978) which is outlined below. Figures relating to yield and specific activity (units/mg of protein) are this author's. One unit of chorismate mutase activity corresponds to an initial rate of formation of one μmole/min of prephenate in the presence of 2.5 mM chorismate at pH 7.5 and at 30°C.

Unless otherwise indicated, all buffers contained 1 mM EDTA and 1 mM DTT, the latter being added to all buffers immediately before use.

(a) Growth of cells, preparation of crude extract and precipitation of nucleic acids

Aerobacter aerogenes Poly 3 was grown, harvested and crude extract prepared essentially by the method of Koch *et al.* (1970 a). Tyrosine, however was not added to buffers, while

phenylmethanesulphonyl fluoride (final concentration 0.02 mg/ml) was added to all buffers used during cell disruption and precipitation of nucleic acids.

(b) Reverse ammonium sulphate fractionation

The supernatant obtained after removal of nucleic acids contained about 1 000 units of chorismate mutase activity at a specific activity about 0.2 units/mg protein. To each 100 ml of this supernatant was added 32.8 g of powdered ammonium sulphate; the resulting suspension was centrifuged and the supernatant discarded. The precipitate was extracted with a succession of buffers whose ammonium sulphate concentration decreased from 40% to 25% saturation. These extraction buffers were made up by diluting saturated ammonium sulphate solution, pH 7.5, with an appropriate volume of 0.2 M Tris-HCl, pH 7.5, containing 1 mM EDTA and 0.2 mM DTT. Those extracts with the highest specific activity were pooled and then the protein was precipitated by adding powdered ammonium sulphate (1.69 g/10 ml) and collected by centrifuging.

(c) Chromatography on AMP-Sepharose

The precipitate from the previous step was dissolved in 0.1 M Tris-acetate buffer, pH 6.0, and dialysed overnight against the same buffer. Precipitated material was removed by centrifuging and the supernatant (which contained about 500 units of chorismate mutase at specific activity about 0.4 units/mg protein) was applied to a column of AMP-Sepharose previously

equilibrated with the above-mentioned buffer which was also used for elution of the enzyme *via* a 0 - 0.5 M NaCl gradient.

(d) Hydroxylapatite chromatography

The pool of active fractions from the previous step (about 350 units of chorismate mutase activity of specific activity about 4 units/mg protein) was applied to a column of hydroxylapatite equilibrated with 0.1 M Tris-acetate, pH 6,0, containing 0.3 M NaCl, and eluted using a phosphate gradient from 0.03 - 0.1 M in 0.1 M Tris-HCl, pH 7.5. Those fractions with the highest specific activity were pooled, sodium azide was added to a final concentration of 0.02%, and aliquots of the enzyme in vials were snap frozen and stored at -15°C.

(e) Purity of the enzyme

Using the above procedures, enzyme preparations of specific activity about 30 units/mg protein were obtained. Such preparations showed one major band on polyacrylamide gel electrophoresis with three faint contaminating bands. Prephenate dehydratase activity was not detectable.

3.2.3 ENZYME ASSAYS

(a) Chorismate mutase

Routine assay of chorismate mutase was performed by the stopped-time method of Koch *et al*. (1970 a) with the exceptions that the assays were carried out at 30°C and for much shorter periods, usually 2 - 6 min for location of active frac-

tions from columns, and 1 - 2 min for determination of activity in pooled material.

(b) Prephenate dehydrogenase

Prephenate dehydrogenase activity was measured by continuous monitoring at 340 nm of the formation of NADH. The molar extinction coefficient for the products NADH and 4-hydroxyphenylpyruvate was taken to be 6 500 (R.K. Ghambeer, unpublished results). The instrument used was either a Cary 118C or a Varian 635 spectrophotometer. Quartz cuvettes of 1.0 cm light path were used for all assays except in experiments investigating inhibition by NADH at fixed NAD concentration. For those assays, cuvettes of 0.5 cm light path were used because of the high concentration of NADH required. Reactions were carried out at 30°C, and stock solutions of buffer were prepared so that the final pH was 8.3 at this temperature. The reaction mixtures contained 0.1 M Tris-HCl, 0.5 mM EDTA and 0.5 mM DTT in a final volume of 1.0 ml. Substrates, products and other compounds were added at the concentrations specified in Section 3.3. Reaction was initiated by the addition of enzyme with a Hamilton syringe (fitted with dispenser) to pre-warmed assay mixtures. The amount of enzyme used for each assay was between 0.3 and 1 μg depending on the enzyme preparation. Linearity of velocity with respect to enzyme concentration was checked from time to time. Velocity of reaction was determined by estimating the slope of the initial linear portion of the progress curve, and is expressed in terms of μmoles product formed/min/mg of protein.

(c) Prephenate dehydrogenase in the presence of thionicotinamide adenine dinucleotide

Thionicotinamide adenine dinucleotide (Thio-NAD) is an alternative substrate for prephenate dehydrogenase and undergoes spectral changes on reduction. In experiments involving both NAD and Thio-NAD, NADH formation was monitored at the isosbestic point of Thio-NAD reduction which was determined to be 341.8 nm on the Cary 118C spectrophotometer under the conditions of the experiments. The molar extinction coefficient for equimolar mixtures of NADH and 4-hydroxyphenylpyruvate was taken to be 6 500 at 341.8 nm, which is estimated to be less than 2% higher than the true value. (The estimation is based on the spectrum of NADH in the Circular OR-18, P.L. Biochemicals, Inc., and spectra of 4-hydroxyphenylpyruvate recorded in this laboratory.)

In the absence of NAD, reduction of Thio-NAD was followed at 395 nm, and, for calculation of velocities of reaction the molar extinction coefficient of Thio-NADH was taken to be 11 300 (Circular OR-18, P.L. Biochemicals, Inc.).

3.2.4 ESTIMATION OF SUBSTRATE AND OTHER CONCENTRATIONS

Chorismate and prephenate concentrations were determined enzymically using the procedures described in Section 2.2. NAD was estimated by the same enzymic procedure as that used for prephenate, except that the concentration of prephenate was in large excess over NAD concentration.

NADH, AMP and ADP were estimated by procedures to be

found in Dawson et al. (1969).

Protein concentration of crude extracts was determined using the Biuret method (Gornall et al., 1949). Protein estimation of purified preparations was based on the absorbance, against an appropriate blank, at 280 nm using an extinction coefficient of 1.0 absorbance unit/cm/mg.

3.2.5 DATA ANALYSIS

Inspection of double reciprocal plots for each set of data was used to determine the form of equation to be used for computer analysis. Data analysis programs were those of Cleland (1967), written in FORTRAN, and were run on a Univac 1100/42 computer. If graphical inspection suggested that more than one equation be tested, each equation was fitted, and the equation of best fit determined on the basis of the variance values.

Depending on the context in which the computer programs are used, either true or apparent kinetic parameters are obtained. For the quantitative assessment of kinetic mechanisms true constants were calculated using equations relating them to the apparent constants yielded by analysis of experimental data and other parameters which could be determined independently. This aspect will be treated in more detail in Section 3.4.

Weighted mean values ($\bar{x}$) of kinetic parameters and their standard errors (S.E.($\bar{x}$)) were calculated according to the formulae :

$$\bar{x} = \sum(w_i x_i)/\sum w_i$$

$$S.E.(\bar{x}) = 1/\sqrt{\sum w_i}$$

where $w_i = 1/(S.E.(x_i))^2$

The standard errors of sums and differences were determined using the formula :

$$S.E.(x \pm y) = \sqrt{(S.E.(x))^2 + (S.E.(y))^2}$$

while the standard errors of products and quotients were calculated using the formula :

$$S.E.\left(\frac{xy}{z}\right) = \frac{xy}{z}\sqrt{\left[\frac{S.E.(x)}{x}\right]^2 + \left[\frac{S.E.(y)}{y}\right]^2 + \left[\frac{S.E.(z)}{z}\right]^2}$$

3.2.6 NOMENCLATURE AND NOTATION

The nomenclature and notation used in this thesis are those of Cleland (1963 a and b) except that for reasons of convenience, some of the schemes depicting kinetic mechanisms do not conform to the graphical descriptions adopted by that author. In addition, Cleland's inhibition constants, $K_{i\ intercept}$ and $K_{i\ slope}$, have been abbreviated to K_{ii} and K_{is}, respectively, and are followed by a shorthand notation indicating the experiment from which they are derived. The following examples explain the notation. $K_{is}(P/A)$ indicates the inhibition constant determined from a change in slope when the inhibition by P is investigated while varying the concentration of substrate A (keeping all other substrates at constant concentration). $K_{ii}(Q/B)$ represents the inhibition constant determined from the change in vertical intercept when the inhibition by Q with res-

pect to substrate B is investigated.

K_{is} and K_{ii} are determined by fitting experimental data to the equations :

$$v = \frac{VA}{K_a(1 + I/K_{is}) + A}$$

$$v = \frac{VA}{K_a(1 + I/K_{is}) + A(1 + I/K_{ii})}$$

$$v = \frac{VA}{K_a + A(1 + I/K_{ii})}$$

for competitive, noncompetitive and uncompetitive inhibition, respectively.

It should be pointed out that the term "noncompetitive" inhibition is used in the general sense that refers to inhibition characterised by changes in both the slope and the vertical intercept of double reciprocal plots, irrespective of whether the cross-over point of the pattern is above, below or on the horizontal axis.

3.3 RESULTS

3.3.1 DEPENDENCE OF THE STEADY STATE VELOCITY ON SUBSTRATE CONGENTRATIONS

Experiments investigating the dependence of initial velocity of reaction on the substrate concentrations yielded double reciprocal plots which were intersecting (Figs. 3.1 and 3.2), a result indicative of a sequential mechanism, where both of the substrates must bind to the enzyme before a product may dissociate. However, inspection of the patterns suggested that at a saturating concentration of NAD, the velocity was independent of prephenate concentration, since the double reciprocal plots of Fig. 3.2 intersect with each other on the vertical axis. Although this result is predicted for an equilibrium ordered mechanism, the same result may be obtained with a rapid equilibrium random mechanism, if there is marked synergism in the substrate binding (as discussed in Section 1.1.2). Therefore it was important to repeat the initial velocity experiment using different ranges of substrate concentrations. Such experiments indicated that the maximum velocity does, in fact, depend on prephenate concentration, and the results of one such experiment are illustrated in Figs. 3.3 and 3.4. Table 3.1 records the Michaelis and inhibition constants for NAD and prephenate determined from the data of Figs. 3.1 - 3.4 and other similar data. These constants have been used in the calculations reported in Section 3.4.

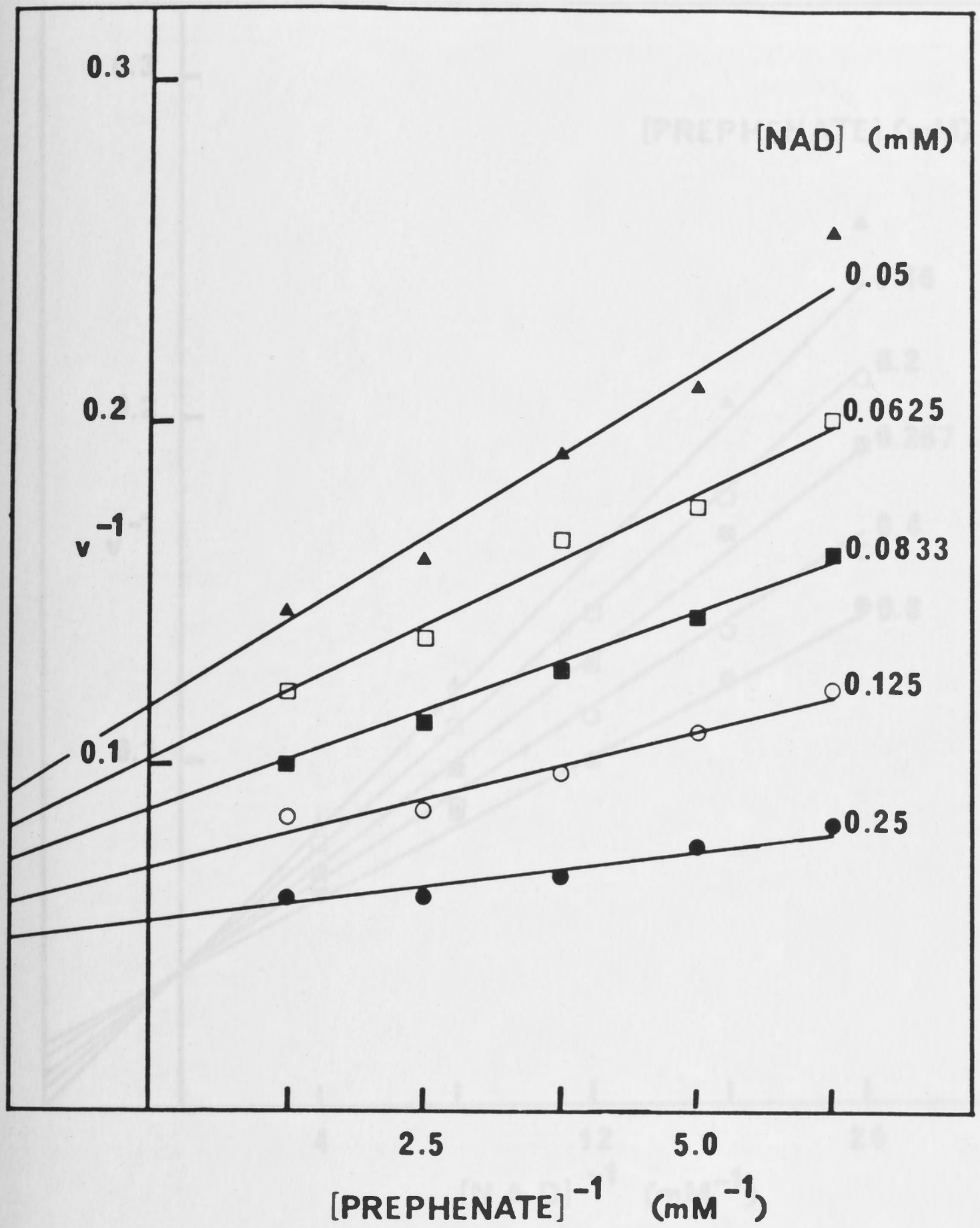

FIGURE 3.1 Initial velocity pattern obtained for prephenate dehydrogenase at pH 8.3 when prephenate concentration is varied (0.8 - 0.16 mM) at different fixed levels of NAD (0.25 - 0.05 mM). Lines through the data points are calculated from the fit of the data to the equation :

$$v = \frac{VAB}{K_{ia}K_b + K_bA + AB}$$

where A and B represent prephenate and NAD, respectively.

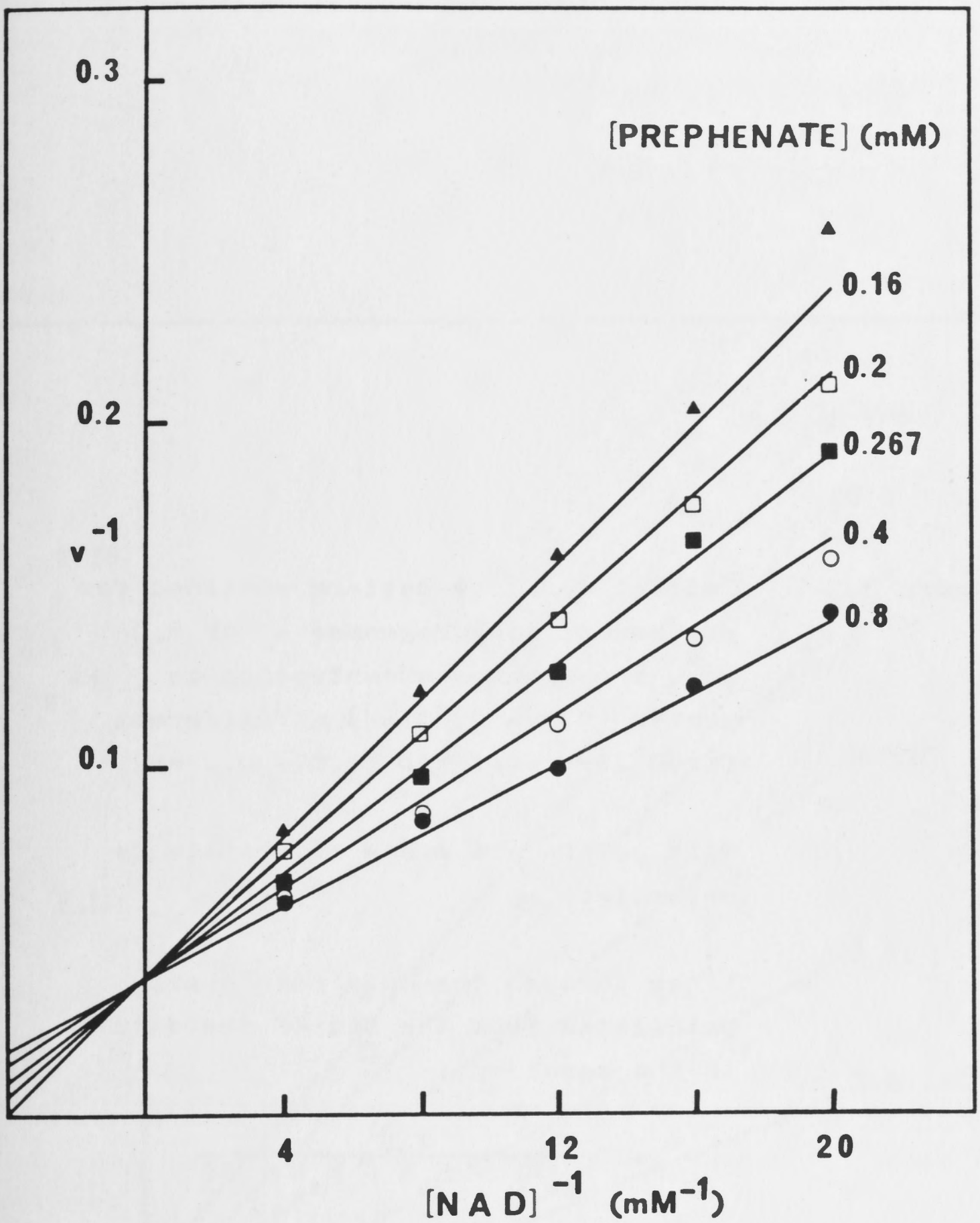

FIGURE 3.2 Initial velocity pattern obtained for prephenate dehydrogenase at pH 8.3 when NAD concentration is varied (0.25 - 0.05 mM) at different fixed levels of prephenate (0.8 - 0.16 mM). Lines through the data points are calculated from the fit of the data to the equation :

$$v = \frac{VAB}{K_{ia}K_b + K_bA + AB}$$

where A and B represent prephenate and NAD, respectively.

Figure 3.3 Initial velocity pattern obtained for prephenate dehydrogenase at pH 8.3 when prephenate concentration is varied (0.5 - 0.05 mM) at different fixed levels of NAD (2.0 - 0.2 mM).

Data points are means of triplicate estimates.

Lines through the data points are calculated from the fit of the data to the equation :

$$v = \frac{VAB}{K_{ia}K_b + K_bA + K_aB + AB}$$

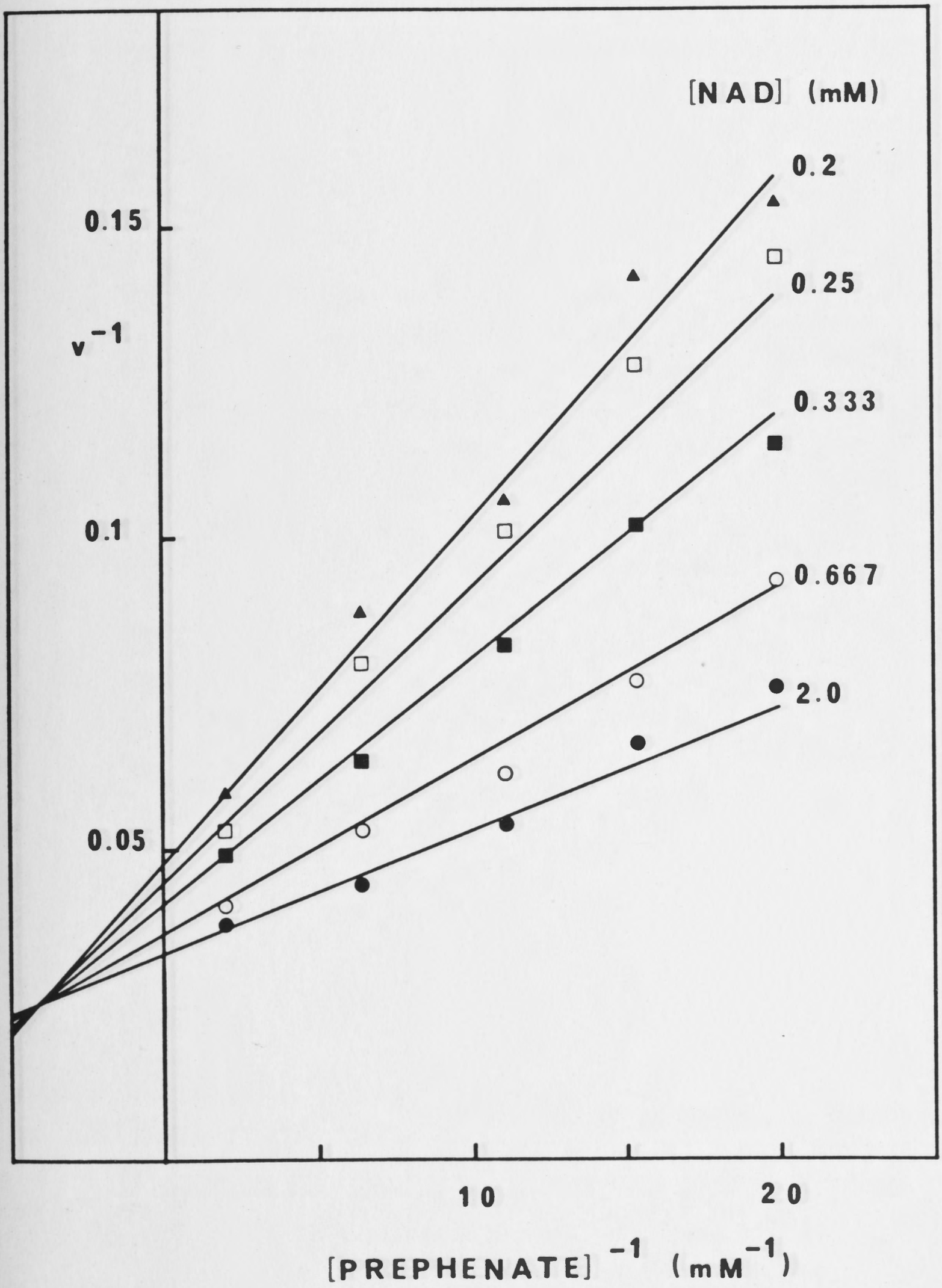
[NAD] (mM)
0.2
0.25
0.333
0.667
2.0
0.15
0.1
0.05
v⁻¹
10
20
[PREPHENATE]⁻¹ (mM⁻¹)

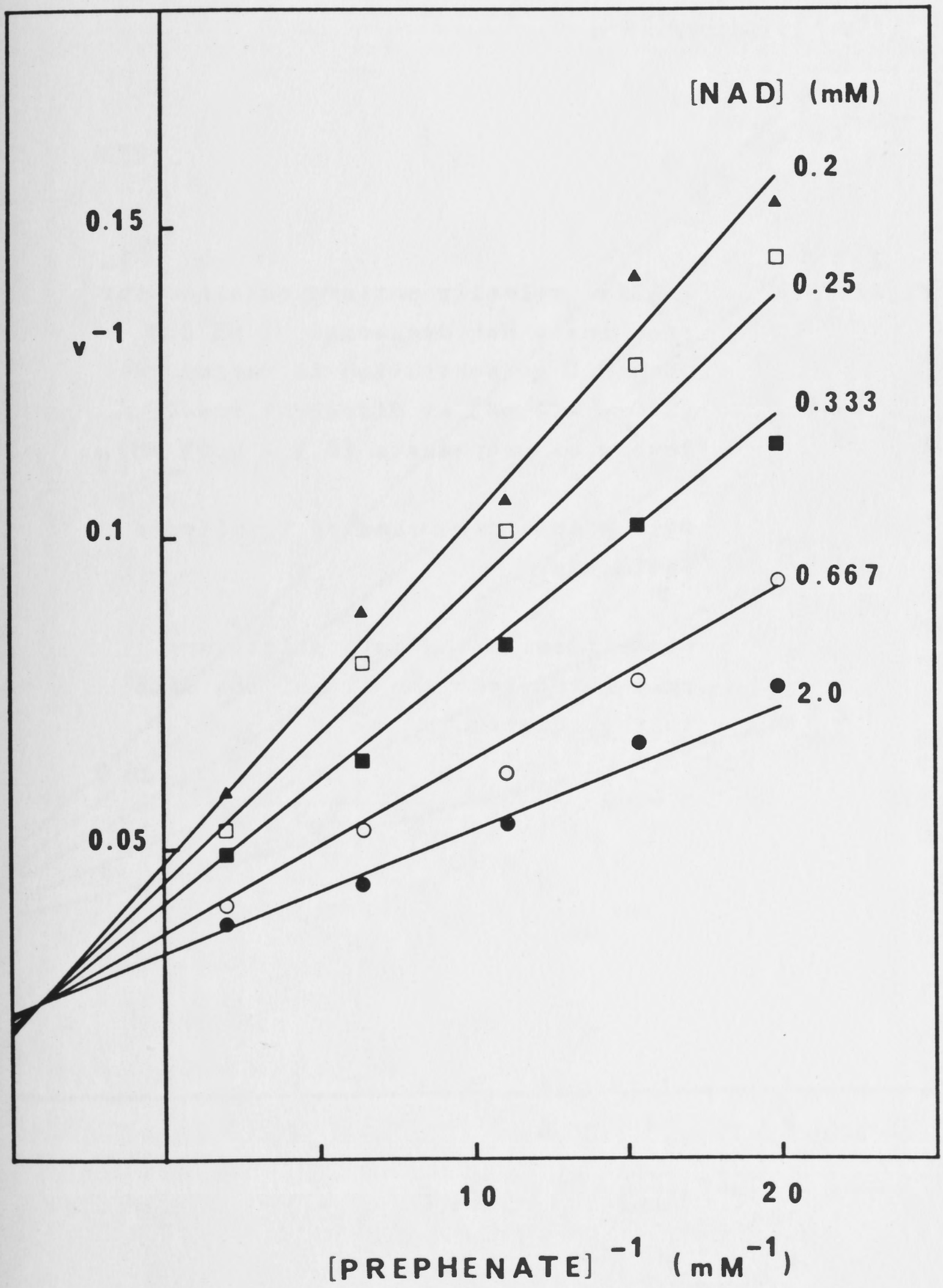
[NAD] (mM)
0.2
0.25
0.333
0.667
2.0
0.15
0.1
0.05
v^{-1}
10
20
[PREPHENATE] $^{-1}$ (mM^{-1})

Figure 3.4 Initial velocity pattern obtained for prephenate dehydrogenase at pH 8.3 when NAD concentration is varied (2.0 - 0.2 mM) at different fixed levels of prephenate (0.5 - 0.05 mM).

Data points are means of triplicate estimates.

Lines through the data points are calculated from the fit of the data to the equation :

$$v = \frac{VAB}{K_{ia}K_b + K_bA + K_aB + AB}$$

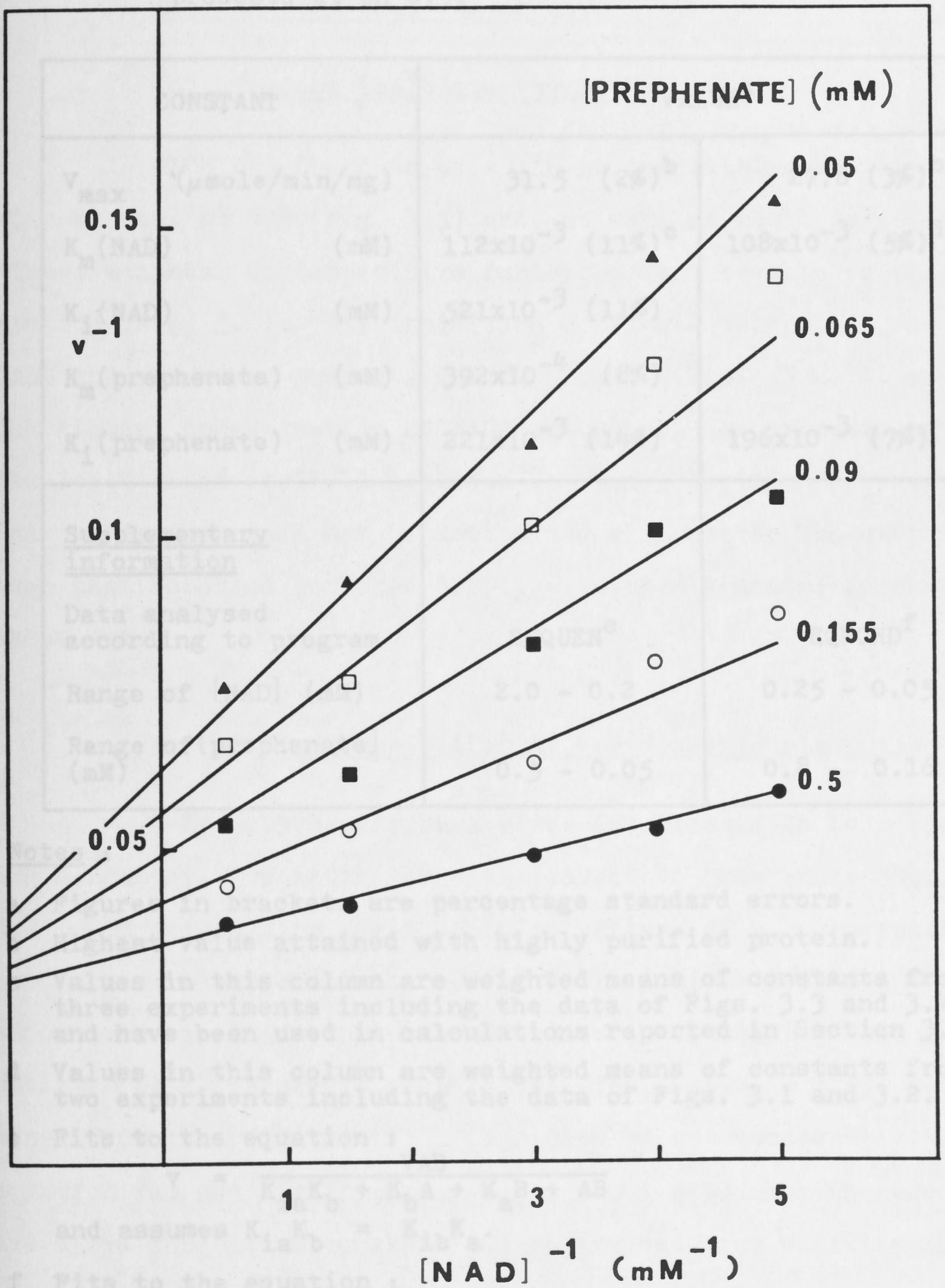
[PREPHENATE] (mM)
0.05
0.065
0.09
0.155
0.5
0.15
0.1
0.05
v⁻¹
1
3
5
[NAD]⁻¹ (mM⁻¹)

TABLE 3.1 Values of the kinetic constants associated with prephenate dehydrogenase as determined from steady state velocity studies in the absence of added products at pH 8.3.

CONSTANT	VALUE[a]	
V_{max} (μmole/min/mg)	31.5 (2%)[b]	27.8 (3%)[b]
K_m(NAD) (mM)	112×10^{-3} (11%)[c]	108×10^{-3} (5%)[d]
K_i(NAD) (mM)	521×10^{-3} (11%)	
K_m(prephenate) (mM)	392×10^{-4} (8%)	
K_i(prephenate) (mM)	221×10^{-3} (14%)	196×10^{-3} (7%)
<u>Supplementary information</u>		
Data analysed according to program	SEQUEN[e]	EQNORD[f]
Range of [NAD] (mM)	2.0 - 0.2	0.25 - 0.05
Range of [prephenate] (mM)	0.5 - 0.05	0.8 - 0.16

<u>Notes</u> :

a Figures in brackets are percentage standard errors.

b Highest value attained with highly purified protein.

c Values in this column are weighted means of constants from three experiments including the data of Figs. 3.3 and 3.4, and have been used in calculations reported in Section 3.4.

d Values in this column are weighted means of constants from two experiments including the data of Figs. 3.1 and 3.2.

e Fits to the equation :

$$v = \frac{VAB}{K_{ia}K_b + K_bA + K_aB + AB}$$

and assumes $K_{ia}K_b = K_{ib}K_a$.

f Fits to the equation :

$$v = \frac{VAB}{K_{ia}K_b + K_bA + AB}$$

3.3.2 STEADY STATE VELOCITY INVESTIGATIONS IN THE PRESENCE OF PRODUCTS

(a) Product inhibition by NADH

NADH was found to be a linear competitive inhibitor with respect to NAD (Fig. 3.5) and, as well as could be determined, a linear noncompetitive inhibitor with respect to prephenate (Fig. 3.6). The inhibition constants determined for NADH and the other products are recorded in Table 3.2. Because the highest concentration of NADH which could be used was below the lower limit of the inhibition constant, K_{is}(NADH/prephenate), this parameter could not be determined with better accuracy than that recorded in Table 3.2, i.e. with a standard error of about 20%.

(b) Product inhibition by 4-hydroxyphenylpyruvate

4-Hydroxyphenylpyruvate was established to be a linear noncompetitive inhibitor with respect to prephenate (Fig. 3.7). In determining the inhibition pattern of 4-hydroxyphenylpyruvate with respect to NAD (Fig. 3.8), similar problems were encountered as those in the experiments investigating NADH inhibition with respect to prephenate. The change in slope determined from the computer fit of the data to the noncompetitive equation was not significant : $K_{is} \approx 500 \pm 2200$ mM. Therefore the slope inhibition constant was determined from experiments in which each point of the baseline and the double reciprocal plot at 1.2 mM 4-hydroxyphenylpyruvate was assayed in triplicate;

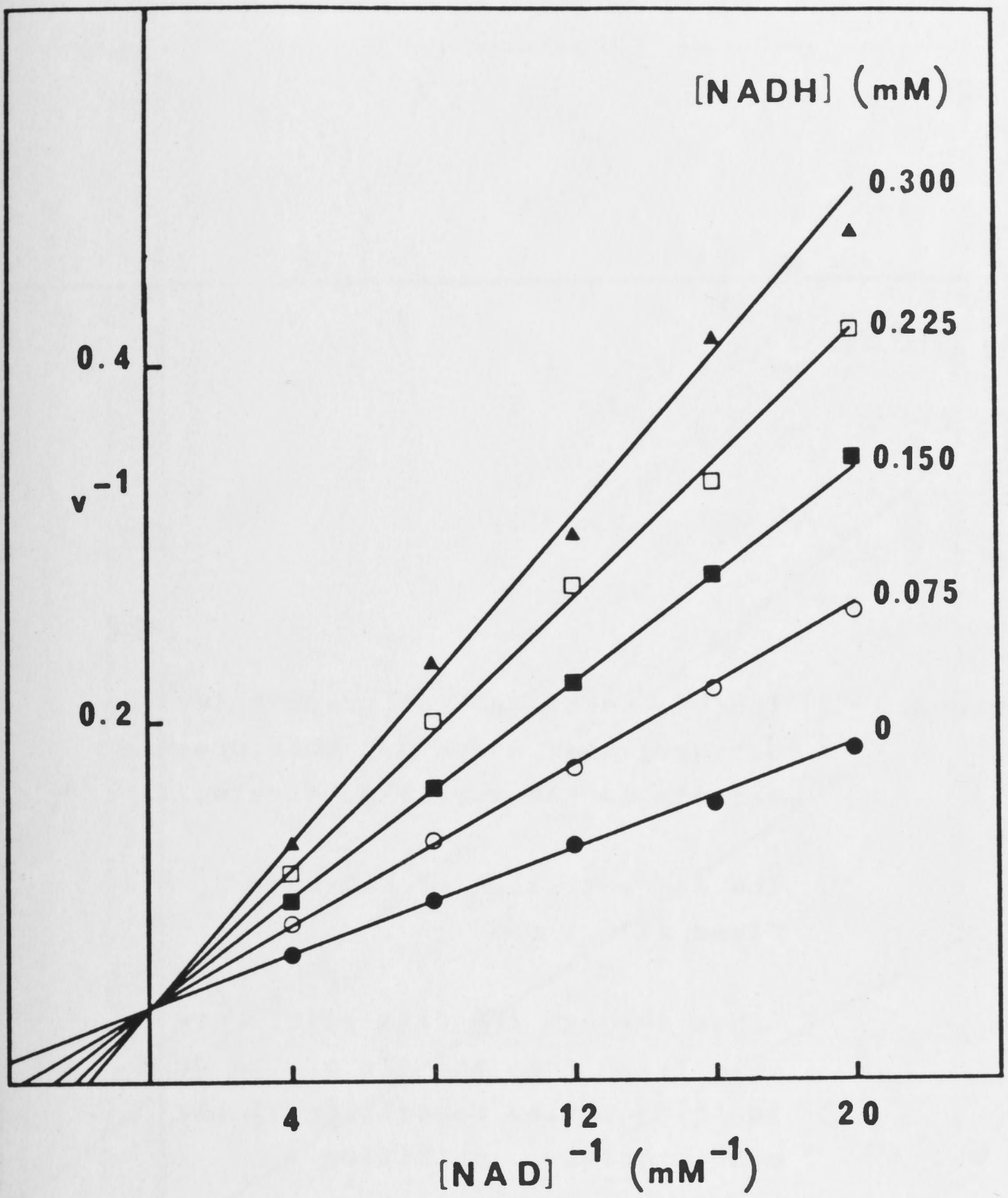

FIGURE 3.5 Inhibition by NADH of prephenate dehydrogenase at pH 8.3 when NAD is the varied substrate. The concentration of prephenate was fixed at 0.1 mM. Lines through the data points are calculated from the fit of the data to the equation describing linear competitive inhibition :

$$v = \frac{VA}{K_a(1 + I/K_{is}) + A}$$

Figure 3.6 Inhibition by NADH of prephenate dehydrogenase at pH 8.3 when prephenate is the varied substrate.

The concentration of NAD was fixed at 0.1 mM.

Lines through the data points are calculated from the fit of the data to the equation describing linear noncompetitive inhibition :

$$v = \frac{VA}{K_a(1 + I/K_{is}) + A(1 + I/K_{ii})}$$

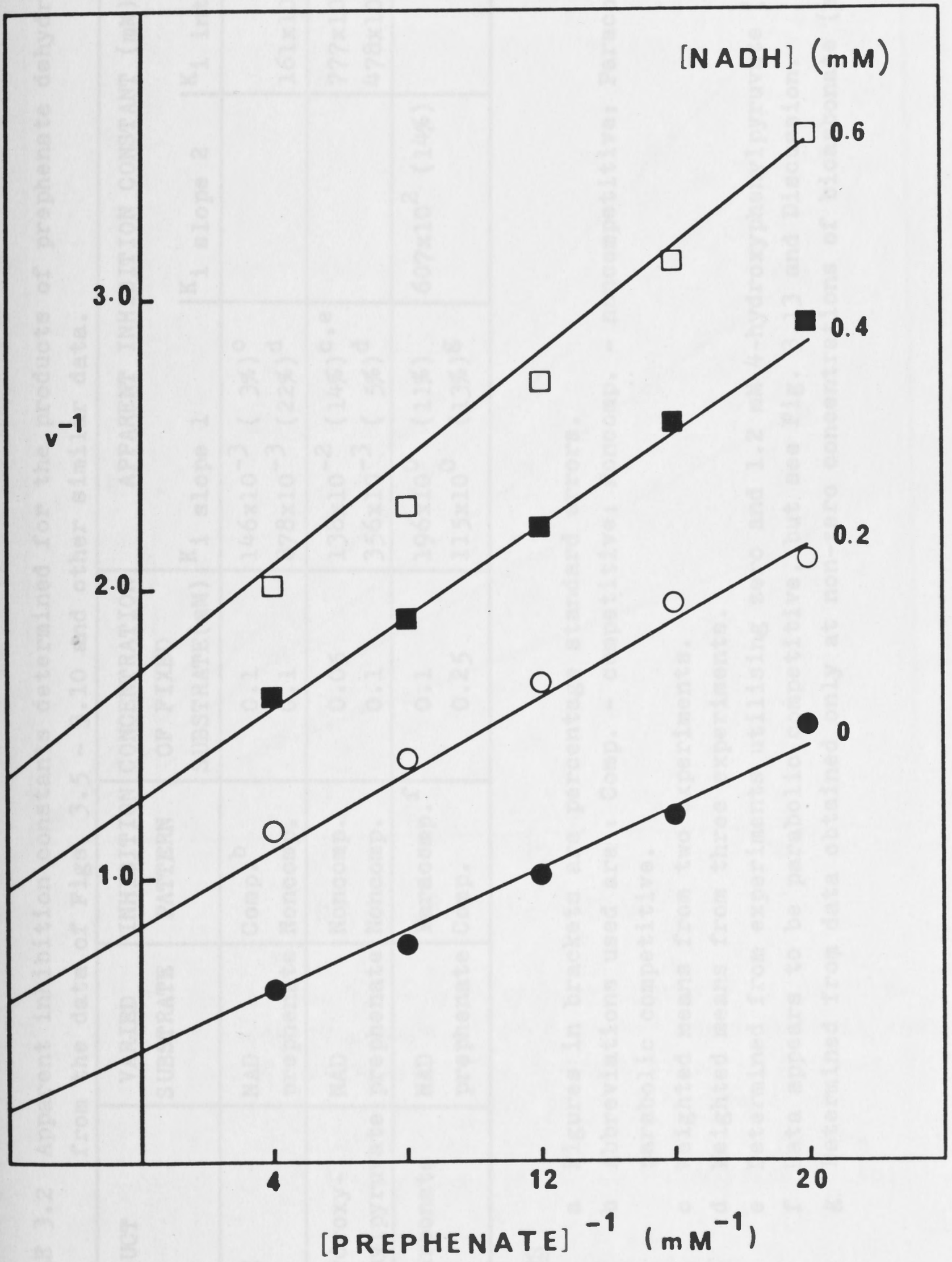
[NADH] (mM)
0.6
0.4
0.2
0
3·0
2·0
1·0
v⁻¹
4
12
20
[PREPHENATE]⁻¹ (mM⁻¹)

TABLE 3.2 Apparent inhibition constants determined for the products of prephenate dehydrogenase from the data of Figs. 3.5 - 3.10 and other similar data.

PRODUCT	VARIED SUBSTRATE	INHIBITION PATTERN	CONCENTRATION OF FIXED SUBSTRATE(mM)	APPARENT INHIBITION CONSTANT (mM)[a]		
				K_i slope 1	K_i slope 2	K_i intercept
NADH	NAD	Comp.[b]	0.1	146×10^{-3} (3%)[c]		
	prephenate	Noncomp.	0.1	878×10^{-3} (22%)[d]		161×10^{-3} (6%)[d]
4-hydroxy-phenylpyruvate	NAD	Noncomp.	0.05	138×10^{-2} (14%)[c,e]		777×10^{-4} (2%)[c]
	prephenate	Noncomp.	0.1	356×10^{-3} (5%)[d]		478×10^{-3} (7%)[d]
bicarbonate	NAD	Paracomp.[f]	0.1	196×10^{0} (11%)	607×10^{2} (14%)	
	prephenate	Comp.	0.25	115×10^{0} (13%)[g]		

NOTES

a Figures in brackets are percentage standard errors.

b Abbreviations used are : Comp. - competitive; Noncomp. - noncompetitive; Paracomp. - parabolic competitive.

c Weighted means from two experiments.

d Weighted means from three experiments.

e Determined from experiments utilising zero and 1.2 mM 4-hydroxyphenylpyruvate (see text).

f Data appears to be parabolic competitive, but see Fig. 3.13 and Discussion.

g Determined from data obtained only at non-zero concentrations of bicarbonate (see Fig. 3.11).

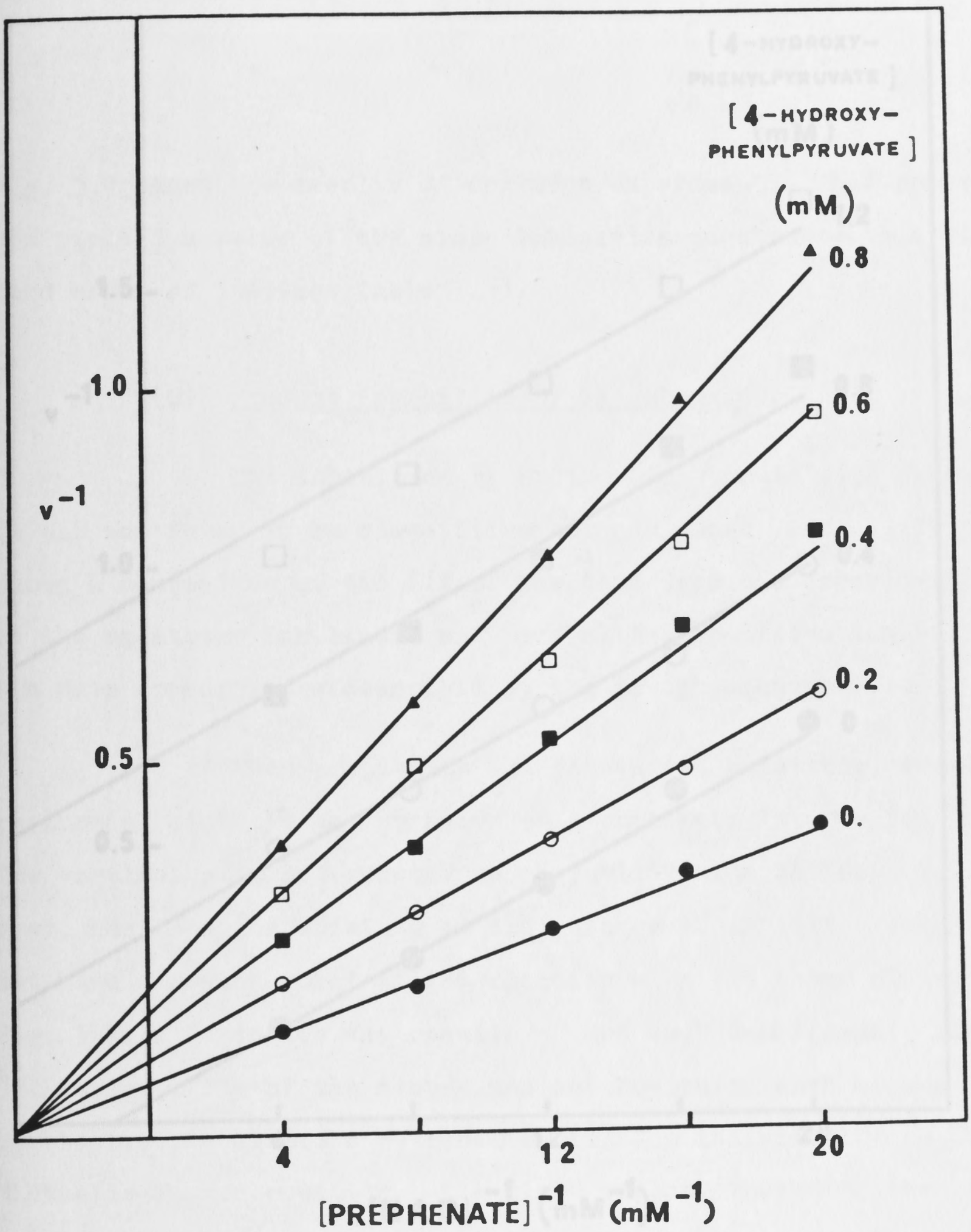

FIGURE 3.7 Inhibition by 4-hydroxyphenylpyruvate of prephenate dehydrogenase at pH 8.3 when prephenate is the varied substrate. The concentration of NAD was fixed at 0.1 mM. Lines through the data points are calculated from the fit of the data to the equation describing linear noncompetitive inhibition :

$$v = \frac{VA}{K_a(1 + I/K_{is}) + A(1 + I/K_{ii})}$$

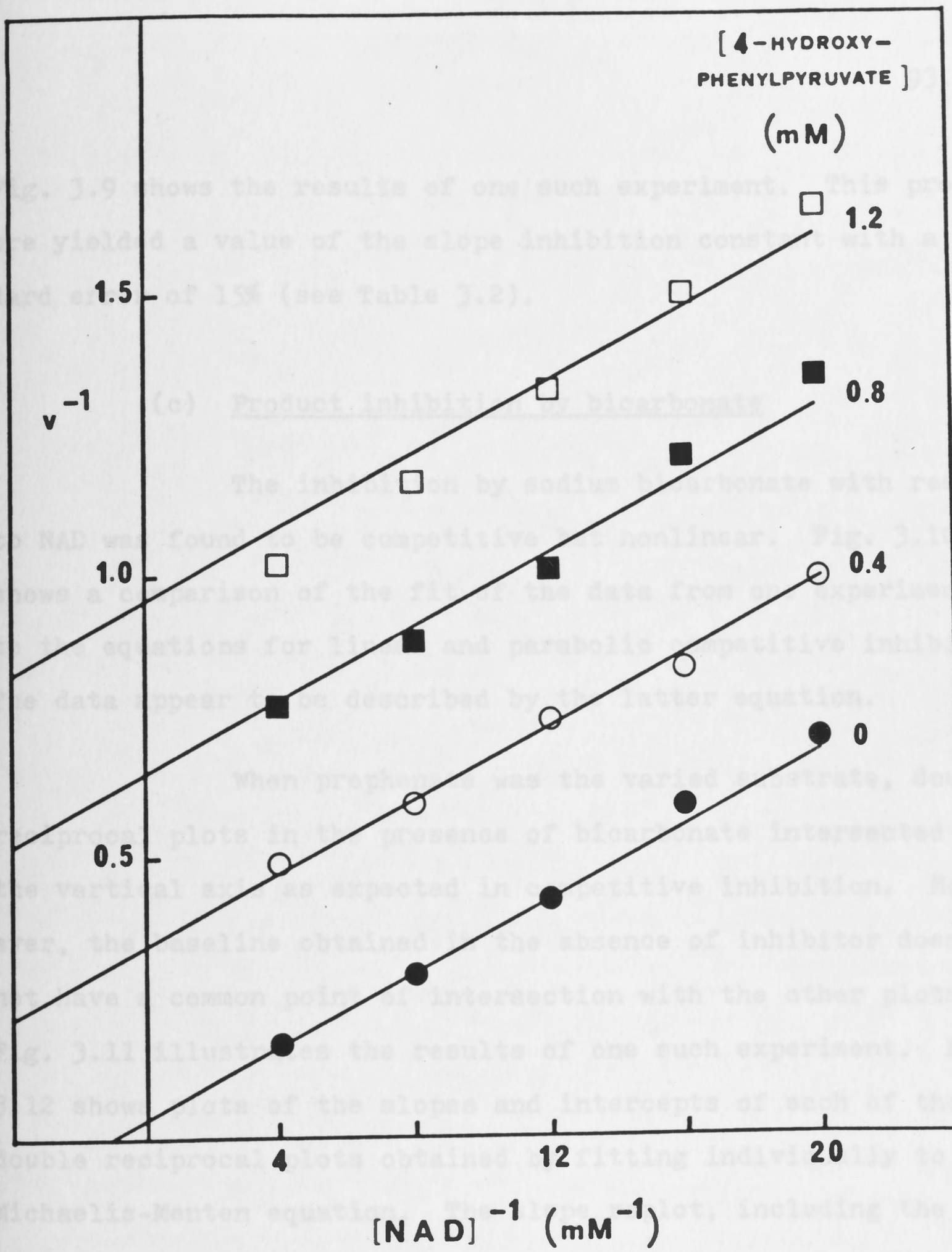

FIGURE 3.8 Inhibition by 4-hydroxyphenylpyruvate of prephenate dehydrogenase at pH 8.3 when NAD is the varied substrate. The concentration of prephenate was fixed at 0.05 mM. Lines through the data points are calculated from the fit of the data to the equation describing linear noncompetitive inhibition :

$$v = \frac{VA}{K_a(1\ I/K_{is}) + A(1 + I/K_{ii})}$$

Fig. 3.9 shows the results of one such experiment. This procedure yielded a value of the slope inhibition constant with a standard error of 15% (see Table 3.2).

(c) Product inhibition by bicarbonate

The inhibition by sodium bicarbonate with respect to NAD was found to be competitive but nonlinear. Fig. 3.10 shows a comparison of the fit of the data from one experiment to the equations for linear and parabolic competitive inhibition. The data appear to be described by the latter equation.

When prephenate was the varied substrate, double reciprocal plots in the presence of bicarbonate intersected on the vertical axis as expected in competitive inhibition. However, the baseline obtained in the absence of inhibitor does not have a common point of intersection with the other plots. Fig. 3.11 illustrates the results of one such experiment. Fig. 3.12 shows plots of the slopes and intercepts of each of the double reciprocal plots obtained by fitting individually to the Michaelis-Menten equation. The slope replot, including the point corresponding to the baseline, is quite normal. The intercept replot for non-zero bicarbonate concentrations is also normal, but bicarbonate increases the normal maximum velocity by about half. The activation at relatively low bicarbonate concentrations was reproducible, and, as shown in Fig. 3.13, is evident at prephenate concentrations as low as 0.1 mM.

In view of the relatively high concentrations of

Figure 3.9 Inhibition by 4-hydroxyphenylpyruvate of prephenate dehydrogenase at pH 8.3 when NAD is the varied substrate.

The concentration of prephenate was fixed at 0.05 mM.

Data points on the baseline (▲) are means of triplicate estimates.

Lines through the data points are calculated from the fit of the data to the equation describing linear noncompetitive inhibition:

$$v = \frac{VA}{K_a(1 + I/K_{is}) + A(1 + I/K_{ii})}$$

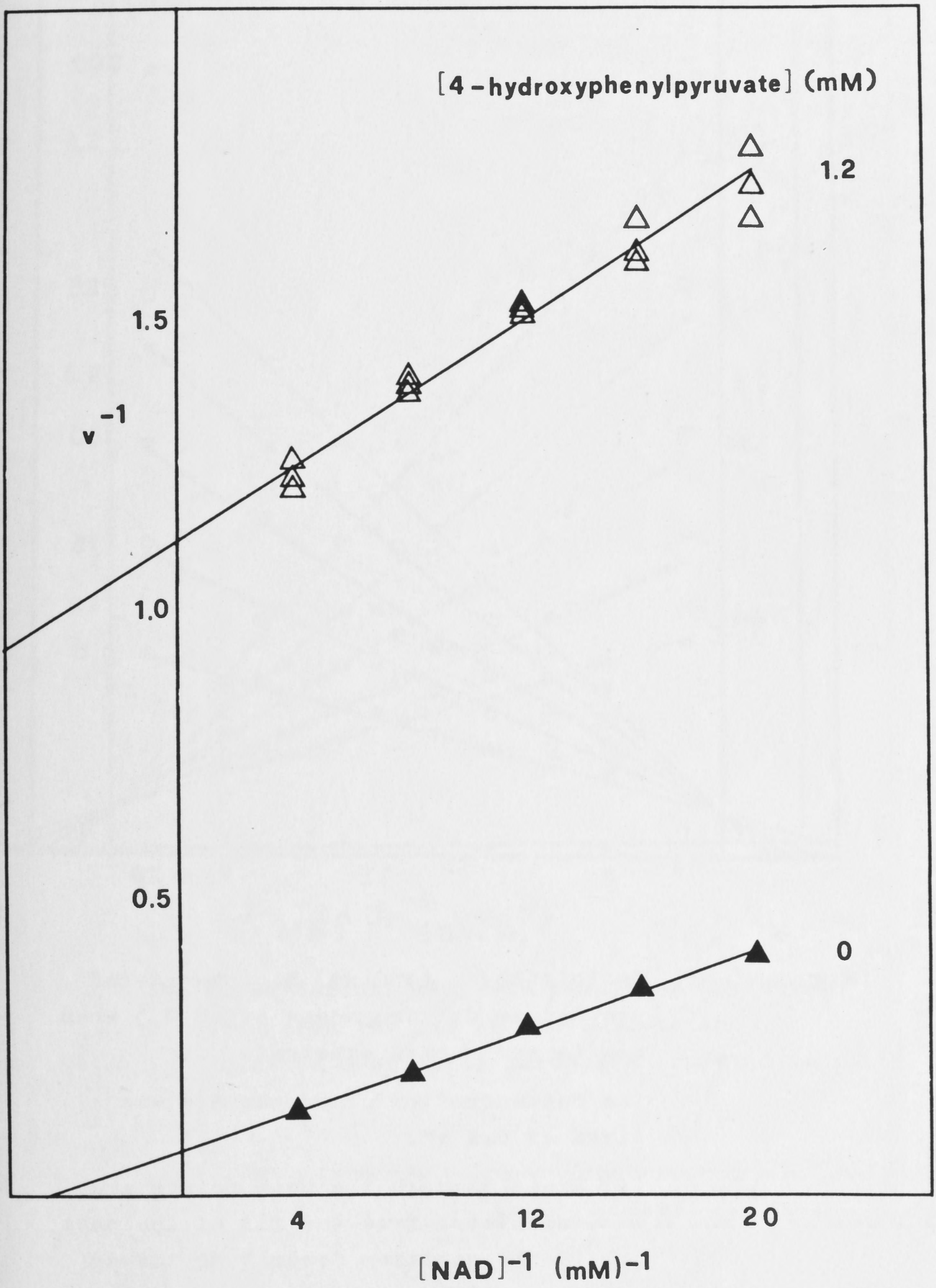
[4-hydroxyphenylpyruvate] (mM)
1.2
1.5
v -1
1.0
0.5
0
4
12
20
[NAD]-1 (mM)-1

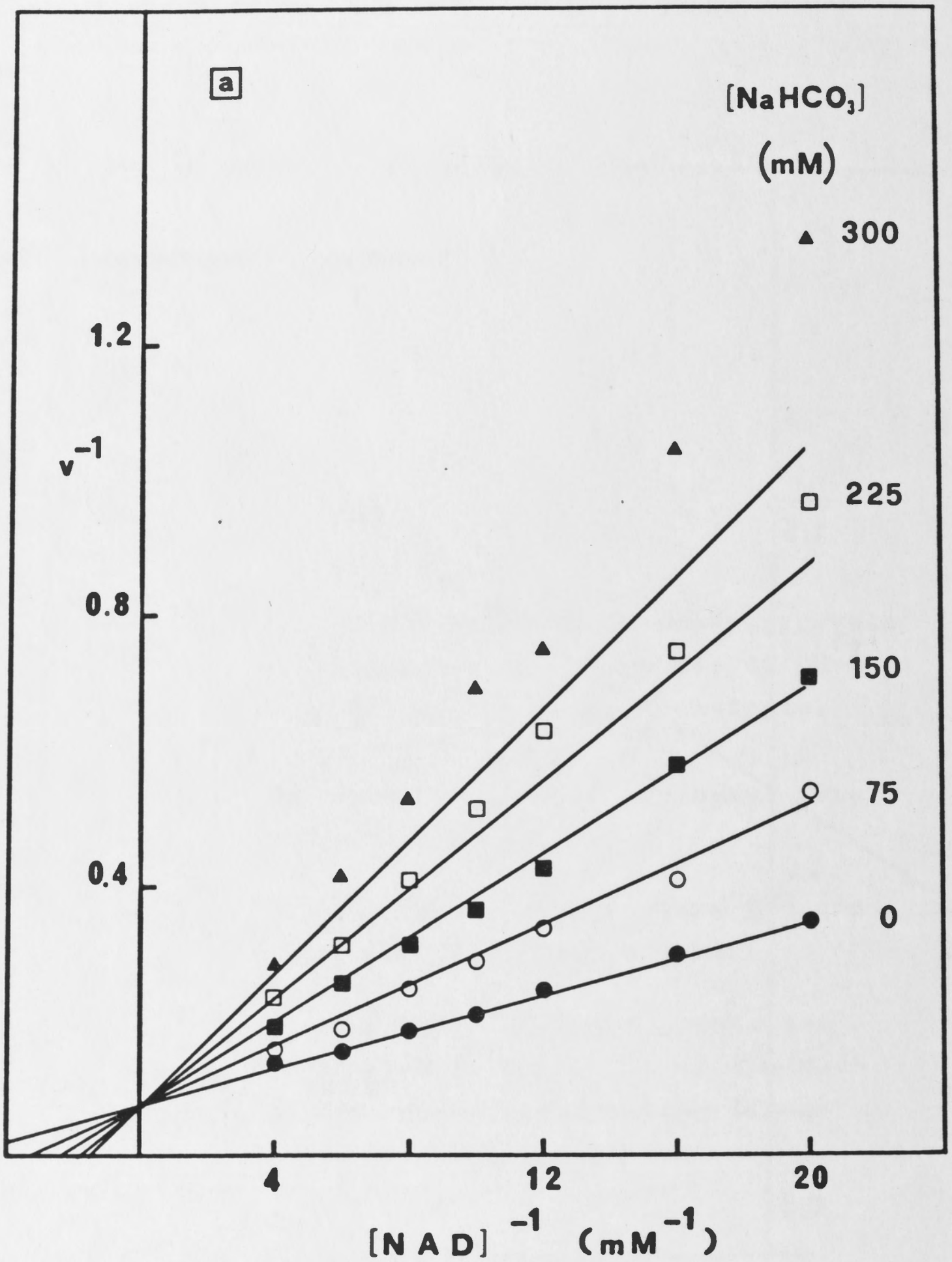

Figure 3.10 Inhibition by (sodium) bicarbonate of prephenate dehydrogenase at pH 8.3 when NAD is the varied substrate.

The concentration of prephenate was fixed at 0.1 mM.

(a) Lines through the data points are calculated from the fit of the data to the equation describing linear competitive inhibition :

$$v = \frac{VA}{K_a(1 + I/K_{is}) + A}$$

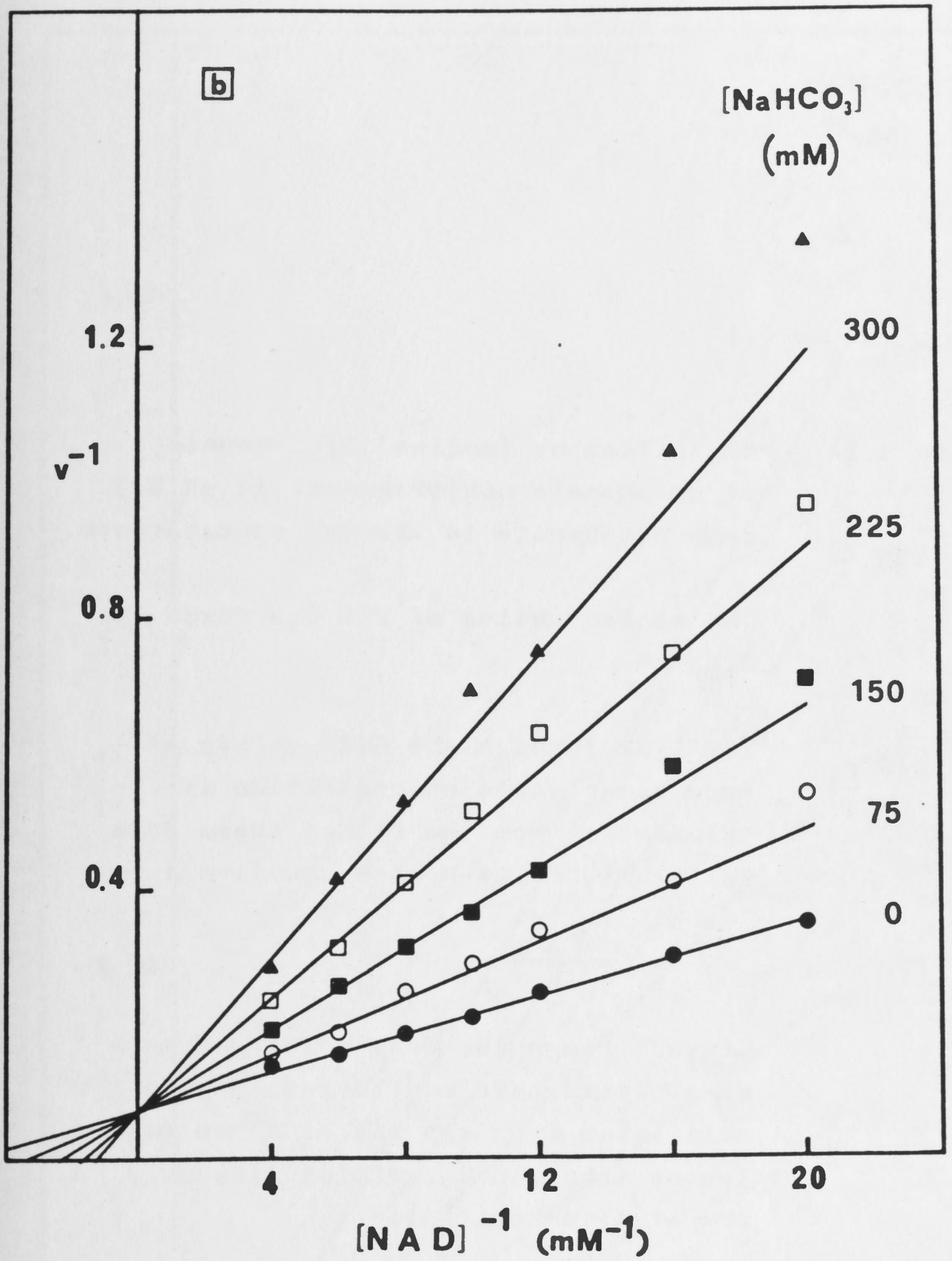

(b) Lines through the data points are calculated from the fit of the data to the equation describing parabolic competitive inhibition :

$$v = \frac{VA}{K_a(1 + I/K_{is1} + I^2/K_{is2}) + A}$$

Figure 3.11 Inhibition by (sodium) bicarbonate of prephenate dehydrogenase at pH 8.3 when prephenate is the varied substrate.

The concentration of NAD was fixed at 0.25 mM.

The line through the data points at zero bicarbonate concentration is calculated from the fit of these data to the Michaelis-Menten equation :

$$v = \frac{VA}{K_a + A}$$

Lines through the data points at non-zero bicarbonate concentrations are calculated from the fit of these data to the equation describing linear competitive inhibition :

$$v = \frac{VA}{K_a(1 + I/K_{is}) + A}$$

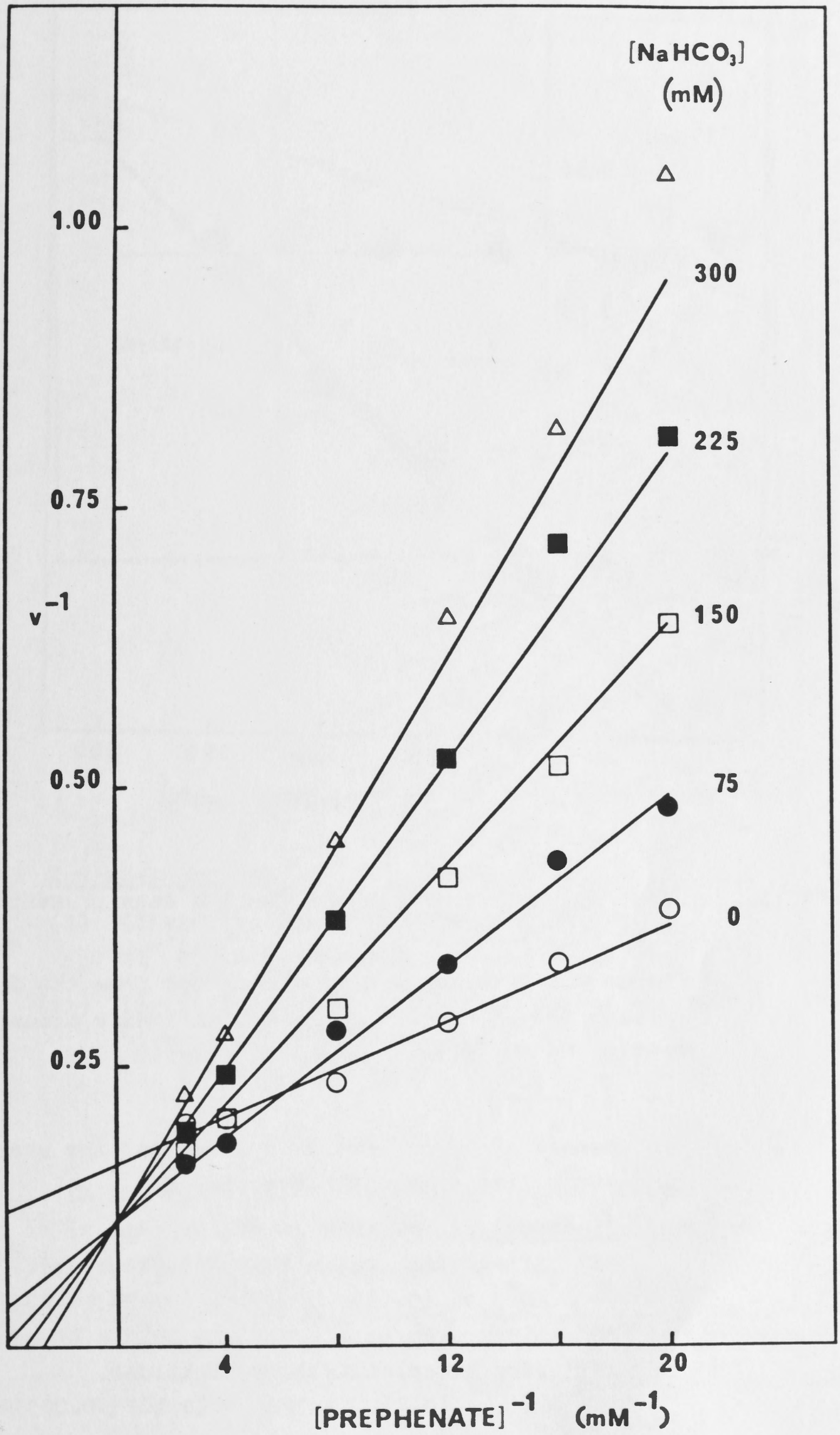
[NaHCO3]
(mM)
300
225
150
75
0
1.00
0.75
0.50
0.25
v-1
4
12
20
[PREPHENATE]-1 (mM-1)

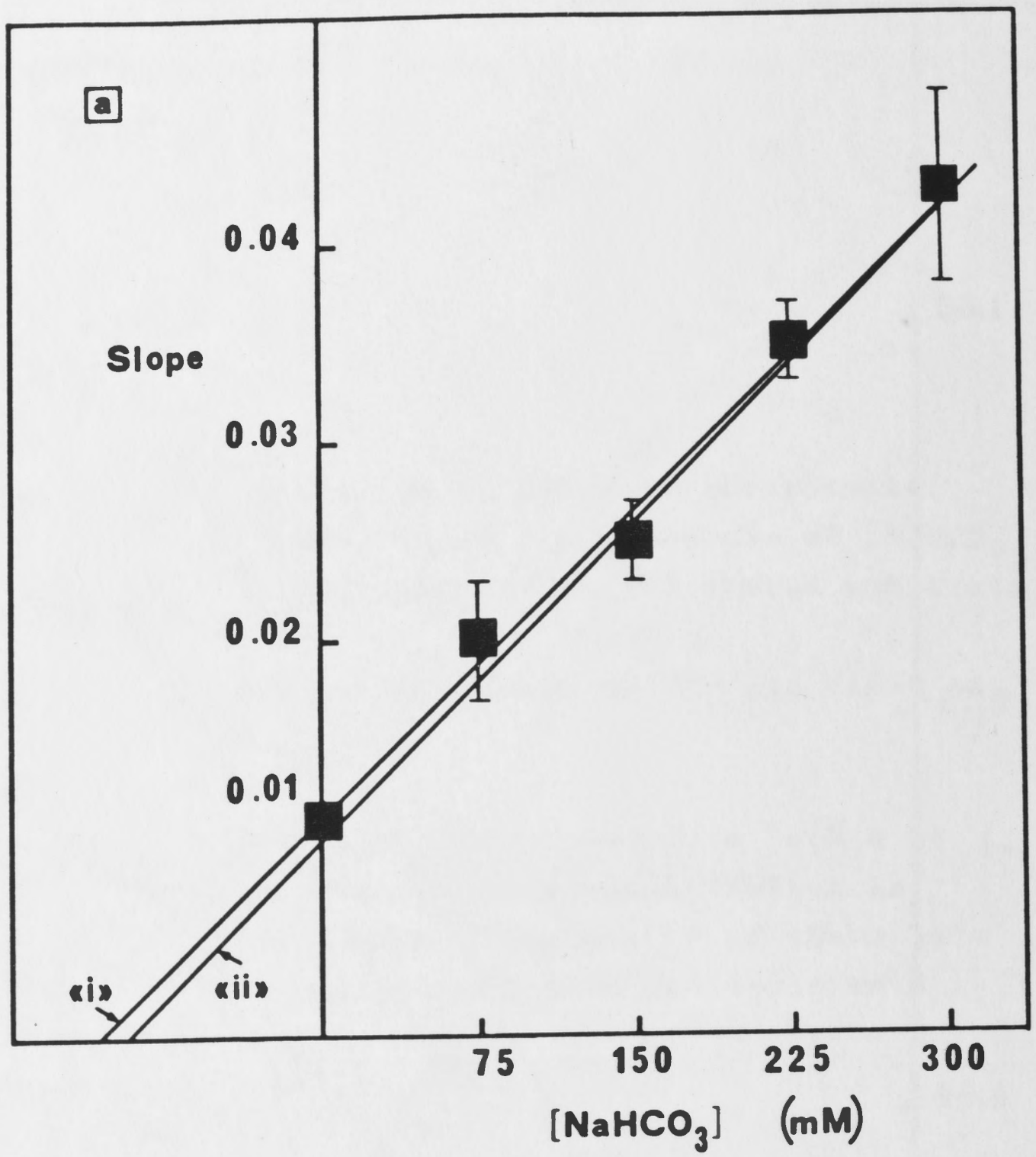

FIGURE 3.12 Slope and intercept replots for the data presented in Fig. 3.11.

Slopes and intercepts were determined from the fit of each set of data at a given bicarbonate concentration to the Michaelis-Menten equation

$$v = \frac{VA}{K_a + A}$$

The absence of error bars indicates that the standard error lies within the symbols used.

(a) Slope replot

(i) Linear regression through all points.

$YS^{*} = (0.011 \pm 0.001) + (0.104 \pm 0.005)X$

(ii) Linear regression through points at non-zero bicarbonate concentrations.

$YS = (0.010 \pm 0.002) + (0.107 \pm 0.005)X$

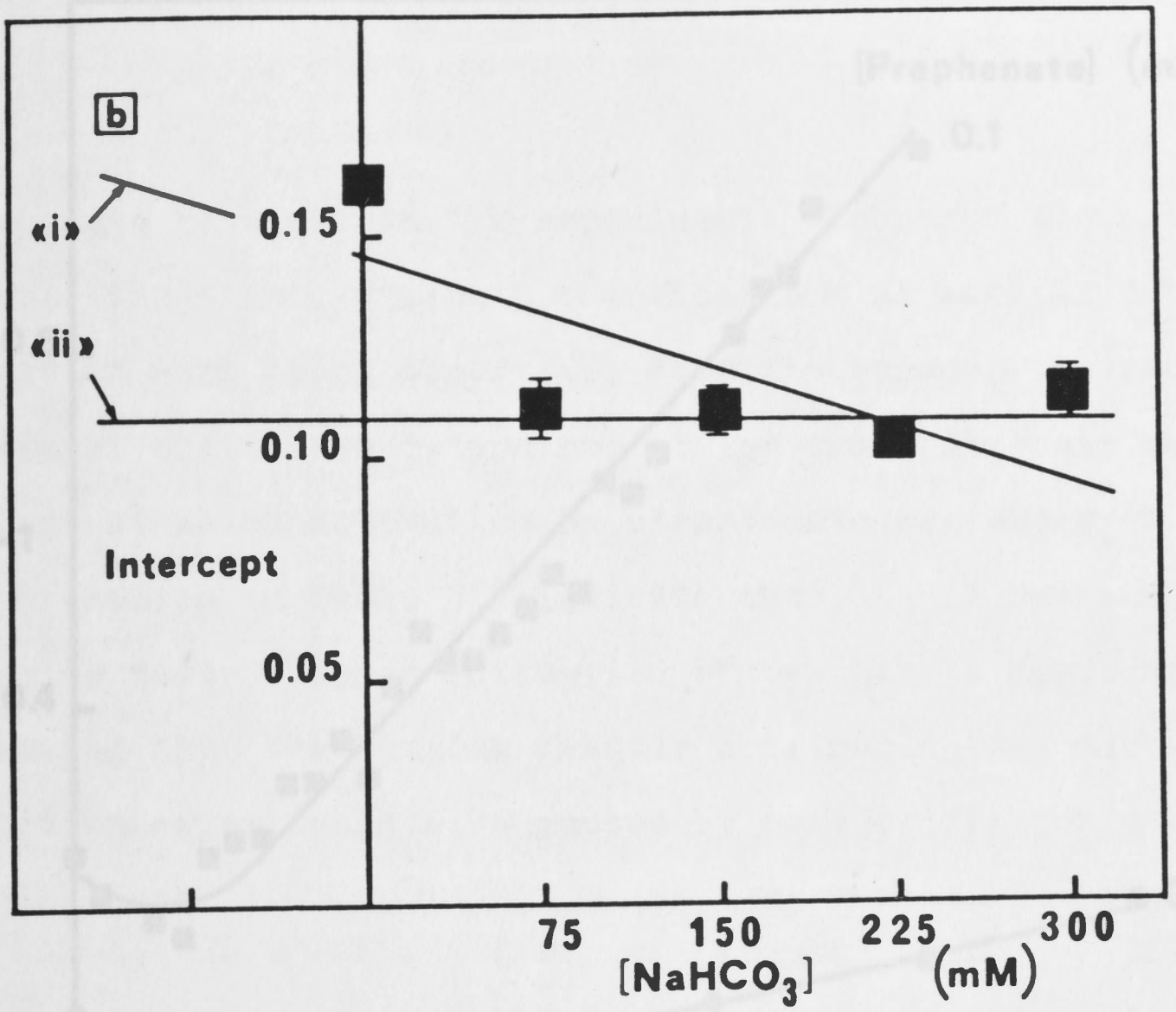

(b) Intercept replot

(i) Linear regression through all points.

$YI = (0.146 \pm 0.015) - (0.173 \pm 0.780)X$

(ii) Linear regression through points at non-zero bicarbonate concentrations.

$YI = (0.109 \pm 0.009) - (0.004 \pm 0.044)X$

* X, YS and YI represent bicarbonate concentration, slope of double reciprocal plot and intercept of double reciprocal plot, respectively.

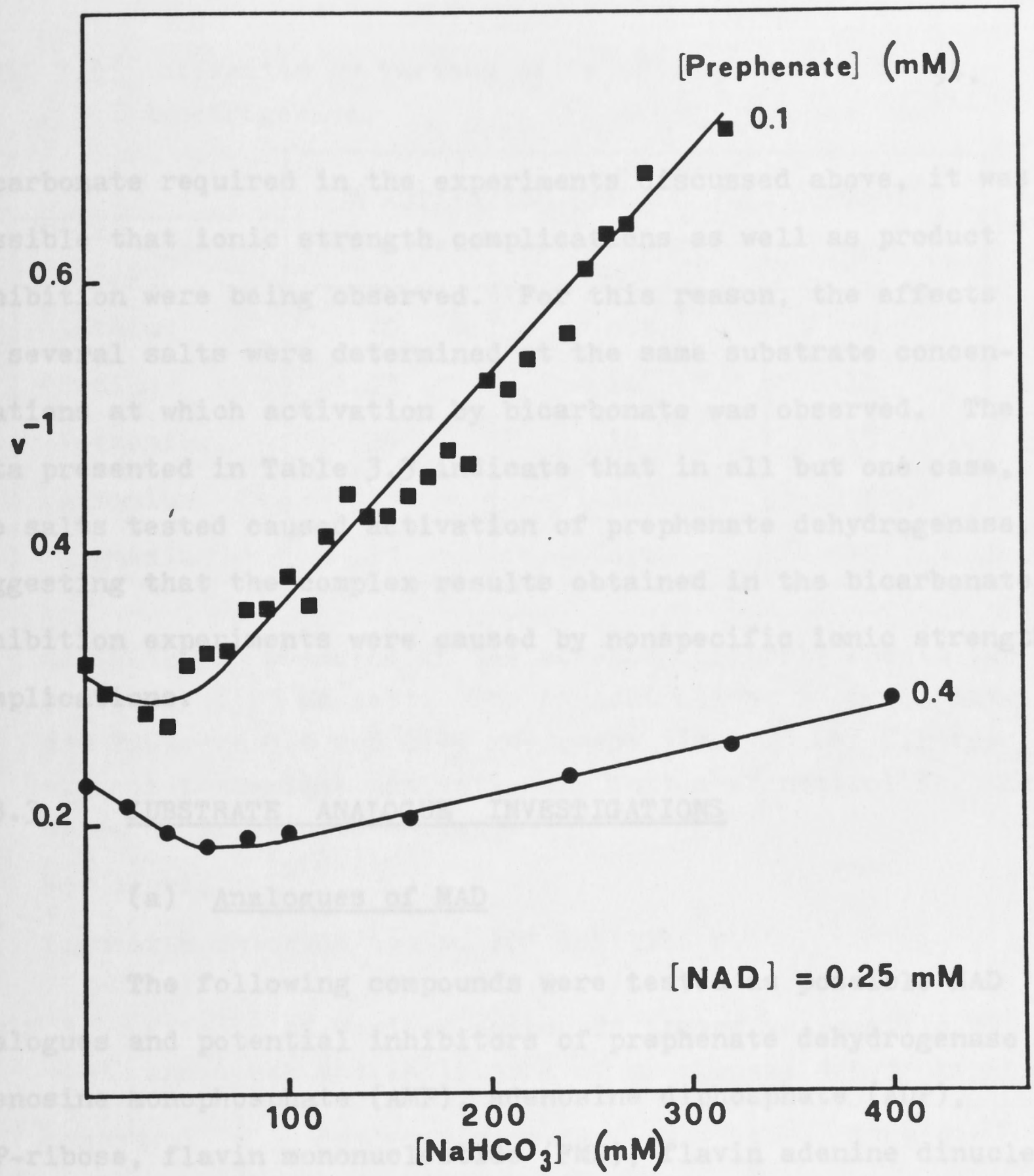

Figure 3.13 Dixon plots illustrating activation of prephenate dehydrogenase at relatively low concentrations of sodium bicarbonate, inhibition at higher concentrations.

Points at 0.4 mM prephenate concentration (●) are means of duplicate estimations whose range is less than 5% of the mean.
Lines through the points are fitted by eye, and are only meant to show trends.

N.B. Dixon plots for parabolic inhibition have their minimum at zero inhibitor concentration (see Results and Discussion).

bicarbonate required in the experiments discussed above, it was possible that ionic strength complications as well as product inhibition were being observed. For this reason, the effects of several salts were determined at the same substrate concentrations at which activation by bicarbonate was observed. The data presented in Table 3.3 indicate that in all but one case, the salts tested caused activation of prephenate dehydrogenase, suggesting that the complex results obtained in the bicarbonate inhibition experiments were caused by nonspecific ionic strength complications.

3.3.3 SUBSTRATE ANALOGUE INVESTIGATIONS

(a) Analogues of NAD

The following compounds were tested as possible NAD analogues and potential inhibitors of prephenate dehydrogenase : adenosine monophosphate (AMP), adenosine diphosphate (ADP), ADP-ribose, flavin mononucleotide (FMN), flavin adenine dinucleotide (FAD) and thionicotinamide adenine dinucleotide (Thio-NAD). As seen from the data in Table 3.4, AMP and Thio-NAD were the only substances which caused enough inhibition to warrant further investigation. Fig. 3.14 records the linear competitive inhibition by AMP with respect to NAD. However, when prephenate was the varied substrate, double reciprocal plots were reproducibly concave-up in the presence of AMP (Fig. 3.15). Because of the small degree of inhibition at higher prephenate concentrations, it is not possible to determine with certainty whether there is an effect of AMP on the vertical intercept.

TABLE 3.3 Activation by various salts of prephenate dehydrogenase.

cation \ anion	% ACTIVATION BY SALT OVER CONTROL* Acetate	Bicarbonate	Chloride
Lithium	20	n.t.**	6
Sodium	23	16	11
Potassium	24	18	13
Ammonium	18	16	6
Magnesium	27	n.t.	-10***

* Activity was measured in the absence (control) and in the presence of 75 mM salt. The concentrations of prephenate and NAD were 0.4 and 0.25 mM, respectively. The figures express percentage activation by salt over control for the means of triplicate estimates.

** Not tested.

*** Magnesium chloride caused 10% inhibition.

TABLE 3.4 Effects of various compounds tested as possible NAD analogues and inhibitors of prephenate dehydrogenase.

COMPOUND	CONCENTRATION (mM) OF test compound	prephenate	NAD	EFFECT
AMP	0.4	0.1	0.1	16% inhibition
ADP	0.4	0.1	0.1	18% activation
ADP-ribose	0.4	0.1	0.1	none
Thio-NAD	0.4	0.1	0.1	60% inhibition
FAD	0.28	0.05-0.25	0.1	no significant effect

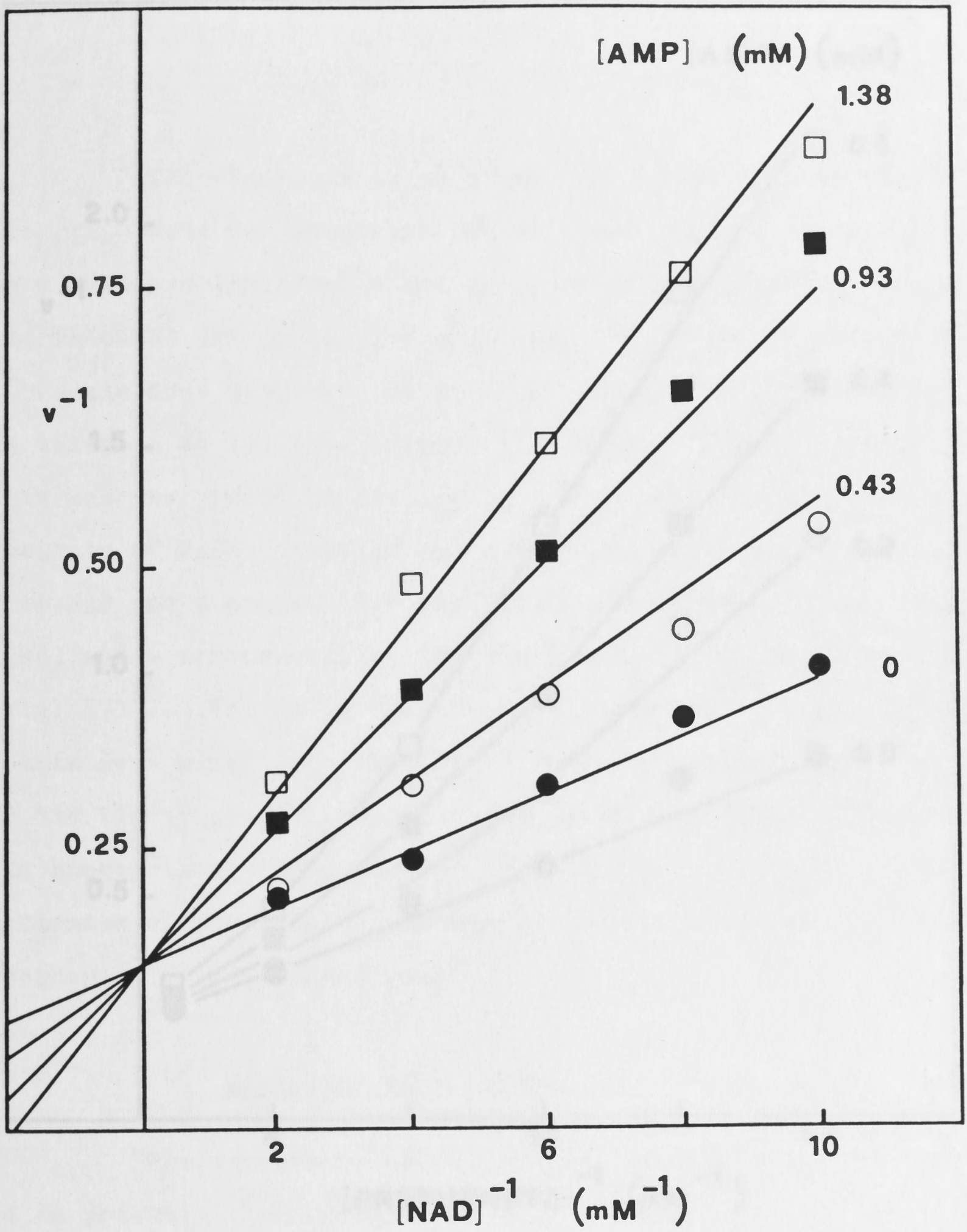

FIGURE 3.14 Inhibition by AMP of prephenate dehydrogenase at pH 8.3 when NAD is the varied substrate. The concentration of prephenate was fixed at 0.4mM. Lines through the data points are calculated from the fit of the data to the equation describing linear competitive inhibition :

$$v = \frac{VA}{K_a(1 + I/K_{is}) + A}$$

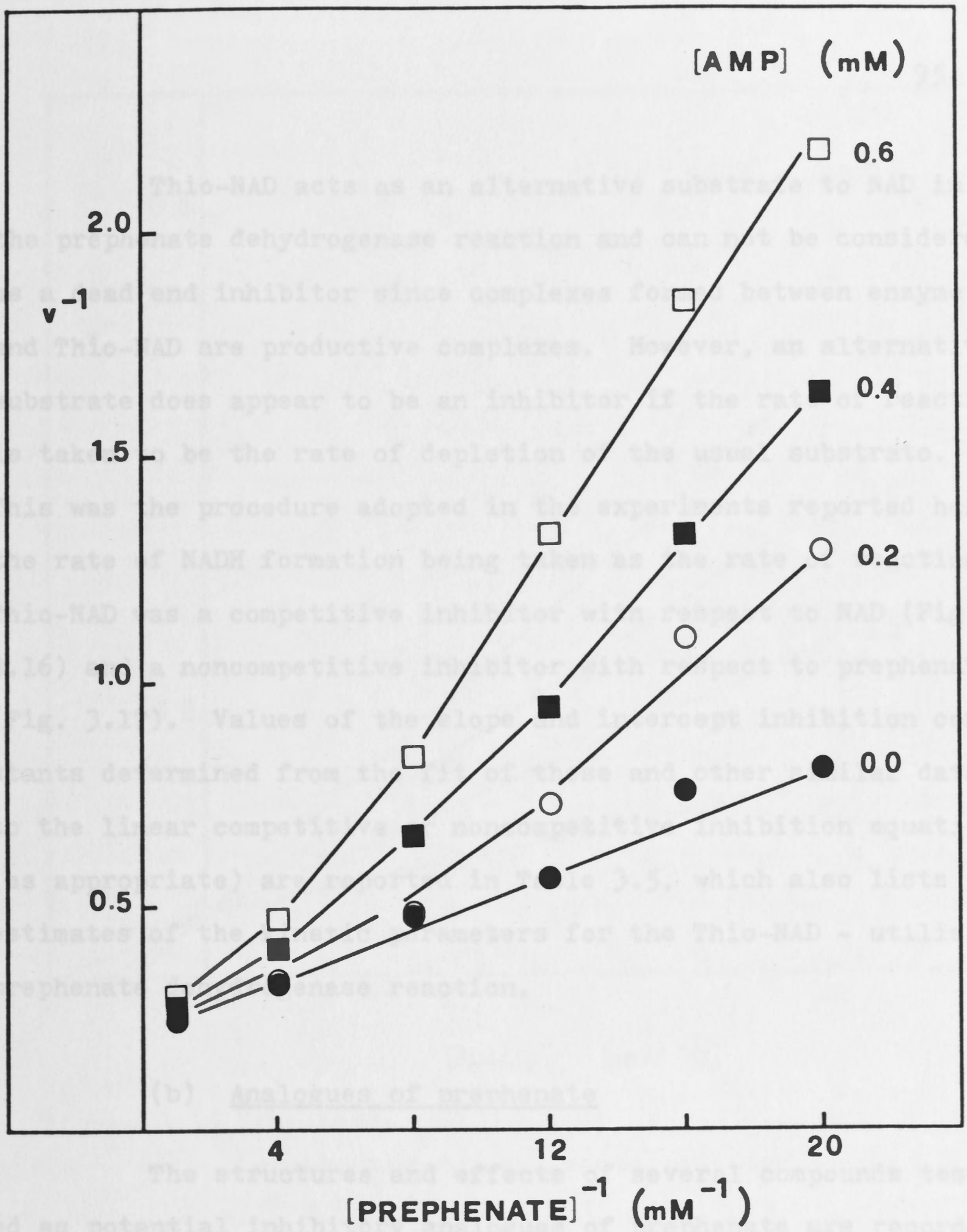

FIGURE 3.15 Inhibition by AMP of prephenate dehydrogenase at pH 8.3 when prephenate is the varied substrate. The concentration of NAD was fixed at 0.25 mM. Lines through the data points are fitted by eye.

Thio-NAD acts as an alternative substrate to NAD in the prephenate dehydrogenase reaction and can not be considered as a dead end inhibitor since complexes formed between enzyme and Thio-NAD are productive complexes. However, an alternative substrate does appear to be an inhibitor if the rate of reaction is taken to be the rate of depletion of the usual substrate. This was the procedure adopted in the experiments reported here, the rate of NADH formation being taken as the rate of reaction. Thio-NAD was a competitive inhibitor with respect to NAD (Fig. 3.16) and a noncompetitive inhibitor with respect to prephenate (Fig. 3.17). Values of the slope and intercept inhibition constants determined from the fit of these and other similar data to the linear competitive or noncompetitive inhibition equation (as appropriate) are reported in Table 3.5, which also lists estimates of the kinetic parameters for the Thio-NAD - utilising prephenate dehydrogenase reaction.

(b) Analogues of prephenate

The structures and effects of several compounds tested as potential inhibitory analogues of prephenate are recorded in Table 3.6. Of the compounds which were more fully investigated, several induced concave-up double reciprocal plots when NAD was the varied substrate (*viz.* 1-adamantane acetic acid (Fig. 3.18) and *cis*-aconitate, 4-hydroxybenzaldehyde and mimosine). *Trans*-aconitate was a more effective inhibitor than the *cis* isomer, and the double reciprocal plots in its presence remained linear. The inhibition appeared to be competitive with respect to prephenate and noncompetitive with respect to NAD,

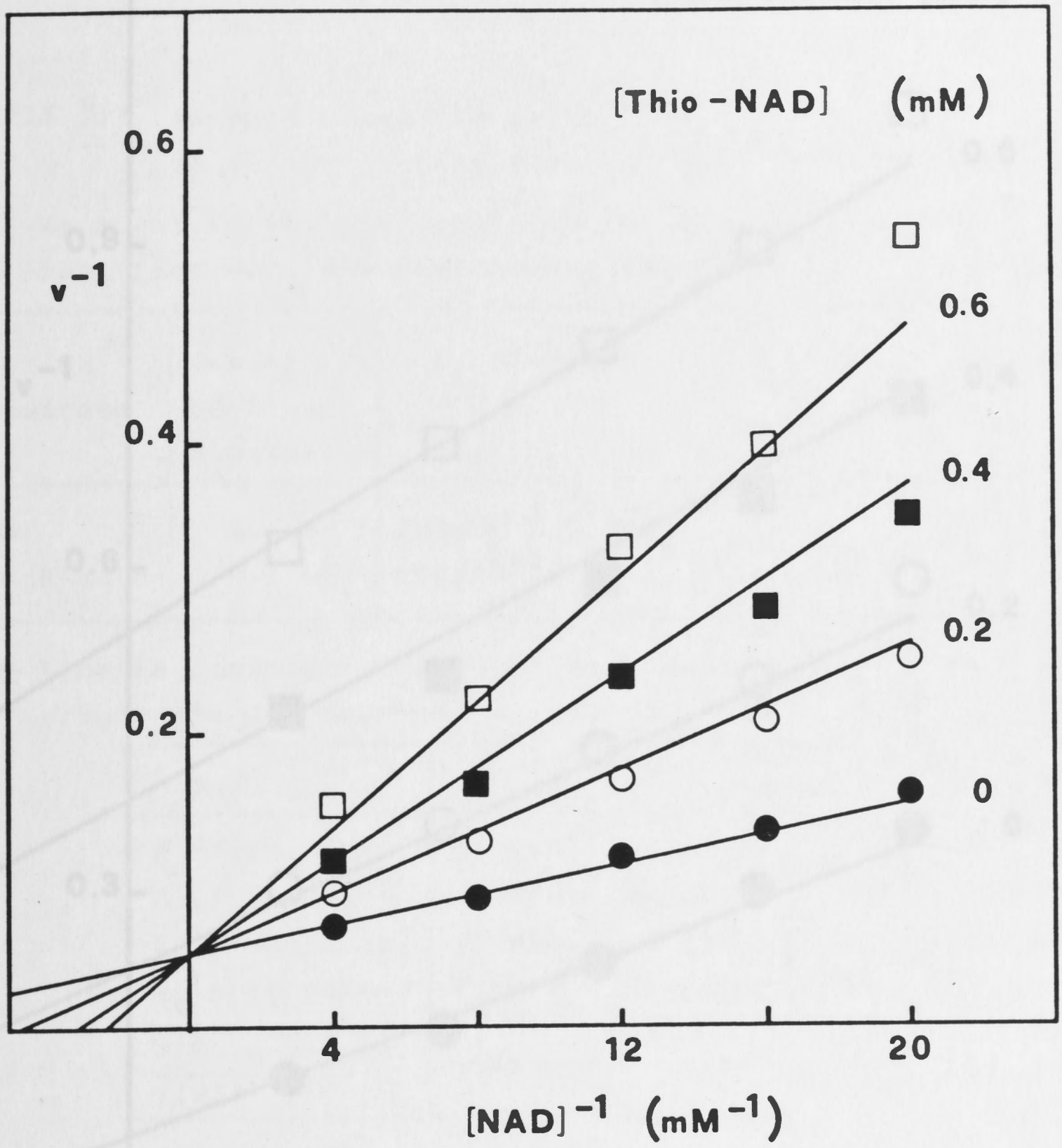

Figure 3.16 Inhibition by Thio-NAD of the NAD-utilising prephenate dehydrogenase reaction at pH 8.3 when NAD is the varied substrate.

The concentration of prephenate was fixed at 0.1 mM.

Assays were performed as specified in Section 3.2.3.

Lines through the data points (means of duplicate estimates) are calculated from the fit of the data to the equation describing linear competitive inhibition :

$$v = \frac{VA}{K_a(1 + I/K_{is}) + A}$$

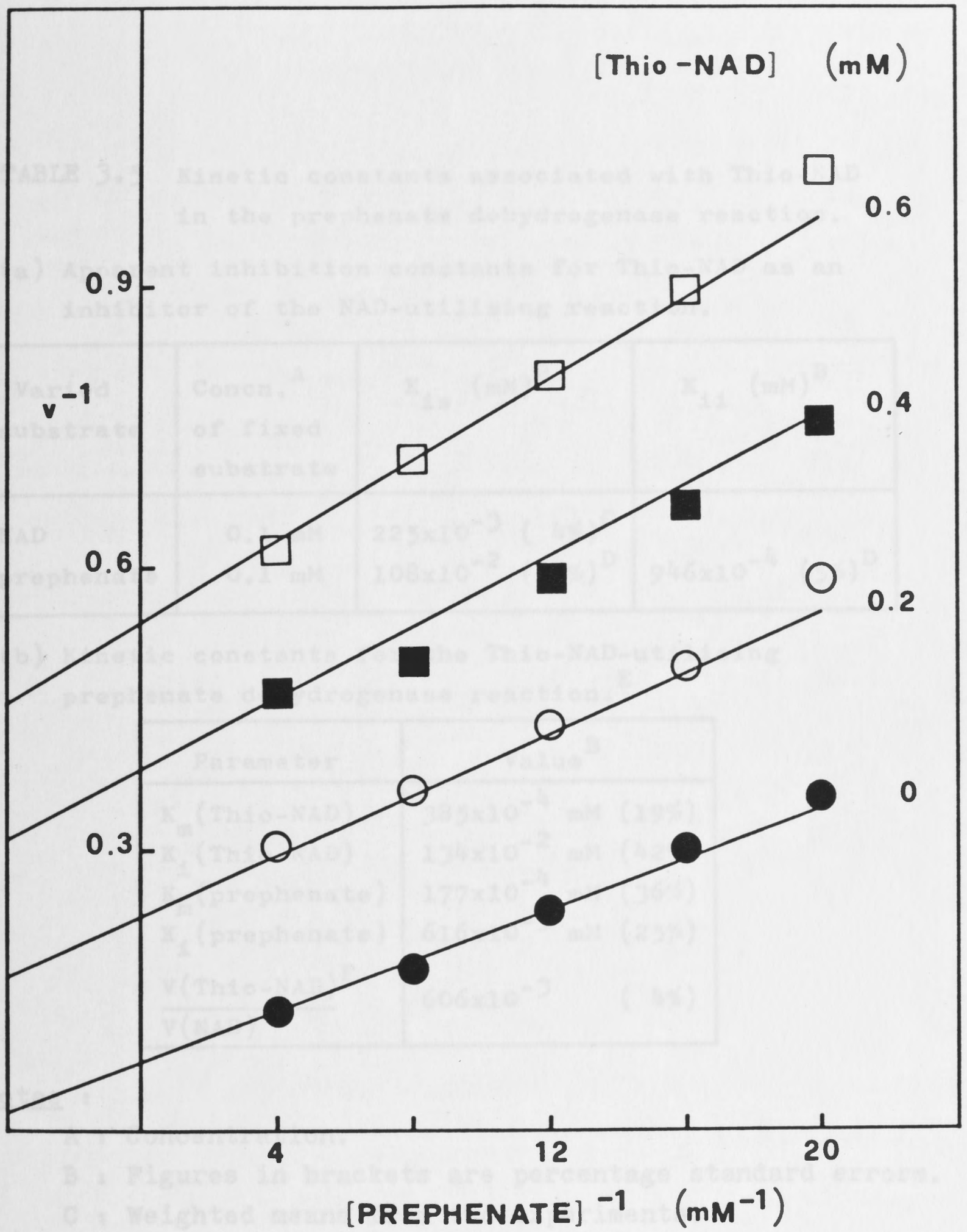

FIGURE 3.17 Inhibition by Thio-NAD of the NAD - utilising prephenate dehydrogenase reaction at pH 8.3 when prephenate is the varied substrate. The concentration of NAD was fixed at 0.1 mM. Assays were performed as specified in Section 3.2.3. Lines through the data points are calculated from the fit of the data to the equation describing linear noncompetitive inhibition :

$$v = \frac{VA}{K_a(1 + I/K_{is}) + A(1 + I/K_{ii})}$$

TABLE 3.5 Kinetic constants associated with Thio-NAD in the prephenate dehydrogenase reaction.

(a) Apparent inhibition constants for Thio-NAD as an inhibitor of the NAD-utilising reaction.

Varied substrate	Concn.[A] of fixed substrate	K_{is} (mM)[B]	K_{ii} (mM)[B]
NAD	0.1 mM	225×10^{-3} (4%)[C]	
prephenate	0.1 mM	108×10^{-2} (27%)[D]	946×10^{-4} (5%)[D]

(b) Kinetic constants for the Thio-NAD-utilising prephenate dehydrogenase reaction.[E]

Parameter	Value[B]
K_m(Thio-NAD)	385×10^{-4} mM (19%)
K_i(Thio-NAD)	134×10^{-2} mM (42%)
K_m(prephenate)	177×10^{-4} mM (36%)
K_i(prephenate)	616×10^{-3} mM (25%)
$\frac{V(\text{Thio-NAD})}{V(\text{NAD})}$[F]	606×10^{-3} (4%)

Notes :

A : Concentration.

B : Figures in brackets are percentage standard errors.

C : Weighted means from two experiments.

D : Weighted means from three experiments.

E : Determined from a single initial velocity experiment with 12 data points.

F : Ratio of maximum velocity of Thio-NAD - utilising reaction to that of NAD - utilising reaction.

TABLE 3.6(a) Structures and effects of some compounds tested as potential prephenate analogues and inhibitors of prephenate dehydrogenase.

Compound	Structure
α-ketoglutarate	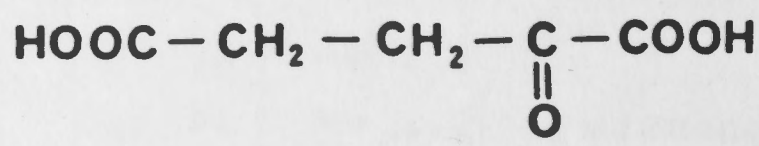
oxaloacetate	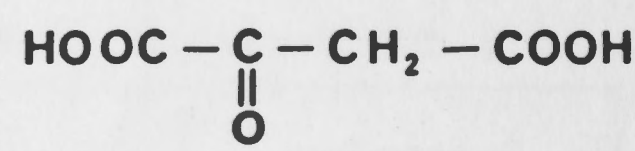
succinate	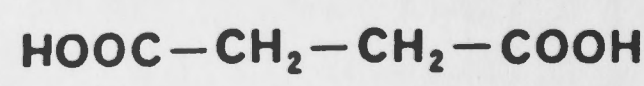
citrate	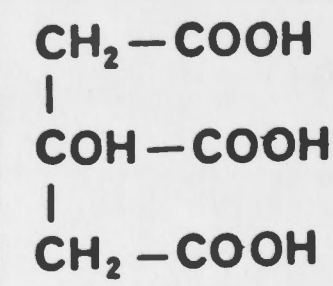
phenylacetate	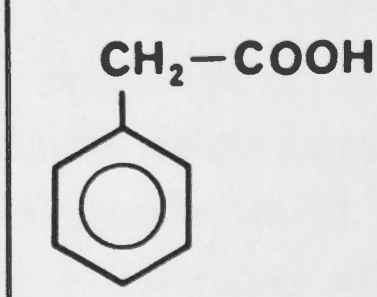
3,4-dihydroxybenzoate	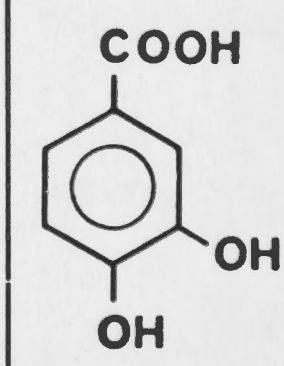

Concentration (mM) of test compound	prephenate	NAD	Effect
7	0.05	0.1	15% inhibition
9,18	0.1	0.05-0.25	none
7	0.05	0.1	none
7	0.05	0.1	none
0.4	0.1	0.1	none
1	0.1	0.1	none

TABLE 3.6(b) Structures and effects of some compounds tested as potential prephenate analogues and inhibitors of prephenate dehydrogenase.

Compound	Structure
<u>cis</u>-aconitate	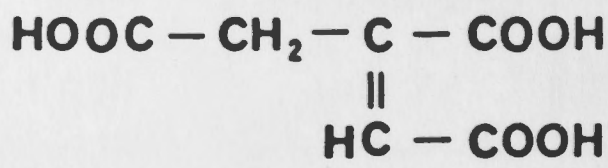
<u>trans</u>-aconitate	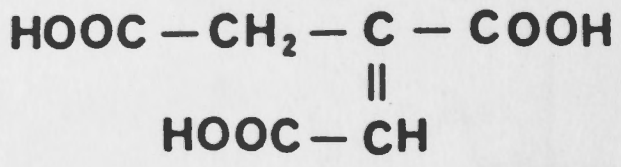
1-adamantane acetic acid	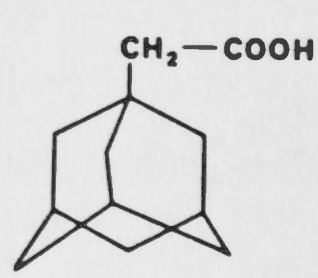
4-hydroxybenzaldehyde	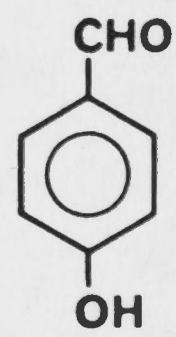
mimosine	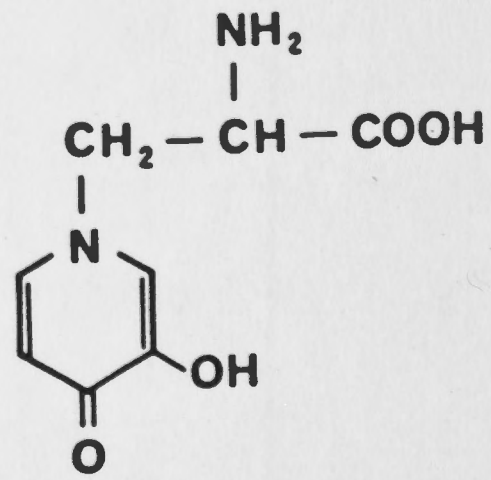

Effect
Induces concave-up double reciprocal plots with NAD as the varied substrate. Effectiveness: at 80 mM results in 20% and 39% inhibition at NAD concentrations of 0.5 and 0.056 mM, respectively, with prephenate fixed at 0.08 mM.
Linear double reciprocal plots, but slopes not linear function of inhibitor concentration (see Figs. 3.19 and 3.20). High concentrations required.
Effective inhibitor; induces concave-up double reciprocal plots with NAD as the varied substrate (see Fig. 3.18).
Induces concave-up double reciprocal plots with NAD as the varied substrate. Effectiveness: at 0.1 mM results in 8% and 29% inhibition at NAD concentrations of 0.25 and 0.05 mM, respectively, with prephenate fixed at 0.1 mM.
Induces concave-up double reciprocal plots with NAD as the varied substrate. Effectiveness: at 2 mM results in 41% and 73% inhibition at NAD concentrations of 0.25 and 0.05 mM, respectively, with prephenate fixed at 0.1 mM.

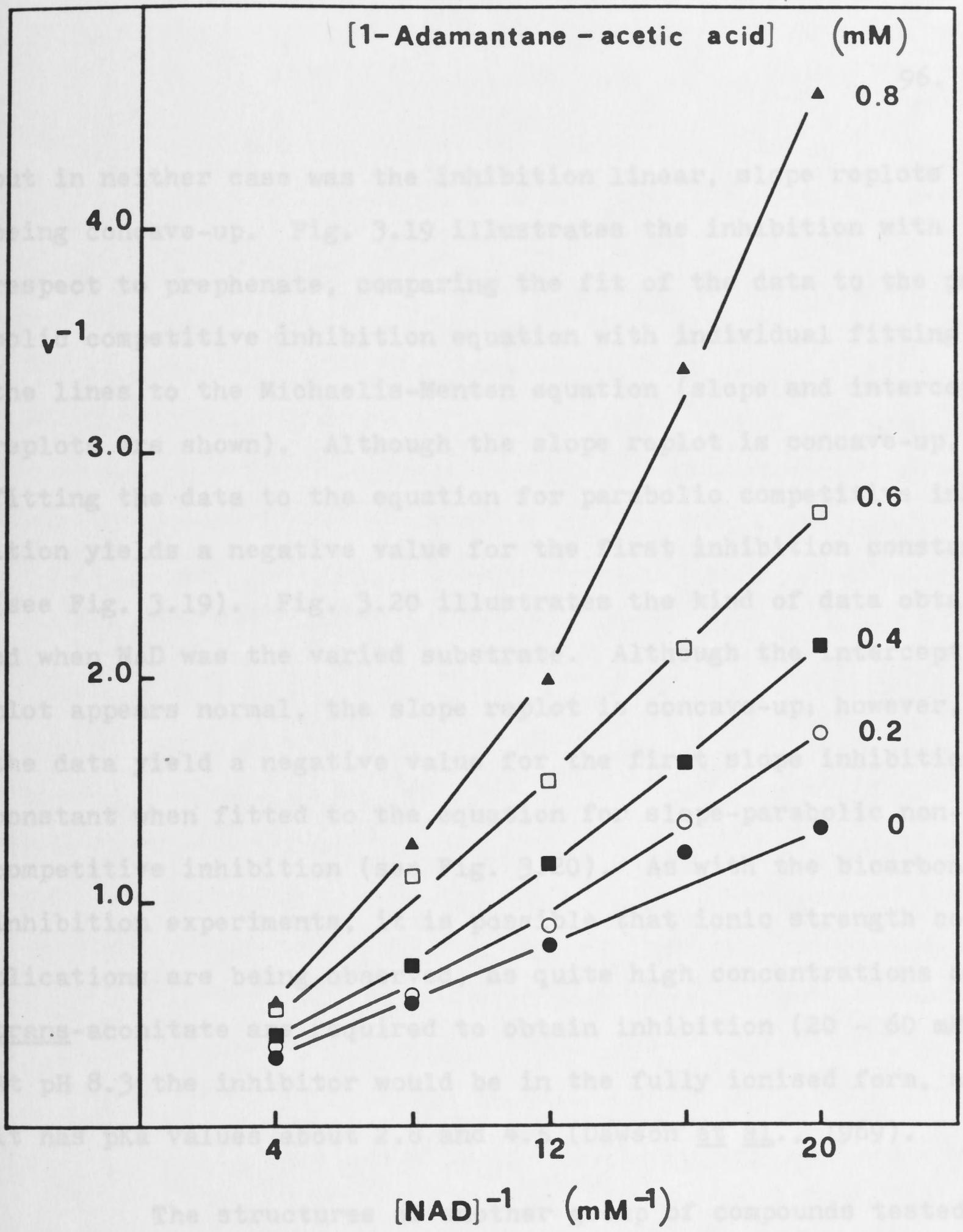

FIGURE 3.18 Inhibition by 1-adamantane acetic acid of prephenate dehydrogenase at pH 8.3 when NAD is the varied substrate. The concentration of prephenate was fixed at 0.05 mM. Lines through the data points are fitted by eye.

but in neither case was the inhibition linear, slope replots being concave-up. Fig. 3.19 illustrates the inhibition with respect to prephenate, comparing the fit of the data to the parabolic competitive inhibition equation with individual fitting of the lines to the Michaelis-Menten equation (slope and intercept replots are shown). Although the slope replot is concave-up, fitting the data to the equation for parabolic competitive inhibition yields a negative value for the first inhibition constant (see Fig. 3.19). Fig. 3.20 illustrates the kind of data obtained when NAD was the varied substrate. Although the intercept replot appears normal, the slope replot is concave-up; however, the data yield a negative value for the first slope inhibition constant when fitted to the equation for slope-parabolic non-competitive inhibition (see Fig. 3.20). As with the bicarbonate inhibition experiments, it is possible that ionic strength complications are being observed, as quite high concentrations of trans-aconitate are required to obtain inhibition (20 - 60 mM). At pH 8.3 the inhibitor would be in the fully ionised form, as it has pKa values about 2.8 and 4.5 (Dawson et al., 1969).

The structures of another group of compounds tested as possible analogues of prephenate are indicated in Fig. 3.21. With the exception of 4-hydroxycinnamate, none of these compounds was suitable because of the low degree of inhibition (if any) at the highest concentration which could be tested (determined by the background absorbance at 340 nm contributed by the potential inhibitor). Of all the compounds tested, only 4-hydroxycinnamate was found suitable as a prephenate analogue

Figure 3.19 Inhibition by trans-aconitate of prephenate dehydrogenase at pH 8.3 when prephenate is the varied substrate.
The concentration of NAD was fixed at 0.1 mM.

(a) Lines through the data points are calculated from the fit of the data to the equation describing parabolic competitive inhibition :

$$v = \frac{VA}{K_a(1 + I/K_{is1} + I^2/K_{is2}) + A}$$

The values obtained for the apparent inhibition constants were : -

$$K_{is1} = -148 \times 10^0 \text{ mM } (80\%)*$$
$$K_{is2} = 121 \times 10^1 \text{ mM } (16\%)*$$

* Figures in brackets are percentage standard errors.

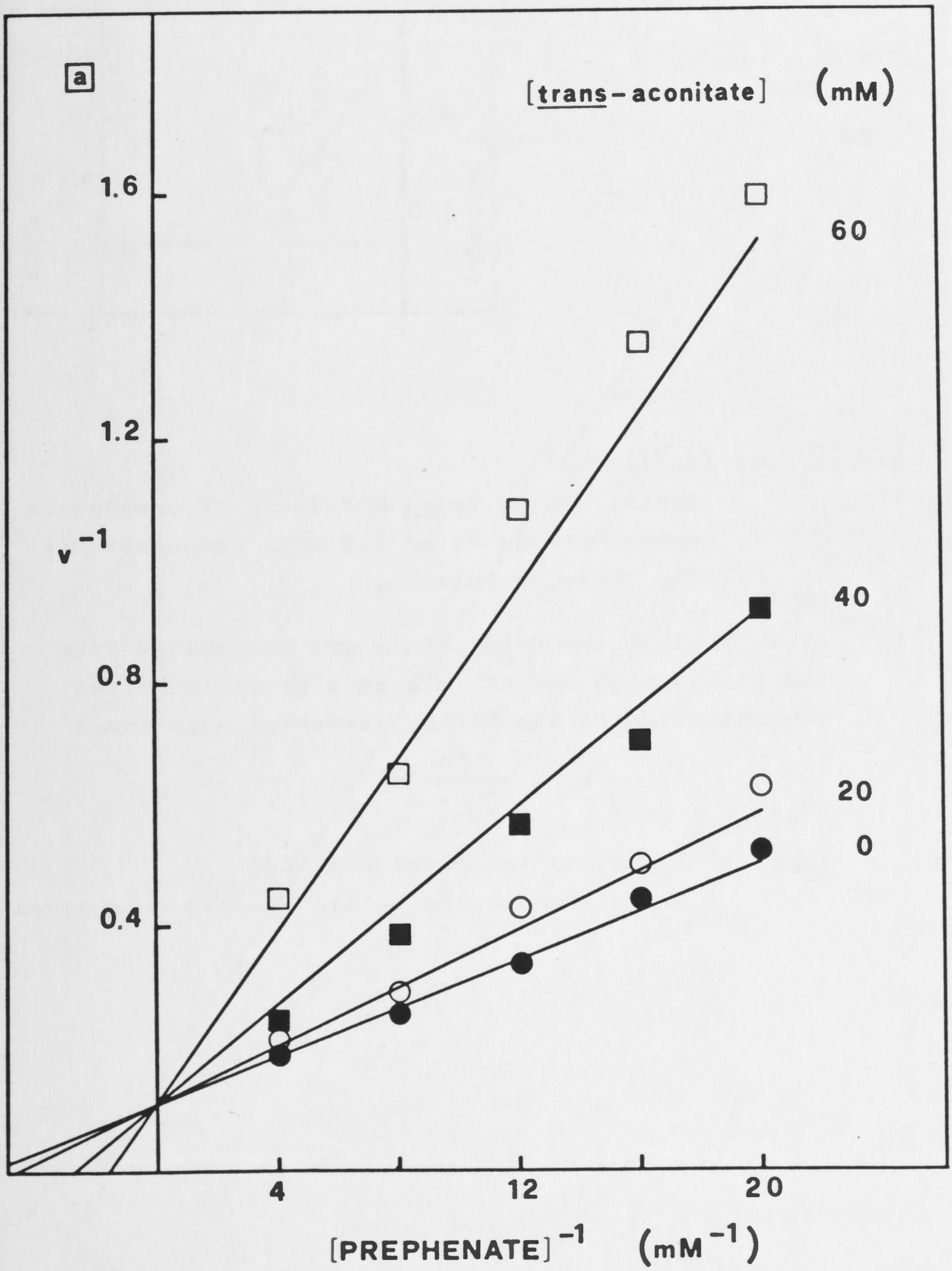
a
[trans-aconitate] (mM)
1.6
1.2
0.8
0.4
v^-1
60
40
20
0
4
12
20
[PREPHENATE]^-1 (mM^-1)

Figure 3.19 (continued)

Inhibition by <u>trans</u>-aconitate of prephenate dehydrogenase at pH 8.3 when prephenate is the varied substrate.

(b) Lines through the data points are calculated from the fit of each set of data at a given inhibitor concentration to the Michaelis-Menten equation :

$$v = \frac{VA}{K_a + A}$$

<u>Inset</u> : Slope and intercept replots.
Lines through the points are not calculated.

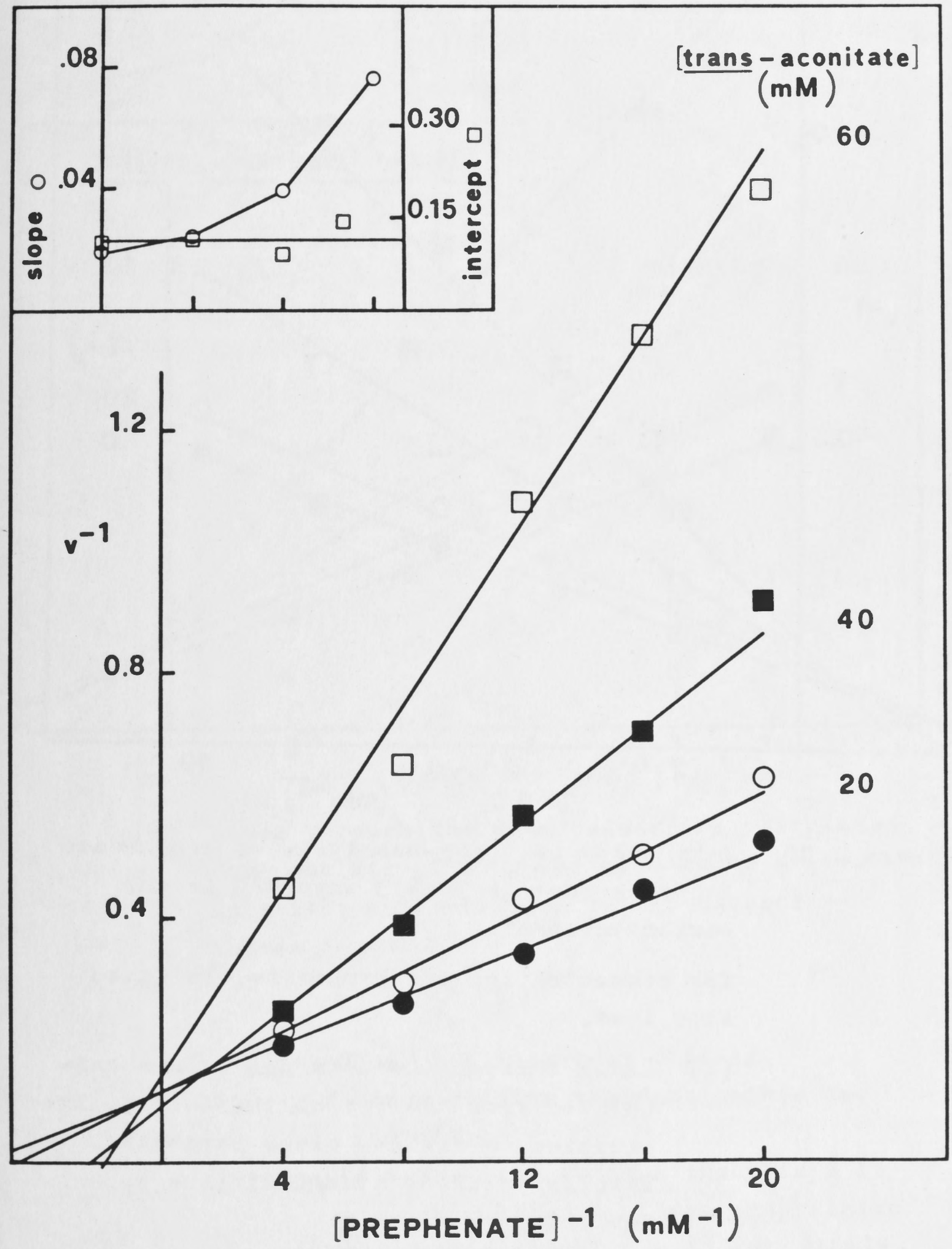
slope
.08
.04
intercept
0.30
0.15
[trans-aconitate]
(mM)
60
40
20
1.2
0.8
0.4
v⁻¹
4
12
20
[PREPHENATE]⁻¹ (mM⁻¹)

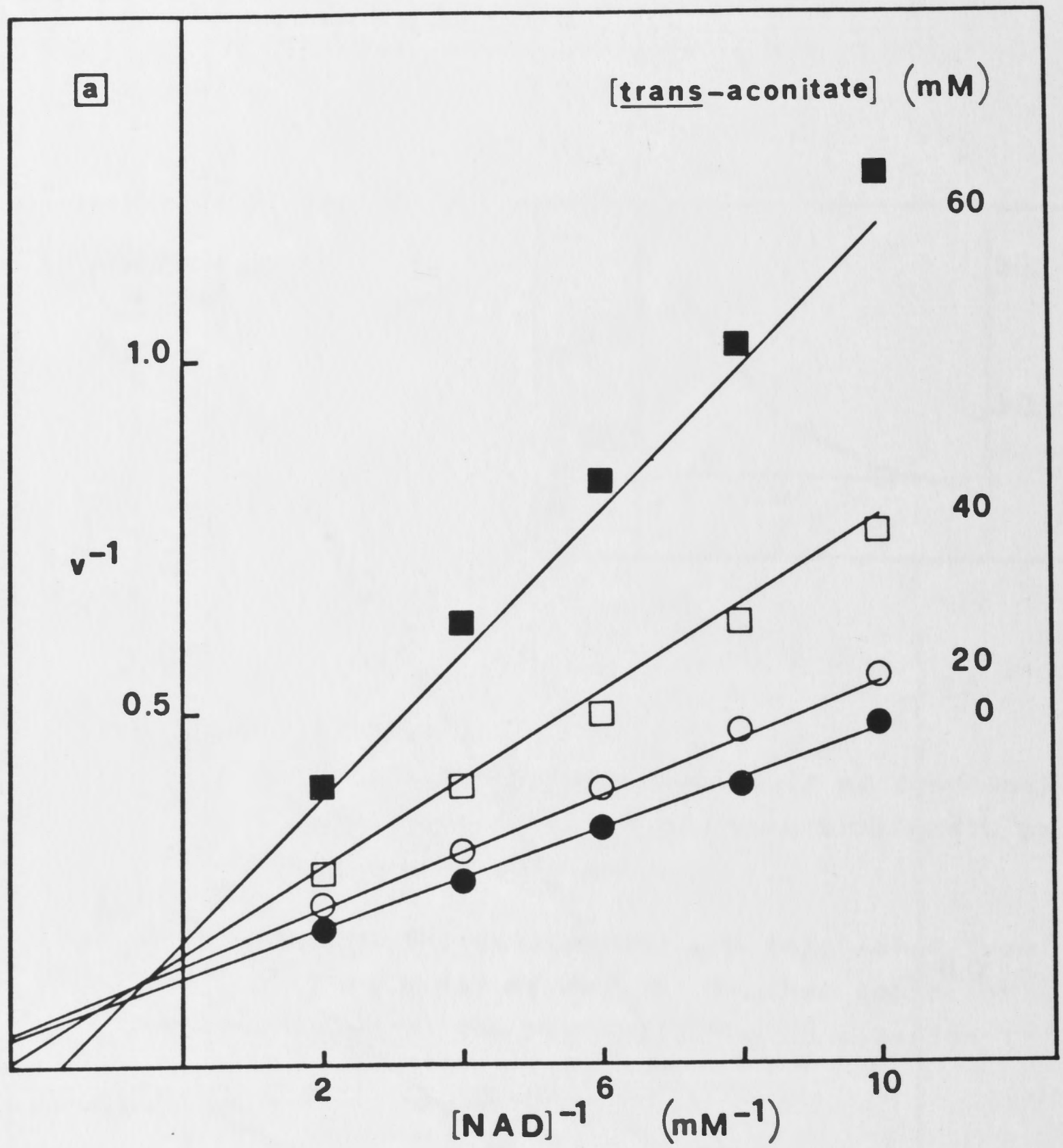

Figure 3.20 Inhibition by trans-aconitate of prephenate dehydrogenase at pH 8.3 when NAD is the varied substrate.

The concentration of prephenate was fixed at 0.1 mM.

(a) Lines through the data points are calculated from the fit of the data to the equation describing slope parabolic, intercept linear noncompetitive inhibition :

$$v = \frac{VA}{K_a(1 + I/K_{is1} + I^2/K_{is2}) + A(1 + I/K_{ii})}$$

The values obtained for the apparent inhibition constants were : K_{is1} = -191 mM (60%)*, K_{is2} = 1640 mM (10%)*, K_{ii} = 124 mM (29%)*.

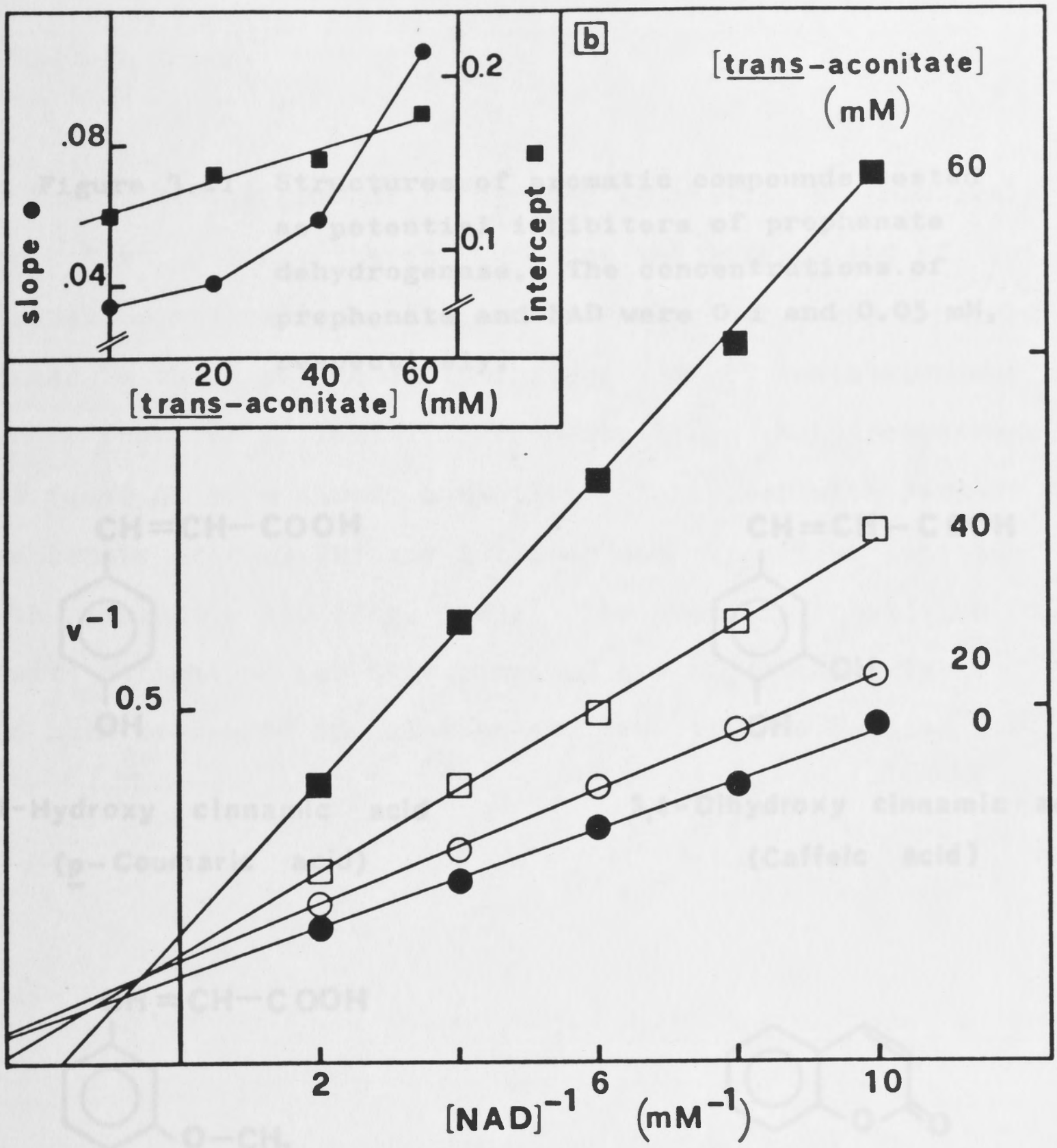

(b) Lines through the data points are calculated from the fit of each set of data at a given inhibitor concentration to the Michaelis-Menten equation :

$$v = \frac{VA}{K_a + A}$$

Inset : Slope and intercept replots.

Slopes : Lines joining the data points are not fitted.

Intercepts : The line through the points is calculated by linear regression and yields K_{ii} = 134 mM (16%)*.

*Figures in brackets are percentage standard errors.

Figure 3.21 Structures of aromatic compounds tested as potential inhibitors of prephenate dehydrogenase. The concentrations of prephenate and NAD were 0.1 and 0.05 mM, respectively.

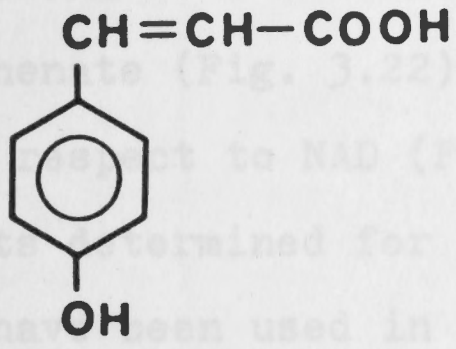

4-Hydroxy cinnamic acid
(p-Coumaric acid)

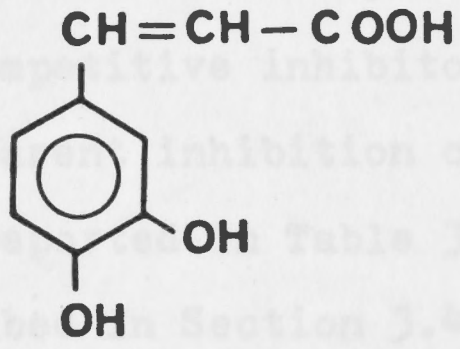

3,4-Dihydroxy cinnamic acid
(Caffeic acid)

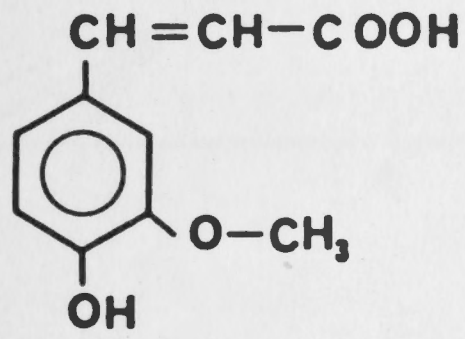

4-Hydroxy, 3-methoxy
cinnamic acid
(Ferulic acid)

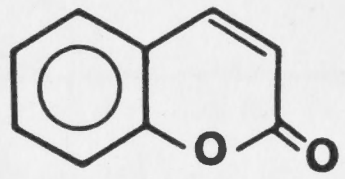

Coumarin

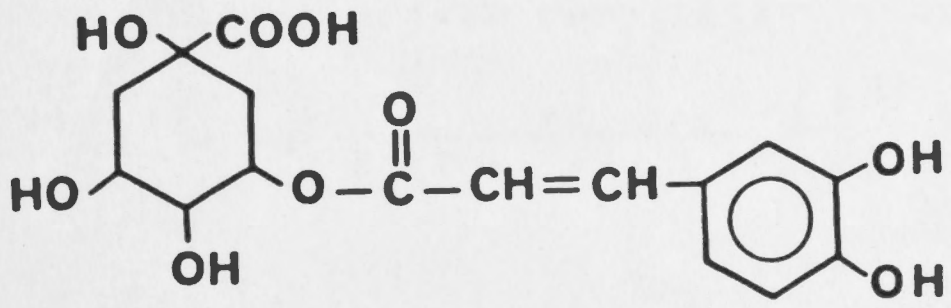

Chlorogenic acid

on the following grounds : (a) good inhibition at relatively low concentrations, thereby avoiding the possibility of ionic strength complications, (b) double reciprocal plots remained linear in the presence of inhibitor, and (c) inhibition was a linear function of inhibitor concentration. 4-Hydroxycinnamate was found to be a linear competitive inhibitor with respect to prephenate (Fig. 3.22) and a linear noncompetitive inhibitor with respect to NAD (Fig. 3.23). The apparent inhibition constants determined for this compound are reported in Table 3.7 and have been used in calculations described in Section 3.4.

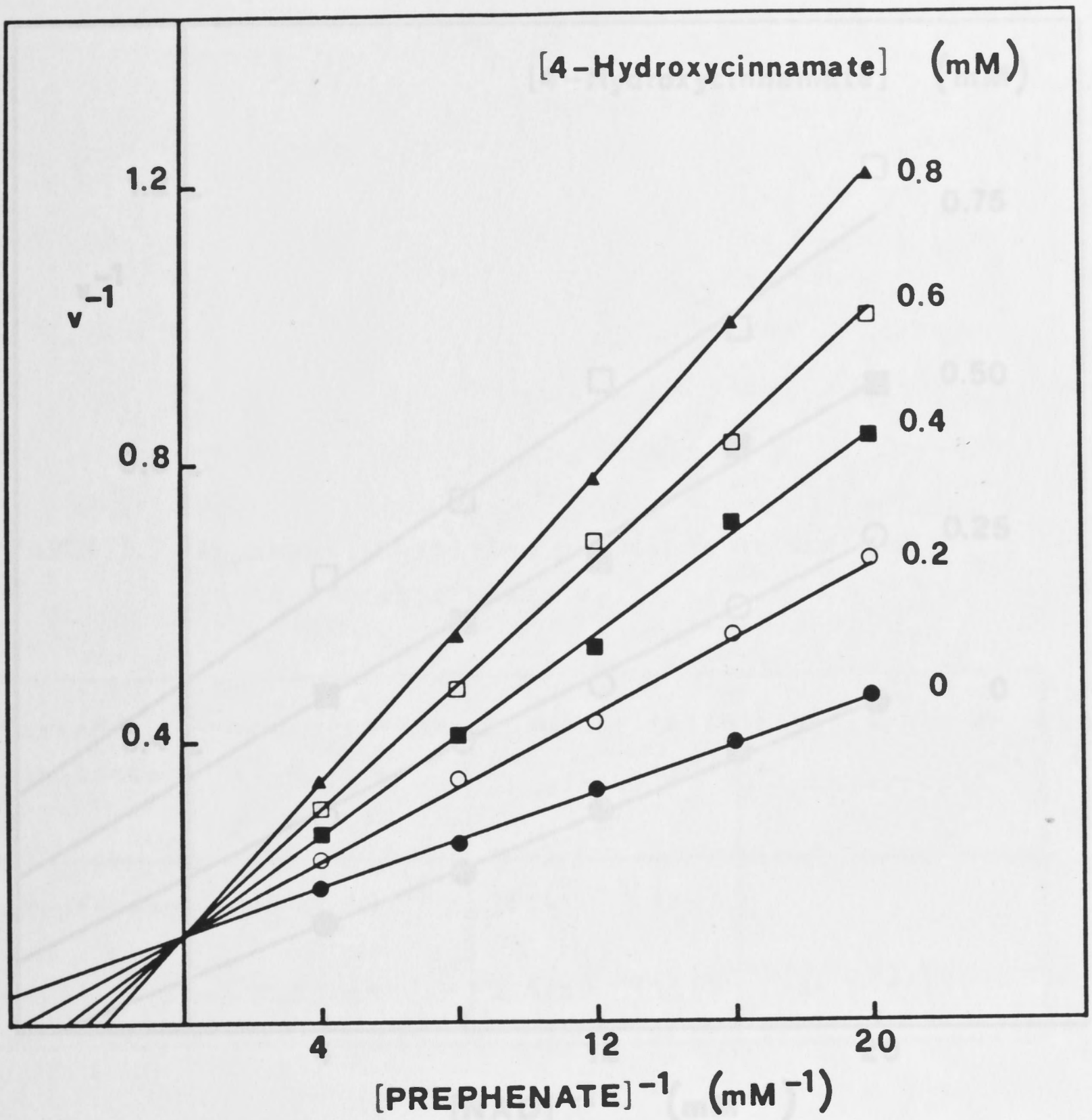

Figure 3.22 Inhibition by 4-hydroxycinnamate of prephenate dehydrogenase at pH 8.3 when prephenate is the varied substrate.

The concentration of NAD was fixed at 0.05 mM. Lines through the data points are calculated from the fit of the data to the equation describing linear competitive inhibition :

$$v = \frac{VA}{K_a(1 + I/K_{is}) + A}$$

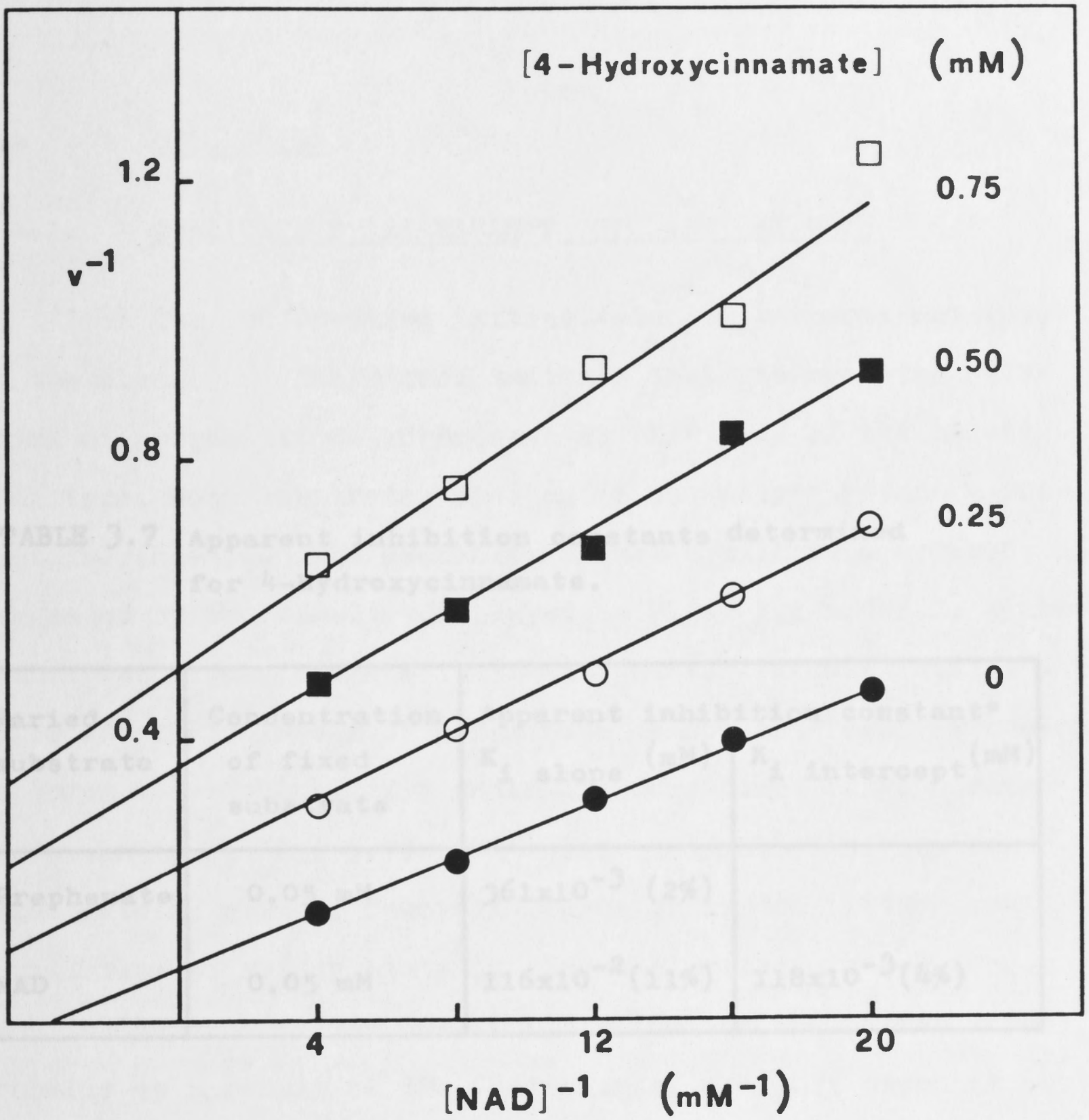

Figure 3.23 Inhibition by 4-hydroxycinnamate of prephenate dehydrogenase at pH 8.3 when NAD is the varied substrate.

The concentration of prephenate was fixed at 0.05 mM.

Lines through the data points are calculated from the fit of the data to the equation describing linear noncompetitive inhibition :

$$v = \frac{VA}{K_a(1 + I/K_{is}) + A(1 + I/K_{ii})}$$

TABLE 3.7 Apparent inhibition constants determined for 4-hydroxycinnamate.

Varied substrate	Concentration of fixed substrate	Apparent inhibition constant* K_i slope (mM)	K_i intercept (mM)
Prephenate	0.05 mM	361×10^{-3} (2%)	
NAD	0.05 mM	116×10^{-2} (11%)	118×10^{-3} (4%)

* Figures in brackets are percentage standard errors. All apparent constants are weighted means from two experiments.

3.4 DISCUSSION

3.4.1 QUALITATIVE ASSESSMENT OF THE RESULTS

The intersecting initial velocity patterns obtained in the absence of inhibitors indicate that the reaction mechanism of prephenate dehydrogenase at pH 8.3 is of the sequential type, both substrates binding to the enzyme before a product is released. The mechanism is not equilibrium ordered, as suggested by the results displayed in Figs. 3.1 and 3.2, since double reciprocal plots with NAD as the varied substrate at different fixed levels of prephenate do not intersect with each other on the vertical axis under all conditions of substrate variation (e.g. Fig. 3.4). Therefore the mechanism may be ordered (steady state), Theorell-Chance or random (either rapid equilibrium or steady state*). Now the prephenate dehydrogenase reaction is essentially irreversible (Cotton and Gibson, 1967), probably as a result of the formation of a highly resonant product from prephenate (Schwinck and Adams, 1959); if a Theorell-Chance mechanism were operative, the irreversibility of the reaction would have to be on the release side, since intersecting initial velocity patterns were obtained (as discussed in Section 1.1.2)

---

*Cleland (1970) reports that "simulation studies have shown that random mechanisms, unless very unusual values are assumed for the rate constants, resemble rapid equilibrium mechanisms in their initial velocity and product inhibition patterns, even though the rate limiting step is not solely the interconversion of two central complexes".

The product inhibition patterns observed for prephenate dehydrogenase are listed in Table 3.8, together with those predicted for the simple Bi-Ter mechanisms allowed by the initial velocity data; as can be seen, the observed data do not conform to any of these simple mechanisms. When the possible formation of dead end complexes is considered, the product inhibition patterns are consistent with a rapid equilibrium random mechanism involving the formation of the dead end complexes enzyme-prephenate-NADH, enzyme-prephenate-4-hydroxyphenylpyruvate and enzyme-NAD-4-hydroxyphenylpyruvate, if the nonlinearity of the inhibition by bicarbonate is not taken into account. If the bicarbonate inhibition data are ignored altogether on the grounds of ionic strength effects, the inhibition patterns for the other two products are consistent with :(a) an ordered mechanism in which NAD binds first to the enzyme, and products are released in the order - 4-hydroxyphenylpyruvate, bicarbonate then NADH, or (b) a Theorell-Chance mechanism in which prephenate binds first to the enzyme, and products are released in the order - NADH, bicarbonate then 4-hydroxyphenylpyruvate, and involving the formation of an enzyme-prephenate-4-hydroxyphenylpyruvate dead end complex on the addition side of the reaction. (Were this dead end complex formation to occur on the release side, double reciprocal plots with prephenate as the varied substrate would be nonlinear.) That a non-specific ionic strength effect, however, would compensate exactly for the intercept effects predicted in both the ordered and Theorell-Chance mechanisms to result in competitive inhibition by bicarbonate is highly unlikely. The product inhibition results,

TABLE 3.8

(a) Product inhibition patterns observed for prephenate dehydrogenase at pH 8.3.

Product	Varied substrate	
	prephenate	NAD
4-hydroxy-phenylpyruvate	NC*	NC
bicarbonate	C**	C**
NADH	NC	C

(b) Product inhibition patterns predicted for simple sequential Bi-Ter mechanisms. The fixed substrate is assumed to be at non-saturating concentration.

Mechanism	Product	Varied substrate	
		A	B
Rapid equilibrium random	P,Q,R	C	C
Ordered	P	NC	NC
	Q	UC	UC
	R	C	NC
Theorell-Chance	P	NC	C
	Q	UC	UC
	R	C	NC

* Abbreviations used are : C - competitive, NC - noncompetitive, UC - uncompetitive.

** Inhibition not simple - see text.

therefore, would suggest that neither the ordered nor the Theorell-Chance mechanism is operative.

The dead end inhibition patterns observed with inhibitors of prephenate dehydrogenase are listed in Table 3.9, together with those predicted for sequential bisubstrate mechanisms. Although the results obtained with AMP were not simple, a definite slope effect was observed when prephenate was the varied substrate. No uncompetitive patterns were observed, as expected in an ordered or Theorell-Chance mechanism. If the AMP results are set aside as anomalous, however, the results are consistent with :(a) a rapid equilibrium random mechanism, (b) a Theorell-Chance mechanism in which prephenate binds to the enzyme before NAD, and (c) an ordered mechanism in which prephenate is the first-bound substrate. The choice of the ordered mechanism (c), however, would contradict the conclusion from the product inhibition patterns that if the mechanism is ordered, then NAD binds to the enzyme before prephenate. Therefore, on the basis of initial velocity, product and dead end inhibition data, the mechanism operative for prephenate dehydrogenase could be the random mechanism (a) involving dead end complex formation as previously specified, or the Theorell-Chance mechanism (b) involving enzyme-prephenate-4-hydroxyphenylpyruvate dead end complex formation.

The results obtained with the NAD analogue, Thio-NAD, can not be interpreted on the basis of dead end inhibition, since this compound acts as an alternative substrate in the prephenate dehydrogenase reaction. In the NAD-utilising reaction,

TABLE 3.9

(a) Dead end inhibition patterns observed for prephenate dehydrogenase at pH 8.3.

Inhibitor	Varied substrate	
	prephenate	NAD
4-hydroxycinnamate	C*	NC
trans-aconitate	C**	NC**
AMP	NC?**	C

(b) Dead end inhibition patterns predicted for sequential bisubstrate mechanisms.

Mechanism	Inhibitor is an analogue of	Varied substrate	
		A	B
Ordered, Theorell-Chance	A	C	NC
	B	UC	C
Rapid equilibrium random	A	C	NC
	B	NC	C

* Abbreviations used are : C - competitive, NC - noncompetitive, UC - uncompetitive.

** Inhibition not simple - see text.

Thio-NAD was found to act as a competitive inhibitor with respect to NAD and a noncompetitive inhibitor with respect to prephenate, and double reciprocal plots in the presence of Thio-NAD remained linear. These results, taken together with the interpretation of the previously discussed data, are consistent with either a rapid equilibrium random mechanism or a Theorell-Chance mechanism in which prephenate is the first substrate to bind to the enzyme.

If a rapid equilibrium random mechanism is operative, three dead end complexes must be postulated to explain the product inhibition patterns, viz. enzyme-prephenate-NADH, enzyme-NAD-4-hydroxyphenylpyruvate and enzyme-prephenate-4-hydroxyphenylpyruvate. Now dead end complexes involving the unlike substrate/product pairs can be expected in a rapid equilibrium random mechanism (Cleland, 1970). Thus with creatine kinase, enzyme-creatine-MgADP and enzyme-MgATP-creatine phosphate complexes form (Morrison and James, 1965). Therefore, it is not surprising that with prephenate dehydrogenase, dead end complexes involving prephenate and NADH, or NAD and 4-hydroxyphenylpyruvate might form. The formation of an enzyme-prephenate-4-hydroxyphenylpyruvate complex, as required for the postulated rapid equilibrium random and Theorell-Chance mechanisms, is more difficult to envisage, but not impossible. Heyde and Morrison (1978) have found that at pH 7.5 there is interaction between the mutase and dehydrogenase of this bifunctional enzyme, the mutase being inhibited by prephenate and 4-hydroxyphenylpyruvate and activated by NAD and NADH, while the dehydrogenase is act-

ivated by chorismate. Binding of 4-hydroxyphenylpyruvate at a mutase site might occur, resulting in a conformational change which prevents the binding of NAD but not prephenate at the dehydrogenase site. However, Heyde (1978) presents evidence for a single active site catalysing both mutase and dehydrogenase activities, suggesting that chorismate is converted to prephenate on the part of the dehydrogenase site that binds prephenate. If this were the case, the formation of an enzyme-prephenate-4-hydroxyphenylpyruvate dead end complex as described above would not be possible. An alternative explanation is that 4-hydroxyphenylpyruvate, being structurally similar to the end product inhibitor, tyrosine, might combine with the enzyme at the tyrosine binding site, resulting in the formation of catalytically incompetent dead end complex(es). Wherever a second site for 4-hydroxyphenylpyruvate might exist, it must be assumed that if the mechanism is rapid equilibrium random, the binding of this product at one of the two sites precludes its binding at the other, since simultaneous binding at both sites predicts squared terms in inhibitor concentration in the rate equation, and therefore nonlinear inhibition. There was no evidence that this was the case.

In summary, the combination of product, dead end and alternative substrate inhibition results argues against the mechanism of the prephenate dehydrogenase reaction being an ordered one. On the other hand, only the noncompetitive inhibition by 4-hydroxyphenylpyruvate with respect to prephenate might suggest that the mechanism is not random, but enzyme-pre-

phenate-4-hydroxyphenylpyruvate dead end complex formation is not inconceivable.

3.4.2 QUANTITATIVE ASPECTS OF THE RESULTS

(a) The kinetic constants associated with prephenate and NAD.

No detailed kinetic studies of the dehydrogenase reaction catalysed by chorismate mutase - prephenate dehydrogenase isolated from A. aerogenes had been reported at the beginning of this work. Both Cotton and Gibson (1967) and Koch et al. (1970 a) reported only apparent Michaelis constants for prephenate and NAD. Table 3.10 compares the kinetic constants obtained in the present study with the parameters determined in this laboratory in a parallel study at pH 7.5 (Heyde and Morrison, 1978). While the Michaelis constants do not vary from one pH to the other, the inhibition constants do, that for prephenate being higher and that for NAD being lower at the higher pH.

For a rapid equilibrium random mechanism, the inhibition constant is the dissociation constant for the enzyme-substrate binary complex, and the Michaelis constant is the dissociation constant for the substrate from the ternary complex. Now it can be seen (Table 3.10) that the inhibition constant for each substrate in the prephenate dehydrogenase reaction is some five times higher than the Michaelis constant. This means that, if the mechanism is rapid equilibrium random, the binding of prephenate to the enzyme-NAD complex at pH 8.3 is five times higher than its binding to free enzyme, and the same is true for

TABLE 3.10 Comparison of kinetic constants for the interaction of substrates with prephenate dehydrogenase at pH 7.5 and at pH 8.3.

PARAMETER	VALUE (mM)	
	pH 7.5[(a)]	pH 8.3[(b)]
K_i prephenate	0.17 ± 0.02[(c)]	0.22 ± 0.03[(c)]
K_m prephenate	0.030 ± 0.003	0.039 ± 0.003
K_i NAD	0.72 ± 0.09	0.52 ± 0.06
K_m NAD	0.11 ± 0.01	0.11 ± 0.01

Notes

(a) Values in this column taken from Heyde and Morrison (1978).

(b) Values in this column taken from Table 3.1.

(c) Assuming (K_i NAD)(K_m prephenate)/K_m NAD is equal to K_i prephenate for individual experiments.

the binding of NAD to the enzyme-prephenate complex; that is to say, there is marked synergism of binding. (The parameters at pH 7.5 are similar.) As discussed in Section 1.1.2, a rapid equilibrium random mechanism with synergism of substrate binding can be forced to behave as an equilibrium ordered mechanism by judicious manipulation of the substrate concentrations. The data presented in Figs. 3.1 and 3.2 show that the prephenate dehydrogenase reaction does appear to be equilibrium ordered when the NAD concentration is varied below its inhibition constant at relatively high concentrations of prephenate.

For a bisubstrate Theorell-Chance mechanism (assuming no isomerisation of the EA complex), K_{ia} is equal to k_2/k_1, the dissociation constant for A from EA, while K_{ib} is equal to k_2/k_3, a partition coefficient for EA, and therefore K_{ib}/K_{ia} is equal to k_1/k_3, the ratio of the rate of binding of A to free enzyme to the rate of binding of B to the EA complex. For prephenate dehydrogenase, K_i(NAD)/K_i(prephenate) equals 2.4 $\pm$ 0.4, and therefore if the mechanism were Theorell-Chance, prephenate would bind about twice as fast to free enzyme as NAD would to the enzyme-prephenate complex.

(b) Quantitative discrimination between mechanisms

(i) Ordered mechanisms

Although as discussed in Section 3.4.1, an ordered mechanism is almost certainly ruled out on the basis of the product, dead end and alternative substrate inhibition patterns,

it will be assumed for the present analysis that the reaction mechanism is ordered with NAD binding first, and 4-hydroxyphenylpyruvate and NADH being the first and last products, respectively to be released :

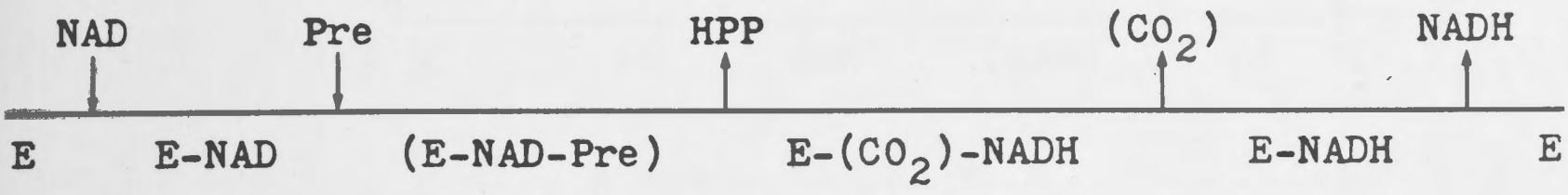

where E, Pre and HPP represent enzyme, prephenate and 4-hydroxyphenylpyruvate, respectively. (3.1)

Such a mechanism would explain at least the NADH and 4-hydroxyphenylpyruvate inhibition patterns. The complete rate equation for this mechanism has been derived by the method of King and Altman (1956) (Equation 3.2 - see following pages). By elimination of all terms in products other than the one of interest, one obtains the initial rate equation for the inhibition experiments involving that product. Thus the initial rate equation for the NADH inhibition experiments would be :

$$v = \frac{VAB}{K_{ia}K_b + K_bA + K_aB + AB + K_{ia}K_bR/K_{ir} + K_aBR/K_{ir}} \qquad (3.3)$$

where A, B and R represent the concentrations of NAD, prephenate and NADH, respectively, and the kinetic constants are as defined for Equation 3.2. It can be shown that K_{ir}, the inhibition constant for NADH, from the enzyme-NADH complex, may be determined in three ways from the NADH inhibition data (see Table 3.11). Similarly, examination of the initial rate equation for inhibition by 4-hydroxyphenylpyruvate shows two ways of determining the value of the ratio K_q/K_pK_{iq} (where K_p is the

EQUATION 3.2 Scheme and full rate equation for an ordered Bi Ter mechanism.

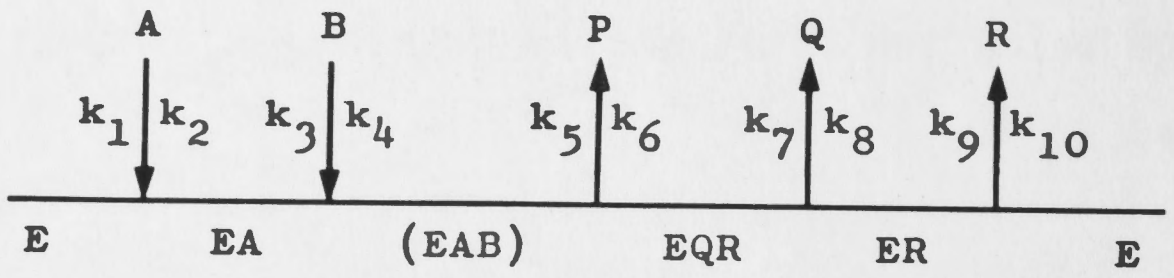

$$v = \frac{V_1 AB - V_1 PQR/K_{eq}}{K_{ia}K_b + K_b A + K_a B + AB}$$

$$+ \frac{K_{ia}K_b K_q P}{K_p K_{iq}} + \frac{K_b K_q AP}{K_p K_{iq}} + \frac{K_b K_q ABP}{K_{ib} K_p K_{iq}}$$

$$+ \frac{K_b K_{ip} K_r ABQ}{K_{ib} K_p K_{iq} K_{ir}} + \frac{K_{ia} K_b R}{K_{ir}} + \frac{K_a BR}{K_{ir}}$$

$$+ \frac{K_{ia} K_b K_r PQ}{K_p K_{iq} K_{ir}} + \frac{K_{ia} K_b K_q PR}{K_p K_{iq} K_{ir}} + \frac{K_{ia} K_b QR}{K_{iq} K_{ir}}$$

$$+ \frac{K_b K_r APQ}{K_p K_{iq} K_{ir}} + \frac{K_a BQR}{K_{iq} K_{ir}} + \frac{K_{ia} K_b PQR}{K_p K_{iq} K_{ir}}$$

$$+ \frac{K_b K_r ABPQ}{K_{ib} K_p K_{iq} K_{ir}} + \frac{K_a BPQR}{K_{ip} K_{iq} K_{ir}}$$

EQUATION 3.2(Cont.) Definitions of the kinetic constants and Haldane relationships.

$$K_a = \frac{k_5k_7k_9}{k_1(k_5k_7 + k_5k_9 + k_7k_9)} \qquad K_{ia} = k_2/k_1$$

$$K_b = \frac{k_7k_9(k_4 + k_5)}{k_3(k_5k_7 + k_5k_9 + k_7k_9)} \qquad K_{ib} = k_4/k_3$$

$$K_p = \frac{k_2(k_4 + k_5)}{k_6(k_2 + k_4)} \qquad K_{ip} = k_5/k_6$$

$$K_q = \frac{k_2k_4}{k_8(k_2 + k_4)} \qquad K_{iq} = k_7/k_8$$

$$K_r = \frac{k_2k_4}{k_{10}(k_2 + k_4)} \qquad K_{ir} = k_9/k_{10}$$

$$V_1 = \frac{k_5k_7k_9E_t}{k_5k_7 + k_5k_9 + k_7k_9}$$

$$V_2 = \frac{k_2k_4E_t}{(k_2 + k_4)}$$

$$K_{eq} = \frac{K_{ip}K_{iq}K_{ir}}{K_{ia}K_{ib}} = \frac{V_1K_pK_{iq}K_{ir}}{V_2K_{ia}K_b} = \frac{k_1k_3k_5k_7k_9}{k_2k_4k_6k_8k_{10}}$$

TABLE 3.11 Quantitative assessment of the plausibility of the ordered mechanism depicted in Scheme 3.1. Calculations were performed using the product inhibition data recorded in Table 3.2 and values of kinetic constants reported in Table 3.1.

Parameter	Derived value (mM) §	Determined from relationship :
K_q/K_pK_{iq} ℘	281×10^{-2} (5%)	$K_{is}(HPP/PRE) = K_pK_{iq}/K_q$
	925×10^{-3} (15%)	$K_{is}(HPP/NAD) = \dfrac{1 + K_aB/K_{ia}K_b}{K_q/K_pK_{iq}}$
K_{ir}	146×10^{-3} (3%)	$K_{is}(NADH/NAD) = K_{ir}$
	736×10^{-3} (22%)	$K_{is}(NADH/PRE) = K_{ir}(1 + A/K_{ia})$
	849×10^{-4} (8%)	$K_{ii}(NADH/PRE) = K_{ir}(1 + A/K_a)$

Notes :

§ : Figures in brackets are percentage standard errors.

℘ : Symbols and abbreviations used are : -

HPP : 4-hydroxyphenylpyruvate

PRE : prephenate

A : NAD

B : prephenate

K_a : Michaelis constant for NAD

K_b : Michaelis constant for prephenate

K_p : Michaelis constant for 4-hydroxyphenylpyruvate

K_q : Michaelis constant for bicarbonate

K_{ia} : Inhibition constant for NAD

K_{iq} : Inhibition constant for bicarbonate

K_{ir} : Inhibition constant for NADH.

Michaelis constant for 4-hydroxyphenylpyruvate and K_q and K_{iq} are the Michaelis and inhibition constants for bicarbonate (CO_2), respectively). It should be noted that the value of K_q/K_pK_{iq} can not be determined from the intercept inhibition constants, since these involve K_{ib}, the inhibition constant for prephenate. While for some mechanisms K_{ib} can be calculated from the equality of $K_{ia}K_b$ and $K_{ib}K_a$, this relationship does not hold for the ordered mechanism, and K_{ib} can not be determined from the initial velocity data.

Table 3.11 compares the three values determined for K_{ir} and the two values determined for K_q/K_pK_{iq} from the apparent inhibition constants obtained experimentally. The highest value calculated for K_{ir} is an order of magnitude higher than the lowest, while one estimate of K_q/K_pK_{iq} is three times higher than the other. These inconsistencies are further indications of the invalidity of the ordered mechanism. The bicarbonate inhibition data can not be used as a check, since the competitive inhibition by bicarbonate with respect to both substrates is the foremost reason for rejecting an ordered mechanism on the basis of product inhibition patterns; these patterns should have been uncompetitive for the mechanism of Scheme 3.1.

It will be recalled that, on a qualitative basis, a Theorell-Chance mechanism in which prephenate is the first-bound substrate and involving the formation of an enzyme-prephenate-4-hydroxyphenylpyruvate dead end complex (Scheme 3.4) would be consistent with the experimental data, with the exception of the bicarbonate inhibition results. The plausibility

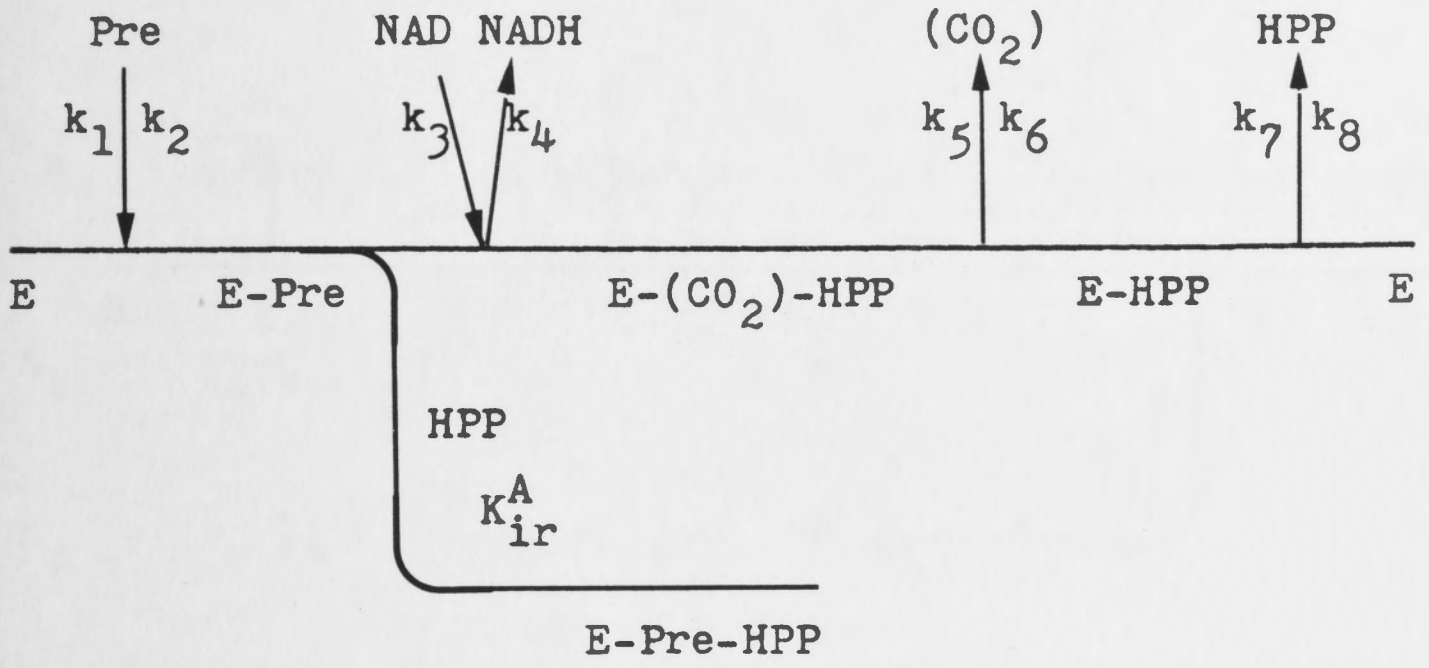

where E, Pre, HPP and K_{ir}^A represent enzyme, prephenate, 4-hydroxyphenylpyruvate and the dissociation constant for 4-hydroxyphenylpyruvate from enzyme-prephenate-4-hydroxyphenylpyruvate dead end complex, respectively.

(3.4)

of this mechanism may also be quantitatively examined by making use of the full rate equation (Equation 3.5 - see following pages).

K_{ip}, the inhibition constant for NADH, can be determined in three ways (see Table 3.12); K_{ir}, the inhibition constant for 4-hydroxyphenylpyruvate, can be determined in two ways; K_{ir}^A, the dissociation constant for 4-hydroxyphenylpyruvate from the enzyme-prephenate-4-hydroxyphenylpyruvate dead end complex, can be calculated from K_{ii} (4-hydroxyphenylpyruvate/prephenate); finally, the values of K_{ir} and K_{ir}^A previously determined can be used to calculate the predicted value of K_{is} (4-hydroxyphenylpyruvate/NAD). The above-mentioned determinations are summarised in Table 3.12. The large discrepancies for K_{ip}

EQUATION 3.5 Full rate equation for a Bi Ter Theorell-Chance mechanism involving the formation of an EAR dead end complex.

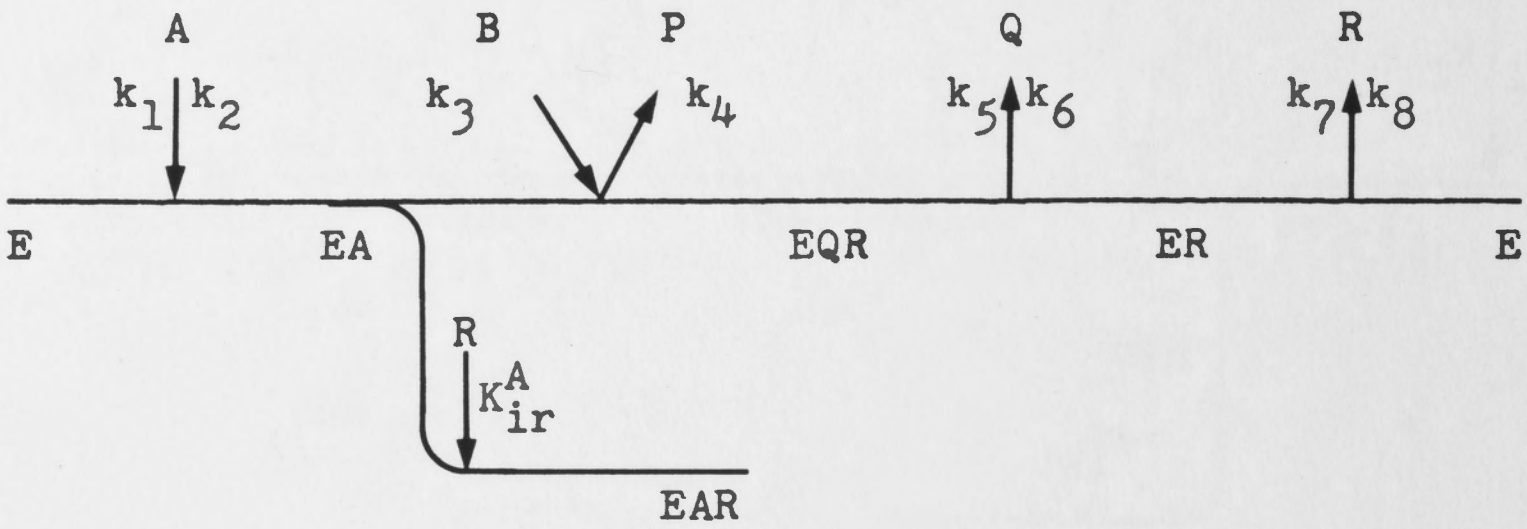

$$v = \frac{V_1AB - V_1PQR/K_{eq}}{K_{ia}K_b + K_bA + K_aB + AB + \frac{K_{ia}K_bP}{K_{ip}} + \frac{K_bAP}{K_{ip}} + \frac{ABQ}{K_{iq}} + \frac{K_{ia}K_bR}{K_{ir}} + \frac{K_bAR}{K_{ir}^{A}} + \frac{K_aBR}{K_{ir}} + \frac{K_{ia}K_bK_rPQ}{K_{ip}K_qK_{ir}} + \frac{K_{ia}K_bPR}{K_{ip}K_{ir}} + \frac{K_{ia}K_bK_pQR}{K_{ip}K_qK_{ir}} + \frac{K_bK_rAPQ}{K_{ip}K_qK_{ir}} + \frac{K_bAPR}{K_{ip}K_{ir}^{A}} + \frac{K_aK_pBQR}{K_{ip}K_qK_{ir}} + \frac{K_{ia}K_bPQR}{K_{ip}K_qK_{ir}} + \frac{K_{ia}K_bPQR^2}{K_{ip}K_qK_{ir}K_{ir}^{A}} + \frac{K_bK_rAPQR}{K_{ip}K_qK_{ir}K_{ir}^{A}}}$$

EQUATION 3.5(Cont.) Definitions of the kinetic constants and Haldane relationships.

$$K_a = \frac{k_5 k_7}{k_1(k_5+k_7)} \qquad K_{ia} = k_2/k_1$$

$$K_b = \frac{k_5 k_7}{k_3(k_5+k_7)} \qquad K_{ib} = k_2/k_3$$

$$K_p = k_2/k_4 \qquad K_{ip} = k_5/k_4$$

$$K_q = k_2/k_6 \qquad K_{iq} = \frac{(k_5+k_7)}{k_6}$$

$$K_r = k_2/k_8 \qquad K_{ir} = k_7/k_8$$

$$V_1 = \frac{k_5 k_7 E_t}{(k_5+k_7)} \qquad V_2 = k_2 E_t$$

$$K_{eq} = \frac{K_{ip} K_q K_{ir}}{K_{ia} K_b} = \frac{V_1 K_p K_{iq} K_r}{V_2 K_{ia} K_b} = \frac{k_1 k_3 k_5 k_7}{k_2 k_4 k_6 k_8}$$

Note that $K_{ia}K_b = K_{ib}K_a$ in this mechanism.

TABLE 3.12 Quantitative assessment of the plausibility of the Theorell-Chance mechanism depicted in Scheme 3.4. Relationships between kinetic constants and apparent inhibition constants were derived by manipulation of the full rate equation (Equation 3.5). Calculations were performed using the product inhibition data of Table 3.2 and values of kinetic constants in Table 3.1.

PARAMETER	DERIVED VALUE (mM)[a]	DETERMINED FROM :
K_{ip}[b]	I. 146×10^{-3} (3%)	$K_{is}(NADH/NAD) = K_{ip}$
	II. 849×10^{-4} (8%)	$K_{ii}(NADH/Pre) = K_{ip}(1 + B/K_b)$
	III. 736×10^{-3} (22%)	$K_{is}(NADH/Pre) = K_{ip}(1 + B/K_{ib})$
K_{ir}	I. 356×10^{-3} (5%)	$K_{is}(HPP/Pre) = K_{ir}$
	II. 341×10^{-4} (5%)	$K_{ii}(HPP/NAD) = K_{ir}(1 + A/K_a)$
K_{ir}^A	253×10^{-3} (9%)	$K_{ii}(HPP/Pre) = K_{ir}^A(1 + B/K_b)$
$K_{is}(HPP/NAD)$	I. 138×10^{-2} (14%)	Fit of experimental data to equation for noncompetitive inhibition.

K_{is}(HPP/NAD)	II. 290×10^{-3} (11%)	Calculated from : $K_{is}(HPP/NAD) = \frac{K_{ir}(1 + A/K_{ia})}{1 + (A/K_{ia})(K_{ir}/K^{A}_{ir})}$ using calculated value I. for K_{ir} and calculated value for K^{A}_{ir}.
	III. 663×10^{-4} (7%)	Calculated using same relatioship as that used for value II., but using value II. for K_{ir}.

Notes : (a) Figures in brackets are percentage standard errors.

(b) Symbols and abbreviations used are :

Pre - prephenate; HPP - 4-hydroxyphenylpyruvate; A - prephenate; B - NAD; K_a - Michaelis constant for prephenate; K_b - Michaelis constant for NAD; K_{ia} - inhibition constant for prephenate; K_{ib} - inhibition constant for NAD; K_{ip} - inhibition constant for NADH; K_{ir} - inhibition constant for 4-hydroxyphenylpyruvate; K^{A}_{ir} - dissociation constant for 4-hydroxyphenylpyruvate from the enzyme-prephenate-4-hydroxyphenylpyruvate dead end complex.

are the same as those mentioned for the ordered mechanism (Scheme 3.1) since the calculations are identical. The two values of K_{ir} are an order of magnitude apart, and the use of these two values for K_{ir} yields values of K_{is}(4-hydroxyphenylpyruvate/NAD) which are an order of magnitude apart, and only one of which approximates the experimentally determined value of this slope inhibition constant. It is, therefore, clear that these wide discrepancies rule out the plausibility of the Theorell-Chance mechanism depicted in Scheme 3.4.

(ii) Random mechanisms

The simplest random mechanism which accounts for the data obtained in this investigation is a rapid equilibrium random mechanism involving the formation of the dead end complexes : enzyme-prephenate-NADH, enzyme-NAD-4-hydroxyphenylpyruvate and enzyme-prephenate-4-hydroxyphenylpyruvate (Fig. 3.24). The way in which the last complex might form has been discussed previously. The full initial rate equation (Equation 3.6 - see after Fig. 3.24) for this mechanism has been derived using Cha's (1968) modification of the method of King and Altman (1956). It should be noted that if 4-hydroxyphenylpyruvate binds at two different sites (and this seems more realistic), then EP in Fig. 3.24 represents two species of enzyme-4-hydroxyphenylpyruvate complex, and K_{ip} in Fig. 3.24 and in Equation 3.6 is not a simple dissociation constant, but is defined by the relationship :

$$1/K_{ip} = 1/K_{ip1} + 1/K_{ip2} \qquad (3.7)$$

FIGURE 3.24 Schemes for a Bi Ter rapid equilibrium random mechanism (b), involving EAP, EBP and EBR dead end complex formation (a). If this is the mechanism of the prephenate dehydrogenase reaction then A, B, P, Q and R represent NAD, prephenate, 4-hydroxyphenylpyruvate and bicarbonate (CO_2), and NADH, respectively.

(a) Dead end (nonproductive) complex formation.

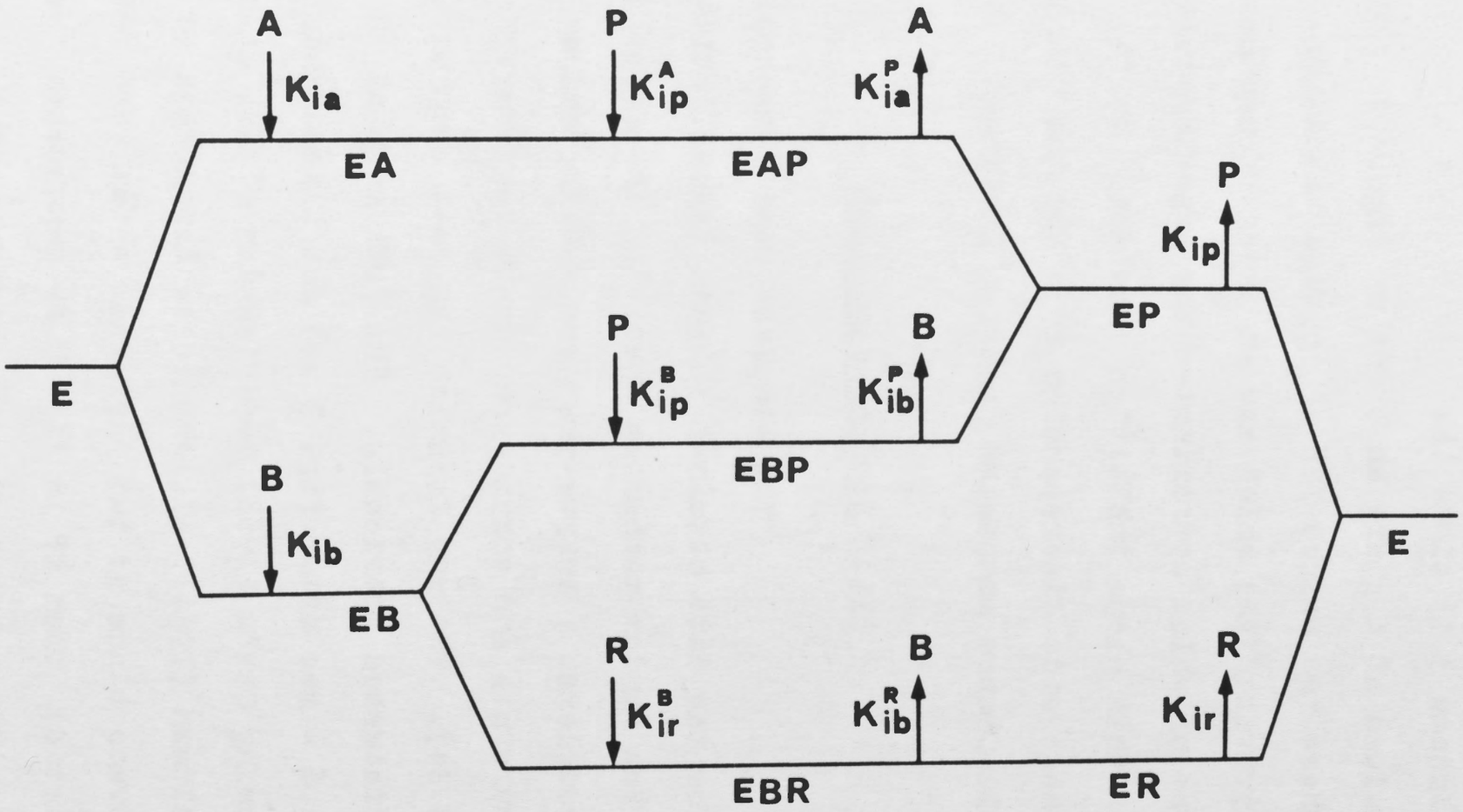

(b) Main reaction sequence involving productive complex formation.

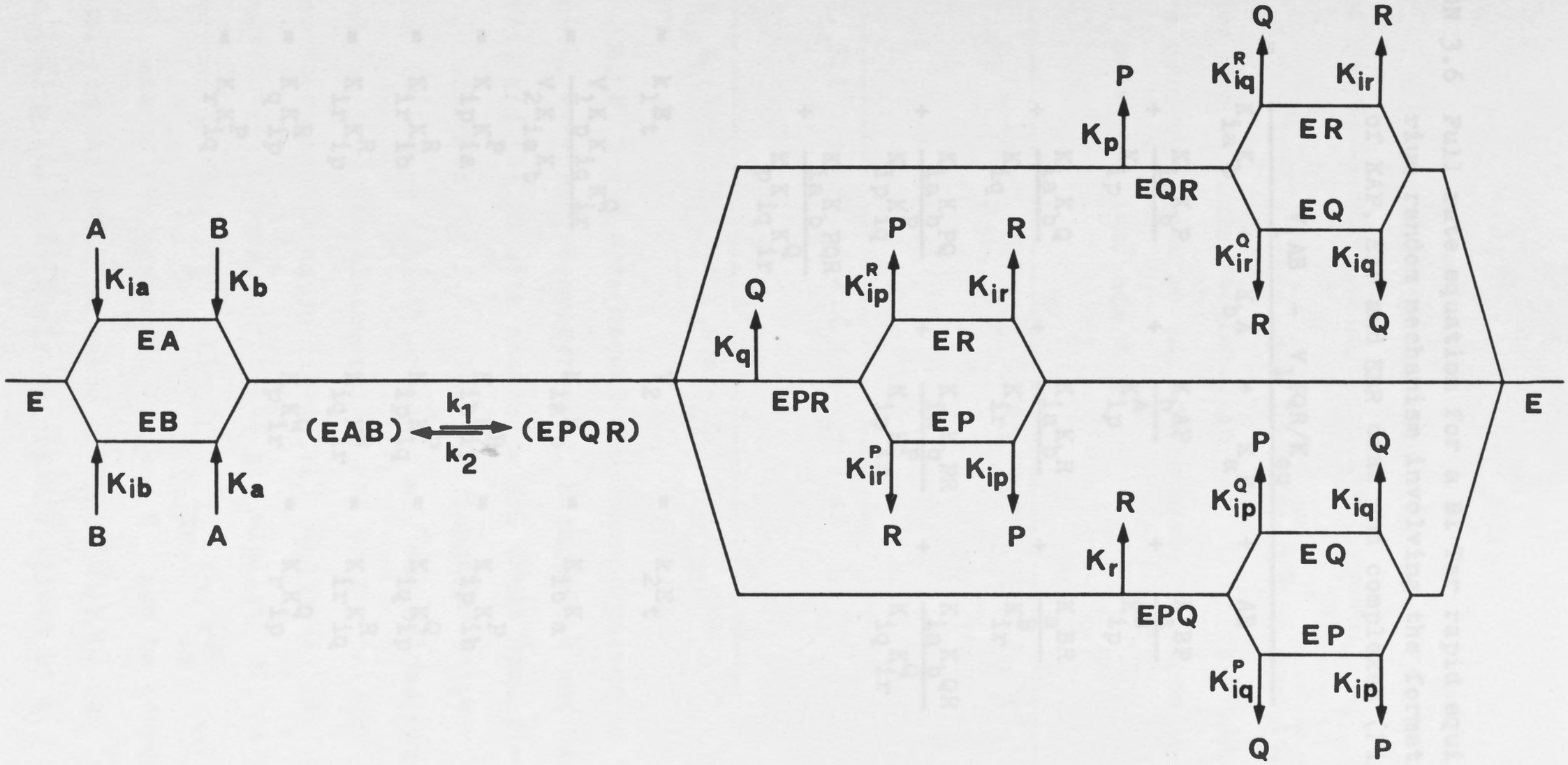

EQUATION 3.6 Full rate equation for a Bi Ter rapid equilibrium random mechanism involving the formation of EAP, EBP and EBR dead end complexes (Fig. 3.24).

$$v = \frac{V_1 AB - V_1 PQR/K_{eq}}{K_{ia}K_b + K_bA + K_aB + AB + \frac{K_{ia}K_bP}{K_{ip}} + \frac{K_bAP}{K_{ip}^A} + \frac{K_aBP}{K_{ip}^B} + \frac{K_{ia}K_bQ}{K_{iq}} + \frac{K_{ia}K_bR}{K_{ir}} + \frac{K_aBR}{K_{ir}^B} + \frac{K_{ia}K_bPQ}{K_{ip}K_{iq}^P} + \frac{K_{ia}K_bPR}{K_{ip}K_{ir}^P} + \frac{K_{ia}K_bQR}{K_{iq}K_{ir}^Q} + \frac{K_{ia}K_bPQR}{K_pK_{iq}K_{ir}^Q}}$$

$V_1 = k_1E_t$ $\quad V_2 = k_2E_t$

$K_{eq} = \frac{V_1K_pK_{iq}K_{ir}^Q}{V_2K_{ia}K_b}$ $\quad K_{ia}K_b = K_{ib}K_a$

$K_{ia}K_{ip}^A = K_{ip}K_{ia}^P$ $\quad K_{ib}K_{ip}^B = K_{ip}K_{ib}^P$

$K_{ib}K_{ir}^B = K_{ir}K_{ib}^R$ $\quad K_{ip}K_{iq}^P = K_{iq}K_{ip}^Q$

$K_{ip}K_{ir}^P = K_{ir}K_{ip}^R$ $\quad K_{iq}K_{ir}^Q = K_{ir}K_{iq}^R$

$K_pK_{iq}^R = K_qK_{ip}^R$ $\quad K_pK_{ir}^Q = K_rK_{ip}^Q$

$K_qK_{ir}^P = K_rK_{iq}^P$

where K_{ip1} and K_{ip2} are dissociation constants for the two forms of enzyme-4-hydroxyphenylpyruvate complex.

The initial rate equations describing product inhibition for the mechanism depicted in Fig. 3.24 (obtained by setting the concentrations of two of the three products to zero in the full rate equation) are :

$$v = \frac{VAB}{K_{ia}K_b(1 + P/K_{ip}) + K_bA(1 + P/K^A_{ip}) + K_aB(1 + P/K^B_{ip}) + AB} \qquad (3.8)$$

$$v = \frac{VAB}{K_{ia}K_b(1 + Q/K_{iq}) + K_bA + K_aB + AB} \qquad (3.9)$$

$$v = \frac{VAB}{K_{ia}K_b(1 + R/K_{ir}) + K_bA + K_aB(1 + R/K^B_{ir}) + AB} \qquad (3.10)$$

where A, B, P, Q and R represent the concentrations of NAD, prephenate, 4-hydroxyphenylpyruvate, bicarbonate and NADH, respectively, and the kinetic constants are those specified in Fig. 3.24 and Equation 3.6. The relationships between the slope and intercept inhibition constants determined experimentally and the true kinetic constants and concentrations of fixed substrates are listed in Table 3.13, and have been used in the quantitative assessment of the plausibility of the mechanism depicted in Fig. 3.24. K^A_{ip}, K^B_{ip}, K_{ir} and K^B_{ir} can be calculated, each of the constants K_{ip} and K_{iq} can be determined in two ways, and the expected value of K_{is}(NADH/NAD) can be calculated (using the previously determined values of K_{ir} and K^B_{ir})

TABLE 3.13 Expressions relating apparent inhibition constants to true kinetic constants and the concentration of the fixed substrate for the rapid equilibrium random mechanism depicted in Fig. 3.24.

Product	Varied substrate	K_{is}	K_{ii}
P*	A	$\dfrac{1 + B/K_{ib}}{1/K_{ip} + B/K_{ib}K_{ip}^{B}}$	$K_{ip}^{A}(1 + B/K_{b})$
	B	$\dfrac{1 + A/K_{ia}}{1/K_{ip} + A/K_{ia}K_{ip}^{A}}$	$K_{ip}^{B}(1 + A/K_{a})$
Q	A	$K_{iq}(1 + B/K_{ib})$	
	B	$K_{iq}(1 + A/K_{ia})$	
R	A	$\dfrac{1 + B/K_{ib}}{1/K_{ir} + B/K_{ib}K_{ir}^{B}}$	
	B	$K_{ir}(1 + A/K_{ia})$	$K_{ir}^{B}(1 + A/K_{a})$

* Kinetic constants are the dissociation constants indicated in Fig. 3.24.
A and B represent the substrates NAD and prephenate, respectively, or their concentrations.
P,Q and R represent 4-hydroxyphenylpyruvate, bicarbonate and NADH, respectively.

and compared with the experimentally obtained value. The results of the above-mentioned determinations are reported in Table 3.14.

The predicted slope inhibition constant for NADH with respect to NAD is in reasonable agreement with the experimentally determined value. Certain assumptions were made for the calculations of K_{iq}, the dissociation constant for bicarbonate from the enzyme-bicarbonate binary complex. It will be recalled that when prephenate was the varied substrate in bicarbonate inhibition experiments, the slope and intercept replots were characteristic of linear competitive inhibition with the exception of the baseline intercept. The activation by bicarbonate has been interpreted as an ionic strength effect in view of the results obtained with other salts. The data obtained only in the presence of bicarbonate were therefore fitted to the equation describing linear competitive inhibition and the apparent inhibition constant thus obtained has been used in the calculations. When NAD was the varied substrate, bicarbonate inhibition was not linear. The Dixon plots obtained indicate that the inhibition is not parabolic competitive inhibition since, if this were the case, the Dixon plots would have their minimum at zero bicarbonate concentration, and this was not the case. However, the parabolic competitive inhibition equation appears to describe the data. Therefore it has been assumed that the inhibition constant associated with the linear term in bicarbonate concentration approximates the specific interaction by bicarbonate as a product of the reaction, while a nonspecific ionic

TABLE 3.14 Quantitative assessment of the plausibility of a rapid equilibrium random mechanism involving the formation of the dead end complexes enzyme-prephenate-NADH, enzyme-prephenate-4-hydroxyphenylpyruvate and enzyme-NAD-4-hydroxyphenylpyruvate (see Fig. 3.24). Determinations were made using the relationships expressed in Table 3.13, values of kinetic constants reported in Table 3.1 and the product inhibition data of Table 3.2.

PARAMETER	DERIVED VALUE (mM)[a]	DETERMINED FROM :
K_{ip}^{A} [b]	341×10^{-4} (5%)	$K_{ii}(HPP/NAD) = K_{ip}^{A}(1 + B/K_b)$
K_{ip}^{B}	252×10^{-3} (9%)	$K_{ii}(HPP/Pre) = K_{ip}^{B}(1 + A/K_a)$
K_{ir}	736×10^{-3} (22%)	$K_{is}(NADH/Pre) = K_{ir}(1 + A/K_a)$
K_{ir}^{B}	849×10^{-4} (8%)	$K_{ii}(NADH/Pre) = K_{ir}^{B}(1 + A/K_a)$
K_{ip}	I. -210×10^{0} (3700%)	$K_{is}(HPP/NAD) = \dfrac{1 + B/K_{ib}}{1/K_{ip} + B/K_{ib}K_{ip}^{B}}$

K_{ip}	II. -439×10^{-3} (23%)	$K_{is}(HPP/Pre) = \dfrac{1 + B/K_{ib}}{1/K_{ip} + A/K_{ia}K_{ip}^{A}}$
K_{iq} (c)	I. 135×10^{0} (12%)	$K_{is1}(HCO_3^-/NAD) = K_{iq}(1 + B/K_{ib})$
	II. 776×10^{-1} (14%)	$K_{is}(HCO_3^-/Pre) = K_{iq}(1 + A/K_{ia})$
$K_{is}(NADH/NAD)$	I. 146×10^{-3} (3%)	Fit of experimental data to equation for competitive inhibition.
	II. 217×10^{-3} (14%)	$K_{is}(NADH/NAD) = \dfrac{1 + B/K_{ib}}{1/K_{ir} + B/K_{ib}K_{ir}^{B}}$

Notes :

(a) Figures in brackets are percentage standard errors.

(b) Symbols and abbreviations used are :

A, B - concentrations of NAD and prephenate, respectively.

Pre, HPP - prephenate and 4-hydroxyphenylpyruvate, respectively.

K_{ia}, K_{ib}, K_{ip}, K_{iq} and K_{ir} - dissociation constants for NAD, prephenate, 4-hydroxyphenylpyruvate, bicarbonate and NADH, respectively, from the appropriate enzyme-reactant binary complexes.

K_a, K_b - dissociation constants for NAD and prephenate, respectively, from the ternary complex, enzyme-prephenate-NAD.

K_{ip}^A, K_{ip}^B - dissociation constants for 4-hydroxyphenylpyruvate from the dead end complexes, enzyme-NAD-4-hydroxyphenylpyruvate and enzyme-prephenate-4-hydroxyphenylpyruvate, respectively.

K_{ir}^B - dissociation constant for NADH from the dead end complex, enzyme-prephenate-NADH.

(c) Calculated on the basis of assumptions detailed in the text.

strength effect is responsible for any further anomalies. Although these assumptions may be oversimplifications, there is relatively good agreement between the two calculated values of K_{iq}. The magnitude of this constant, about 100 mM, suggests that there is little tendency for bicarbonate to associate with free enzyme. The nonsense values calculated for K_{ip} arise because of the nature of the expressions relating K_{ip} to the slope inhibition constants. However, by substituting known values for A, B, K_{ia} and K_{ib}, and calculated values for K_{ip}^{A} and K_{ip}^{B} into the expressions :

$$K_{is}(P/A) = \frac{1 + B/K_{ib}}{1/K_{ip} + B/K_{ib}K_{ip}^{B}} \qquad (3.11)$$

$$K_{is}(P/B) = \frac{1 + A/K_{ia}}{1/K_{ip} + A/K_{ia}K_{ip}^{A}} \qquad (3.12)$$

the lower and upper limits of these slope inhibition constants can be determined. For the experimental conditions employed, $K_{is}(P/A)$ can vary between zero and 1.35 mM as K_{ip} varies from zero to infinity, while $K_{is}(P/B)$ varies between zero and 0.23 mM. The experimentally determined values are $K_{is}(P/A)$ = 1.35 mM and $K_{is}(P/B)$ = 0.36 mM, suggesting that K_{ip} tends towards infinity, and therefore that EP does not form by combination of P (4-hydroxyphenylpyruvate) with free enzyme.

A modified scheme in which an enzyme-4-hydroxyphenylpyruvate complex does not form is depicted in Fig. 3.25 and is followed by the complete rate equation for the mechanism (Equa-

FIGURE 3.25 Schemes for a rapid equilibrium Bi Ter mechanism in which all reactants except P bind randomly (P does not bind to free enzyme), and involving EAP, EBP and EBR dead end complex formation. If this is the mechanism of the prephenate dehydrogenase reaction, then A, B, P, Q and R represent NAD, prephenate, 4-hydroxyphenylpyruvate, bicarbonate (CO_2) and NADH, respectively.

(a) Dead end (nonproductive) complex formation.

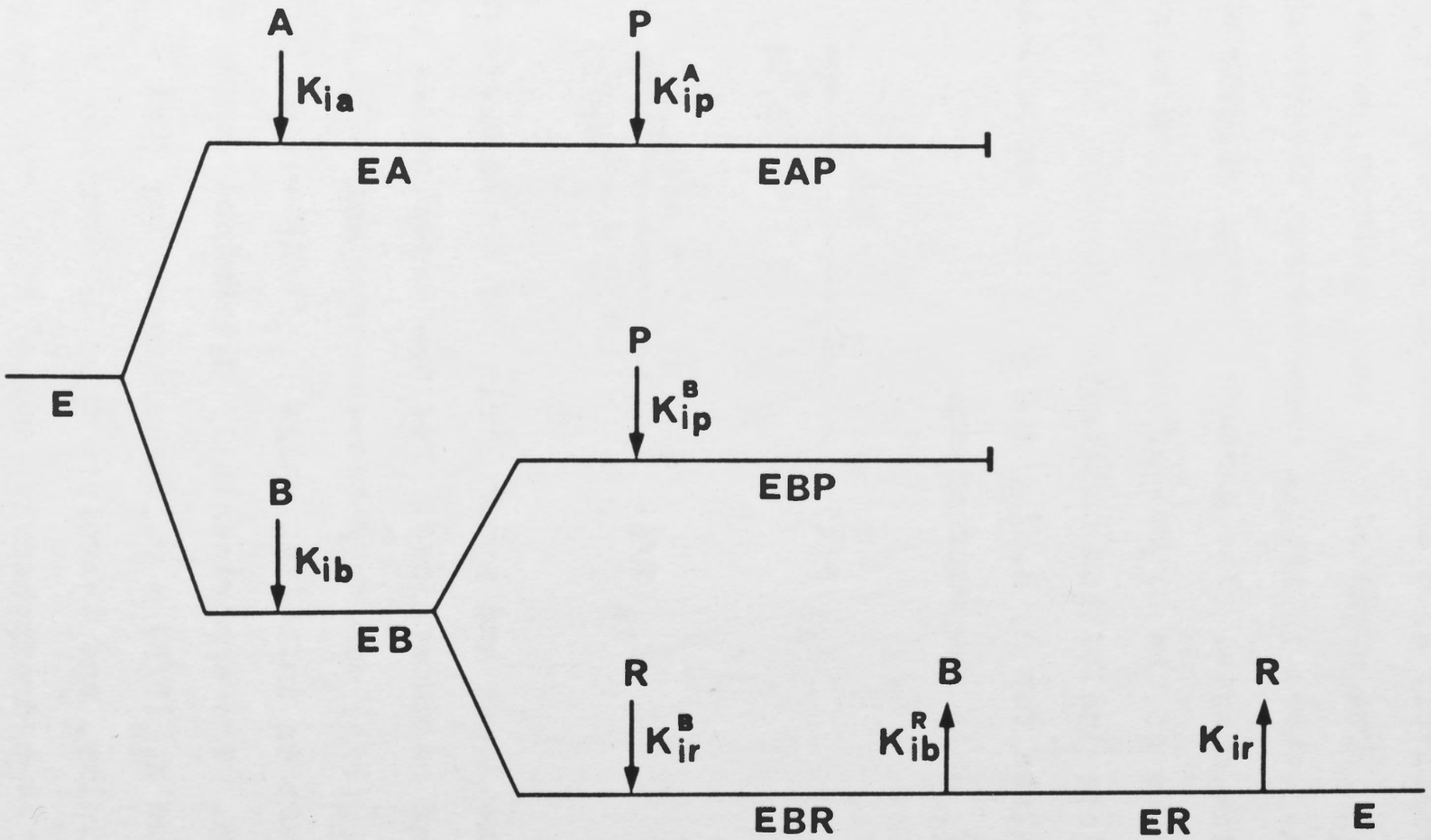

(b) Main reaction sequence involving productive complex formation.

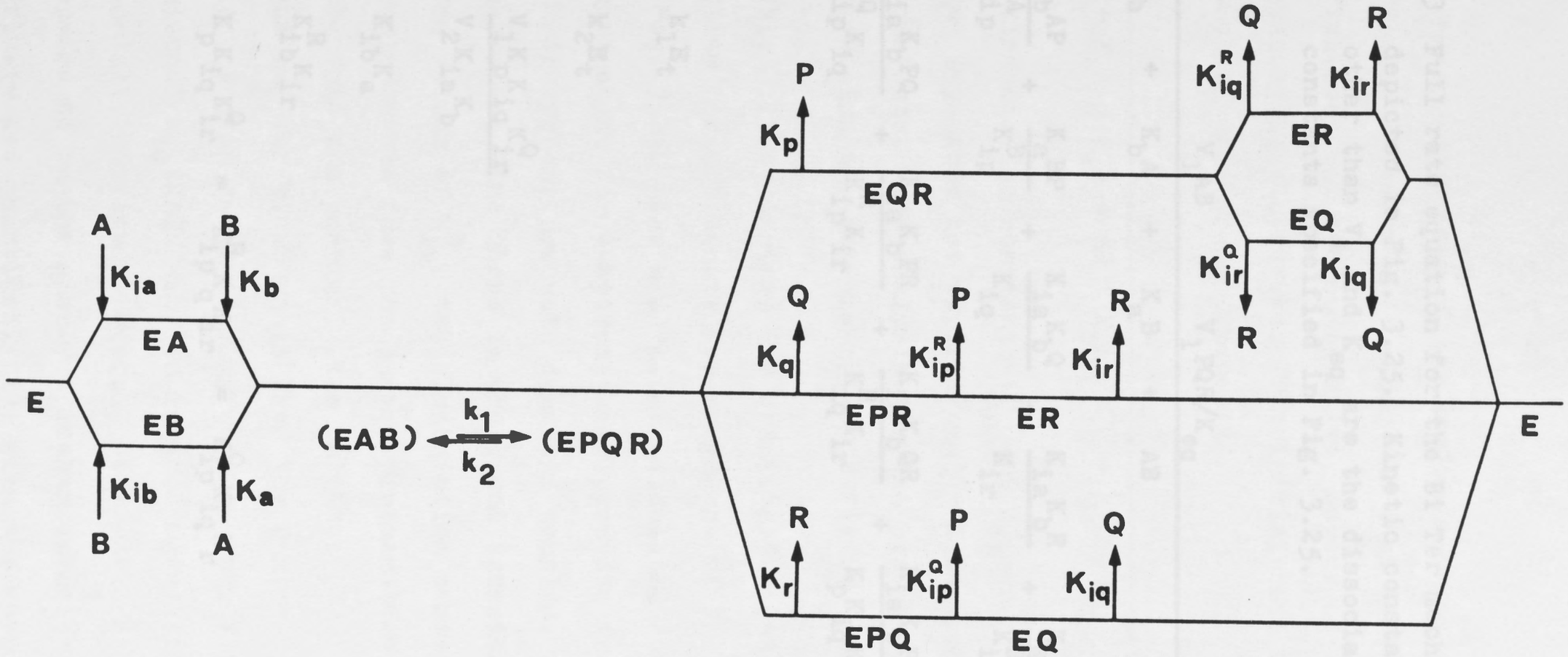

EQUATION 3.13 Full rate equation for the Bi Ter mechanism depicted in Fig. 3.25. Kinetic constants other than V_1 and K_{eq} are the dissociation constants specified in Fig. 3.25.

$$v = \frac{V_1AB - V_1PQR/K_{eq}}{K_{ia}K_b + K_bA + K_aB + AB + \frac{K_bAP}{K_{ip}^A} + \frac{K_aBP}{K_{ip}^B} + \frac{K_{ia}K_bQ}{K_{iq}} + \frac{K_{ia}K_bR}{K_{ir}} + \frac{K_aBR}{K_{ir}^B} + \frac{K_{ia}K_bPQ}{K_{ip}^QK_{iq}} + \frac{K_{ia}K_bPR}{K_{ip}^RK_{ir}} + \frac{K_{ia}K_bQR}{K_{iq}^RK_{ir}} + \frac{K_{ia}K_bPQR}{K_pK_{iq}K_{ir}^Q}}$$

$$V_1 = k_1E_t$$

$$V_2 = k_2E_t$$

$$K_{eq} = \frac{V_1K_pK_{iq}K_{ir}^Q}{V_2K_{ia}K_b}$$

$$K_{ia}K_b = K_{ib}K_a$$

$$K_{ib}K_{ir}^B = K_{ib}^RK_{ir}$$

$$K_pK_{iq}^RK_{ir} = K_pK_{iq}K_{ir}^Q = K_{ip}^RK_qK_{ir} = K_{ip}^QK_{iq}K_r$$

tion 3.13). For the purposes of the analysis being undertaken, the only difference between this model and that of Fig. 3.24 is the quantitative, but not qualitative, aspect of the inhibition by 4-hydroxyphenylpyruvate. The initial rate equation in the presence of this product becomes :

$$v = \frac{VAB}{K_{ia}K_b + K_bA + K_aB + AB + K_bAP/K_{ip}^{A} + K_aBP/K_{ip}^{B}} \qquad (3.14)$$

Each of the dissociation constants K_{ip}^{A} and K_{ip}^{B} can now be calculated in two ways from the experimentally determined apparent inhibition constants. The analysis for the products bicarbonate and NADH remains the same as that for Figure 3.24.

Table 3.15 summarises the quantitative analysis of the plausibility for prephenate dehydrogenase of the mechanism depicted in Fig. 3.25. The two values calculated for K_{ip}^{A}, the dissociation constant for 4-hydroxyphenylpyruvate from the enzyme-NAD- 4-hydroxyphenylpyruvate dead end complex, are in reasonable agreement, and there is excellent agreement of the two calculated values of K_{ip}^{B}, the dissociation constant for 4-hydroxyphenylpyruvate from the enzyme-prephenate-4-hydroxyphenylpyruvate dead end complex. The values of K_{iq}, the dissociation constant for bicarbonate from the enzyme-bicarbonate binary complex, are in reasonable agreement, and, finally, the predicted value of K_{is}(NADH/NAD) is in good agreement with that experimentally obtained. Overall, the model depicted in Fig. 3.25 appears to be the simplest mechanism which is accord both qualitatively and quantitatively, with the results of the

TABLE 3.15 Quantitative assessment of the plausibility for prephenate dehydrogenase of the rapid equilibrium random mechanism depicted in Fig. 3.25. Determinations were made using Equation 3.13 and the data of Tables 3.1 and 3.2.

PARAMETER	DERIVED VALUE (mM)[a]	DETERMINED FROM :
K_{ip}^{A} [b]	I. 574×10^{-4} (11%) II. 341×10^{-4} (5%)	$K_{is}(HPP/Pre) = K_{ip}^{A}(1 + K_{ia}/A)$ $K_{ii}(HPP/NAD) = K_{ip}^{A}(1 + B/K_{b})$
K_{ip}^{B}	I. 254×10^{-3} (18%) II. 252×10^{-3} (9%)	$K_{is}(HPP/NAD) = K_{ip}^{B}(1 + K_{ib}/B)$ $K_{is}HPP/Pre) = K_{ip}^{B}(1 + A/K_{a})$
K_{iq} [c]	I. 135×10^{0} (12%) II. 776×10^{-1} (14%)	$K_{is1}(HCO_3^-/NAD) = K_{iq}(1 + B/K_{ib})$ $K_{is}(HCO_3^-/Pre) = K_{iq}(1 + A/K_{ia})$
K_{ir}	736×10^{-3} (22%)	$K_{is}(NADH/Pre) = K_{ir}(1 + A/K_{a})$
K_{ir}^{B}	849×10^{-4} (8%)	$K_{ii}(NADH/Pre) = K_{ir}^{B}(1 + A/K_{a})$

K_{is}(NADH/NAD)	I. 146×10^{-3} (3%) II. 217×10^{-3} (14%)	Fit of experimental data to equation for competitive inhibition. $K_{is}(NADH/NAD) = \frac{1 + B/K_{ib}}{1/K_{ir} + B/K_{ib}K_{ir}^{B}}$

Notes :

(a) Figures in brackets are percentage standard errors.

(b) Symbols and abbreviations used are the same as those used in Table 3.14.

(c) Calculated on the basis of assumptions detailed in the text (pp 111 &112).

product inhibition experiments, and qualitatively with the results of the substrate analogue inhibition experiments.

The inhibition by 4-hydroxycinnamate may be described by the following equation :

$$v = \frac{VAB}{K_{ia}K_b(1 + J/K_{ij}) + K_bA(1 + J/K_j) + K_aB + AB} \qquad (3.15)$$

where, in addition to symbols previously defined, J represents the concentration of 4-hydroxycinnamate, and K_{ij} and K_j are dissociation constants for the inhibitor from the complexes, enzyme-4-hydroxycinnamate and enzyme-NAD-4-hydroxycinnamate, respectively.

The dissociation constants have been calculated from the data of Table 3.7 by procedures analogous to those detailed for the analysis of the product inhibition data. In addition, the expected slope constant K_{is}(4-hydroxycinnamate/prephenate) has been calculated. The relevant data are presented in Table 3.16. It will be noted that the predicted value of K_{is}(4-hydroxycinnamate/prephenate) is in excellent agreement with that obtained experimentally, and that 4-hydroxycinnamate binds some twenty times more easily to the enzyme-NAD complex than to free enzyme, in parallel with the synergism of binding of the substrates and products.

The experimental data obtained by studying Thio-NAD inhibition of the NAD-utilising prephenate dehydrogenase reaction can be utilised to calculate the kinetic parameters for Thio-NAD and prephenate in the Thio-NAD-utilising reaction.

TABLE 3.16 Quantitative analysis of the 4-hydroxycinnamate inhibition data. Calculations were performed using the data of Tables 3.1 and 3.7.

PARAMETER	DERIVED VALUE (mM)[a]	DETERMINED FROM :
K_j[b]	519×10^{-4} (6%)	$K_{ii}(J/A) = K_j(1 + B/K_b)$
K_{ij}	946×10^{-3} (11%)	$K_{is}(J/A) = K_{ij}(1 + B/K_{ib})$
$K_{is}(J/B)$	I. 361×10^{-3} (2%)	Fit of experimental data to equation for competitive inhibition.
	II. 377×10^{-3} (10%)	Calculated using : $K_{is}(J/B) = \dfrac{1 + A/K_{ia}}{1/K_{ij} + A/K_{ia}K_j}$

Notes :

(a) Figures in brackets are percentage standard errors.

(b) Symbols used are :

A - NAD.
B - prephenate.
J - 4-hydroxycinnamate.
K_j - dissociation constant for J from EAJ.
K_{ij} - dissociation constant for J from EJ.
K_{ia} - dissociation constant for NAD from E-NAD.
K_{ib} - dissociation constant for prephenate from enzyme-prephenate.
K_b - dissociation constant for prephenate from enzyme-prephenate-NAD.

These constants can be compared with those determined from the initial velocity data for the Thio-NAD-utilising reaction. On the basis of a rapid equilibrium random mechanism, the initial rate equation for the inhibition is :

$$v = \frac{VAB}{K_{ia}K_b + K_bA + \frac{K_aK_b^*A^*}{K_a^*} + K_aB + AB + \frac{K_aA^*B}{K_a^*}} \qquad (3.16)$$

where, in addition to previously defined symbols,
A^* represents the concentration of Thio-NAD, and
K_a^* and K_b^* are the Michaelis constants for Thio-NAD and prephenate in the Thio-NAD-utilising reaction.

The calculations require the use of the relationships :

$$K_{ib} = \frac{K_{ia}K_b}{K_a} = \frac{K_{ia}^*K_b^*}{K_a^*}$$

where K_{ia}^* is the dissociation constant for the enzyme-ThioNAD complex. Table 3.17 summarises the results of these calculations, and compares the calculated constants with those experimentally determined. As can be seen, there is reasonable agreement, and the data indicate that the synergism of binding seen with the usual substrate is also observed when Thio-NAD acts as a substrate.

In summary, the quantitative analysis of the data is consistent with the mechanism depicted in Fig. 3.25.

TABLE 3.17 Comparison of kinetic constants for Thio-NAD and prephenate obtained by initial velocity experiments and by calculation from the apparent inhibition constants for Thio-NAD in the NAD-utilising reaction.

Constant	Value (mM) from initial velocity§	Calculated value (mM)	Relationship used for calculation:
K_{ib}	616×10^{-3} (25%)	221×10^{-3} (14%)	Fixed: must be the same in both NAD- and Thio-NAD utilising reactions.
K^{*}_{ia}	134×10^{-2} (42%)	908×10^{-3} (27%)	$K_{is}(A^{*}/B) = K^{*}_{ia}(1 + A/K_{ia})$
K^{*}_{a}	385×10^{-4} (19%)	499×10^{-4} (7%)	$K_{ii}(A^{*}/B) = K^{*}_{a}(1 + A/K_{a})$
K^{*}_{b}	177×10^{-4} (36%)	122×10^{-4} (31%)	$K^{*}_{b} = K_{ib}K^{*}_{a}/K^{*}_{ia}$

§ Figures in brackets are percentage standard errors.

Symbols used are:

K^{*}_{a} and K^{*}_{ia} - Michaelis and inhibition constants, respectively, for Thio-NAD.

K^{*}_{b} and K_{ib} - Michaelis constant for prephenate in the Thio-NAD utilising reaction, and inhibition constant for prephenate, respectively.

A^{*}, A and B- Thio-NAD, NAD and prephenate, respectively.

3.4.3 CONCLUSIONS

On the basis of both qualitative and quantitative assessments, an ordered or Theorell-Chance mechanism for the reaction catalysed by prephenate dehydrogenase must be rejected. Three competitive inhibition patterns by products were observed compared with one expected in an ordered mechanism, and two in a Theorell-Chance. Moreover, in both cases the values of the kinetic parameters which can be evaluated independently in different ways are not consistent with each other.

On the other hand, the evidence available is consistent with the mechanism depicted in Fig. 3.25. The essential features of this mechanism are :

1. the mechanism is rapid equilibrium (or approximately). That is, the sole rate-limiting step is the interconversion of the central complexes, and all other steps are so fast compared with the rate-limiting step that they can be considered to be at thermodynamic equilibrium.

2. the substrates bind randomly and synergistically, although

3. 4-hydroxyphenylpyruvate is not the last product released. There is no evidence, however, to indicate that it must be the first product released.

4. the mechanism involves the formation of the dead end complexes enzyme-prephenate-NADH, enzyme-prephenate-

4-hydroxyphenylpyruvate and enzyme-NAD-4-hydroxyphenylpyruvate.

Table 3.18 summarises the dissociation constants at pH 8.3 for interaction of reactants with free enzyme and different enzyme-reactant complexes, and compares them with the available constants at pH 7.5. The only difference of note is that NADH binds to free enzyme and to the enzyme-prephenate complex much less readily at pH 8.3, the dissociation constants being comparable with the respective constants for the substrate NAD, unlike the situation at pH 7.5 where the product NADH binds much more readily to free enzyme and to enzyme-prephenate than does the substrate NAD. In addition, at pH 7.5, there is no need to postulate the formation of an enzyme-prephenate-4-hydroxyphenylpyruvate dead end complex, since 4-hydroxyphenylpyruvate was a competitive inhibitor with respect to prephenate. On the other hand, it has been observed that 4-hydroxyphenylpyruvate is a noncompetitive inhibitor with respect to prephenate in the reaction catalysed by monofunctional prephenate dehydrogenase from B. subtilis NP 40 (Champney and Jensen, 1970). The lack of evidence for the binding of 4-hydroxyphenylpyruvate to free enzyme at pH 8.3 is most likely explained by a very high dissociation constant, outside of the concentration range which it was possible to utilise in the product inhibition experiments. At pH 7.5, this product appears to bind to free enzyme with a dissociation constant of 0.44 mM (Heyde and Morrison, 1978). In connection with the unusual bicarbonate effects observed in this study, simulation of data from equations involving random, non-rapid equilibrium release of products has indic-

TABLE 3.18 Summary of dissociation constants for the interaction of reactants with free enzyme and enzyme-reactant complexes derived in this study, and comparison with their values at pH 7.5.

REACTANT	SYMBOL FOR DISSOCIATION CONSTANT	ENZYME SPECIES INVOLVED	DISSOCIATION CONSTANT (mM)	
			pH 7.5[a]	pH 8.3
NAD	K_{ia}	E[b]	0.72 ± 0.09	0.52 ± 0.06[c]
	K_a	E-Pre	0.11 ± 0.01	0.11 ± 0.01[c]
	K_{ia}^J	E-HCIN	-	0.030 ± 0.005[d]
Prephenate	K_{ib}	E	0.17 ± 0.02	0.22 ± 0.03[c]
	K_b	E-NAD	0.030 ± 0.003	0.039 ± 0.003[c]
	K_{ib}^R	E-NADH	-	0.027 ± 0.009[e]
	K_b^*	E-TNAD	-	0.014 ± 0.003[f]
Thio-NAD	K_{ia}^*	E	-	1.0 ± 0.2[f]
	K_a^*	E-Pre	-	0.048 ± 0.003[f]

4-hydroxy-phenylpyruvate	K_{ip}^{A}	E	0.032 ± 0.002	0.036 ± 0.002(g)
	K_{ip}^{B}	E-Pre	-	0.25 ± 0.02(g)
Bicarbonate	K_{iq}	E	-	95 ± 9(g)
NADH	K_{ir}	E	0.09 ± 0.02	0.7 ± 0.2(h)
	K_{ir}^{B}	E-Pre	0.023 ± 0.002	0.085 ± 0.007(h)
4-hydroxy-cinnamate	K_{ij}	E	-	0.9 ± 0.1(j)
	K_{j}	E-NAD	-	0.052 ± 0.003(j)

Notes :

(a) Taken from Heyde and Morrison (1978).

(b) Abbreviations used are : E - enzyme, Pre - prephenate, HCIN - 4-hydroxy-cinnamate, TNAD - Thio-NAD.

(c) Taken from Table 3.1.

(d) Calculated using relationship $K_{ia}^{J} = K_{ia}K_{j}/K_{ij}$ and values for the known constants from this table.

TABLE 3.18 Notes (Continued) :

(e) Calculated using relationship $K^{R}_{ib} = K_{ib}K^{B}_{ir}/K_{ir}$ and values for the known constants from this table.

(f) Weighted mean of calculated an experimentally obtained values from Table 3.17.

(g) Weighted mean of calculated values from Table 3.15.

(h) Calculated value from Table 3.15.

(j) Calculated value from Table 3.16.

ated that activation by a product such as that observed with bicarbonate may theoretically occur, but depends on complex relationships between rate constants. Although ionic strength complications are a more likely explanation for the bicarbonate activation, it is possible that these results are an indication that the rapid equilibrium condition is not fulfilled in the reaction catalysed by prephenate dehydrogenase at pH 8.3.

Fig. 3.26 repeats the postulated mechanism for the reaction catalysed by prephenate dehydrogenase at pH 8.3 and indicates the values of the dissociation constants determined in this study. The marked synergism of reactant binding is an especially notable feature of the findings of this investigation.

FIGURE 3.26 Postulated mechanism of the prephenate dehydrogenase reaction at pH 8.3. Nonstandard abbreviations used are : E, enzyme; HCIN, 4-hydroxycinnamate; HPP, 4-hydroxyphenylpyruvate; PRE, prephenate; TNAD, Thio-NAD. Numbers accompanying symbols for dissociation constants are the values (mM) of these dissociation constants.

(a) Main reaction pathway. The scheme indicates the most general mechanism of product release consistent with the data. Other alternatives not ruled out by the data are that product release occurs <u>via</u> the branches labelled I, OR I and II, OR I and III, OR II and III.

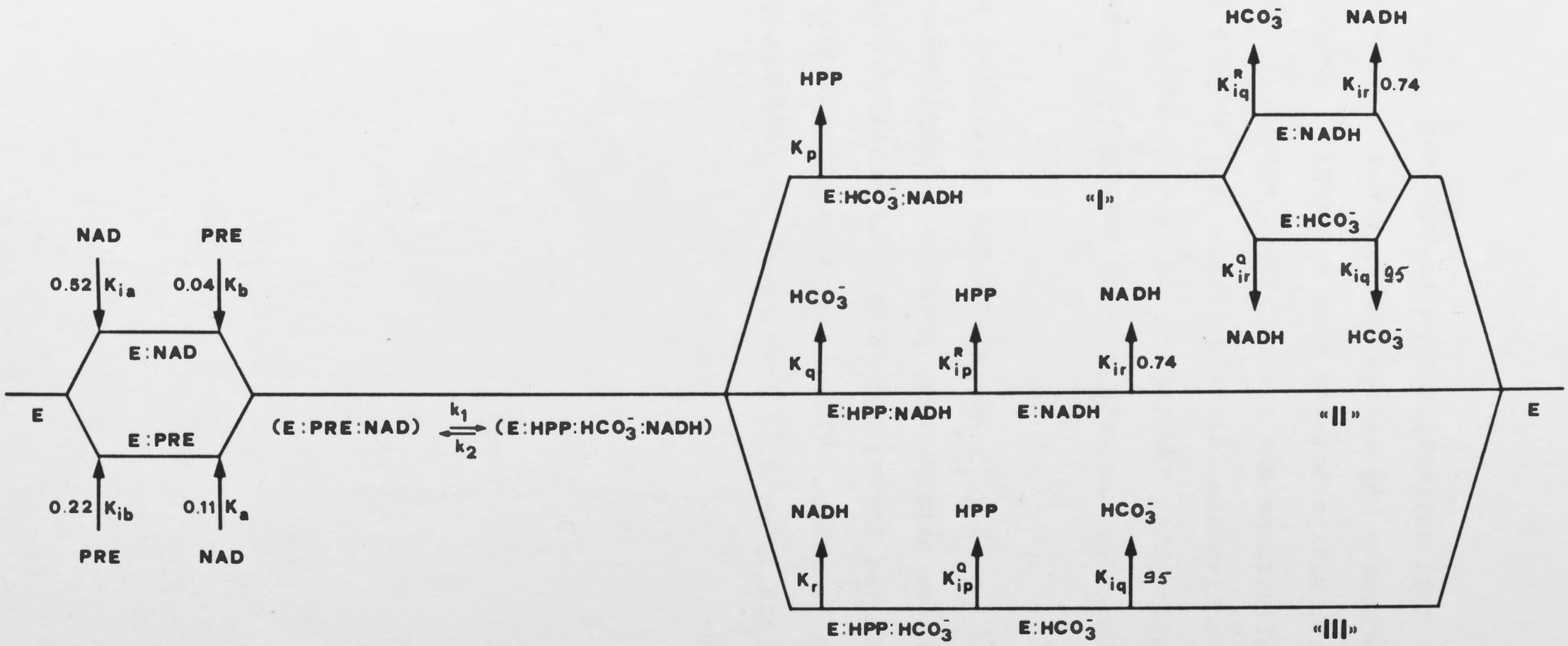

(b) Dead end (nonproductive) complex formation.

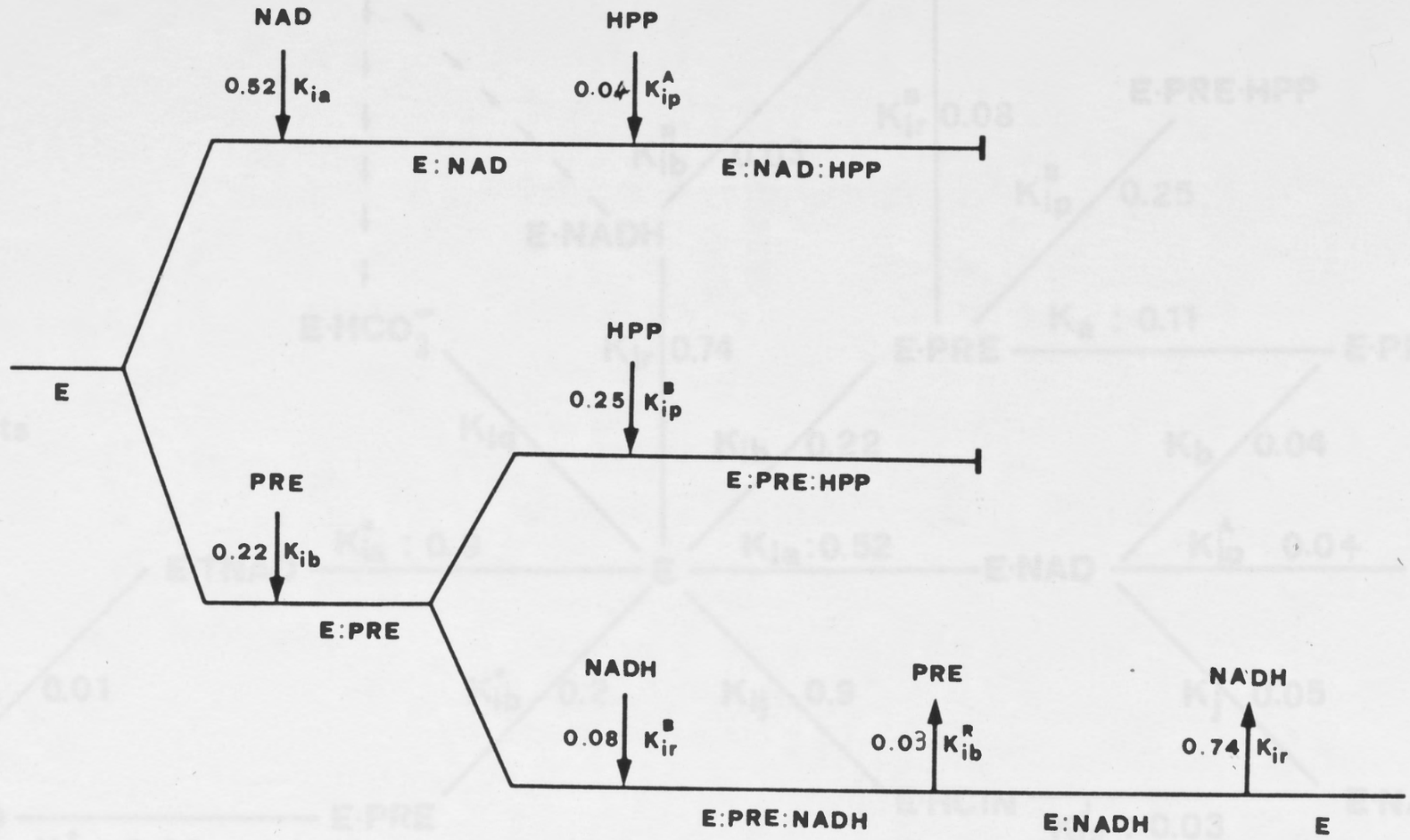

(c) Alternative representation for the purposes of emphasizing synergism of binding. The scheme includes the main reaction pathway, dead end complex formation, the Thio-NAD-utilising reaction and 4-hydroxycinnamate binding.

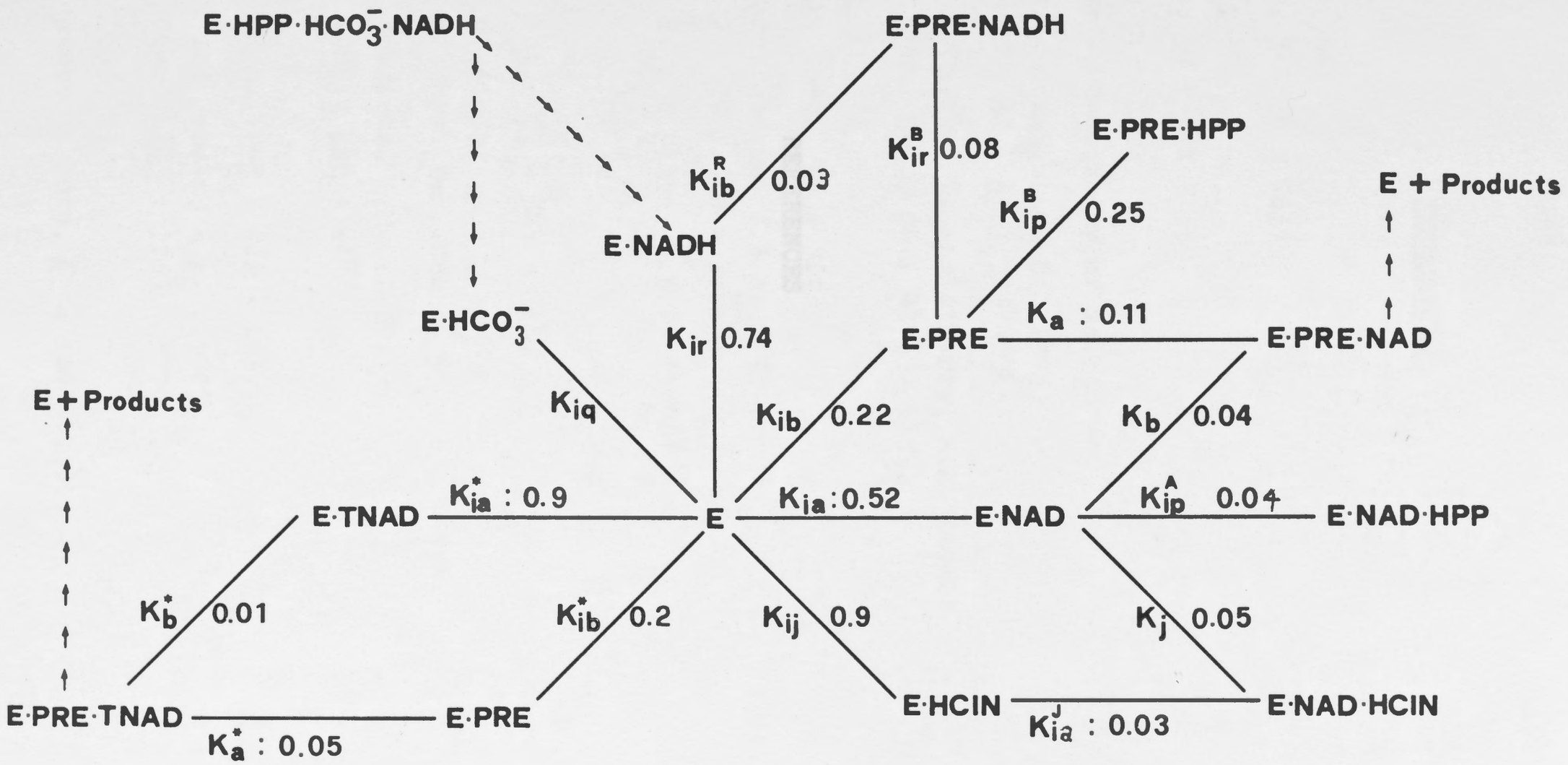

REFERENCES

REFERENCES

Baker, T.I. (1966)
Biochem., 5:2654 - 2657.

Baker, T.I. (1968)
Genetics, 58 : 351 - 359.

Baldwin, G.S. (1974)
Ph.D Thesis, University of Melbourne.

Bardsley, W.G. and Waight, R.D. (1976)
J. Theoret. Biol., 63 : 325 - 345.

Bloomfield, V., Peller, L. and Alberty, R.A. (1962)
J. Amer. Chem. Soc., 84 : 4375 - 4381.

Bodenstein, M. (1913)
Z. physik. Chem., 85 : 329.

Briggs, G.E. and Haldane, J.B.S. (1925)
Biochem. J., 19 : 338 - 339.

Brocklehurst, K. and Dixon, H.B.F. (1976)
Biochem. J., 155 : 61.

Brown, A.J. (1902)
J. Chem. Soc., 81 : 373 - 388.

Catcheside, D.E. (1969)
Biochem. Biophys. Res. Comm., 36 : 651 - 656.

Cedar, H. and Schwartz, J.H. (1969)
J. Biol. Chem., 244 : 4122.

Cha, S. (1968)
J. Biol. Chem., 243 : 820 - 825.

Champney, W.S. and Jensen, R.A. (1970)
J. Biol. Chem., 245 : 3763 - 3770.

Cleland, W.W. (1963 a)
Biochim. Biophys. Acta, 67 : 104 - 137.

Cleland, W.W. (1963 b)
Biochim. Biophys. Acta, 67 : 173 - 187.

Cleland, W.W. (1963 c)
Biochim. Biophys. Acta, 67 : 188 - 196.

Cleland, W.W. (1967)
Ann. Rev. Biochem., 36 : 77.

Cleland, W.W. (1967)
Advan. Enzymol., 29 : 1 - 32.

Cleland, W.W. (1970)
in "The Enzymes" vol.II pp 1 - 65.
P.D.Boyer, ed., Academic Press, New York and London.

Cleland, W.W. (1977)
Advan. Enzymol., 45 : 273 - 387.

Cornish-Bowden, A. (1976)
Biochem. J., 153 : 455.

Cotton, R.G.H. and Gibson, F. (1965)
Biochim. Biophys. Acta, 100 : 76 - 88.

Cotton, R.G.H. and Gibson, F. (1967)
Biochim. Biophys. Acta, 147 : 222 - 237.

Cotton, R.G.H. and Gibson, F. (1968)
Biochim. Biophys. Acta, 160 : 188 - 195.

Crawford, I.P. (1975)
Bacteriol. Rev., 39 : 87 - 120.

Dalziel, K. (1957)
Acta Chem. Scand., 11 : 1706 - 1723.

Darvey, I.G. (1976)
Molec. and Cellul. Biochem., 11 : 3 - 8-

Davidson, B.E., Blackburn, E.H. and Dopheide, T.A.A. (1972)
J. Biol. Chem., 247 : 4441 - 4446.

Dawson, R.M.C., Elliott, D.C., Elliott, W.H. and Jones, K.M. (1969)
"Data for Biochemical Research" 2nd ed. Oxford University Press, London.

Dayan, J. and Sprinson, D.B. (1970)
Meth. Enzymol., XVII Pt.A : 559 - 561.

Dixon, H.B.F. (1976)
Biochem. J., 153 : 627 - 629.

Dopheide, T.A.A., Crewther, P. and Davidson, B.E. (1972)
J. Biol. Chem., 247 : 4447 - 4452.

Doy, C.H. (1960)
Nature, 186 : 529 - 531.

Duggleby, R.G., Sneddon, M.K. and Morrison, J.F. (1978)
Biochemistry, 17 : 1548 - 1554.

Edwards, J.M. and Jackman, L.M. (1965)
Aust. J. Chem., 18 : 1227 - 1239.

Friedrich, B., Friedrich, C.G. and Schlegel, H.G. (1976 a)
J. Bacteriol., 126 : 712 - 722.

Friedrich, C.G., Friedrich, B. and Schlegel, H.G. (1976 b)
J. Bacteriol., 126 : 723 - 732.

Friedrich, B. and Schlegel, H.G. (1972)
Arch. Mikrobiol., 83 : 17 - 31.

Fromm, H.J. (1964)
Biochim. Biophys. Acta 81 : 413 - 417.

Gamborg, O.L. and Keeley, F.W. (1966)
Biochim. Biophys. Acta, 115 : 65 - 72.

Gething, M.J.H. (1973)
Ph.D. Thesis, University of Melbourne.

Gething, M.J.H. and Davidson, B.E. (1976)
Eur. J. Biochem., 71 : 327 - 336.

Gibson, F. (1964)
Biochem. J., 90 : 256 - 261.

Gibson, F. (1968)
Biochem. preps., 12 : 94 - 97.

Gibson, M.I. and Gibson, F. (1964)
Biochem. J., 90 : 248 - 256.

Gilchrist, D.G. and Kosuge, T. (1974)
Arch. Biochem. Biophys. 164 : 95 - 105.

Gilchrist, D.G. and Kosuge, T. (1975)
Arch. Biochem. Biophys., 171 : 36 - 42.

Görisch, H. and Lingens, F. (1972)
Arch. Mikrobiol., 82 : 147 - 154.

Görisch, H. and Lingens, F. (1974)
Biochem., 13 : 3790 - 3794.

Gornall, A.G., Bardwill, C.J. and David, M.M. (1949)
J. Biol. Chem., 177 : 751 - 766.

Haldane, J.B.S. (1930)
"Enzymes" Longmans, London.

Henri, V. (1903)
"Lois Générales de l'Action des Diastases", Hermann, Paris.

Heyde, E. (1978)
Biochemistry, 18 : 2766 - 2775.

Heyde, E. and Morrison, J.F. (1978)
Biochemistry, 17 : 1573 - 1580.

Hoch, J.A. and Nester, E.W. (1973)
J. Bacteriol., 116 : 59 - 66.

Huang, L., Montoya, A.L. and Nester, E.W. (1974 a)
J. Biol. Chem., 249 : 4473 - 4479.

Huang, L., Montoya, A.L. and Nester, E.W. (1975)
J. Biol. Chem., 250 : 7675 - 7681.

Huang, L., Nakatsukasa, W.M. and Nester, E. (1974 b)
J. Biol. Chem., 249 : 4467 - 4472.

Jensen, R.A. (1969)
J. Biol. Chem., 244 : 2816 - 2823.

Jensen, R.A. and Nester, E.W. (1965)
J. Mol. Biol., 12 : 468.

Jensen, R.A. and Stenmark, S.L. (1975)
J. Mol. Evol., 4 : 249 - 259.

King, E.L. and Altman, C. (1956)
J. Phys. Chem., 60 : 1375.

Knox, W.E. and Pitt, B.M. (1957)
J. Biol. Chem., 225 : 675 - 688.

Knowles, J.R. (1976)
CRC Critical Reviews in Biochemistry, Nov., p 165.

Koch, G.L.E., Shaw, D.C. and Gibson, F. (1970 a)
Biochim. Biophys. Acta, 212 : 375 - 386.

Koch, G.L.E., Shaw, D.C. and Gibson, F. (1970 b)
Biochim. Biophys. Acta 212 : 387 - 395.

Koch, G.L.E., Shaw, D.C. and Gibson, F. (1971 a)
Biochim. Biophys. Acta, 229 : 795 - 805.

Koch, G.L.E., Shaw, D.C. and Gibson, F. (1971 b)
Biochim. Biophys. Acta, 229 : 805 - 812.

Koch, G.L.E., Shaw, D.C. and Gibson, F. (1972)
Biochim. Biophys. Acta, 258 : 719 - 730.

Lepesant-Kejzlarovà, J., Lepesant, J.A., Walle, J.,
Billault, A. and Dedonder, R. (1975)
J. Bacteriol., 121 : 823 - 824.

Lingens, F., Goebel, W. and Uesseler, H. (1966)
Biochem. Z. 346 : 357 - 367.

Lingens, F., Goebel, W. and Uesseler, H. (1967)
Eur. J. Biochem., 2 : 442 - 447.

Llewellyn, D.J. and Smith, G.D. (1977)
Aust. Biochem. Soc. (Proc.) 10 : 1.

Lowe, D.A. and Westlake, D.W.S. (1972)
Can. J. Biochem., 50 : 1064 - 1073.

Metzenberg, R.L. and Mitchell, H.K. (1956)
Arch. Biochem. Biophys., 64 : 51 - 56.

Michaelis, L. and Menten, M.L. (1913)
Biochem. Z., 49 : 333 - 369.

Michaelis, L. and Pechstein, H. (1914)
Biochem. Z., 60 : 79.

Michaelis, L. and Rona, P. (1914)
Biochem. Z. 60 : 62.

Morrison, J.F. and James, E. (1965)
Biochem. J., 97 : 37.

Nakatsukasa, W.M. and Nester, E.W. (1972)
J. Biol. Chem., 247 : 5972 - 5979.

Nester, E.W. and Jensen, R.A. (1966)
J. Bacteriol., 91 : 1594 - 1598.

Painter, H.A. and Zilva, S.S. (1947)
Biochem. J., 41 : 520 - 522.

Patel, N., Pierson, D.L. and Jensen, R.A. (1977)
J. Biol. Chem., 252 : 5839 - 5846.

Pierson, D.L. and Jensen, R.A. (1974)
J. Mol. Biol., 90 : 563 - 579.

Pittard, J. and Wallace, B.J. (1966)
J. Bacteriol., 91 : 1494 - 1508.

Plieninger, H. (1962)
Angew. Chem. internat. Edit., 1 : 367 - 372.

Plowman, K.M. (1972)
"Enzyme kinetics" M^{C}Graw-Hill Book Company, New York.

Rebello, J.L. and Jensen, R.A. (1970)
J. Biol. Chem., 245 : 3738 - 3744.

Richards, J.H. (1970)
in "The Enzymes" vol. II, pp 321 - 333.
P.D. Boyer, ed., Academic Press, New York and London.

Rose, I.A. (1970)
in "The Enzymes" vol. II, pp 281 - 320.
P.D. Boyer, ed., Academic Press, New York and London.

Rose, I.A., O'Connell, E.L., Litwin, S. and Bar-Tana, (1974)
J. Biol. Chem., 249 : 5163.

Rudolph, F.B and Fromm, H.J. (1970)
Biochemistry, 9 : 4660 - 4665.

Schimerlik, M.I., Rife, J.E. and Cleland, W.W. (1975)
Biochemistry, 14 : 5374.

Schmit, J.C., Artz, S.W. and Zalkin, H. (1970)
J. Biol. Chem., 245 : 4019 - 4027.

Schmit, J.C. and Zalkin, H. (1969)
Biochemistry, 8 : 174 - 181.

Schmit, J.C. and Zalkin, H. (1971)
J. Biol. Chem., 246 : 6002 - 6010.

Schwinck, I. and Adams, E. (1959)
Biochim. Biophys. Acta, 36 : 102.

Segal, H.L. (1959)
in "The Enzymes" (2nd Ed.) vol. I pp 1 - 48.
Academic Press, New York.

Sørenson, S.P.L. (1909)
Biochem. Z., 21 : 131.

Sprössler, B., Lenssen, U. and Lingens, F. (1970)
Hoppe Seyler's Z. Physiol. Chem., 351 : 1178 - 1182.

Sprössler, B. and Lingens, F. (1970)
Hoppe Seyler's Z. Physiol. Chem. 351 : 448 - 458.

Van Slyke, D.D. and Cullen, G.E. (1914)
J. Biol. Chem., 19 : 141.

Van Slyke, D.D. and Zacharias, G. (1914)
J. Biol. Chem., 19 : 181.

Vining, L.C. and Westlake, D.W.S. (1964)
Can. J. Microbiol., 10 : 705 - 716.

Weber, H.L. and Böck, A. (1968)
Arch. Mikrobiol., 61 : 159.

Weber, H.L. and Böck, A. (1969)
Arch. Mikrobiol., 66 : 250.

Weber, H.L. and Böck, A. (1970)
Eur. J. Biochem., 16 : 244 - 251.

Weiss, U., Gilvarg, C., Mingioli, E.S. and Davis, B.D. (1954)
Science, 119 : 774 - 775.

Wong, J.T.-F. and Hanes, C.S. (1962)
Can. J. Biochem. Physiol., 40 : 763 - 804.

Woodin, T.S. and Nishioka, L. (1973 a)
Biochim. Biophys. Acta, 309 : 224 - 231.

Woodin, T.S. and Nishioka, L. (1973 b)
Biochim. Biophys. Acta, 309 : 211 - 223.

Woolf, B. (1929)
Biochem. J., 23 : 472 - 482.

Woolf, B. (1931)
Biochem. J., 25 : 342 - 348.

Young, I.G., Gibson, F. and MacDonald, C.G. (1969)
Biochim. Biophys. Acta, 192 : 62 - 72.

Zewe, V., Fromm, H.J. and Fabiano, R. (1964)
J. Biol. Chem., 239 : 1625 - 1634.

Zurawski, G. and Brown, K.D. (1975)
Biochim. Biophys. Acta, 377 : 473 - 481.